THE CONTROLLED RELEASE OF MACROMOLECULES FROM MACROPOROUS HYDROPHILIC POLYMER MATRICES

Roisin Lesley McCALLION

Thesis submitted for the degree of Doctor of Philosophy

The University of Aston in Birmingham

May 1990

The University of Aston in Birmingham

Roisin Lesley McCallion 1990

Summary of Thesis submitted for the Degree of Doctor of Philosophy

THE CONTROLLED RELEASE OF MACROMOLECULES FROM MACROPOROUS HYDROPHILIC POLYMER MATRICES

This work has used novel polymer design and fabrication technology to generate bead form polymer based systems, with variable, yet controlled release properties, specifically for the delivery of macromolecules, essentially peptides of therapeutic interest. The work involved investigation of the potential interaction between matrix ultrastructural morphology, in vitro release kinetics, bioactivity and immunoreactivity of selected macromolecules with limited hydrolytic stability, delivered from controlled release vehicles.

The underlying principle involved photo-polymerisation of the monomer, hydroxyethyl methacrylate, around frozen ice crystals, leading to the production of a macroporous hydrophilic matrix. Bead form matrices were fabricated in controllable size ranges in the region of 100μm - 3mm in diameter. The initial stages of the project involved the study of how variables, delivery speed of the monomer and stirring speed of the non solvent, affected the formation of macroporous bead form matrices. From this an optimal bench system for bead production was developed. Careful selection of monomer, solvents, crosslinking agent and polymerisation conditions led to a variable but controllable distribution of pore sizes (0.5 - 4μm).

Release of surrogate macromolecules, bovine serum albumin and FITC-linked dextrans, enabled factors relating to the size and solubility of the macromolecule on the rate of release to be studied. Incorporation of bioactive macromolecules allowed retained bioactivity to be determined (glucose oxidase and interleukin-2), whilst the release of insulin enabled determination of both bioactivity (using rat epididymal fat pad) and immunoreactivity (RIA).

The work carried out has led to the generation of macroporous bead form matrices, fabricated from a tissue biocompatible hydrogel, capable of the sustained, controlled release of biologically active peptides, with potential use in the pharmaceutical and agrochemical industries.

KEY WORDS: Controlled release. Bioactive macromolecules. Macroporous hydrophilic polymer matrices.

DEDICATION

This thesis is dedicated to my parents, Patrick and Lesley, and my sister, Katherine. A million thanks for your love and support.

Also, to the memory of my Grandparents.

ACKNOWLEDGEMENTS

Grateful thanks to my Supervisor, Dr T W Atkins for all his help, advice and encouragement. Many thanks to Mr J Elston and Mr K Mynett for their invaluable technical assistance throughout the course of this work. Thanks also to the following people for their help:-

Drs. B J Tighe and S M Murphy, Speciality Materials Research Group, for their advice on polymeric formulations.

Dr. A J H Gearing, N.I.B.S.C., for the assay of interleukin-2.

Members of the technical staff in the Biology Division, Department of Pharmaceutical Sciences, for all their assistance.

Drs. R Armstrong and P Hanson for their advice on the statistical analyses used in this work.

Finally, many thanks to Mrs Lesley June McCallion for typing this thesis and to Ms Elizabeth Graves for the help she gave to her.

CONTENTS

LIST OF TABLES, FIGURES AND PLATES

TABLES

FIGURES

PLATES

CHAPTER 1

INTRODUCTION

1.1 INTRODUCTION TO CONTROLLED DELIVERY

Biologically active molecules, when used therapeutically are generally administered in a cyclic fashion, by periodic injections or via oral dosage forms. This is not always a satisfactory means of delivery, since great fluctuations in the systemic concentration of the bioactive agent can occur between administrations. Typically, when a bioactive agent is injected or ingested as a basis for clinical therapy the systemic level initially achieved exceeds the therapeutic level for a brief period and subsequently declines from therapeutic to ineffective levels until the next dose is administered. This method of application is undesirable, since the kinetics are difficult to control and the fluctuating concentrations can make treatment unreliable, particularly when toxic and therapeutic concentrations of the bioactive agent are of the same order (1). Continuously maintained plasma levels can also enhance the therapeutic actions of certain clinically employed bioactive agents.

Once a therapeutic agent has entered the systemic circulation, the time course of its effects are entirely determined by its intrinsic rate of action, degradation and excretion. Therefore, controlling the

rate at which the bioactive agent enters the systemic circulation, ie the bioavailability of the agent, provides the only practical means for the control of the safety and effectiveness of a therapeutic agent (2). To achieve and maintain a steady therapeutic level, devices must be designed which deliver the bioactive agent at controlled rates over extended periods of time. The controlled delivery of a bioactive agent, refers specifically to the precise control of the dose, based on the predetermined and controllable rate at which a particular bioactive agent is released, unchanged, from a delivery vehicle over an extended time period. This differs from a sustained delivery device, which simply prolongs the dosage from a depot, with little control and often over only a short time period.

Controlled delivery devices assume particular importance for the administration of bioactive agents with short plasma half lives, especially if the agent must be administered by injection and/or the therapeutic range is narrow. This work is specifically concerned with the controlled delivery of macromolecules, especially peptides of therapeutic interest, from a polymeric delivery system. Biotechnology has made available an increasing number and quantity of clinically significant peptides, such

as hormones, growth factors and cytokines, of high specific activity, which must be injected to avoid hydrolytic breakdown in the stomach, often have short plasma half lives and toxic side effects at concentrations close to their therapeutic level. The potential of these macromolecules in clinical application would be improved if devices were designed for their controlled delivery, in an active form, close to their site of action. However, these macromolecules are generally so prone to thermal and hydrolytic instability that their incorporation into controlled delivery devices is difficult. Immobilisation of biologically active polypeptides within a polymeric delivery system is often difficult due to the ease with which some macromolecules denature when exposed to organic solvents or to temperatures appreciably higher than room temperature. The high molecular weight of many biologically active macromolecules often further prohibits their delivery from currently employed polymeric delivery devices, the majority of which are only capable of the delivery of relatively small molecules.

Controlled delivery systems can be broadly defined as either chemical or mechanical devices, as shown in Table 1.1, designed to deliver bioactive agents into a system at a predetermined rate. It is the polymeric

devices with which this work is concerned. The development of controlled delivery systems requires a knowledge not only of the physical and chemical properties of the bioactive agent and the condition to be treated, but of the physical and chemical properties of the delivery vehicle and its method of fabrication.

Table 1.1 The main classes of controlled delivery systems.

MECHANICAL DEVICES	CHEMICAL DEVICES
Infusion Pumps Osmotic Pumps	Prodrug design Biological devices Polymeric devices

1.2 POLYMER BASED CONTROLLED DELIVERY DEVICES.

Synthetic polymer based delivery devices are highly developed forms of bioactive agent delivery system. Delivery devices have been constructed from inert, bioerodible and biodegradable polymers. Langer and colleagues (3,4) have attempted a classification of the various types of polymeric vehicle used for controlled release, based upon the mechanisms of release, as shown in Table 1.2.

Table 1.2: Broad classification of the types of polymer based drug delivery devices available, based upon the mechanism by which release is effected.

MECHANISM OF RELEASE	TYPE OF SYSTEM
Diffusion Controlled	Matrix system Reservoir system
Chemically Controlled	Bioerodible/ biodegradable system. Pendent chain system.
Swelling Controlled	Swelling controlled system.
Magnetically Controlled	Magnetically controlled system.

Although these categories are greatly oversimplified, they represent a useful summary of the wide variety of the potential polymer based delivery devices available. However, it must be remembered that any one delivery device may exhibit a combination of mechanisms by which release is effected.

1.2.1 Diffusion controlled delivery systems

The first category suggested by Langer and colleagues (3,4), described polymeric delivery devices in which the rate of diffusion of the bioactive agent through the polymer is the controlling factor in the rate of release of a bioactive agent from the device. Diffusion controlled systems may be further subdivided into either reservoir, or matrix type systems.

(a) Reservoir systems

In a reservoir system, a core of bioactive agent is surrounded by a diffusion-rate limiting polymer. This category may include the encapsulation of bioactive agents by polymeric membranes, forming nanoparticles and microcapsules, film 'sandwiches' in which a layer of bioactive agent is sandwiched between two polymeric membranes, or larger, monolith-type devices. Reservoir systems may be constructed from inert, bioerodible or biodegradable polymers.

The inert polymers most widely used for reservoir system are poly 2-hydroxyethyl methacrylate (polyHEMA) ethylene-vinyl acetate copolymer (EVAc) and silicone rubber (3), in the form of a non-porous or microporous film, in which water is homogenously dispersed. Two

basic mechanisms have been proposed to explain the transport of a solute, such as an incorporated bioactive agent in solution, through an homogenous polymeric membrane, either via a pore mechanism, in the case of a microporous membrane, or by a partition mechanism in a non-porous membrane. In the pore mechanism of release, the core of bioactive agent starts dissolving at its outside edge first, in response to an influx of aqueous environmental medium (if the bioactive agent is incorporated in a crystalline form) and solute transport then occurs through micropores in the polymeric membrane (5). In the partition mechanism the transport of bioactive agent is thought to occur by dissolution of the bioactive agent within the polymer, followed by its diffusion between and along polymer chains (5). However, non-porous and microporous inert polymer films are generally only permeable to low molecular weight species (MW<600).

The principle advantage of a reservoir system is the ease with which it can be designed to release the bioactive agent at a zero-order release rate, ie a constant amount of bioactive agent released per day. This can be achieved by loading the reservoir, encompassed by the polymer, with a solid core of bioactive agent, far above the level of its solubility

in the environmental medium. The influx of aqueous medium, such as tissue fluid on implantation, causes the bioactive agent to be dissolved first around the outer edges of the core and only the amount required to reach saturation concentration can be dissolved at any one time. Therefore, as long as the bioactive agent is available in its solid form its concentration at the internal wall of the membrane will be its saturation concentration and the rate of release from the membrane will be constant. If the bioactive agent is encapsulated in solution, as is the case with some nanoparticles and microcapsules, the kinetics of release will tend to be first order, decreasing with time as the reservoir of bioactive agent is quickly depleted. Such systems tend to be designed for short term delivery and are employed more to protect the bioactive agent or to reduce its toxicity than to provide sustained delivery of the bioactive agent over long periods of time. Under these circumstances zero-order release kinetics are not of prime importance.

In general, the rate of diffusion of a solute through a microporous membrane depends on the molecular diameter of the solute, smaller molecules are transported quicker than larger molecules. Diffusion through a 'non porous' partition mechanism membrane depends on the affinity of the solute for the polymer

and its ability to move between polymeric chains (6). The diffusion of a solute through any one particular polymer may be by either pore flow or partition mechanism or by both, depending upon the composition of the polymer. For example, it has been shown that the permeation of steroids through a polyHEMA matrix, without crosslinker, occurs predominantly by the pore mechanism, with about a 20% contribution from the partition mechanism, the amount dependant upon the solute. However, when ethylene dimethacrylate was added as a crosslinking agent, permeation occurred via the partition mechanism (7). Release rates can also be altered by varying the membrane thickness and geomerty of the device. Mathematical models describing the rates of release of bioactive agents from different reservoir devices have been well documented (3-5).

Non-porous reservoir devices have been marketed commercially by the Alza Corporation (California - USA). Progestasert^{R}(8,9) and Ocusert^{R}(10,11) are fabricated from non-degradable, hydrophobic ethylene-vinyl acetate (EVAc) copolymer. Such hydrophobic polymers tend to have a minimal water content and show relatively high permeation for lipophilic bioactive agents. Progestasert is a T-shaped intrauterine device composed of a microcrystalline progesterone reservoir, within a liquid poly dimethyl siloxane

core, surrounded by an EVAc membrane. Progesterone diffuses by partition through the EVAc membrane, then into the uterine fluid. The diffusion of the progesterone out of the device is slow compared with its more rapid dissipation into the uterine fluid and hence a negative concentration gradient is maintained. Such devices release about 65µg of progesterone per day in utero at a nearly constant rate for one year (8,9). This type of intrauterine device has advantages over oral methods of contraception since the required doses of the hormone are very much reduced and compliance is improved. Ocusert was designed to deliver pilocarpine continuously over a one week period for the treatment of glaucoma. Two devices, fabricated using EVAc were designed to release either 20 or 40µg of pilocarpine per hour directly into the eye from its position under the lower eyelid (10,11). The mechanism of release is similar in principle to the Progestasert system. Pilocarpine is released at a near zero order rate after an initial burst release covering the first hour of insertion. Using Ocusert, a reduced amount of pilocarpine is required to reduce intraocular pressure and the device improves patient compliance.

Reservoir systems have a number of disadvantages; they are unsuitable for the controlled delivery of high molecular weight bioactive agents because of the

microporous or non-porous nature of the membranes employed. They are potentially dangerous if a rupture should occur in the polymeric membrane because the contents would be rapidly released. Reservoir devices also tend to be more difficult to fabricate and hence more expensive to produce than other types of polymeric delivery devices. As a rule, their use and development has tended to be towards the treatment of acute conditions of specific duration rather than chronic conditions which require routine long term treatment.

(b) Matrix systems

In matrix systems, the bioactive agent is dispersed uniformly throughout the polymeric structure. In common with reservoir systems, the diffusion of bioactive agent through the polymer matrix is usually the rate-limiting process. Many different types of matrix systems have been investigated involving inert, bioerodible and biodegradable polymers. In inert matrices, the bioactive agent may be either dispersed or dissolved within a non-porous or microporous polymer, such as EVAc or polyHEMA. Diffusion out of the vehicle occurs via a pore-flow or a partition mechanism, as described for reservoir systems. However, if a non-porous or microporous polymer is employed the matrix device will generally only be

suitable for the delivery of low molecular weight compounds.

In contrast to reservoir systems, matrix systems have been designed to facilitate the long term delivery of macromolecules such as insulin. One approach has been to incorporate crystalline macromolecules in solvent cast polymers such as EVAc, which is usually impermeable to macromolecules (12). In these studies, casting solutions of EVAc were made by dissolving the copolymer in methylene chloride at 37°C. The macromolecule was then added to the solution in a powdered form and the solution poured into moulds. The solvent was evaporated off, under a mild vacuum (60 mmHg), leaving the macromolecule trapped within the polymer matrix. When exposed to aqueous medium, the EVAc pellets released the incorporated macromolecules for over 100 days (13). The reproducibility of the release kinetics was poor, due to settling of the powdered macromolecules in the polymer solution, however, low temperature (-80°C) casting and two step drying, at -20°C and then 20°C has subsequently improved the reliability of this vehicle (14).

Macromolecules are too large to dissolve through the EVAc and the presence of the powdered macromolecule forms a network of channels throughout the polymer.

Thus, in contact with aqueous environmental medium,the macromolecules at the surface of the device diffuse away first leaving open pores in the polymer. As the medium penetrates further into the polymer, more macromolecule dissolves and diffuses out of the device via the gaps vacated by the dissolved macromolecule at the surface. A network of interconnecting pores is thereby created, allowing the eventual diffusion of all the incorporated macromolecule. The release profiles obtained from these devices reveal three phases; an initial 'burst' release due to the rapid dissolution and diffusion of the macromolecule from the surface of the device, a second, extended period, when release rates approach zero-order and a final period, in which the rate of release gradually declines due to the depletion of the incorporated macromolecule (14). Macromolecules incorporated into these matrix systems have included bovine serum albumin (MW 68,000), ß-lactoglobulin (MW 18,000), lysozyme (MW 14,400), alkaline phosphatase (MW 88,000) and catalase (MW 250,000) (12-14). Biologically active bovine insulin (MW 5640) has been delivered by this type of solvent-cast EVAc matrix system, at a rate of 2 - 5U/day when implanted subcutaneously into diabetic rats, achieving normoglycaemia for 30 - 100 days (15-8). There is some suggestion that <u>in vitro</u> release experiments carried out with this type of matrix system can accurately predict the rates of release of

the macromolecules in vivo, at least over the two month period release rates were compared (19).

A number of factors have been found to affect the rates of release of macromolecules from these solvent-cast matrix systems. These include the particle size of the macromolecule and the percentage loading of the macromolecule into the polymer solution (14). High loading levels of macromolecule and a large particle size create a wider pore diameter and more extensive porous network within the polymer and allow the macromolecule to diffuse out faster (20). The degree of solubility of the macromolecule in the release medium is another important factor (16,21,22). For example, studies have shown that sodium insulin (solubility = 120mg/ml pH7.4) is released 7.5 times faster than zinc insulin (solubility = 0.33mg/ml pH7.4) from comparable matrices (16). It is evident that a simple diffusion model alone cannot account for the varying rates of release of different macromolecules from this type of matrix system, since there is no clear relationship between the molecular weight of an incorporated macromolecule and its rate of release (12,14). However, the molecular weight of the EVAc itself has been shown to influence the rate of release of incorporated bovine serum albumin (BSA). The higher the molecular weight of the polymer, the slower the rate of release of the macromolecule. It

is thought that bovine serum albumin particles swell in the environmental medium more easily in a lower molecular weight, easily deformable matrix, opening up larger pores and hence producing a faster release rate (23).

An alternative approach to the delivery of bioactive macromolecules, is to utilise synthetic polymer based, macroporous hydrophilic matrix systems, through which an incorporated macromolecule can diffuse. Such a system may be achieved by the heterogenous dispersion of water within a hydrogel polymer, using a freeze-thaw method of polymerisation, described by Haldon and Lee (24). This yields a polymer in which water is heterogenously dispersed between a polymeric network of low water content and a porous network in which water molecules predominate, through which macromolecules can diffuse. It is the formulation of such a delivery vehicle with which the present work is principally concerned, more specifically, the use of bead formed, hydrophilic macroporous matrices composed of polyHEMA for the controlled delivery of macromolecules.

The main advantage of the use of matrix type systems is their relative ease of fabrication. The most often perceived disadvantage in the use of such systems is difficulty in obtaining zero-order release rates of

bioactive agent, particularly when slab shaped devices are used (3). However, manoeuvres such as coating the device with a second, bioerodible or biodegradable polymer, to provide an additional rate controlling layer, or changing the geometry of the device to a sphere or hemisphere, have facilitated zero-order release of bioactive agents (3,4,17).

1.2.2 Chemically controlled delivery systems

The main factor controlling the release of an incorporated bioactive agent is the chemical cleavage of the polymer by one of a number of chemical mechanisms. The rate of chemical cleavage of the polymer is not necessarily the rate limiting step for the release of the bioactive agent, diffusion of the incorporated bioactive agent as the polymer cleaves may also be an important factor. Chemically controlled systems can be further subdivided into bioerodible and biodegradable polymer based delivery systems and pendent chain systems.

(a) Bioerodible and biodegradable systems

Bioerodible and biodegradable polymers can be used to fabricate a matrix-type delivery system in which the bioactive agent is uniformly dispersed throughout the polymer. The difference between bioerodible/biodegradable polymer based systems and

diffusion controlled matrix systems is that, in the latter, the polymer remains chemically unchanged with time and the diffusion of the bioactive agent is the rate limiting process for release. However, in bioerodible/biodegradable systems the polymer degrades with time, by any one of a number of mechanisms, and the rate and extent of cleavage of the polymer chains is an important factor in the control of the release rate. There is often little distinction made between the use of the terms bioerodible and biodegradable and where the terms are defined, they often vary between authors. Biodegradation has been defined as the biological breakdown of the polymer as opposed to simple hydrolytic cleavage (25,26) or any polymer which undergoes in vivo degradation (27). Bioerosion has been variously described as the dissolution and diffusion away of the soluble product (28), the conversion of a water insoluble to a water soluble material (29) or the ability of the rate of erosion of the polymer to control the rate of release of a bioactive agent (30). A more precise definition is to consider biodegradation as the enzymatic, hydrolytic or bacteriological cleavage of a polymer in which the physical form of the polymer is not necessarily altered during the release period and in which the rate of diffusion of an incorporated bioactive agent out of the device is the rate controlling step. Bioerosion is considered to necessitate physical

weight loss from the device following either homogenous or heterogenous (surface) erosion and where the incorporated bioactive agent is released only with physical loss of the polymer (31).

In addition to matrix-like systems, in which the bioactive agent is uniformly dispersed throughout the polymer, bioerodible and biodegradable polymers may be used to fabricate reservoir-type microcapsules, nanoparticles, or they may be used to coat devices to provide an additional rate controlling barrier to the release of the incorporated bioactive agent. The use of biodegradable and bioerodible polymers in the fabrication of vehicles for the delivery of bioactive agents has been the subject of a large number of reviews (3-5,28,30-32). Most have been directed towards the delivery of relatively low molecular weight bioactive agents such as steroids and narcotic antagonists (32-35), however, biodegradable and bioerodible polymers have also been successfully employed in the fabrication of delivery vehicles for macromolecules. Torchilin and coworkers have used the bioerodible polymer polyvinyl pyrrolidone, crosslinked with N, N-methylene bisacrylamide, to entrap the enzyme α-chymotrypsin (E.C. 3.4.4.5) (36). These workers synthesised microspheres comprised of a range of polymeric formulations with characteristics which ranged from complete solubility of the poly vinyl

pyrrolidone in 0.05M phosphate buffer, pH8.2 (37°C) in several days, yielding rapid release of the enzyme, to virtual insolubility of devices composed of more than about 1% N, N-methylene bisacrylamide. Bioerosion within useful time periods occurred only at low crosslinking densities and the resultant polymers were quite hydrophilic. Therefore, this type of system is only useful for the release of macromolecules of low solubility in the medium into which they are to be released, since soluble compounds rapidly leach out of the matrix, independant of the rate of erosion of the polymer. If the crosslinking density of the polymer is increased to a level sufficient to trap the soluble macromolecule, the erosion rate is too slow to be practicable. Heller and Baker (37), confirmed these observations when they used devices of the same formulation to release bovine serum albumin (BSA) and concluded that more easily erodible polymers would need to be employed to immobilise macromolecules within the matrix and only allow release to occur with concomitant erosion of the polymer.

Heller, Helwing, Baker and Tuttle have described the controlled release of BSA into agitated tris-buffered saline (pH7.4, 37°C) from bioerodible hydrogel microspheres (38). The devices were based on water-soluble, unsaturated polyesters which released

incorporated macromolecule as the ester linkages hydrolysed. Their results showed good immobilisation of BSA within the polymeric matrix and controllable release rates dependant upon the type and amount of crosslinking agent or acid group, incorporated to enhance hydrolysis of the poly ethylene glycol based polymer. For example, approximately 20% of the incorporated BSA was released over about 45 days from a hydrogel consisting of poly ethylene glycol, fumaric acid and 60% N-vinly pyrrolidone, as a crosslinking agent. When the crosslinking agent was reduced to 20% about 40% of the incorporated BSA was released over the same time period. When fumaric acid was replaced with a 4:1 ratio of ketomalonic: fumaric acid (to enhance hydrolysis), the release of BSA increased to 100% in less than 20 days. Heller et al concluded that the rate of release of BSA from these microspheres was controlled principally by the rate of erosion of the polymer and not by the rate of diffusion of the macromolecule. However, these matrices do not degrade to metabolites normally found in the body (38).

During implantation, matrices composed of hydrophilic biodegradable and bioerodible polymers and copolymers, such as the biodegradable poly glycolic acid (39-44) and poly lactic acid (45,46) generally erode in a

homogenous manner from the entire matrix and not just at the surface of the device. A progressive loosening of the matrix occurs, causing an increase in the permeability and a decrease in the mechanical strength of the device. A more useful device is one which undergoes surface erosion only, leading to zero order release of an incorporated bioactive agent provided that release of the molecule due to diffusion alone is minimal and the geometry of the device is such that the surface area remains fairly constant throughout the useful life of the device (generally a slab) (47). Poly n-alkyl α-cyanoacrylates are another group of bioerodible polymers which have been investigated for use in the fabrication of controlled delivery devices for macromolecules. These polymers are thought to degrade by surface erosion which is dependant upon pH, length of the alkyl side chains of the monomer, molecular weight and molecular weight distribution of the polymer as well as polymer particle size and surface area (48). These polymers have been used to fabricate nanoparticles for use as colloidal carriers for clinically useful molecules such as insulin and actionmycin D (49,50). Laurencin and coworkers have investigated polyphosphazenes for the release of macromolecules (51). The polyphosphazenes are high molecular weight polymers with backbones composed of nitrogen and phosphorous atoms. Many side chain constituents, such as amino acid and alkyl esters

confer hydrolytic instability to the polymer backbone (52) and the degradation products consist of ammonia, phosphate, water and side chain substituents (53). The biocompatibility of these polymers has been reported to be good (54) and no adverse reactions have been observed after implantation into rats (51) Laurencin et al demonstrated the sustained release of BSA for up to 1000 hours and both in vitro and in vivo release of progesterone for up to 1000 hours from poly imedazole-methyl phenoxy phosphazene, in rats (51).

The major potential advantage of the use of any bioerodible and/or biodegradable controlled delivery systems is that surgical removal of the matrix, depleted of bioactive agent should not be required. On the other hand, in some clinical situations, the physician may wish to retrieve the implant to alter or discontinue therapy and this is a potential disadvantage when employing bioerodible and/or biodegradable system. The possibility of long term toxicity or carcionogenicity of the breakdown products, particularly those which do not naturally occur in the body must also be carefully considered.

(b) Pendent chain systems

In its simplest form a pendent chain system is a bioactive agent, attached to a polymeric backbone.

These systems are so called since the pharmacologically active agent is present as pendent side chains of the polymer backbone. The bioactive agent is chemically bound to the polymer, which may be soluble or insoluble and the agent may exert its biological effect whilst bound to the polymer or may require hydrolytic or enzymatic cleavage from the polymer to exert its biological effect. These systems are not designed for long term delivery, but for short term release to reduce the toxicity of the bioactive agent, as in the case of cancer chemotherapy agents (55,56). They are also designed to increase the agent's therapeutic efficiency and/or to target the agent towards specific cells or organs. There appears to be little evidence of the delivery of macromolecules by pendent chain systems, indeed, the attachment of macromolecules to a polymer backbone in pendent chain systems appears to be used only in an attempt to target a second bioactive agent to its site of action. Site specific targeting of bioactive agents is only likely with the attachment of 'recognition ligands' such as enzymes, hormones and immunoglobulins to the polymer backbone (56). Rowland and coworkers bound cytotoxic -phenylenediamine mustard to the polymer backbone of poly L- glutamic acid, along with rabbit immunoglobulin against mouse lymphoma (57). They reported this system to have greater activity against mouse lymphoma than the

individual components alone. There are a number of limitations to the use of pendent chain systems such as possible immunogenicity, and uptake by cells of the reticuloendothelial system. The bioactive agent is chemically bound in pendent chain systems, unlike other devices and this limits the number of molecules which can be successfully delivered.

1.2.3 Swelling controlled delivery systems

In swelling controlled systems, the bioactive agent is dispersed within an initially glassy, hydrophilic polymer and is unable to diffuse out until contact with aqueous medium causes swelling of the polymer. The rate of release of the bioactive agent from these systems is determined by the rate of influx of the aqueous medium and hence the rate of swelling of the polymer. Polymers which may be employed include poly vinyl alcohol and its copolymers with vinyl acetate and methyl methacrylate, poly N-vinyl pyrrolidone and its copolymers with vinyl acetate and various acrylates, polyHEMA and its copolymers with methyl methacrylate and vinyl acetate and other polymers of hydroxyethyl methacrylates and their copolymers (58). The rate of release of a bioactive agent from the polymer is dependant upon two simultaneous processes, the penetration of aqueous medium into the polymer and the diffusion of the bioactive agent out of the gel

phase (59). Since the bioactive agent must diffuse out through the non-porous or microporous gel these systems are only suitable for the delivery of low molecular weight molecules. In addition, heat treatment up to 80°C is often used in the fabrication of these devices and this necessarily restricts the number of bioactive agents which can be successfully incorporated (60).

1.2.4 Magnetically controlled delivery systems

Magnetically modulated systems have been developed by Hsieh and coworkers for the delivery of biologically active macromolecules from ethylene-vinyl acetate copolymer (EVAc) matrices. In this type of system, powdered bioactive agent and small magnetic steel beads are uniformly dispersed within the polymer matrix. On exposure to aqueous medium, the bioactive agent is released in a fashion typical of the EVAc diffusion controlled matrices described earlier (Pages 23-26). However, upon exposure to an external oscillating magnetic field the bioactive agent is released at a much higher rate (61). No such effect was observed when the devices were exposed to a continuous magnetic field. Initial experiments using bovine serum albumin (BSA) as a marker macromolecule showed that these matrices released up to 100% more BSA over a six hour period when exposed to an

oscillating (18 cycles per min.) magnetic field (1,000 gauss) than they did over six hours in the absence of an externally applied magnetic field (62). The biocompatibility of this device was tested by implantation in the rabbit cornea and no significant inflammation was detected (61). Work investigating the mechanism of magnetically modulated release has shown a number of parameters to be important in controlling release rates. These are, the strength of the applied oscillating magnetic field (63), the frequency of the magnetic field (64), magnetic strength, orientation of the magnetic field and the position of the embedded magnet in the polymer film (64). The composition of the EVAc was an additional factor in controlling the rate of release of macromolecules from the polymeric matrix, increasing the vinyl acetate content of the copolymer increased the amount of magnetically modulated release obtained (65). It is thought that the movement of the magnets in response to the magnetic field is responsible for the alternating dilation and compression of pores within the EVAc, caused by the physical presence of the powdered macromolecule. The pulsatile stimulus caused by the oscillation of the magnetic field is thought to cause a piston-like motion, forcing the bioactive agent out of the pores. It is also recognised that the movement of the magnets may cause alterations to the porous network such as causing

connections to form between pores (64). 50% vinyl acetate copolymer was the mechanically weakest polymer tested, offering least resistance to the motion of the magnets and hence, showing the greatest modulated release rates (65). Kost and coworkers have evaluated this type of magnetically modulated release device in vivo for the controlled delivery of insulin into diabetic rats (66). These workers found that a basal level of released insulin 41μU/ml, was increased to 126μU/ml on application of an external oscillating magnetic field, decreasing the blood glucose levels of diabetic rats by a further 30%. Magnetically modulated release devices have the advantage that external control of the rate of release of the bioactive agent can be achieved, even after implantation and a modulated release pattern can be achieved. This type of device has potential use for the treatment of diabetes where a basal rate of insulin release would be supplemented by 'triggering' an additional bolus to counteract post-prandial hyperglycaemia. These devices however do have a number of potential problems, for instance, it would be important to ensure protection from adjacent or neighbouring magnetic fields which could produce an unintentional burst of therapeutic agent from the device. It is also possible that movement of the implant in vivo may change the orientation of the magnets in relation to the field, changing the

expected rate of release. The long term biocompatibility of these devices also requires monitoring, not only in relation to the polymer, but also in terms of the integrity of the magnetic beads in vivo.

1.3 CRITERIA FOR THE SELECTION OF SYNTHETIC POLYMERS FOR IMPLANTABLE CONTROLLED DELIVERY DEVICES.

The selection of a suitable synthetic polymer formulation is critical in the development of a controlled delivery system. Candidate polymers must comply with a range of requirements which may arise from either the structure of the polymer, the nature of the biologically active macromolecule to be delivered, or the environment in which the device is required for use.

Critical to the development of an implantable controlled delivery device is the biocompatibility of the proposed polymer formulation. It is important to establish the biocompatibility of the polymer before a delivery device is developed, saving time and money if the polymer should prove unsuitable. A biocompatible polymer may be defined as one which can exist in a physiological environment without adversely affecting the recipient and is not itself adversely affected by conditions in the body (67). Incompatibility may occur as a short term, acute

response or as a long term, chronic affect, either at local or systemic levels.

The most common cause of acute incompatibility of a polymer is the presence of biologically active toxic leachable substances in or on the material. These leachables may be intentional components of a polymer fomulation such as residual monomers and catalysts, or unintentional contaminants introduced in the fabrication or sterilization process. Toxic leachables can usually be eliminated from polymers by modification of the fabrication processes and careful attention to washing and sterilization procedures. Toxic leachables, absorbed into the circulation may cause systemic toxicity, the degree of which will depend on dose. HEMA monomer causes intradermal irritation in rats which is dose dependant, although, at low concentrations (<1%) little irritation is observed (68). Cathers and colleagues have compared the response obtained in the peritoneal cavity of rats to HEMA which had been prepolymerised and washed for two months and to HEMA polymerised in situ. Significantly higher inflammatory cell counts were obtained from the rats with HEMA polymerised in situ. On the basis of these observations it was suggested that HEMA monomer could cause toxic effects in cells by the eventual production of formaldehyde (69). In vitro tissue culture testing is the most sensitive

indicator of the presence of toxic leachables within a polymer. The actual degree of toxicity observed does tend to be dependant upon the cell line used, although if a range of substances were to be ranked from most to least toxic, their order would tend to be the same, irrespective of the cell line used. However, tissue culture experiments cannot evaluate the degree of inflammatory response to any possible leachables and therefore *in vivo* tests are also required to test the suitablity of a polymer formulation for use as an implant. The muscle is often the chosen site for the implantation of test materials as this tends to be a more sensitive area than the abdominal cavity where washing away of the toxic substances can more easily occur (70). Lawrence has provided an extensive summary of both the *in vivo* and *in vitro* tests available for the evaluation of biomaterials for the presence of toxic leachables (71).

If the results of short term acute toxicity testing of a polymer are favourable, long term, chronic implications of implantation can then be considered. Long term contact of a polymer material with living tissues and biological fluids may result in the biodegradation of the polymer, even those polymers which are nominally stable may be susceptible to hydrolysis *in vivo* (72,73). It is therefore

important that inert devices as well as bioerodible and biodegradable matrices are considered in the context of their breakdown products' ability to induce tumours or other effects due to cumulative toxicity, particularly if the degradation products are unlikely to be metabolised. Carcinogenesis is an important problem to be considered as regards the long term implantation of polymers. This may be induced by the presence of a carcinogen in the polymer (74) by generation of a carcinogen through degradation or through physical 'solid-state carcinogenesis' (75).

Since the first description of the suitability of some hydrogels for biological applications by Wichterle and Lim in 1960, (76), polyHEMA biocompatibility has been the subject of extensive research. Many reports have confirmed the tissue biocompatibility of polyHEMA (13,77-82). Langer and colleagues have used the rabbit cornea as the implantation site for in vivo testing of polymers (13,82) since the cornea is known to be very sensitive to inflammatory stimuli (83,84). These authors noted that a milder reaction may be seen in other tissues. Polyacrylamide, polyvinyl pyrrolidone, and poly vinyl alcohol caused significant inflammation, whilst ethylene-vinyl acetate copolymer caused mild inflammation over a two month test period. An extensive washing procedure (100 changes of alcohol at 37°C, minimum of 3 hours per change of alcohol) was

required to obtain a 100% inflammation free response from ethylene-vinyl acetate copolymer, completely unsuitable for the incorporation of biologically active peptides. Of all the polymers thus tested, only polyHEMA produced no inflammation in any test cornea and no washing procedure was required (82). It is the proven biocompatibility of polyHEMA which makes it the polymer of choice for use in the present work. However, there have been some problems associated with the long term implantation of polyHEMA. Winter and Simpson found evidence of woven bone formation in pieces of macroporous polyHEMA sponges implanted for over two months in young pigs, an effect which was easily reproducible (85). Sprincl and colleagues investigated the effects of porosity of a hyrdogel implant on its calcification (86-88). Homogenous hydrogels and porous hydrogels with a water content of less than 70% healed as normal with encapsulation with a thin fibrous capsule and no calcification was seen. Implants containing 70% water, or more were surrounded by a much thinner fibrous capsule and newly formed blood capillaries penetrated the implant. Mineralisation was attributed to the necrosis of cells penetrating the implant, the more porous the implant, the more extensive the effect. It would, therefore, seem appropriate to limit the water content of the polyHEMA matrices used in the present work to less than 70%. Hydrogels of high water content tend to be

mechanically weak, so this precaution is also advantageous in minimising the risk of structural breakdown of the device. Investigation into the removal of residual contaminants from polyHEMA crosslinked with ethylene dimethacrylate showed an unindentified compound leached from the matrix after some months (89). Brynda and colleagues suggested that the polymer matrix was being hydrolytically degraded. The unidentified degradation product produced no irritating response when tested intradermally on rats . It can be concluded that polyHEMA is a suitable candidate polymer for the design of implantable delivery devices. A macroporous network should allow both the delivery of macromolecules and any residual contaminants to be easily washed out of the network.

Biocompatibility, although critical is not the only aspect of a polymer which needs to be considered in controlled release applications. Mechanical strength of the polymer should be considered since a dangerous surge of bioactive agent could occur if the implant were to break up in vivo. It is also important to prevent interaction between the bioactive agent and polymer or any other constituent, such as buffers, which may be required for the incorporation of the bioactive agent. The bioactive macromolecule must be released in a biologically active form. Chemical

reactions between the bioactive agent and constituents of the monomer solution such as polymerisation initiators may bring about denaturation of an incorporated protein. The long term storage and sterilization of the device are also factors to be considered if the device is to be used surgically.

1.4 PROPERTIES OF HYDROGEL POLYMERS

A hydrogel is a polymer gel, hydrophilic in character which can imbibe water and retain a significant fraction of this water within its structure without dissolution of the polymer matrix (90). A variety of materials from plant and animal origin and synthetic polymeric materials may be classed as hydrogels. Three types of hydrogel have been defined (91).

(i) Non-ionic hydrogels

In non-ionic hydrogels, the matrix is formed by primary chemical bonds between chains of monomer, such as the hydrogels of poly 2-hydroxyethyl-methacrylate (polyHEMA), crosslinked with ethylene dimethacrylate (EDM).

(ii) Thermally reversible hydrogels

The matrix structure of thermally reversible hydrogels is held together by weak secondary forces, eg hydrogen bonding. The hydrogels of polyelectrolyte complexes such as poly vinlybenzyl trimethyl-ammonium chloride (Ioplex 101) and polystyrene sulfonate, are examples of thermally reversible hydrogels.

(iii) Novel microcrystal hydrogels

Novel microcrystal hydrogels contain discrete colloidal particles of microcrystals, such as gels of collagen, cellulose and nylon.

All three types of hydrogel have been utilised in biomedical applications, however, it is the synthetic non-ionic hydrogels, specifically polyHEMA crosslinked with EDM, which are relevant to the present work.

1.4.1 Synthetic non-ionic hydrogels

Most synthetic non-ionic hydrogels are made by the polymerisation of hydrophilic monomers. A number of monomers have been used for the synthesis of non ionic hydrogels, including the arcylamides, methacrylamides, N-vinyl lactams and the hydroxyalkyl acrylates and methacrylates, the most important of these methacrylate monomers

being hydroxyethyl methacrylate, which has the following structure (92).

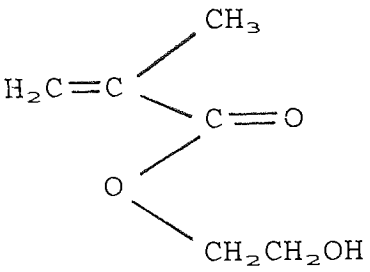

hydroxyethyl methacrylate. (HEMA)

Crosslinking agents are employed to hold the gel together, one of the most important, ethylene dimethacrylate, has the following structure (92).

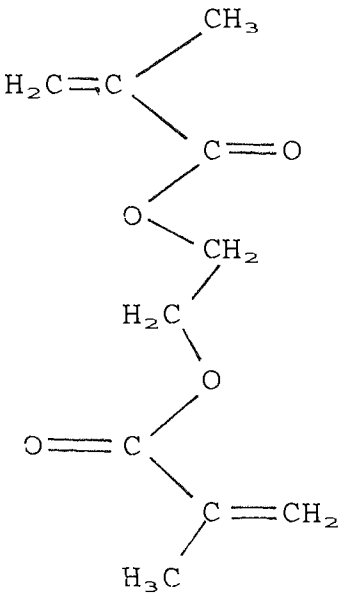

Ethylene dimethacrylate (EDM)

The present work utilised polyHEMA hydrogels, prepared by free radical polymerisation of HEMA monomer in the presence of the hydrophobic divinyl crosslinking agent EDM. A number of solvents have been used in the polymerisation of HEMA (93) although an aqueous

solvent, usually water or buffer, is most common if the polymer is intended for biomedical applications. The free radicals for the polymerisation reaction may be generated by chemical initiators such as ammonium persulphate and benzoyl peroxide, ionizing radiation or ultraviolet (UV) radiation in the presence of a photosensitive chemical. The kinetics of these polymerisation reactions have been discussed in detail by Peppas and Mikos (94). Throughout the course of this work polymerisation of polyHEMA crosslinked with EDM was effected using UV light with uranyl nitrate as the photoinitiator.

The choice and concentration of the solvent used in the polymerisation of polyHEMA determines whether the gel will be homogenous or heterogenous in nature. If HEMA monomer and crosslinking agent, such as EDM, is polymerised in a good solvent for both monomer and polymer (such as ethylene glycol or glycerine) an homogenous gel will result (90). If the monomer and crosslinking agent is polymerised in a poor solvent system for the polymer a heterogenous gel is formed. Since HEMA monomer is a good solvent for polyHEMA, if the concentration of water is less than about 45% (water is a non-solvent for polyHEMA) an homogenous gel will result (95). This critical concentration for water has been variously reported, ranging from

40 - 60% (95). The specific nature of the water within a hydrogel is one of its most important properties, related to the permeability, biocompatibility and the mechanical strength of the hydrogel.

1.4.2 Properties of synthetic, non-ionic hydrogels

In 1960, Wichterle and Lim indicated that polyHEMA was indifferent to biological materials and could withstand heat sterilization without damage (76). It is also known to be resistant to acid hydrolysis, resistant to reaction with amines (96) and, by extension of the data for a similar polymer, to incur alkaline hydrolysis only at high pH and temperature (97). One of the greatest advantages of polyHEMA over many other hydrogels, such as acrylamide, is its stability to varying conditions of tonicity, pH and temperature (98).

Hydrophilicity of a hydrogel, ie the affinity for water, is one of its most important properties since it is integrally related to the mechanical strength, permeability and biocompatibility of the polymer. Hydrophilicity is the result of the presence of hydrophilic groups (for example the hydroxyl groups in polyHEMA) on the polymeric chains and enables the swelling of crosslinked hydrogels when they are

equilibrated with water. The amount of water absorbed by a hydrogel can be expressed as the equilibrium water content (EWC) (98) and is represented by the equation:

$$EWC = \frac{\text{Weight of water in the hydrogel}}{\text{Total weight of hydrated hydrogel [at 20°C]}} \times 100\%$$

The EWC of a hydrogel is controllable, since it depends on the hydrophilicity of the polymer and the experimental conditions used in the preparation of the hydrogel. Water is a poor solvent for HEMA, about 45% miscible at room temperature and an EWC of approximately the same amount is expected for an homogenous polyHEMA hydrogel (99). The fact that water is a poor solvent for HEMA is thought to be the predominant factor controlling the EWC of the homogenous hydrogel and tends to overshadow other determinants which may influence the EWC of other hydrogels such as crosslinking density and initial dilution of the monomer (99). The EWC of homogeneous polyHEMA has been shown to be insensitive to the concentration of cross-linking agent in the range 0-4mol% and to vary little with changing temperature and pH (100,101).

The presence of some solutes in the hydrating medium may have some effect on the swelling behaviour of polyHEMA. For example, $NaClO_4$ causes an increase in the EWC compared to that obtained with pure water whilst NaCl and $NaSO_4$ cause a decrease (102,103). It

has been proposed, based on the insensitivity of the EWC of homogenous polyHEMA to the concentration of crosslinking agent and anomalous swelling behaviour in the presence of urea and other solutes (104), that a secondary, non-covalent structure exists within the polymer network. This secondary structure is proposed to consist of hydrogen bonded hydroxyl groups, stabilized by the exclusion of water molecules from the regions containing the bonds (104). Increased swelling, in response to a solute such as urea has been explained by assuming the breaking of the hydrophobic bonds in the polymer, whilst the deswelling effect of electrolytes such as chlorides and sulphates has been attributed to the ability of these electrolytes to decrease the solubility of polyHEMA segments in water (salting out effect) strengthening the hydrophobic bonds in the polymer (102).

The EWC of a hydrogel gives no indication of the various possible states in which this water may exist in the hydrogel and there has been some dispute as to the precise nature of this water. It has been suggested that the specific nature of the water within a hydrogel and the relative amounts of each type of water have a considerable bearing on the permeability and biocompatability of the hydrogel (105). A three-state model for the distribution of water within

hydrogels has been proposed (106) and determined experimentally (107), comprising, bound water (non-freezing), interfacial water (intermediate) and bulk water (free or freezing water). The bulk water is a free fraction, which does not take part in direct hydrogen bonding with the polymer. The bound water fraction is strongly associated with the polymer, bound by hydrogen bonding and the interfacial water is thought to represent a form of water intermediate between the two groups, indicating a continuum of water states between the bound water and water unaffected (bulk) by the polymer (108).

Hydrophilic solutes diffuse primarily by a 'pore flow' mechanism through the bulk water fraction of the hydrogel (109). The 'pore flow' mechanism is also a major means for the diffusion of hydrophobic solutes through hydrogels but these solutes will also diffuse by a 'partition mechanism' by associating with the bound and interfacial water and diffusing along polymer chains (110). Lee, Johon and Andrade (107) showed that a homogenous polyHEMA gel, made with 20% water contained mostly bound water, whilst the gel tested by these workers to have the most bulk water (free) was made with 50% water, a heterogenous hydrogel and these workers indicated that the amount of bulk water increased with increasing water content above 35-40%. The fraction of interfacial water

appeared to reach a maximum at about 12% of the total water. However, the way in which water is structured in homogenous polyHEMA has been disputed. Roorda and colleagues have indicated that it is unlikely that any bulk water can exist in a homogenous gel because of the small amount of total water within the polymer (111). These authors found no evidence for the structuring of water in polyHEMA gels made with 35% water and regarded the water to have a continuous distribution. This work however does not necessarily contradict the observations of either Lee et al (107) or Pedley and Tighe (108) since significant bulk water has only been found in heterogenous gels.

In contrast to homogenous polyHEMA, the EWC of heterogenous polyHEMA gels strongly depends on the amount of water present during the polymerisation reaction. The EWC of the polymer increases linearly with increasing initial monomer dilution (99). This dependance of the EWC is thought to be associated with increasing the bulk water fraction in a heterogenous gel when the amount of bound water has reached a maximum. Increasing the cross-linking density of a heterogenous gel decreases the EWC and is thought to increase the amounts of bound and interfacial water and to decrease the amount of bulk water in the polymer (112).

The surface characteristics of a hydrogel are important factors for consideration in terms of the biocompatibility of the gel; Chain mobility, ie the ability of the polymeric chains to rotate within the gel is an important parameter and Holly and Refojo have demonstrated that polyHEMA chains can undergo significant rotation (113). If the polymer surface is in contact with water, the hydroxyl groups are orientated out towards the water phase, in air, methyl groups are exposed due to the thermodynamic force which attempts to direct the system towards the minimisation of interfacial energy (114). Low interfacial tension between the hydrogel and biological fluid (eg serum, tissue fluid) is thought to reduce the tendancy of porteins to adsorb to the surface and to unfold on adsorption (115). Chain mobility also minimises the opportunity for multipoint attachment, thought to be required for protein adsorption (116). Minimal protein interaction between the hydrogel and the surrounding fluid may be important for the biological tolerance of the material since the denaturation of protein at foreign surfaces may serve as triggers for either the initiation of thrombosis or phagocytic attack (117). In vitro studies using whole blood and plasma have shown that proteins (fibrinogen, γ -globulin, haemoglobin, albumin) adsorb less readily to hydrogel than non-hydrogel surfaces and that the higher the water

content of the hydrogel the less protein is adsorbed (116,118). Protein also desorbs more easily from hydrogel surfaces, suggesting that proteins which are adsorbed are not tightly bound and are hence less likely to be denatured.

Heterogenous polyHEMA hydrogels have the advantage over homogenous polyHEMA in that they have a high water content (>40%) and hence the potential for good permeability and biocompatibility, however, their high water content gives them the disadvantage of poor mechanical strength. Ethylene glycol is a better solvent for the polymer than water and its addition to the monomer solution makes it possible to obtain homogenous gels with increased water content (119). The addition of a crosslinking agent such as EDM also allows more water to be tolerated by the system without phase separation occurring and gives the gels produced greater mechanical strength. However, these increased water content homogenous gels have no macroporous structure and the delivery of macromolecules through the bulk water of the polymer cannot be achieved.

One way of increasing the effective pore size of polymers, so as to allow the passage of macromolecules, is to polymerise the monomers around

a crystalline matrix that is subsequently dispersed or dissolved to leave an interconnected meshwork of macropores. Although the application of this technique to polyHEMA was noted by Haldon and Lee (24), the underlying principles have not been greatly explored nor its potential for the controlled delivery of macromolecules exploited. The significance of the technique for hydrophilic monomers lies in the fact that aqueous systems can be used to form ice-based crystalline matrices by rapid cooling of homogenous solutions of these hydrophilic monomers, offering the possibility of incorporating water soluble or dispersable macromolecules into the macroporous matrix for subsequent controlled release.

For the formation of macroporous polyHEMA polymers by this method of freeze-thaw polymerisation, the presence of EDM in the monomer solution is critical since it is only in the presence of the hydrophobic crosslinking agent that sufficient phase separation will occur on freezing to allow ice crystals to separate out, yielding the macroporous structure (24). The amount of EDM which can be tolerated by a HEMA monomer solution of various concentrations at room temperature has previously been established by Skelly (120) and is shown quantitatively in Table 1.3. The addition of ethylene glycol (EG) to the monomer solution allows more EDM to be dissolved without phase

separation of the monomer solution occurring. Increasing the temperature of the solution also enables more EDM to be dissolved, but a hot solution would undergo phase separation before freezing (120).

Table 1.3: Maximum concentrations of EDM which can be tolerated by HEMA:EDM systems, at various monomer: solvent ratios, without phase separation occuring at 22°C (120).

MONOMER:SOLVENT RATIO HEMA : H_2O	SOLVENT RATIO H_2O : EG	LOWEST MOLAR RATIO OBTAINABLE HEMA : EDM
30 : 70	100 : 0	96.6 : 3.4
40 : 60	100 : 0	95.0 : 5.0
50 : 50	100 : 0	93.6 : 6.4
60 : 40	100 : 0	92.0 : 8.0
30 : 70	80 : 20	95.5 : 4.5
40 : 60	80 : 20	94.1 : 5.9
50 : 50	80 : 20	90:0 : 10.0
60 : 40	80 : 20	86.9 : 13.1

Phase separation of the monomer mixture before freezing would result in a non-homogenous mixture of monomer solution constituents. However, the absence of phase separation before feeezing will allow bioactive macromolecules to be incorporated into the macroporous polymer via the aqueous phase of the monomer solution in an homogenous mixture. This will ensure an even distribution of the macromolecule whilst allowing macroporous hydrogels of high water

content and acceptable mechanical strength to be fabricated. A number of factors may govern the porosity and permeability of hydrogels to bioactive macromolecules. These and other factors which may affect the rates of release of incorporated macromolecules such as peptides have been considered below:

1.5 FACTORS WHICH HAVE THE POTENTIAL TO AFFECT THE RATE OF RELEASE OF MACROMOLECULES FROM MACROPOROUS POLYHEMA HYDROGELS.

Factors which may influence the rate of release of an incorporated macromolecule from macroporous polyHEMA are related to the physical and chemical nature of the matrix polymer, the type and properties of the incorporated macromolecule and possibly the character of the environment into which the macromolecule is released.

An important parameter which may govern the rate of release of an incorporated macromolecule is the size and direction of the pores in the polymer matrix. Pore size in homogenous polyHEMA is essentially a theoretical concept. There are no true, discrete pores, only a randomly fluctuating system of hydrated polymer chains. Diffusion of solutes occurs across homogenous polyHEMA along and between the hydrated polymer chains, only by relatively small molecular weight substances. Large, discrete pores must be generated in the polymer matrix to allow the passage of macromolecules (MW>1500). Using the technique of

freeze-thaw polymerisation, Haldon and Lee obtained the most porous films by employing rapid cooling, spreading the monomer solution on a plate which had been pre-cooled to -60°C (24). When the resulting film was compared with a slowly cooled film, in which the monomer solution was spread onto the plate at room temperature and subsequently cooled to -60°C, it was found that the pores were small and random in nature. The rapid cooling process yielded unidirectional pores at right angles to the surface of the membrane. Increasing the proportion of monomer in the monomer solution led to the production of films with fewer, smaller pores and a lower EWC than films of a lower monomer concentration. The diffusion rates through the films were reduced, hence the higher the monomer concentration the lower the permeability of macroporous polyHEMA:EDM films as illustrated in Figure 1.1 below:

Figure 1.1: The effect of monomer concentration on the permeability coefficient (K) of a macroporous polyHEMA film (EDM 15.5% fast frozen) (24).

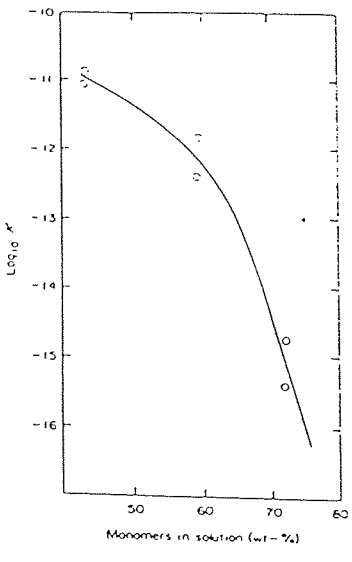

Skelly (120) confirmed these observations for macroporous HEMA:EDM films made by freeze-thaw polymerisation, reporting a decrease in EWC from 56% at a monomer:solvent ratio of 45:55 to an EWC of 36.5% at a ratio of 68:32 (solvent, EG:H_2O ratio 1:4, HEMA:EDM 90:10). The EWC of HEMA:EDM prepared in this way is not directly proportional to the water content of the monomer solution, since, for comparable freezing conditions, ice will separate from different solution concentrations at different temperatures (24). Measurement of the EWC provides a good indication of the permeability of a hydrogel since most solutes diffuse by pore flow, through the bulk water of the polymer (109) and the bulk water fraction increases with increasing water content (107).

The amount of crosslinking agent used may also affect the rate of release of an incorporated macromolecule. The effect of crosslinking agent on the permeability of macroporous HEMA:EDM fabricated by freeze-thaw polymerisation differs from the effect it has on homogenous and non-macroporous heterogenous HEMA:EDM polymers. Increasing the crosslinking density leads to a decrease in the permeability of HEMA:EDM gels not fabricated by freeze-thaw polymerisation (121). This is thought to be due to a reduction in polymer chain mobility and average 'pore size' and a reduction in

the amount of bulk water in the polymer (122). However, in macroporous HEMA:EDM, the permeability of the hydrogel increases with increasing EDM content up to a value of 10% EDM, but beyond 10% EDM the permeability remains fairly constant (24). The presence of EDM in the monomer solution is critical for sufficient phase separation to occur on freezing to allow the formation of the crystalline ice matrix leading to the production of macropores. At very low EDM concentrations, no macropores are formed. However, ice can separate more easily from solutions of high EDM content due to the hydrophobic nature of EDM, hence, increasing the amount of crosslinking agent increases the macroporous nature of the hydrogel. This effect becomes limiting at a 10% concentration of EDM. There is, however, no effect of increasing the crosslinking agent concentration on the EWC (24,120).

The amount of ethylene glycol in the solvent phase of the monomer solution has also been shown to affect the permeability of macroporous HEMA:EDM. Increasing the ethylene glycol content of the solvent leads to a decrease both in the permeability and EWC of the film. Increasing the H_2O:EG ratio results in a lower freezable content of the solvent (effectively reducing water content) and also results in a slower rate of

cooling which also leads to a decrease in the permeability of the hydrogel (24). However, the presence of ethylene glycol, at a ratio of 1:4 in the solvent phase is required to allow sufficient EDM (10%) to be dissolved in the monomer solution for the production of a good macroporous structure (Table 1.3, Page 57). It can be concluded that an optimum formulation for the production of macroporous polyHEMA:EDM would contain 10% EDM, an ethylene glycol:water ratio of 1:4 and that the main factors controlling the macroporosity of the matrix are the rate of freezing and the monomer:solvent ratio.

The level of loading of the macromolecule into the polymer via the aqueous phase of the monomer solution may also affect the rate of release of the bioactive agent. It might be expected that higher loading levels would give greater release rates, simply due to the presence of more bioactive agent within the matrix. However, since the macromolecule is to be loaded into the polymer via the solvent phase, the effects of the macromolecule on the formation of ice crystals and hence pore formation must be considered. High levels of bioactive agent may cause a significant decrease in the freezing temperature of the solvent, resulting in the production of fewer, smaller pores due to a reduced freezing rate.

The geometry of the fabricated device is another factor to be considered with regard to the rate of release of macromolecules. Most matrix-type release devices have been designed as rectangular films or slabs and it has been established that the cumulative release of the bioactive agent is inversely proportional to the square root of time (123). Zero-order release rates are not obtained because of the rapid decrease in the concentration gradient of the bioactive agent with time. The surface area of a film is large and bioactive agent associated with the surface of the film is released first. With time, however, decreasing amounts of bioactive agent are available in the interior of the film and this must diffuse a greater distance prior to being released, hence reducing the release rate (3). A spherical, or bead-shaped device may give release rates approaching zero-order, at least in the early stages of release, since the surface area to volume ratio is reduced from that of a film. Various geometries have been investigated in an attempt to obtain zero-order release rates, including spheres, cylinders and biconvex shapes (124,125). However, alteration of the shape of the device alone has been unsuccessful in obtaining zero-order release rates. The ease of fabrication of a device is an important consideration and simple geometries are likely to be more easy to fabricate than complex shaped devices.

Zero-order release rates from a polymeric device are more easily achieved by the employment of a diffusion rate limiting barrier surrounding the polymer. Lee and colleagues used a highly crosslinked coating of EDM, which had a much lower permeability to solute than the central HEMA or methoxyethoxyethyl methacrylate (MEEMA) matrix (126). These authors demonstrated zero-order release from rod-shaped devices with this highly crosslinked coating. A number of bioerodible and biodegradable polymeric formulations could be considered as coatings to provide an additional rate limiting barrier to the diffusion of macromolecules from a macroporous polyHEMA:EDM device. Polymers which could be considered include poly glycolic acid, poly lactic acid and their copolymers poly hydroxybutyrate and other hydrolytically unstable polymers. Inert polymeric coatings are unlikely to be of use in the controlled delivery of macromolecules since macromolecular diffusion could not occur through the coating. Hsieh, Rhine and Langer utilised both geometrical and coating approaches to produce a hemispherical shaped device, covered in an impermeable coating, except for a small cavity cut into the centre of the flat surface (123). This device was reported to give zero-order release of bovine serum albumin for up to 60 days.

The nature of the incorporated macromolecule itself will exert some influence on the rate of release obtained. Wisniewski and Kim found that for hydrophilic non electrolytes and inorganic chloride salts, with a molecular weight in the range 20 - 500, the diffusion rate decreased exponentially with increasing molecular weight in a HEMA gel containing 45% water and 1 mol% EDM (109). However, Langer and colleagues found no simple relationship between the rate of release of a macromolecule from ethylene vinyl acetate copolymers and the molecular weight of macromolecule (12-14). Refojo and Leong investigated the permeation of macromolecules into 'microporous' polyHEMA and other hydrogel membranes (127). It was found that an FITC-linked dextran with a molecular weight of 150,000 (smallest radius 19Å) was capable of some penetration into a polyHEMA film with a 41.05% water content, whereas, bovine serum albumin (MW 69,000, smallest radius 50Å) did not penetrate the hydrogel. It was suggested by the authors that it is the molecular radius of the macromolecule, rather than its molecular weight which might be important in the diffusion of macromolecules through hydrogel matrices.

The solubility of a macromolecule in the medium hydrating the polymeric vehicle will also be a factor in dictating the rate of release of the macromolecule. A molecule with low solubility in the release medium

will be released at a much slower rate than one with good solubility. If the incorporated macromolecule has a very low solublity, its release rate will tend to be more dependant on its rate of dissolution into the release medium than on the nature of the polymeric matrix in which it is contained (128). Any interaction between the macromolecule and the polymer would also need to be considered when investigating the factors which may affect release rates. For example, it is known that proteins can adsorb to the surface of polyHEMA, although the higher the water content of the hydrogel the less protein is adsorbed (116,118).

Environmental conditions surrounding the polymeric device may also influence release rates. The pH of the release medium may exert an influence on the solubility of the macromolecule and hence its release rate (129). It is possible that the alteration in EWC caused by certain solutes such as chloride or acetate anions (102,103) may also influence the rate of release of an incorporated macromolecule. Physical environmental conditions such as temperature and agitation also have the potential to influence the rate of release of an incorporated macromolecule due to affects on the diffusion rate of the macromolecule. Agitation of the environmental medium can lead to an

increased solvent flow through the polymer and hence may lead to an increased rate of release while increasing the incubation temperature may lead to an increased rate of diffusion of the macromolecule.

1.6 AIMS OF THIS WORK

The present work sets out to utilise a representative, biocompatible hydrogel, polyHEMA, with a view to its use in the fabrication of a vehicle for the controlled delivery of biologically active macromolecules, particularly peptides of therapeutic interest. It is intended to develop a system, using novel polymer design and fabrication technology to generate macroporous bead formed polymer based delivery systems with variable, but controlled release properties. The bioactive macromolecules at which this work is principally aimed are the clinically significant peptides, produced in increasing number, quantity and specific activity by the biotechnology industry. These macromolecules are generally so prone to thermal and hydrolytic instability that the use of a conventional techniques to bring about incorporation into a polymeric matrix is not feasible.

The formation of macroporous polyHEMA matrices, by the freeze-thaw technique (24) consists, in principle of freezing the monomer solution to create a system which

consists of a solid (frozen) monomer matrix around and between solvent crystals. This monomer matrix is polymerised and the solvent subsequently removed by thawing. For successful development of macroporosity it is essential that phase separation of the monomer solution does not occur before ice crystallization takes place. The presence of EDM in the HEMA monomer solution will allow sufficient phase separation to occur on cooling to allow ice crystals to separate out, yielding a macroporous structure. Ethylene glycol is added to the aqueous phase of the monomer solution at a ratio of 1:4 to allow the incorporation of an optimum amount of EDM (10%) in the monomer solution without phase separation occuring (120). Photopolymerisation of the polymer will be carried out using the photoinitiator uranyl nitrate and UV radiation.

The first objective of this study will be to develop and ascertain the practical requirements of a reproducible method for the production of macroporous polyHEMA bead formed vehicles. The main requirement for the formation of macroporous polyHEMA beads is the maintenance of frozen monomer droplets in a non solvent phase until polymerisation is complete. Hexane at a temperature of -70°C will be used as the non-solvent phase throughout the course of this work. The effect of the delivery speed of the monomer

solution to the surface of the hexane and the effect of the stirring speed of the hexane will be investigated with respect to the yield, size distribution of the product beads and the reproducibility of the process. The method of bead production will be scaled up to produce large quantities of beads with well defined physical and chemical characteristics. The ultrastructure of all beads produced will be examined and pore size measured by scanning electron microscopy and the EWC of all beads produced will be routinely monitored. These characterisation procedures will be conducted to test the effects of the alteration in solvent composition and content on the nature of the macropores and the hydrophilicity of the macroporous polyHEMA beads.

Since the biologically active macromolecules to be incorporated into the bead form vehicles are hydrolytically unstable and sensitive to pH they must be incorporated into the monomer solution in physiological buffers. A number of buffers will be used as the aqueous proportion of the solvent phase and their impact on the homogeneity of the monomer solution, polymer bead size distribution and yield, EWC and macropore size and structure will be evaluated.

In order to determine whether the polyHEMA bead formed matrices contain any leachable toxic contaminants such

as uranyl nitrate, hexane or unreacted HEMA monomer, which might influence their future use as implants in animals and man, the cytotoxicity of the beads will be examined using cell culture testing of polyHEMA bead eluates.

Initial studies involving the incorporation of macromolecules into macroporous polyHEMA beads will involve the incorporation of an easily monitored surrogate protein macromolecule, bovine serum albumin (BSA). The macromolecule will be loaded into the macroporous matrix by incorporation in the aqueous phase of the monomer solution. Release of BSA will be monitored over an extended time period. The effect of freeze drying as opposed to air drying BSA loaded beads on the subsequent rate of release of protein will be investigated with a view to establishing the subsequent means of future storage of the bead formed matrices. The effect of agitation on the rate of release of BSA will also be investigated to determine the extent to which the external environment influences the rate of release of a macromolecule from this type of macroporous hydrogel matrix. The effect of the molecular weight of an incorporated macromolecule on its subsequent rate of release will be examined using a relatively low molecular weight (MW 17,500) and a high molecular weight (MW 148,900) FITC-linked dextran. These FITC-linked dextrans were

selected for use as surrogate macromolecules since they are available with a range of molecular weights and their concentration can be reliably monitored by direct spectrophotometry. The influence of the mean diameter of the bead formed vehicles on the rates of release of FITC-linked dextrans will be investigated in order to establish if the surface area to volume ratio of the device is an imporant parameter affecting the release of an incorporated macromolecule. In addition, the temperature at which the FITC-linked dextran loaded matrices are incubated will be varied to examine the influence of environmental temperature on the rates of release.

The first biologically active macromolecule to be incorporated into macroporous polyHEMA vehicles will be the enzyme, glucose oxidase (GOD). This enzyme was selected for study since its assay, by its very nature depends on the biological activity of the macromolecule and hence, only enzyme released from the polymer vehicle in a biologically active form will be measured. The influence of the diameter of the bead formed matrices on the rate of macromolecule release will be further investigated by monitoring the release of GOD from beads in the size range 355 - 500μm and 500 - 1000μm. The first clinically useful macromolecule to be incorporated into polyHEMA bead formed devices will be interleukin-2 (IL-2). The

polypeptide cytokine will be assayed using the IL-2 dependant cell line CTL-L2 and hence only cytokine which has remained biologically active on incorporation and release from the polyHEMA matrices will be assayed. The effect of bead diameter of the rate of release of IL-2 will also be further examined.

In order to investigate more closely the possibility of releasing a clinically important, hydrolytically unstable macromolecule, bovine insulin will be incorporated in neutral buffered solution and its rate of release monitored over an extended period. Three loading levels of insulin (0.4, 0.02 and 0.004% of polymer weight) will be incorporated to establish the effect of percentage loading of the macromolecule on its rate of release. The influence of the environmental conditions of incubation temperature and agitation of the incubation medium and the effect of the presence of a preservative in the incubation medium on the rate of insulin release will be examined. Studies will be carried out aimed at controlling the rate of release of insulin from polyHEMA bead formed matrices by manipulation of the ratio of monomer to solvent in the monomer solution. Insulin release from polyHEMA beads will routinely be measured by radioimmunoassay. However, the immunoreactivity of the insulin molecule is not necessarily indicative of its biological activity.

In order to estimate the biological activity of the insulin released from the polyHEMA vehicles the concentration of biologically active insulin in the incubation medium will be determined using an assay which measures the insulin stimulated rate of D-[U^{14}C]-glucose oxidation to $^{14}CO_2$ using isolated pieces of rat epididymal fat pad.

CHAPTER 2

GENERAL MATERIALS AND METHODS

2.1 MATERIALS

2.1.1 Animals

Male Wistar rats, 150 - 200g, fed ad libitum were used in insulin bioassay studies.

2.1.2 Sources of Chemicals

Reagents of analytical grade and double distilled water were used throughout this work unless otherwise stated. The principle chemicals, tissue culture plastic and sundries used and their sources were as follows:-

Interleukin-2 was a gift from Biotest-Folex Ltd. UK, (obtained by N.I.B.S.C., South Mimms, Herts - UK). 2-hydroxyethyl methacrylate, ethylene dimethacrylate, ethylene glycol, trichloroacetic acid and 95% (v/v) ethanol were supplied by BDH Chemical Ltd., Poole, Dorset - UK. Bovine insulin (0.5% zinc), bovine serum albumin (Fraction V) fluorescein isothiocyanate linked dextrans, 4, 4'dicarboxy 2,2' biquinoline, disodium salt (BCA-NA_2), glucose oxidase, peroxidase, o-dianisidine and ß-D-glucose were purchased from Sigma Chemical Co Ltd., Poole, Dorset - UK. Monocomponant porcine insulin was supplied by Novo Research Institute, Novo Laboratories Limited, Basingstoke, Hampshire - UK, whilst anti-porcine insulin guinea-pig serum and ^{125}I labelled porcine insulin was supplied by Novo Biolabs, Novo Research Institute, Novo Laboratories Ltd.,Bagsraerd,Denmark. Insulin binding reagent and human insulin standards

were purchased from Wellcome Reagents Ltd., Wellcome Research Laboratories, Beckenham - UK. D-(U-^{14}C)-glucose and $Na^{125}I$ were supplied by Amersham International Plc, Aylesbury, Buckinghamshire - UK and NE260 scintillant was obtained from Nuclear Enterprises Ltd., Sighthill, Edinburgh, Scotland - UK. Pencillin-streptomycin (5000 1U/5000µU/ml) solution, foetal calf serum and Earle's minimum essential medium (modified) with Earle's salts and non-essential amino acids (powder) were supplied by Flow Laboratories, Irvine, Scotland - UK. Trypsin (0.05% w/v)/EDTA(0.02% w/v) solution, 50ml tissue culture flasks, vented petri dishes (60 x 15mm) and 1.2ml cryo-ampoules were supplied by Gibco Life Technologies Incorporated, Paisley, Scotland - UK. 200ml Costar tissue culture flasks were obtained from Northumbria Biologicals, Cramlington, Northumberland - UK. Sterivex-GS 0.22µm filter units with filling bell were obtained from Millipore UK Ltd., Harrow, Middlesex - UK and LP3 tubes from LIP Ltd., Shipley, West Yorkshire - UK. G50 Sephadex was supplied by Pharmacia Ltd. Central Milton Keynes, Bucks. - UK.

Uranyl nitrate hexane, chloramine-T, sodium metabisulphite and other chemicals, used in the preparation of buffers were all obtained from Fison's Plc, Loughborough, Leicestershire - UK.

2.2 THE PRODUCTION OF MACROPOROUS POLYHEMA BEADS

2.2.1 The Purification of HEMA monomer

HEMA monomer was supplied containing 0.02% (w/v) 4-methoxyphenol to prevent the polymerisation of monomer during storage. Prior to the bench manufacture of polyHEMA beads, the monomer was purified in small quantities by vacuum distillation using the apparatus shown in Plate 2.1 below:

Plate 2.1 The vacuum distillation of HEMA monomer

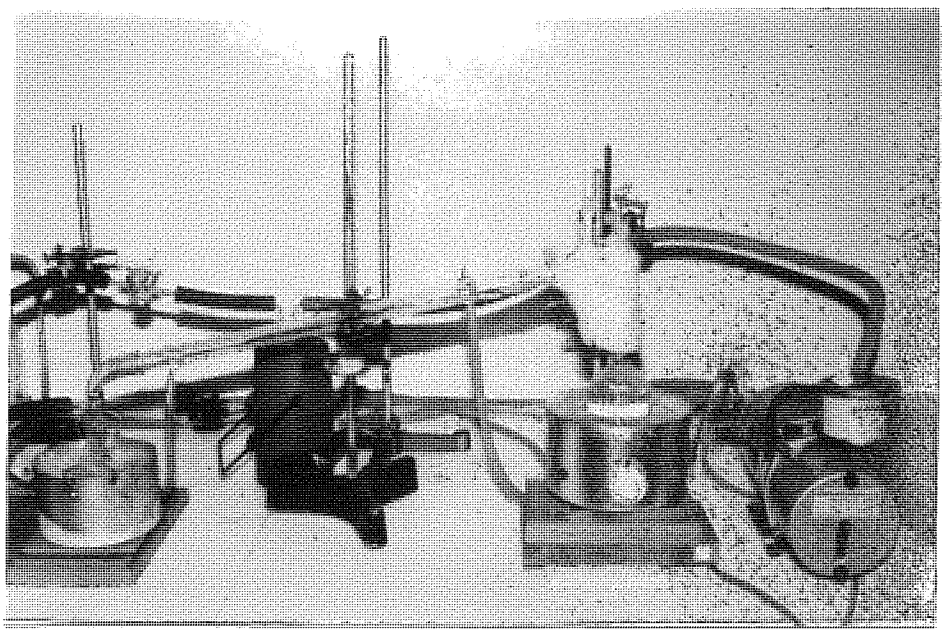

200ml of HEMA monomer was placed in the round bottomed flask, fitted with a fine air bleed and a small amount of copper chloride was added to prevent the polymerisation of the monomer under the influence of heat. Distillate was collected over ice, using an ice/salt bath. The vacuum pump was protected from distillate by employing a cold trap in series, utilising solid CO_2/acetone.

The HEMA monomer was distilled at a temperature of approximately 90°C and a small stream of air passed through the HEMA whilst retaining the vacuum at around 5mmHg. Higher temperatures resulted in polymerisation of the monomer. In some cases, distillate condensed in the neck of the distillation flask, causing it to reflux back into the impure monomer. To avoid this, the neck of the distillation flask was insulated with glass wool to maintain the distillation temperature. After distillation, purified monomer was decanted into a dark bottle to avoid polymerisation under the influence of ultra violet (UV) light and stored at 4°C until required.

2.2.2 Optimum bench process for the fabrication of polyHEMA beads

Macroporous beads used in this work were generated by freeze-thaw polymerisation. Beads were fabricated using the monomer 2-hydroxyethyl methacrylate

(HEMA),crosslinked with hydrophobic ethylene dimethacrylate (EDM) which facilitated the heterogenous dispersal of water throughout the polymer. The method of bead production described below represented the optimum bench system for the fabrication of beads containing a monomer: solvent molar ratio of 50:50. The experimental procedures leading to the development of this system have been described in Chapter 3 (Pages 155-182).

The quantities of each constituent in the monomer solution used to manufacture one batch of polyHEMA beads with a monomer:solvent ratio of 50:50 and a water: ethylene glycol ratio of 4:1 is shown in Table 2.1. For experimental work the production of a x4 batch of polyHEMA beads was often the most convenient and economical. The optimum bench system was used for the production of all polyHEMA beads loaded with macromolecules.

Table 2.1: Constituents of the monomer solution for the fabrication of polyHEMA beads with a 50:50 monomer:solvent molar ratio

Constituent	Weight (g)
HEMA	10.035
EDM	1.526
ETHYLENE GLYCOL	2.312
WATER	9.249
URANYL NITRATE	0.251

10.035g of HEMA was mixed with 1.526g of EDM and these were added to the solvent phase, comprising 9.249g of water and with 2.312g of ethylene glycol. 0.251g uranyl nitrate (2%) was then added to the solution as a photoinitiator. The addition of the monomer solution constituents in this order avoided any phase separation. The monomer solution was filtered and transferred to the reservoir, seen to the left of the apparatus shown in Plate 2.2.

Plate 2.2. The optimum bench system for the fabrication of polyHEMA beads.

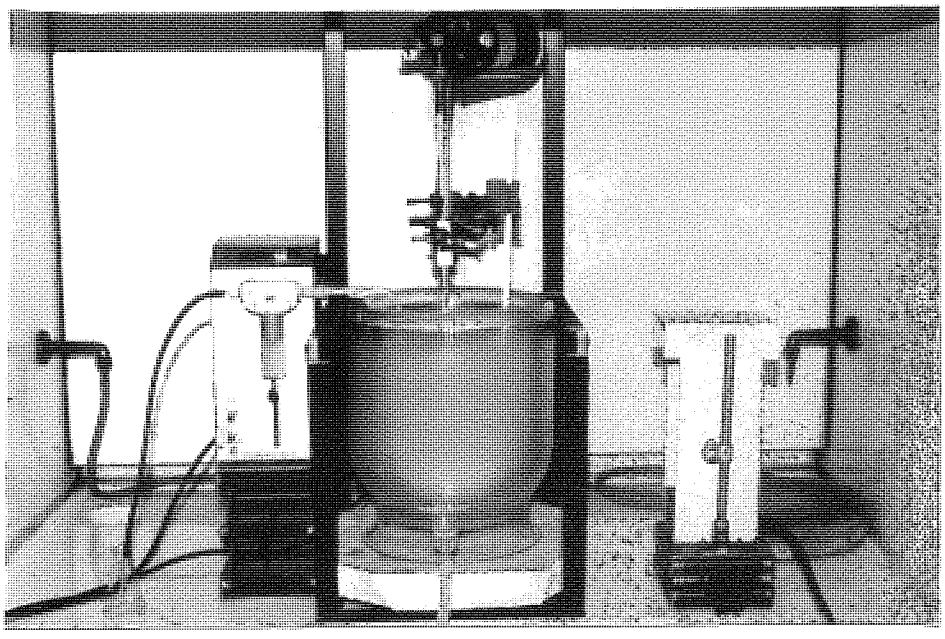

The main criterion for the production of macroporous polyHEMA beads by the freeze-thaw polymerisation process is the maintenance of frozen monomer beads in suspension in a non solvent phase until polymerisation is complete. The bench system used for the production of bead formed matrices was set up in a fume cupboard and is shown in Plate 2.2.

The central 5L dewar flask contained the non-solvent phase, hexane, cooled to a temperature of -70°C by the addition of powdered carbon dioxide. Care was taken during this addition to prevent excess effervescence of the hexane since this caused spillage and deformation of beads produced due to turbulence. The hexane was stirred with an anchor shaped glass paddle using a Citenco stirrer motor (Type KQPS/21, 200-250V, 60W) set at a stirring speed of 300 rpm, as measured with the use of a stroboscope.

The monomer solution was delivered to the surface of the hexane, via a polyethylene catheter (Plate 2.3) using a Brand Multispenser automatic dispenser.

Plate 2.3. Proximity of the delivery nozzle to the surface of the hexane.

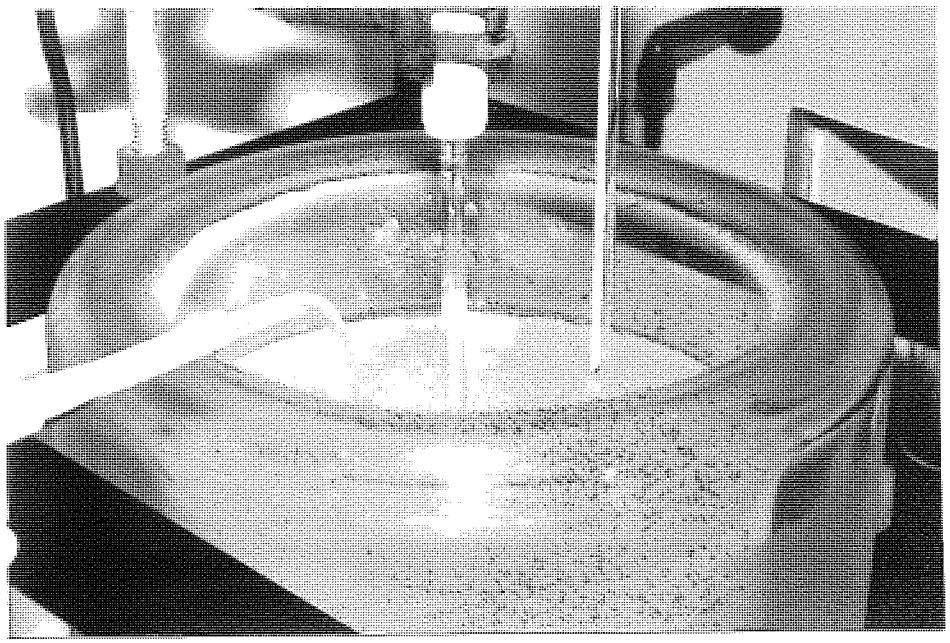

A delivery speed of 9.8ml/sec (Speed IV) was found to be optimum for the fabrication of beads at a stirrer speed of 300rpm. Polymerisation of the suspended frozen beads was carried out with a compact high energy UV light source (250W, 250V, 3-pin glass type

Osram GEC ME/D). The temperature of the hexane was checked periodically, since it tended to rise during the 1½ hour polymerisation time due to the heat generated by the UV lamp. Immediately after use, the delivery system was thoroughly flushed through with x2 distilled water, and the flow directed to a waste reservoir, in order to remove any residual monomer solution remaining in the dispenser which might subsequently polymerise and cause blockage.

After a period of 1½ hours, polymerisation was judged to the complete. The resultant polyHEMA beads were harvested by draining off the hexane from the base of the dewar, via the spring loaded tap. Beads were collected in a fine mesh sieve (100μm) and the hexane was filtered and stored for subsequent reuse. The resultant beads were washed thoroughly in x2 distilled water to remove contaminants such as small particles of dry ice, ethylene glycol, residual uranyl nitrate and hexane. The beads were then freeze dried overnight at -65°C and 0.2 atmospheres, using an Edwards 4K Modulyo freeze-drier. The freeze-dried dehydrated beads were white in colour and of good spherical shape.

The size range of the freeze dried dehydrated beads was established using stacked Endicott sieves of varying mesh sizes (1700 - 106μm). The beads

FIGURE 2.1: Typical mean bead size distribution obtained using the optimum bench system, expressed as the percentage dry weight of the total bead yield (Mean values ± SEM, n=10).

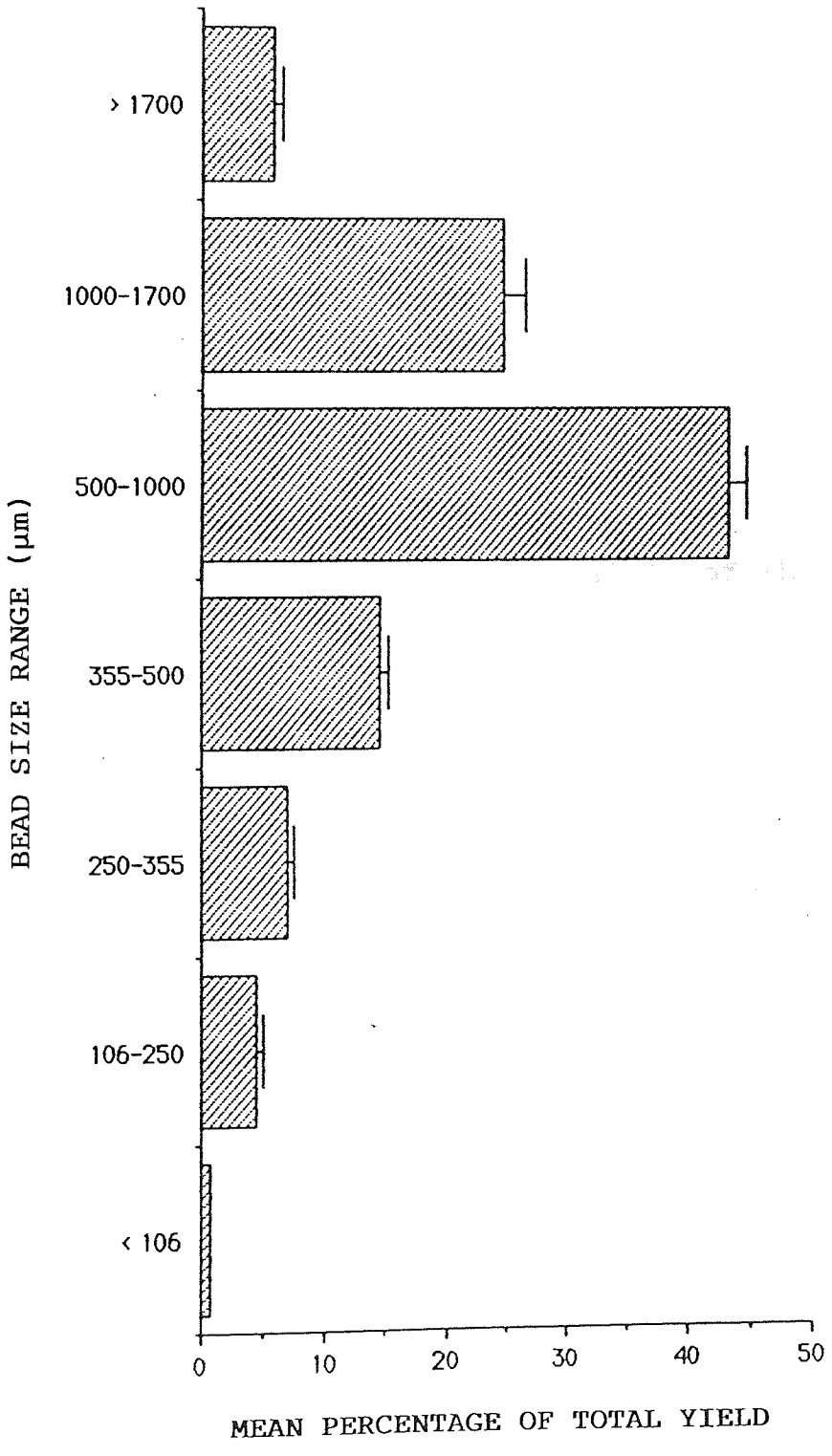

retained in each sieve were weighed and the percentage, by weight, of the total yield of beads determined. The typical size distribution of the beads produced, expressed as a percentage of the total yield of beads and fabricated using a monomer:solvent ratio of 50:50 is shown in Figure 2.1. The largest proportion of beads separated in the 500 - 1000μm size range.

The mean total bead yield obtained in each batch was calculated, using the following equation:-

$$\frac{\text{Total weight of beads produced}}{\text{Total weight of monomer used}} \times 100\%$$

The mean total bead yield was 76.79% ± 3.75% (n = 10).

The equilibrium water content (EWC) of the polyHEMA beads was routinely established, by determining the hydrated weight of a sample of beads, which had been rehydrated in x2 distilled water for seven days, then drying them to constant weight at room temperature and re-weighing. The EWC was then calculated using the equation below:

$$EWC = \frac{\text{Weight of water in beads}}{\text{Total weight of rehydrated beads}} \times 100\% \text{ (at 20°C)}$$

The mean EWC of unloaded polyHEMA beads, fabricated using a monomer:solvent ratio of 50:50 was found to be 60.02 ± 0.13% (n = 15).

The internal ultrastructural morphology and the external topography of polyHEMA beads was determined by scanning electron microscopy (SEM), using freeze dried beads mounted on stubs and coated with a gold electron conducting coating. Samples were stored in a vacuum desiccator, over silica gel and only removed just prior to examination, over a magnification range of X100 - X5000. Black and white photomicrographs taken and examined for the presence and distribution of macropores.

2.2.3 The loading of surrogate and clinically significant macromolecules into polyHEMA beads.

Macromolecules were loaded into polyHEMA beads by dissolving the required macromolecule in the water or buffer component of the aqueous phase of the monomer solution. This was carried out immediately prior to mixing the components of the monomer solution for subsequent bead fabrication in order to minimise the possibility of degradation of the macromolecule. The percentage loading level of the macromolecule was expressed as a percentage of the dry weight of polymer used, assuming 100% incorporation. Fabricated beads loaded with macromolecule were washed for either 5 or 10 minutes in x2 distilled water. The wash time was kept constant in order to try and standardise any loss of macromolecule from the surface of the beads.

2.2.4 Release monitoring protocol.

Generally beads from a number of batch productions were pooled for use in release experiments. A unit weight of 1g of dehydrated beads was used for release studies with an incubation volume of 10ml of either x2 distilled water or buffer. Before setting up the release experiment the small amount of incubation medium required for the complete rehydration of 1g of the appropriate beads was calculated using the known EWC as shown below. This allowed for the 'dead volume' of water within the beads and ensured that the amount of incubation medium in contact with the beads and available for sampling remained at 10ml. This water of rehydration was added to the incubation of volume on the first day of the release experiment.

$$\text{Water of rehydration} = \text{Wet weight of beads} - \text{Dry weight of beads}$$

$$\text{Wet weight of Beads} = \frac{\text{Dry Weight}}{1 - \frac{\text{EWC}}{100}}$$

1g of dehydrated beads, loaded or unloaded, were inserted into each of a number of 25ml siliconised flasks. The flasks were siliconised in order to minimise the adsorption of the macromolecule to the glass. 10ml of water or the appropriate buffer (plus water of rehydration on the first day) was added to each of the flasks. The flasks were sealed to avoid water loss through evaporation and maintained at either 4°C, 37°C or room temperature, under static or agitated conditions.

After 24 hours incubation, a sample of the medium was transferred to an LP3 tube and immediately frozen for subsequent assay. The remainder of the medium was aspirated off and discarded. The flasks containing beads were then replenished with 10ml of fresh incubation medium. This routine sampling and replacement was continued daily throughout the course of the experiments. This procedure was selected as the standard method of monitoring the release kinetics of macromolecules, to provide 'sink' conditions of release as far as possible and to limit the possibility of microbial contamination of the released macromolecule in solution.

Cumulative profiles for the release of each macromolecule were constructed by summating the amount of macromolecule released per day, per 10ml of incubation medium per gramme of beads. Approximation of the cumulative rate of release of the macromolecule to zero order kinetics was computed using linear regression. The proportion of the total loading released over the time period of the experiment, expressed as a percentage of the total load was then computed and recorded alongside each release profile constructed.

Changes in the size distribution, EWC or ultrastructure of beads, caused by the incorporation

of a specific macromolecule have been discussed in the appropriate section. Bovine serum albumin, the first surrogate macromolecule to be used was incorporated via the water portion of the solvent phase of the monomer solution. FITC-linked dextrans needed to be buffered both during incorporation and during release studies since their absorbance maxima were affected by changes in pH. Glucose oxidase, insulin and interleukin-2, biologically active macromolecules, required buffering at physiological pH7.4. Both glucose oxidase and insulin were incorporated using a 0.01M sodium acetate/0.12M sodium chloride buffer pH7.4, while interleukin-2 was incorporated using a 0.01M phosphate buffer.

2.3 DETERMINATION OF BOVINE SERUM ALBUMIN CONCENTRATION USING BICINCHONINIC ACID

The bicinchoninic acid (BCA) method of protein determination (130) was used for the assay of BSA in preference to the Folin-Lowry method (131). This was because the BCA method has been found to accurately detect the presence of protein at much lower concentrations than the Folin-Lowry method, ie. 0.5 µg/ml compared with 40 µg/ml minimum detection point for the Folin-Lowry method (130). The BCA method is also reputed to be unaffected by a non-ionic detergents and some simple buffer salts which interfere with the colour reaction in the Folin-Lowry assay. In addition, the instability of the

Folin-Ciocalteau reagent in alkaline solution demands that exacting technique be exercised in the timing of both reagent addition and mixing with the sample in order to obtain accurate results. The assay response is also known to fall considerably upon storage of the working Folin-Ciocalteau reagent and fresh reagent must be prepared daily. In contrast, the BCA reagent is stable for at least one week at room temperature and the stability of the chromaphore in the reaction allows for a simple, one step analysis and flexibility in protocol selection.

In the form of its water soluble sodium salt, BCA is a sensitive, stable and highly specific reagent for cuprous ion CU^{1+} , forming an intense purple complex with Cu^{1+} in an alkaline environment. This colour generation forms the basis of an analytical method, capable of monitoring the amount of Cu^{1+} produced when the peptide bonds of a protein complex with alkaline Cu^{2+} (biuret reaction). The purple colour produced from the BCA reaction is stable and its intensity at 562nm increases proportionally over a broad range (0.5 - 1200µg/ml) of increasing protein concentrations (130).

The incubation temperature chosen for colour development in the standard BCA assay depended upon the concentration of BSA judged to be present in the

test sample. For the determination of protein concentrations in the range 100-1200µg/ml a "standard protocol" was used. When lower BSA concentrations were to be assayed (5-250µg/ml) a "standard microprotocol" was selected. Extremely dilute BSA solutions, 0.5-10µg/ml could be assayed using a "microassay" which employed more concentrated reagents than in the standard assays.

2.3.1 Preparation of reagents for BCA protein assays

(a) "Standard protocol" and "Standard Microprotocol" reagents

Reagent A: consisted of solution of 1% BCA-Na_2, 2% Na_2CO_3 .H_2O, 0.16% $Na_2C_4H_4O_6$ 0.4% NaOH and 0.95% $NaHCO_3$ in deionised water. When required, 50% NaOH was added to adjust the pH to 11.25.

Reagent B: consisted of 4% $CuSO_4.5H_2O$ in deionised water.

Standard working reagent (SWR): was prepared by the addition of reagent A to reagent B at a ratio of 50:1 (vol/vol).

(b) "Microassay" reagents

Micro-reagent A (MA); consisted of a solution of 8% Na_2CO_3 .H_2O, 1.6% NaOH, 1.6% $Na_2C_4H_4O_6$ in deionised water and sufficient NaOH to adjust the pH to 11.25.

Micro-reagent B (MB); consisted of 4% BCA - Na_2 in deionised water.

Micro-reagent C (MC); consisted of a 4% solution of $CuSO_4$ $5H_2O$ added to MB at a ratio of 1:25 (vol/vol).

Micro-working reagent (MWR); was made up from MC and MA using a ratio of 50:50 (vol/vol).

Reagents A, B and SWR, used in the "standard protocols" and reagents MA and MB, used in the "microassay" were stable at room temperature for at least one week, however, reagents MC and MWR were prepared as required.

2.3.2 Protocols for the measurement of BSA concentration by BCA protein assay

In both the "standard protocol" and "standard microprotocol", 2ml of SWR was added to 0.1ml of the sample or standard solution to be assayed, in an LP3 tube. The tubes were then vortex mixed and incubated in a water bath at either 37°C or 60°C for thirty minutes, as shown in Table 2.2. For measurement of BSA concentrations by the "microassay" method, 0.5ml of sample or standard solution was added to 0.5ml MWR in an LP3 tube. The tubes were vortex mixed and incubated in a water bath at 60°C for 60 minutes (Table 2.2).

Table 2.2: Assay protocols for the measurement of BSA using the BCA method.

PROTOCOL	SAMPLE VOLUME (ml)	REAGENT VOLUME (ml)	INCUBATION TEMPERATURE (°C)	INCUBATION TIME (Mins)
"Standard" (100-1200µg/ml)	0.1	2.0 SWR	37	30
"Standard Microprotocol" (5-250µg/ml)	0.1	2.0 SWR	60	30
"Microassay" (0.5-10µg/ml)	0.5	0.5 MWR	60	60

FIGURE 2.2: Standard curve for BSA assay using the BCA "standard protocol" (Mean values ± SEM, n=6).

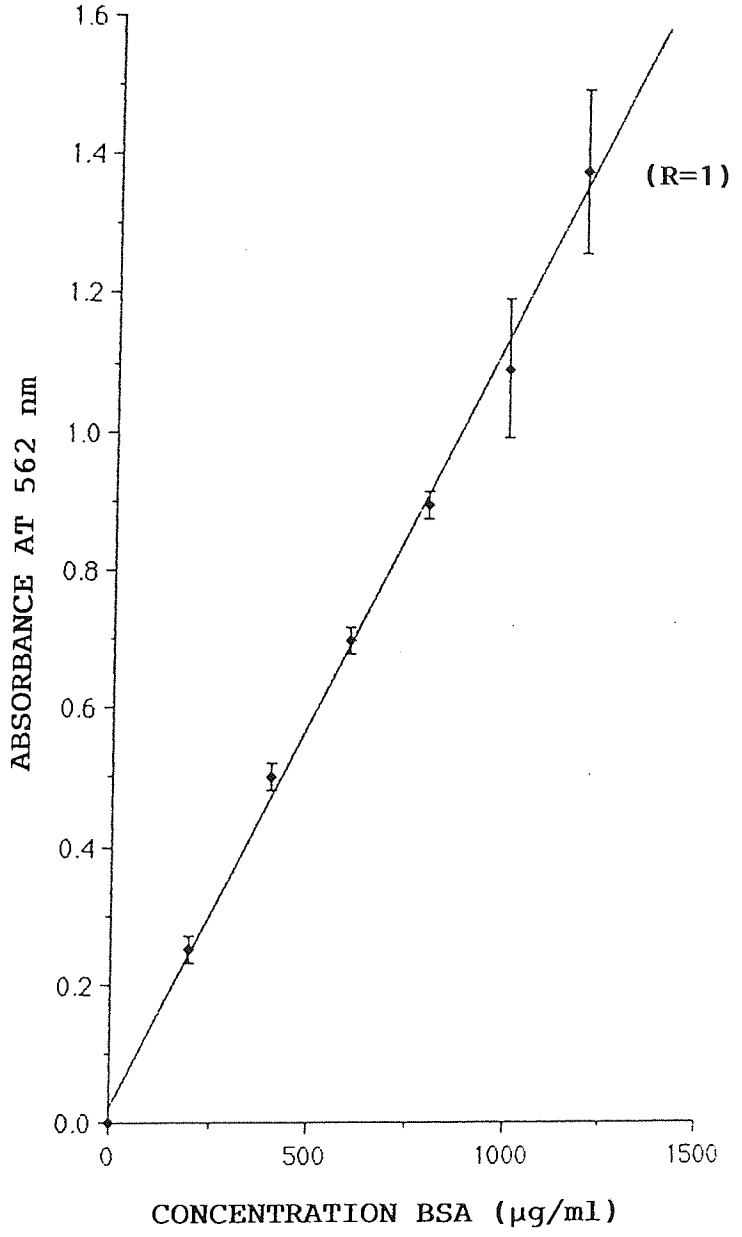

FIGURE 2.3: Standard curve for BSA assay using BCA "standard microprotocol" (Mean values ± SEM, n=6).

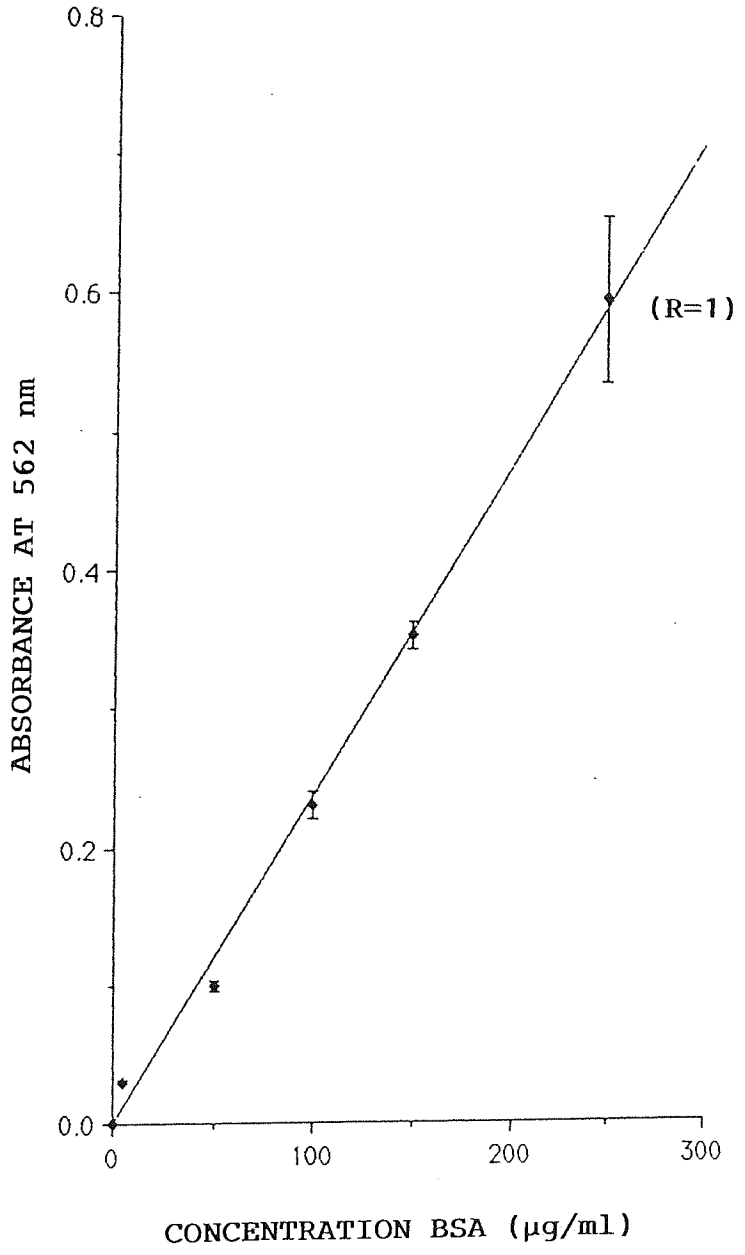

FIGURE 2.4: Standard curve for BSA assay using BCA microassay (Mean values ± SEM, n=6).

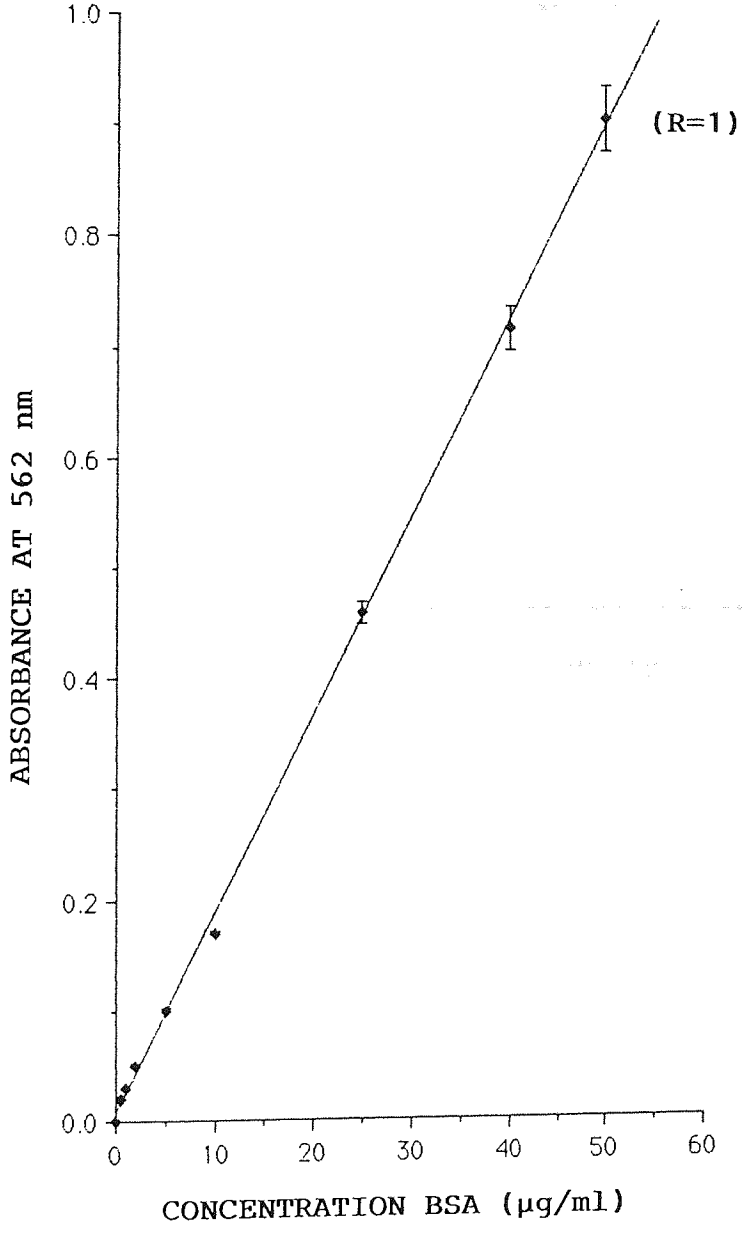

After incubation, samples were cooled to room temperature and their absorbance measured at 562nm, using a programmable LKB ultrospec K 4053 kinetic spectrophotometer, with reference to a reagent blank comprising 2ml of SWR or 0.5ml of MWR to which 0.1 or 0.5ml of deionised water had been added respectively.

The amount of BSA in each sample was computed by reference to standard curves, constructed using the range of BSA concentrations appropriate to each assay protocol, versus the absorbance. Three typical standard curves obtained, covering the three ranges of protein concentration are shown in Figures 2.2, 2.3 and 2.4. These standard curves were programmed into the spectrophotometer so that the BSA concentration in the samples could be obtained directly.

2.4 THE DETERMINATION OF FITC-LINKED DEXTRAN CONCENTRATION BY DIRECT SPECTROPHOTOMETRIC ASSAY

Fluorescein isothiocyanate (FITC) linked dextrans of low (FD-20S) and high (FD-150) molecular weight were incorporated as surrogate macromolecules to investigate the effect of molecular weight on the release of macromolecules from macroporous polyHEMA beads. FITC-linked dextrans are high molecular weight molecules, consisting of repeating glucose units linked by glycosidic bonding to FITC, a fluorescent dye, enabling direct monitoring of dextran

concentration by spectrophotometry, providing the linkage remains intact.

FD-20S (MW 17,500) had a degree of FITC substitution of 0.010 moles of FITC/mole glucose residue while FD-150 (MW 148,900) had a substitution of 0.005 moles of FITC/mole glucose residue. The absorbance maxima of FITC linked dextrans in solution were sensitive to changes in pH (132). Preliminary experiments indicated that the pH of water, adjusted to 7.4, increased to around pH8 when used to incubate beads loaded with FITC-linked dextrans. A buffering system was required which would maintain the pH at 7.4 and yet would be compatible with the other constituents of the monomer solution. 0.2M boric acid-borate buffer, pH7.4 was selected for this use (Appendix A1). This buffer has a buffering capacity of pH7.4 - pH9 and caused no adverse effects either in the monomer solution or the structure of the macroporous matrix. In addition, the buffer did not significantly effect the EWC of polyHEMA beads (Table 3.3, Page 189). The absorbance maxima of FD-20S and FD-150, determined in boric acid-borate buffer, pH7.4, were 491nm and 495 respectively. Standard curves were constructed using the absorbance values of a range of FD-20S and FD-150 concentrations (0.005-0.40 mg/l) in boric acid-borate buffer, pH7.4. Typical standard curves obtained are shown in Figures 2.5 and 2.6. These standard curves

FIGURE 2.5: Standard curve for FD-20S in boric acid - borate buffer, pH7.4 (Mean values ± SEM, n=8).

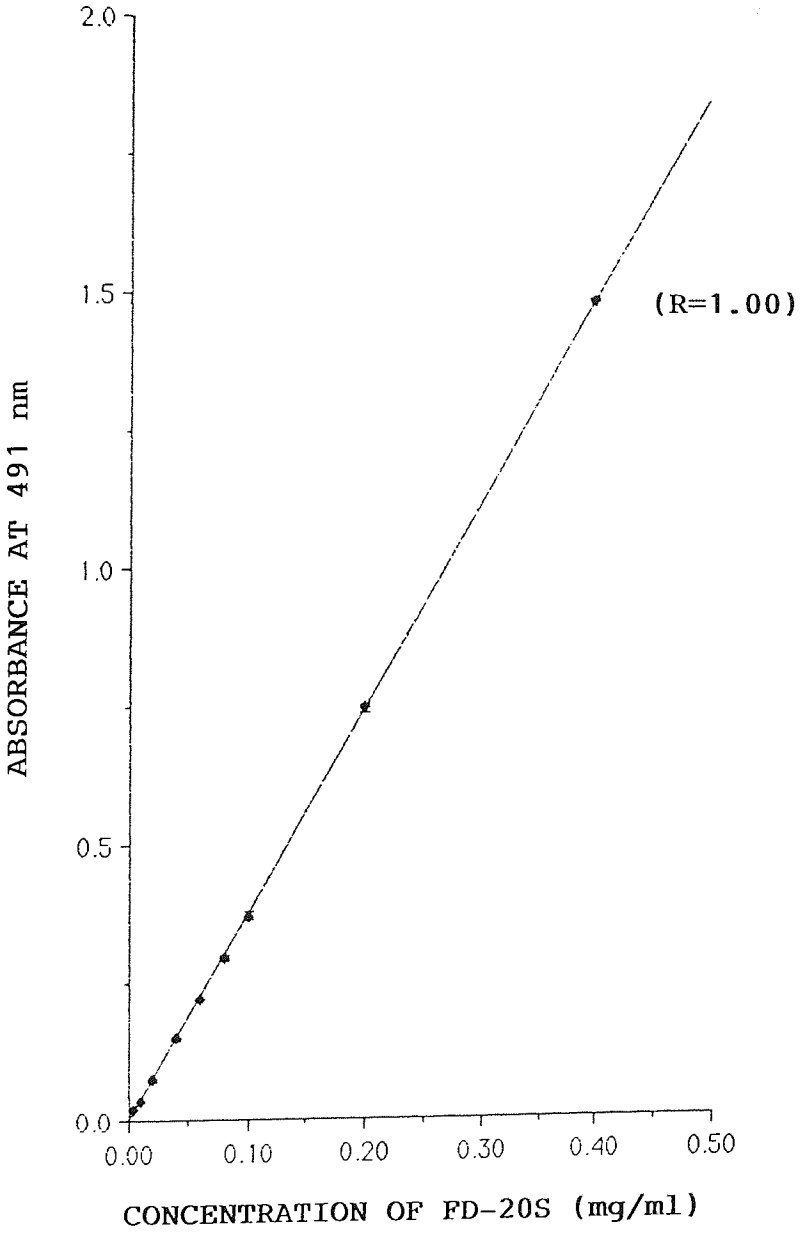

FIGURE 2.6: Standard curve for FD-150 in boric acid - borate buffer, pH7.4 (Mean values ± SEM, n=8).

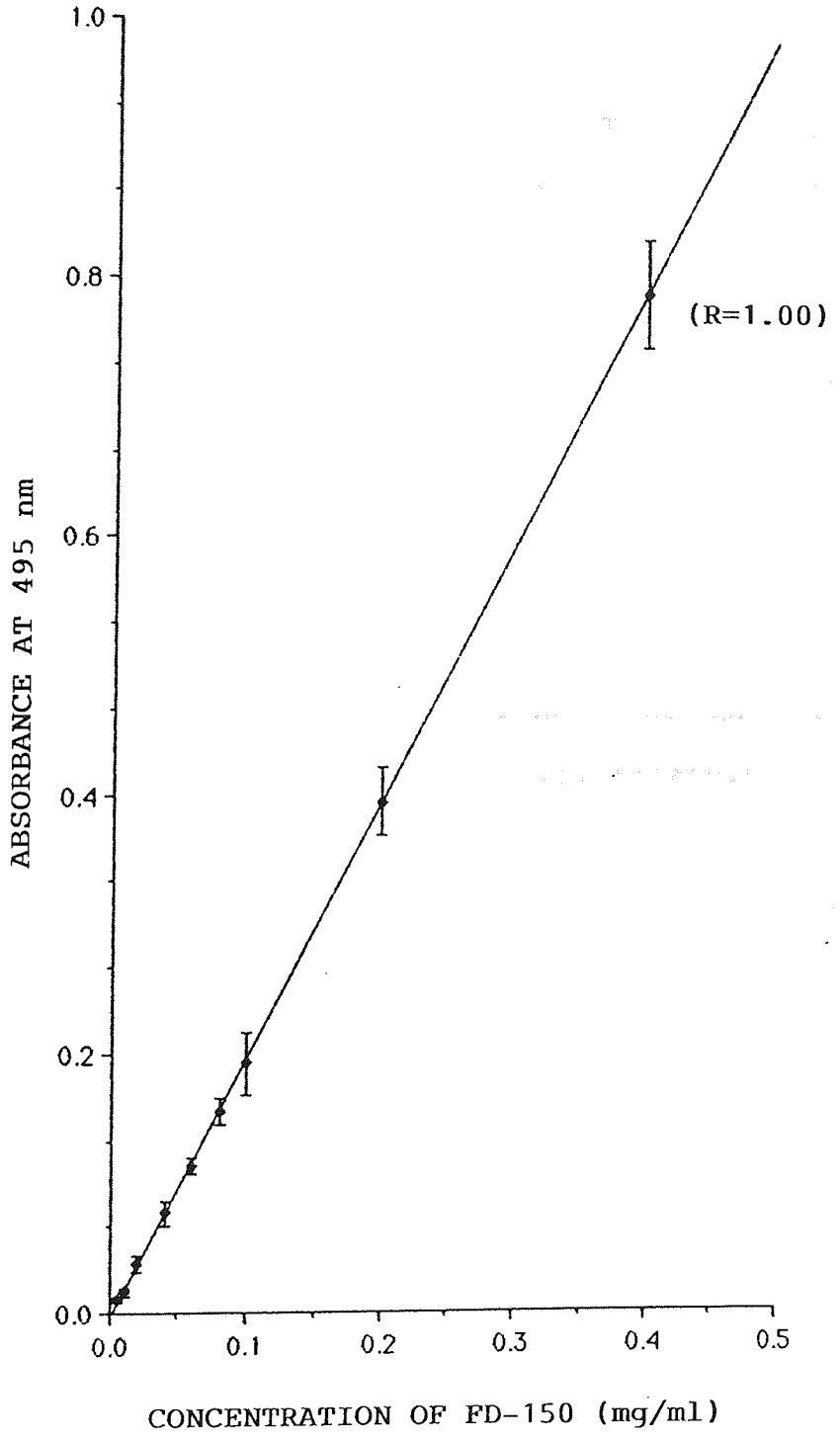

were programmed into an LKB Ultrospec K 4053 kinetic spectrophotometer and the concentrations of FITC-linked dextran samples subsequently obtained from the spectrophotometer directly.

The amount of free FITC in the FITC-linked dextrans used in this work, was measured, both in freshly prepared solutions and samples of the incubation buffer into which FITC-linked dextran had been released from polyHEMA beads, in order to establish if incorporation into polyHEMA beads resulted in any damage to the FITC linkage. Free FITC was separated from FITC-linked dextran by elution on a G50 Sephadex column (flow rate 0.22ml/min) and measuring the absorbance of 10 minute fractions at either 491nm (FD-20S) or 495nm (FD-150), appropriately. FITC-linked dextran was eluted from the column first, by fraction 6 in the case of FD-150 and fraction 16 for FD-20S. Free FITC was displayed by a peak in absorbance at fractions 23-27. The amount of free FITC present in the fresh FITC-linked dextran samples was 3.6% in FD-20S and 3.4% in FD-150. In samples released from polyHEMA beads the percentage of free FITC was increased to 8.36% in FD-20S and 8.27% in FD-150. This result would suggest that bead fabrication did cause some dissociation of FITC from the FITC-linked dextrans, although the proportion was relatively small. Allowance was made for the

proportion of free FITC when computing the release profiles for FD-20S and FD-150 dextrans.

2.5 THE DETERMINATION OF GLUCOSE OXIDASE CONCENTRATION (GOD, EC 1.1.3.4)

The opportunity to incorporate enzyme protein (ie GOD) into a macroporous matrix and the monitoring of its subsequent release provided a convenient and direct assessment of whether bead incorporation would produce any deleterious effect on the biological activity of a protein macromolecule. Released GOD was assayed, using a kinetic assay procedure, such that only enzyme which remained biologically active after release would be assayed (133). The principle of the assay reaction is summarised in the scheme below:-

$$\text{ß-D-Glucose} + O_2 + H_2O \xrightarrow{\text{GOD}} \text{D-Gluconic acid} + H_2O_2$$

$$H_2O + \text{O-Dianisidine (reduced)} \xrightarrow{\text{POD}} \text{O-Dianisidine (oxidised)} + H_2O$$

(Colourless) (Red Colour)

POD = Peroxidase (EC 1.11.1.7)

One unit (µMU) GOD will oxidise 1.0µmol ß-D-glucose to D-gluconic acid and H_2O_2 per minute at pH5.1 and 35°C. 1g of solid GOD supplied contained 128,000 units of enzyme activity.

2.5.1 Reagents for GOD assay

(a) 0.5M sodium acetate buffer, pH5.1 at 35°C

6.81g sodium acetate trihydrate was dissolved in 900ml deionised water and the pH adjusted to 5.1 at 35°C with 1M HC1. The buffer was then made upto 1L with deionised water.

(b) o-dianisidine solution (0.21mM)

13.2mg o-dianisidine was dissolved in 2ml deionised water. 1ml of this solution was then diluted to 100ml with 0.05M sodium acetate buffer, pH5.1 at 35°C.

(c) ß-D-Glucose solution (10% w/v)

1g ß-D-glucose was dissolved in 10ml deionised water.

(d) Peroxidase solution (POD)

A solution of POD was prepared containing 60 purpurogallin units per ml deionised water.
Peroxide was supplied containing 80pu/mg solid and 1 purpurogallin unit will form 1mg of purpurogallin from pyrogallol in 20 seconds at pH6.0 and 20°C.

2.5.2 GOD assay procedure

2.4ml of dye-buffer solution, 0.5ml of glucose solution and 0.1ml POD solution were pipetted into a quartz curvet (1cm light path), mixed and equilibrated

at 35°C. The absorbance was monitored at 500nm, against air, until constant. At zero time, 0.1ml of glucose oxidase sample was quickly added, mixed and the increase in the absorbance at 500nm against air, monitored for two minutes, using a spectrophotometer and chart recorder. The rate of change of absorbance per minute at 500nm was obtained from the maximum linear rate and used to calculate the concentration of glucose oxidase present in the solution as follows:-

$$\mu M \text{ units/ml GOD} = \frac{\Delta A500/min \times 3.1}{7.5 \times 0.1}$$

Where:	ΔA500/min	=	change of absorbance per minute at 500nm
	3.1ml	=	volume of reaction mixture
	$7.5 mmol^{-1} cm^{-1}$	=	millimolar extinction coefficient for the oxidised o-dianiside chromophore.
	0.1ml	=	volume of glucose oxidase sample.

Multiplying by 10 gave the number of units (µMU) released by 1g of beads into 10ml of incubation buffer.

2.6 INSULIN RADIOIMMUNOASSAY

The release of immunoreactive insulin from macroporous polyHEMA beads was initially monitored using double antibody radioimmunoassay (134). However, during the course of this work the double antibody to insulin

ceased to be commercially available, it therefore became necessary to establish an alternative radioimmunoassay method for the determination of insulin concentrations and the ethanol precipitation method was selected for use (135). The principle of radioimmunoassay depends upon the competition between labelled and unlabelled antigen for binding sites on specific antibodies. Increasing the amount of unlabelled antigen in the sample produces a proportional decrease in the binding of labelled antigen to the antibody (136). Therefore, the level of radioactivity associated with the antibody - antigen complex is inversely proportional to the concentration of unlabelled antigen in the sample. A number of procedures for the radioimmunoassay of insulin have been developed, differing principally in the technique used to separate the free hormone from the antibody-insulin complex. These include electrophoretic separation (136,137); sodium sulphite precipitation (138); by means of a second antibody reaction between the insulin-antibody complex and anti- γ -globulin (134,140,141); and by precipitation with 80% ethanol (135,142).

2.6.1 The double antibody method of insulin radioimmunoassay

The antibody system used in the double antibody method of radioimmunoassay consisted of an anti-insulin antibody (first antibody), raised against porcine

insulin in guinea pigs and a second antibody, anti-guinea pig globulin, raised in rabbits, which was used to precipitate the soluble primary antibody-antigen complex. As the binding reaction approached completion the antibody bound insulin was separated from the free insulin by centrifugation and the distribution of radioactivity (^{125}I) was determined by gamma counting. The binding of labelled insulin to the antibody is progressively inhibited by increasing amounts of insulin in the sample to be assayed, due to competition between the labelled and unlabelled insulin for specific binding sites on the antibody. The concentration of insulin in the test sample was determined by reference to a standard curve of $\log_{10}$ of a range of standard insulin concentrations plotted against counts per minute (cpm), constructed at the same time as the assays were performed.

The preparation of ^{125}I labelled insulin for use in the double antibody method of insulin radioimmunoassay.

Radioiodine is convenient for the preparation of labelled insulin since it can be readily substituted into the tyrosine residues of proteins and peptides. Two gamma-emitting isotopes of iodine are widely available ^{125}I and ^{131}I. ^{125}I was the isotope chosen for use in this work since it has a longer half life than ^{131}I (60 days, as compared with 8 days) and a greater counting efficiency (>90%).

It is desirable to obtain an average incorporation of one ^{125}I atom per protein molecule. This ensures a high specific activity with a minimum alteration to the insulin molecule, minimising the effect of the substitution on the biological and immunological activity of the labelled insulin. The chloramine-T method of radioiodination, first described by Hunter and Greenwood for the radioiodination of human growth hormone (143), was routinely used for the preparation of ^{125}I labelled insulin, for use in the double antibody method of insulin radioimmunoassay.

Chloramine-T, the sodium salt of the N-monochloro derivative of p-toluene sulphonamide, breaks down in solution to form hypochlorous acid (a mild oxidising agent). At pH7.4, in the presence of chloramine-T, $Na^{125}I$ is oxidised to form cationic iodine $^{125}I^{+}$. At this pH, the tyrosine residues of the insulin will be slightly anionic and the iodination reaction proceeds through this small proportion of ionised groups. The iodine atom is substituted at the ortho-position to the hydroxyl group on the phenolic ring of tyrosine. 80% of the iodine is incorporated into tyrosine 14 on the A chain of the insulin molecule, the remaining 20% iodinates tyrosines B16 and B26 (144). ^{125}I-insulin, iodinated at tyrosine A14, is known to retain the full immunological and biological activity of the native insulin (145).

The amount of chloramine-T used in the iodination reaction was dependant upon the particular batch of $Na^{125}I$ and the amount of insulin to be iodinated. Excess chloramine-T in the reaction is reduced by the addition of sodium metabisulphite and free iodine is reduced to iodide. Bovine serum albumin (BSA) is included in the reaction volume to act as a carrier for labelled insulin. The concentration of chloramine-T was kept low and the reaction time short, in order to minimise damage to the insulin molecule (143).

Reagents for the iodination of porcine insulin

1 0.5M and 0.05M phosphate buffer, pH 7.4 (Appendix A1).

2 Column eluant:

0.5% BSA and 0.1% sodium azide (as a preservative) dissolved in 0.05M phosphate buffer and pH adjusted to 7.4.

3 Column primer:

2.5% BSA in 0.05M phosphate buffer and adjusted to pH 7.4.

4 Monocomponant porcine insulin (Novo):

0.25mg of porcine insulin was dissolved in 1ml of 0.05M phosphate buffer. 40µl of this solution was aliquoted into each of 25 microfuge tubes (polystyrene, 500µl capacity), frozen and stored at -20°C. A fresh tube of insulin was thawed for each iodination.

5 Chloramine-T and sodium metabisulphite:

25mg of chloramine-T and 50mg of sodium metabisulphite were weighed out into separate LP3 polystyrene tubes which were then wrapped in foil to exclude the effect of light (146). Immediately prior to the iodination each was diluted in 100ml of 0.05M phosphate buffer pH7.4 to provide working concentrations of 0.25mg/ml chloramine-T (Chl-T) and 0.5mg/ml sodium metabisulphite (SMB).

6 $Na^{125}I$ (1mCi): (IMS 30)

10µl of $Na^{125}I$ was supplied by Amersham International UK in a small reactivial. The $Na^{125}I$ was supplied in dilute sodium hydroxide, pH 7-11. 100µl of 0.5M phosphate buffer was added to the reactivial to bring the pH close to 7.4, the optimum required for the chloramine-T reaction.

Procedure for the iodination of insulin

The iodination of porcine insulin was carried out one to two days after $Na^{125}I$ batch synthesis. Iodinations were carried out in the conical glass reactivial supplied, in a fume cupboard, behind a lead screen. The quantities of insulin and chloramine-T used in the reaction were dependant upon the age of the $Na^{125}I$. The 10µl aliquot of $Na^{125}I$ employed for the iodination

of insulin had a projected activity of 1mCi on the 'activity reference day', 15 days after batch synthesis. Therefore, on days two and three after batch synthesis, the activity of the $Na^{125}I$ was in excess of 1mCi. The concentrations of insulin and chloramine-T were therefore adjusted accordingly, as shown in Table 2.3 below:

Table 2.3: Relative proportions of porcine insulin and chloramine-T required in the iodination reaction,1-3 days after $Na^{125}I$ batch synthesis.

Days after Synthesis	$Na^{125}I$ (mCi)	Insulin (µl)	Chl-T (µl)	SMB (µl)	0.5M Phosphate buffer (2.5% BSA) (µl)
1	1.176	11.76 (2.94ng)	23.52 (5.88ng)	20	200
2	1.162	11.62 (2.91ng)	23.24 (5.82ng)	20	200
3	1.149	11.49 (2.87ng)	22.98 (5.78ng)	20	200

In order to minimise the introduction of more than one atom of ^{125}I per insulin molecule, iodination was performed with [^{125}I]/[Insulin] in molar equivalents of 1/10 (147). The iodination of insulin was generally carried out two days after batch synthesis and the quantities of insulin and chloramine-T used in the reaction mixture described are for iodinations on day 2.

100µl of 0.5M phosphate buffer pH7.4 and 11.62µl of porcine insulin (2.91ng), taken from the stock insulin solution (40µl) were added to the reaction vial containing 10µl of $Na^{125}I$. 23.24µl of chloramine-T (5.82ng) was then added and the vial gently inverted twice, to mix the contents. After 20 seconds reaction time, 20µl of sodium metabisulphite (10ng) was added and the vial was again gently inverted twice. After a further 15 seconds (stabilization time), 200µl of 0.05M phosphate buffer, pH7.4 containing 2.5% BSA was added. The labelled insulin was separated from the damaged insulin and free iodide by gel filtration on a Sephadex G50 (fine) column (Pharmacia). The column was first primed with 8ml of 0.05M phosphate buffer, pH7.4 containing 2.5% BSA, in order to purge the column of any material remaining from previous iodinations and to prevent the adsorption of freshly prepared labelled insulin onto the column. A 10µl aliquot of the labelled insulin was removed from the reaction vial immediately after iodination, for the assessment of the percentage incorporation of the ^{125}I into the insulin, the percentage damage and the specific activity.

The remainder of the reaction mixture was transferred to the top of the Sephadex column. The reaction vial was then washed with a further 180µl of 0.05M phosphate buffer, pH7.4 containing 2.5% BSA and this

too was transferred to the top of the column. The column reservoir was then secured and filled with column eluant buffer (0.05M phosphate buffer, pH7.4 containing 0.1% sodium azide and 0.5% BSA). The reaction mixture was then eluted at a flow rate of 1ml per minute. Sixty, one minute fractions were collected in LP3 tubes using a Serva Linear 2 fraction collector. The ^{125}I activity in each tube was counted for three seconds on a ICN Tracerlab gamma counter with a counting efficiency of 72%.

Four well defined peaks of radioactivity could be identified in the elution profile, as shown in Figure 2.7. Peak I represented a high molecular weight fraction containing aggregates of the insulin molecule and was generally contained in fractions 14-18. Peak II (fractions 19-30) contained monoiodinated insulin and demonstrated the maximum levels of radioactivity associated with the elution profile. Peak III was thought to represent free unreacted ^{125}I mixed with small damaged insulin fragments and was usually located in fractions 31-36. Peak IV contained free unreacted ^{125}I and was associated with fractions 37-40. Four to six fractions, representing the apex of Peak II (monoiodinated insulin), were selected and 10µl aliquots removed from each tube in order to assess the percentage of damaged insulin.

FIGURE 2.7: Typical elution profile of iodinated fractions, separated on Sephadex G50 (fine), from the chloramine-T iodination of porcine insulin.

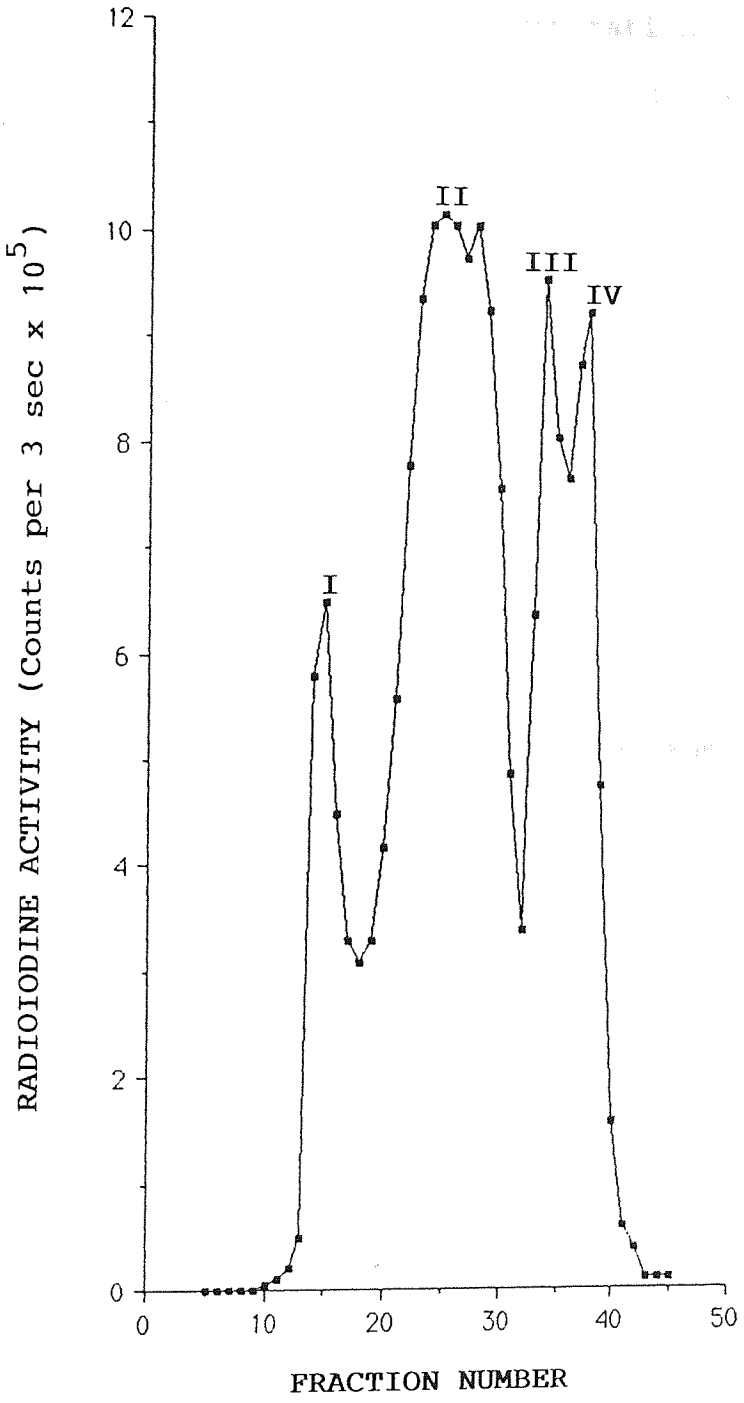

Assessment of the specific activity and integrity of ^{125}I-Insulin preparations.

The 10µl aliquot taken from the reaction vial immediately after the iodination reaction was used to assess the percentage incorporation of ^{125}I into insulin and the specific activity of the preparation. 0.5ml of eluant buffer and 0.5ml of 10% trichloroacetic acid (TCA) were added to the 10µl aliquot. The TCA formed a visible precipitate with the BSA present, which co-precipitated the undamaged ^{125}I insulin. The radioactivity of the total sample was then determined before centrifugation of the tube for 10 minutes at 2000 rpm (MSE Mistral 4L). The supernatant, containing predominantly free ^{125}I was aspirated and the radioactivity associated with the precipitate determined. The percentage incorporation of ^{125}I into undamaged insulin was calculated by the use of the equation below:-

$$\% \text{ Incorporation} = \frac{\text{Radioactivity count of precipitate}}{\text{Radioactivity count of total mixture}} \times 100\%$$

Since the total amount of ^{125}I present in the reaction mixture and the percentage radioactivity incorporated into the insulin were known, the specific activity could be calculated from the following formula:

$$\text{Specific activity } (\mu Ci/\mu g) = \frac{\%\text{incorporation} \times \text{amount of } ^{125}\text{I in reaction mixture } (\mu Ci)}{\text{Amount of insulin present in reaction mixture } (\mu g)}$$

The 10µl aliquots taken from the fractions representing the apex of peak II were also assessed for the percentage of damaged insulin using the TCA precipitation method previously described. The tubes which contained less than 1% damaged insulin were then selected and their contents pooled. 50µl aliquots of the label were then dispensed into LP3 tubes, frozen and stored at -20°C until required for use in the insulin radioimmunoassays. A typical iodination generated about 40 tubes of ^{125}I labelled insulin, with typical iodination characteristics as shown in Table 2.4:

Table 2.4: Mean percentage incorporation of ^{125}I into porcine insulin, percentage of undamaged insulin and specific activity of ^{125}I Insulin

Iodination Characteristics	n=	Mean	± SEM
% incorporation of ^{125}I into insulin	6	63.4%	± 3.92
% undamaged insulin	6	95.4%	± 1.96
Specific activity (µCi/µg)	6	252	± 15.03

The preparation of reagents for use in the double antibody method of insulin radioimmunoassay.

1 Radioimmunoassay (RIA) diluent buffer pH7.4 (Appendix A1).

2 Insulin binding reagent (Wellcome)

The reagent was supplied in a lyophilised form and was reconstituted with 8ml of deionised water on the day of assay.

3 ^{125}I labelled insulin

^{125}I insulin was prepared by the chloramine-T method as described previously (Page 106). The specific activity of a 50µl aliquot was reduced to 50µCi/µg by the addition of unlabelled porcine insulin, the exact amount calculated from the known original specific activity and by reference to an ^{125}I decay curve (Appendix 2). The count rate of the label was then reduced with RIA diluent buffer, such that a 50µl aliquot, used in the assay, provided 9,500 - 11,000 cpm.

4 Insulin standards (Wellcome)

The contents of one bottle of human insulin standard (2.5 - 3.5mU) was dissolved in 2.5 - 3.5ml of RIA diluent buffer to yield a concentration of 1mU/ml. 0.2ml aliquots of this stock solution were dispensed into LP3 tubes,

frozen and stored at -20°C. On the day of assay, one tube was diluted with 0.8ml of diluent buffer to provide a top standard insulin concentration of 200µl/ml. Five further serial dilutions were made of this standard, to yield a range of insulin concentrations from 6.25 - 200µU/ml. The release of bovine insulin from polyHEMA beads was expressed in human insulin equivalents.

Procedure for the radioimmunoassay of insulin

Reagents were added to LP3 tubes in the order indicated in the protocol summary below (Table 2.5):

Table 2.5: Protocol for the addition of reagents in the double antibody of radioimmunoassay of insulin.

Tube Description	Tube Number	Initial Reactants	Binding Reagent [Antibody]	^{125}I Insulin
Total Counts	1-3	-	-	+
Blanks	4-6	RIA Diluent Buffer	RIA Diluent Buffer	+
Insulin Standards (µl/ml)	7-9	6.25	+	+
	10-12	12.5	+	+
	13-15	25	+	+
	16-18	50	+	+
	19-21	100	+	+
	22-24	200	+	+
Zeros	25-27	RIA Diluent Buffer	+	+
Unknown Samples	28-n	+	+	+

All reactants were added in 50µl aliquots.

Insulin standards, total counts (^{125}I insulin only), blanks (no insulin standards or binding reagent) and zeros (no insulin standards), were assayed in triplicate, although samples were generally determined in duplicate. 50µl of each standard insulin concentration and each sample were dispensed into LP3 tubes and 50µl of binding reagent added. The contents of each tube was then vortex mixed and incubated at 4°C for 4 hours. A 50µl aliquot of ^{125}I insulin (50µCi/µg, 9,500 - 11,000 cpm) was then added to each tube, the contents vortex mixed and incubated for a further 18 hours at 4°C.

After the second incubation, 0.5ml of diluent RIA buffer was added to all tubes, except the total counts and the contents again mixed. Free and antibody bound insulin were separated by centrifugation at 2,900 rpm for 30 minutes at room temperature (MSE Mistral 4L). The supernatant, containing free insulin was decanted off and any remaining drops of buffer were aspirated from the neck of the tube. The tubes were then inverted and left to dry, at room temperature, for 4 hours. The ^{125}I activity associated with the precipitate was then counted for one minute, using an LKB 1282 Compugamma Universal gamma counter, with a counting efficiency of 92%.

Computation of results:

The construction of standard curves and the computation of results was performed using a RIA package associated with the gamma counter. Log_{10} of the standard insulin concentration was plotted against the counts per minute of the bound fraction of ^{125}I insulin and the unknown sample insulin concentration was determined automatically by direct extrapolation from the graph. A typical standard curve is illustrated in Figure 2.8. (A copy of a typical printout is shown in Appendix A3).

Quality control assessment of the data obtained in six typical assays is shown in Table 2.6. The double antibody method of insulin radioimmunoassay was found to have an intra and inter-assay coefficient of variation (CV%) of 5.17% and 10.04% respectively. The amount of non-specific binding of the labelled insulin, ie that which was not antibody bound, was calculated by dividing the blank counts obtained by the total counts (4.6%). The minimum detectable concentration of insulin sample, or the minimum sensitivity of the assay, usually defined as that amount of sample two standard deviations away from the zero dose response (148), was found to be 5.02μU/ml.

FIGURE 2.8: Typical standard curve for insulin radioimmunoassay by the double antibody method.

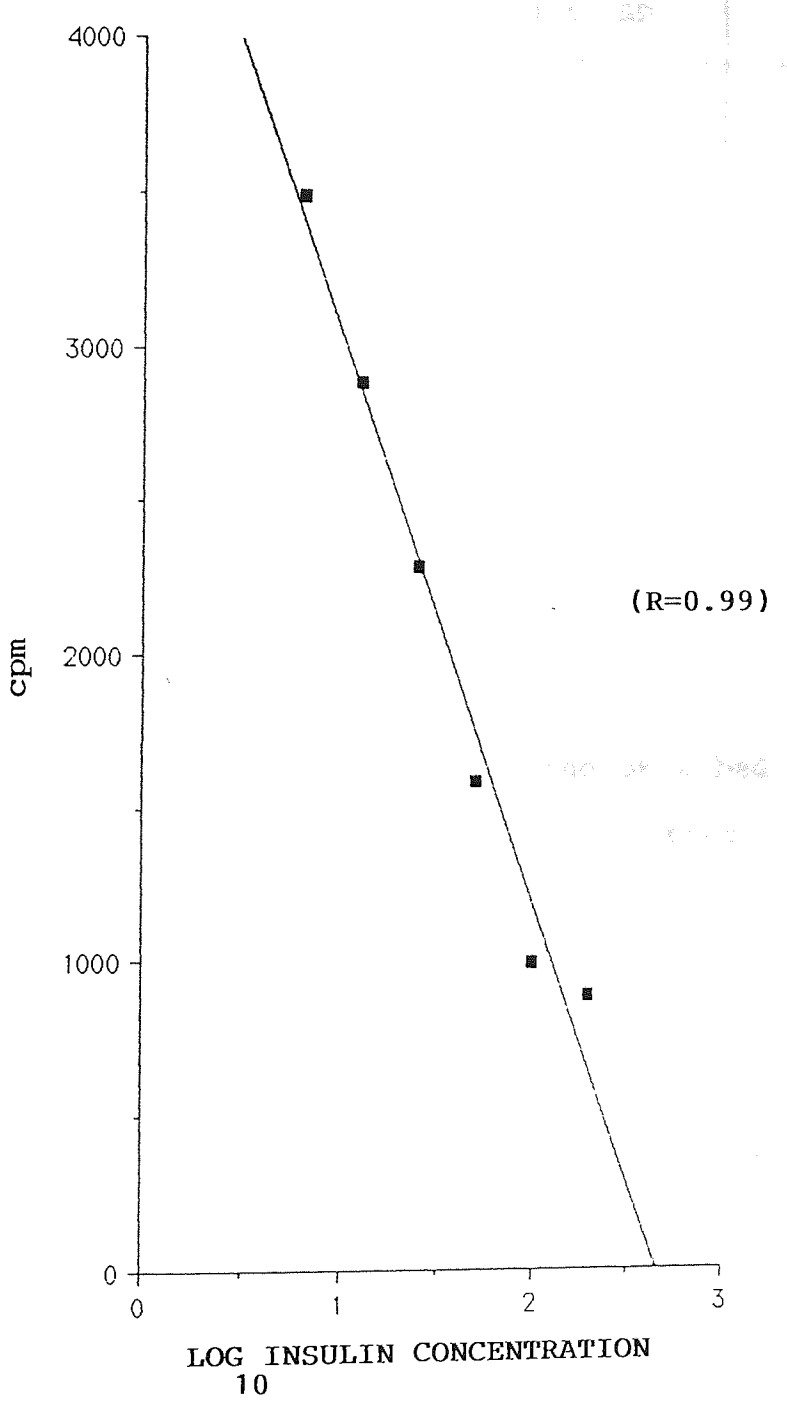

Table 2.6: Quality control assessment of data obtained in six typical insulin radioimmunoassays by the double antibody method

Parameter	Mean ± SD	CV%
Intra-assay variation	-	5.17
Inter-assay variation	-	10.04
Non-specific binding	4.60 ± 0.82	14.60
Minimum Sensitivity	5.02μU/ml	-

The criteria used for the assessment of a satisfactory assay:

There must be good agreement between replicate values. Replicates differing by more than 200 cpm were discarded. The most common causes of poor precision were inaccurate pipetting, mixing or a bad decanting technique. The value obtained for non-specific binding of the labelled insulin identified the efficiency of the buffer wash and this value was routinely less than 5% of the total counts.

2.6.2 Insulin radioimmunoassay by the ethanol precipitation method.

The ethanol precipitation method of insulin radioimmunoassay, first described by Heding (135), was selected for use as the replacement for the double antibody method. In the ethanol precipitation method, free and antibody bound insulin were separated by the addition of 95% (v/v) ethanol. It has been shown that

free insulin remains completely soluble when 95% ethanol makes up as much as 84% of the assay volume, whereas, when it contributes 79% of the assay volume, precipitation of the insulin-antibody complex is complete (135). A concentration of 95% ethanol which contributed 80% of the total assay volume was chosen for use in this assay. This concentration was sufficient to separate antibody bound complex by precipitation from free insulin which remained in solution (135). The antibody used in this technique was a single, first antibody of anti-porcine insulin serum, raised in guinea-pigs (Novo) with an original binding capacity of 3U/ml. When this antiserum was diluted in accordance with the manufacturer's instructions (1:18,000), the maximum binding capacity of the working solution was 160μU/ml. This assay could not therefore be used for the determination of insulin concentrations above 160μU/ml, consequently the value of the highest standard concentration was reduced from 200μU/ml to 100μU/ml. The ^{125}I labelled insulin used in this assay was supplied by Novo (A14,Tyr^{125}I-insulin) and recommended for use, in conjunction with their anti-insulin serum. Monoiodinated ^{125}I Insulin was prepared by Novo according to the method of JΦrgensen and Binder (149). Buffer used for the dilution of insulin standards and samples was the same as that used in the double antibody method (Appendix A1) except that it contained

20mmol/l sodium chloride to ensure complete precipitation of the insulin-antibody complex (142). The insulin concentration in test samples was determined by reference to a standard curve, prepared using a range (6.25 - 100μU/ml) of human insulin concentrations.

The preparation of reagents for use in the radioimmunoassay of insulin by the ethanol precipitation method

1 Diluent phosphate buffer, pH7.4 (Appendix A1).

2 Anti-porcine insulin guinea-pig serum (Novo)

The single insulin antibody was supplied in lyophilised form and reconstituted in 1.4ml x 2 distilled water. 1ml of this stock solution was then diluted with 59ml of diluent phosphate buffer. 10ml aliquots of the working solution were dispensed into universal containers (Sterilin) frozen and stored at -20°C.

3 ^{125}I labelled insulin (Novo)

^{125}I labelled insulin (20-30μCi/μg), was supplied as 20mU of total insulin, combined with 10mg of albumin in a freeze dried form. On the day of receipt, the material was reconstituted in 1.4ml x2 distilled water. 1ml of this solution was diluted with 144ml of diluent buffer and 10ml aliquots were dispensed into universal containers, frozen and stored at -20°C.

4 Human insulin standard solutions (Wellcome)

A range of human insulin standards (6.25 - 100μU/ml) was prepared by serial dilution as described for the double antibody method of insulin radioimmunoassay (Page 116) using diluent phosphate buffer.

5 95% (v/v) ethanol (BDH)

6 Buffer wash

960ml of 95% (v/v) ethanol, 162 ml of x2 distilled water and 18ml of diluent phosphate buffer were combined.

Procedure for the radioimmunoassay of insulin by the ethanol precipitation method

Reagents were added to LP3 tubes in the order indicated in the double antibody method protocol summary shown previously (Table 2.5, Page 117). However, in the ethanol precipitation method the 200μU/ml insulin standard could not be used and the reactants were added in 100μl, rather than 50μl aliquots. Insulin standards, total counts, blanks and zeros were assayed in triplicate and samples were determined in duplicate. 100μl of each standard insulin concentration or sample was dispensed into LP3 tubes and 100μl of anti-insulin serum added. The contents of each tube was vortex mixed and incubated at 4°C for 24 hours, to allow the binding reaction to reach equilibrium. 100μl of ^{125}I insulin (≈15-18,000 cpm) was then added to each tube, maintained at 4°C

over ice. The contents were then vortex mixed and incubated for a further 24 hours at 4°C.

After the second incubation, 1.6ml of 95% (v/v) ethanol was then added to each tube, the contents vortex mixed and centrifuged at 4,000 rpm for 30 minutes. The addition of ethanol to the tubes was performed at room temperature, since it has been shown that co-precipitation of free insulin is increased below 10°C (135). The supernatant was discarded and 2ml of buffer wash was added to each tube. The tubes were then centrifuged for a further 30 minutes at 4,000 rpm. The wash solution was then discarded and the tubes inverted and allowed to dry at room temperature. The ^{125}I activity, associated with the precipitate was then counted for one minute, using an LKB 1282 Compugamma Universal gamma counter, with a counting efficiency of 92%. The computation of results was performed in the same way as for the double antibody method of assay (Page 119). A typical standard curve, of $\log_{10}$ of the standard insulin concentration against counts per minute, for the ethanol precipitation method of insulin radioimmunoassay is shown in Figure 2.9. (A copy of a typical printout is shown in Appendix 3). Quality control assessment of the data obtained from six typical assays is shown in Table 2.7.

FIGURE 2.9: Typical standard curve for insulin radioimmunoassay by the ethanol precipitation method.

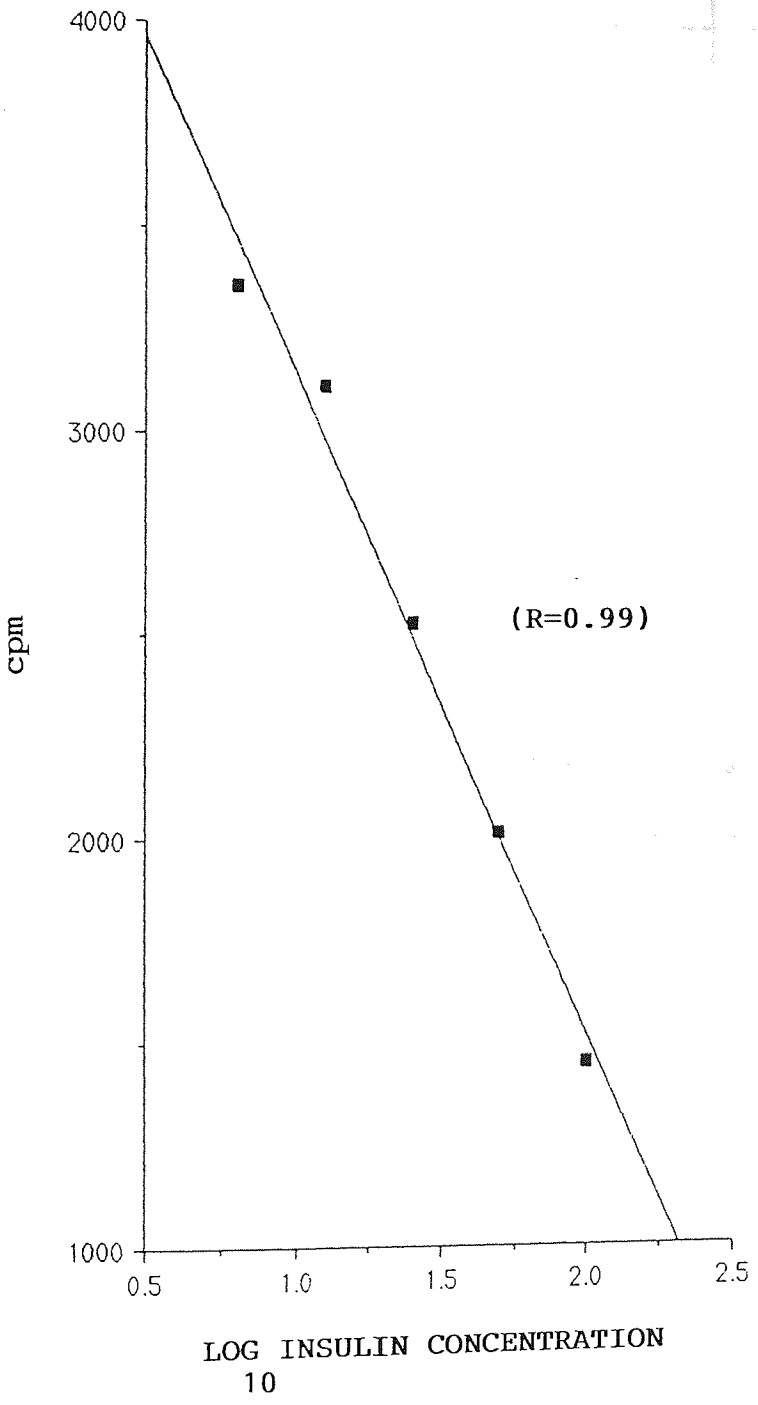

Table 2.7: Quality control assessment of data obtained from six typical insulin radioimmunoassays by the ethanol precipitation method.

Parameter	Mean ± SD	CV%
Intra-Assay Variation	-	5.04
Inter-Assay Variation	-	9.86
Non-Specific Binding	3.70 ± 0.3	12.89
Minimum Sensitivity	4.89 µU/ml	-

The ethanol precipitation method of insulin radioimmunoassay was found to have an intra and inter assay coefficient of variation of 5.04% and 9.86% respectively, with a non-specific binding level of 3.7% and a minimum sensitivity of 4.89µU/ml

The criteria used for the assessment of a satisfactory assay were the same as for the double antibody method of insulin radioimmunoassay (Page 121). However, the concentration of any protein, other than insulin, in the sample can affect the values obtained by the ethanol precipitation method of insulin radioimmunoassay. A high albumin concentration in the diluent buffer, reagents or samples causes increased precipitation of free insulin (135). Therefore, the protein concentration in the standards and samples should be as close as possible. The buffer wash was employed to minimise the co-precipitation of free insulin.

TABLE 2.8: Comparison of standard insulin concentrations determined by double antibody and ethanol precipitation methods of radioimmunoassay.

STANDARD INSULIN CONCENTRATION (μU/ml)	n=	INSULIN CONCENTRATION DETERMINED BY DOUBLE ANTIBODY METHOD		INSULIN CONCENTRATION DETERMINED BY ETHANOL PRECIPITATION METHOD		P
		(μU/ml)	± SEM	(μU/ml)	± SEM	
6.25	8	6.14	0.77	5.93	0.89	ns
12.5	8	13.87	2.46	12.30	1.81	ns
25	8	29.40	1.13	27.43	1.50	ns
50	8	51.79	2.40	56.27	1.76	ns
100	8	105.14	3.58	108.64	2.72	ns

ns = P value not significant.

2.6.3 Comparison of the double antibody and ethanol precipitation methods of insulin radioimmunoassay.

There was no significant difference found between a range of standard insulin concentrations, assayed by both the double antibody and ethanol precipitation methods, as shown in Table 2.8.

The ethanol precipitation method was therefore used as a direct replacement for the double antibody method of radioimmunoassay for the measurement of insulin released from polyHEMA beads.

2.7 ASSESSMENT OF THE BIOLOGICAL ACTIVITY OF INSULIN RELEASED FROM POLYHEMA BEADS, USING THE RATE OF INSULIN STIMULATED GLUCOSE OXIDATION BY RAT EPIDIDYMAL FAT PAD

The radioimmunoassay of insulin measures the immunoreactivity of insulin molecules, however, immunoreactivity of a peptide does not necessarily equate with the biological activity of the macromolecule. The biological activity of incorporated and subsequently released insulin was determined using a well established bioassay and the results obtained, compared with those obtained by double antibody insulin radioimmunoassay method. The major tissue sites of insulin action are the liver, adipose tissue and skeletal muscle, and insulin receptors have been characterised on the plasma membranes of all these cell types (150-152). The immediate effects of insulin involve alterations in the cellular metabolism of glucose and lipids, through changes in the activity of enzymes and membrane

transporters. Insulin rapidly promotes glucose uptake into muscle and fat cells. In muscle cells glycogen production is greatly enhanced and in fat cells, glucose is converted mainly to glycerol and fatty acid moieties of triacylglycerol and lipolysis is reduced. Currently, the primary action of insulin is considered to be an acceleration of glucose transport into the cells of skeletal muscle and adipose tissue (153,154) although the mechanism of the process is poorly understood.

Adipose tissue has long been used for the <u>in vitro</u> estimation of insulin concentration, since insulin causes a marked increase in the rate of glucose oxidation, the conversion of D-glucose to carbon dioxide and water, by the tissue. Two methods are currently available for the measurement of the rate of glucose oxidation employing the measurement of either $^{14}CO_2$ production from D[^{14}C] glucose or $^{3}H_2O$ production from D[^{3}H] glucose (155). The stoichiometry of both these reactions is illustrated below:

<u>$^{14}CO_2$ Production</u>

$$[^{14}C\text{-}C_5]\ H_{12}O_6 + 6O_2 \rightleftharpoons {}^{14}CO_2 + 5CO_2 + 6H_2O + \text{Energy } [\Delta G^{\circ\prime} = -686 \text{ kcal mol}^{-1}]$$

<u>$^{3}H_2O$ Production</u>

$$C_6[^{3}H\text{-}H_{11}]O_6 + 6O_2 \rightleftharpoons 6CO_2 + [^{3}H\text{-}HO] + 5H_2O + \text{Energy } [\Delta G^{\circ\prime} = -686 \text{ kcal mol}^{-1}]$$

In the present study, the assay of bioactive insulin concentration chosen, involved the measurement of the rate of insulin stimulated $^{14}CO_2$ production. This method of measurement has been confirmed to give valid results and work has shown that there is no response by adipose tissue to either the addition of glucose alone, or to insulin in the absence of glucose (156,157). The epididymal fat pad of the rat was chosen for this work. Winegrad and Renold demonstrated that the response of the epididymal fat to insulin was much greater than that obtained with mesenteric and perinephric fat (156). These authors also concluded that the basal activity and magnitude of the insulin effect was markedly reduced by handling and since the epididymal fat pads are discrete and easily removed they are thought to be the most suitable source of adipose tissue for use in the bioassay of insulin concentration. It has been reported that the sensitivity of the different segments of the fan-shaped fat pad to insulin varies, so that the thin, distal part produces a greater response than the thick proximal portion per unit weight (158). Therefore in the current work only the distal portions of the fat pads were used in insulin bioassays. It has also been shown that the steepness of the slope of the standard curve, that is, the sensitivity of the dose response of the adipose tissue to a range of insulin concentrations, is dependent

upon the body weight of the animals and their nutritional regime (159). The most insulin sensitive adipose tissue is obtained from rats weighing about 110g (159), however, rats of this weight yield only small amounts of tissue for experimental purposes. Fat pads from larger rats, weighing over 300g demonstrated a reduced sensitivity to insulin possibly associated with the ageing process (160). In addition, adipose tissue obtained from fasting animals has been demonstrated to be less sensitive to insulin than tissue obtained from rats fed ad libitum. Indeed, dose response curves have been found to be linear over the range 5 - 250μU/ml of insulin when using non-fasted rats (159). The minimum accurate sensitivity of the assay is generally accepted to be of the order of 10μU/ml of insulin (161,162).

2.7.1 Procedure for the biological assay of insulin using rat epididymal fat pad

Modified, oxygenated Kreb's biocarbonate buffer, pH7.4 at 37°C (Appendix A1), containing 1mg/ml glucose was used as the incubation medium for the bioassay. The buffer was warmed to 37°C in a water bath and oxygenated (95% O_2; 5% CO_2), for 30 minutes. After oxygenation, the pH of the buffer was checked and routinely found to be 7.4. The Kreb's buffer contained only half the standard amount of calcium in order to avoid the formation of insoluble calcium phosphates on standing.

D - [U-^{14}C] - glucose of high specific activity (200µCi/ml) was added to 100ml of warm buffer at a concentration of 0.2µci/ml. Sterilin plastic tubes (8cm x 1.5cm) were cut to 3.5cm in depth and positioned upright in standard scintillation vials, to act as reaction tubes. 1.8ml of Kreb's buffer, containing labelled glucose was then added to each of the inner plastic reaction tubes and the whole assembly maintained at 37°C in a water bath with intermittent oxygenation prior to the addition of the adipose tissue.

Free fed rats (150-200g), were killed by stunning and subsequent cervical dislocation. Both epididymal fat pads were excised immediately after death and placed in a petri dish containing oxygenated Kreb's buffer, pH7.4 at 37°C. Extraneous tissue, such as blood vessels and parts of the caput epididymis were dissected away. The thick proximal portion of each fat pad was then removed by a single cut and discarded. The fan-shaped distal portion was cut longitudinally into pieces of 20-40mg in weight. A thorough mixing of the distal pieces of fat from different animals was carried out to limit the effect of individual variation and 3 rats produced sufficient tissue for approximately 35 incubations. Three pieces of fat were rapidly blotted on dry filter paper, weighed and quickly transferred to buffer in the inner

reaction tube of each scintillation vial.

200µl of the appropriate unknown insulin sample, control sample or known standard insulin concentration was then added to the reaction vials containing the tissue. Known standard bovine insulin concentrations of 5, 50 and 500ng/ml were prepared in advance, 200µl of which, when added to the 1.8ml of buffer in the reaction vial, provided working standard insulin concentrations of 0.5, 5 and 50ng/ml of insulin (12.5, 125 and 1,250µU/ml). Blank vials, which received 200µl of buffer alone, were also set up to determine the basal rate of glucose oxidation by adipose tissue, in the absence of exogenous insulin. These controls allow for the possible activity of endogenous insulin present in the pieces of fat. All unknown samples and standard insulin concentrations were assayed in triplicate and standard insulin concentrations were included in every assay. After the addition of the insulin, each vial was quickly oxygenated and sealed with a rubber suba-seal to ensure an air-tight system. The vials were then incubated for one hour in a water bath at 37°C with vigorous shaking (100 cycles/min). After this time, the reaction was quickly terminated by the careful addition of 0.4ml of 10M HCl, injected into the inner reaction tube via a needle extended through the suba-seal. Immediately after the addition of the acid, 0.5ml of 3M NaOH was added to the bottom of the scintillation vial, around the reaction tube,

again, using a needle extended through the suba-seal. The vials were then left overnight in order to allow all the $^{14}CO_2$ produced to be absorbed by the NaOH. After this time the internal reaction tubes were then carefully removed, avoiding spillage and 10ml of toluene based scintillant (NE260 Nuclear Enterprises Limited) was added to each vial. NE260 a micellar scintillant, was chosen because it can accommodate a large aqueous phase. Background vials were set up, containing only NaOH and scintillant. The scintillation vials were capped and left overnight in the dark to reduce any chemoluminescence. Each vial was the counted for ten minutes on a Packard Tri Carb 2660 Liquid Scintillation System ß-counter. The chloroform quench curve used is illustrated in Figure 2.10 and the counting efficiency was always greater than 97%.

The mean background counts (≈400 dpm) were subtracted from the counts obtained for each vial, standards and samples and the dpm per mg fat in each tube was calculated. The rate of glucose oxidation (µmol) per mg of fat per hour was calculated from the following equation:

$$\text{Rate of glucose oxidation (µmol glucose/mg fat/hr)} = \frac{^{14}CO_2 \text{ formed (dpm)}}{\text{specific activity of glucose (dpm/µmol)}}$$

FIGURE 2.10: Chloroform quench curve for ^{14}C showing the relationship between counting efficiency and external standard ratio (ESR). All ESR values were in excess of 0.35 giving a counting efficiency of >97%.

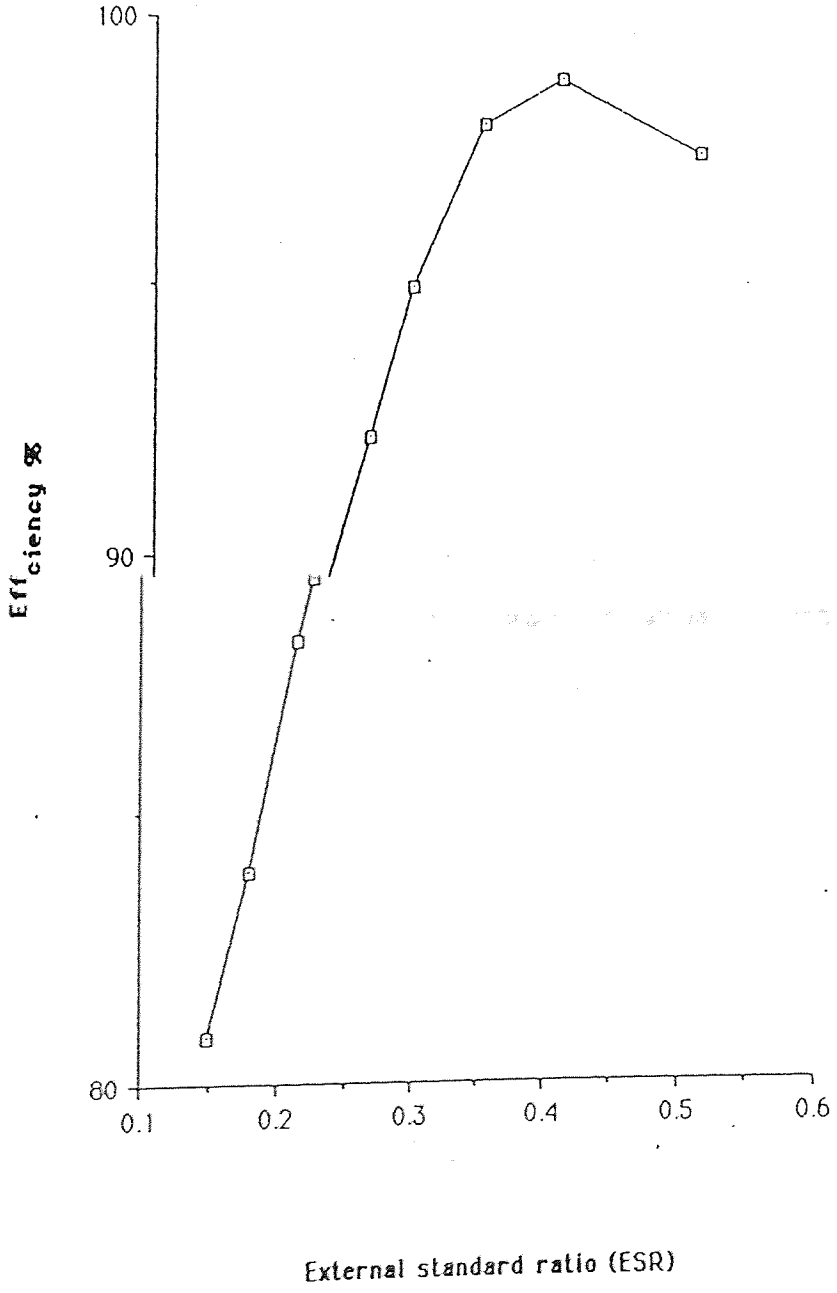

The theoretical dpm of 1μCi is 2.22×10^6 dpm. Since labelled glucose was added at a concentration of 0.2μCi per ml there were 0.36μCi of glucose per reaction tube (1.8ml of buffer x 0.2μCi). The theoretical dpm of 0.36μCi is 7.9×10^5 dpm (0.36μCi x 2.22×10^6 dpm). Therefore, the rate of glucose oxidation can be calculated since the $^{14}CO_2$ formed (dpm) per μmol glucose and the specific activity of the glucose is known (5.6×10^3dpm/μmol).

Therefore:

$\frac{7.9 \times 10^5}{5.6 \times 10^3}$ = 141 dpm per 1μmol D - [U-^{14} C]-glucose oxidised

The rate of glucose oxidation by the fat tissue in the absence of exogenous insulin sample, ie. the basal rate of glucose oxidation was deducted from the rate of glucose oxidation obtained for each standard and sample and a standard curve was constructed in which the rate of insulin stimulated glucose oxidation above basal was plotted against a range of known insulin concentrations. The insulin concentration present in each sample was determined by direct reference to this standard curve. A typical standard curve is shown in Figure 2.11.

Criteria for a satisfactory assay

The handling of the fat pads was kept to a minimum since the response to insulin is known to decrease when the fat is subjected to excessive manipulation (156).

FIGURE 2.11: Typical standard curve for the determination of bioactive insulin by increase in glucase oxidation of rat epidymal fat pad. Mean values ± SEM, n=6).

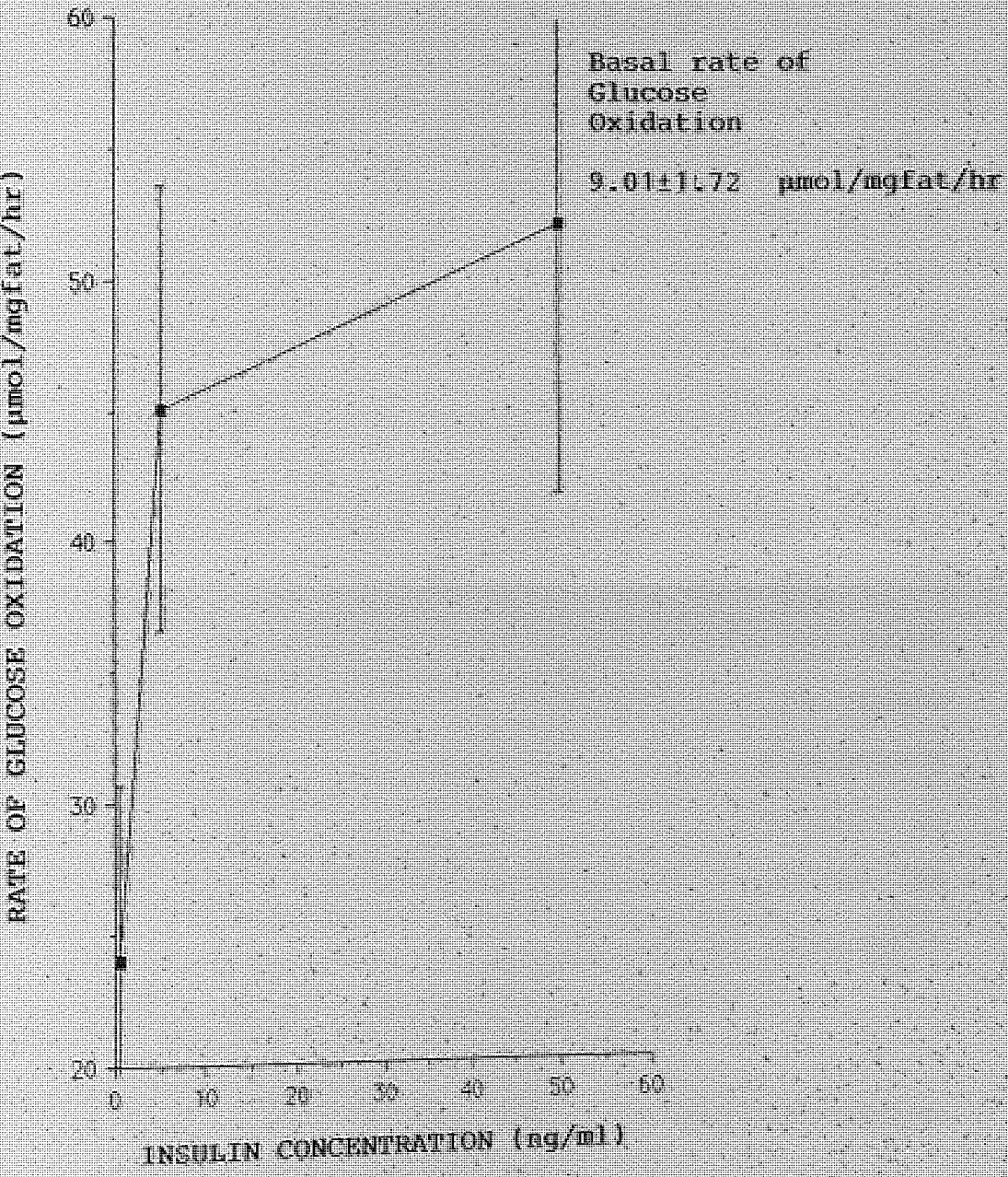

It was also important to thoroughly randomise the pieces of fat from different animals because the insulin sensitivity of the same regions of the fat pad is known to vary between animals and even between two fat pads taken from the same animal (159). The length of incubation time was important and the point in time when each insulin sample was added to a vial was noted so that the incubation time could be kept to exactly 1 hour. The termination of the reaction with HCl and the subsequent removal of the inner reaction tube was performed very carefully to ensure that there was no spillage of D-[U-^{14}C]- glucose into the NaOH.

Values obtained by bioassay had high standard errors of the mean. A 50ng/ml standard was included in the standard curve to test the sensitivity of the assay and the standard curve was not found to be linear above an insulin concentration of approximately 12ng/ml. The basal rate of glucose oxidation by distal portions of the epididymal fat pad in the absence of exogenous insulin was routinely found to be of the order of 9µmol glucose/mg fat/hour.

2.8 THE CYTOTOXICITY TESTING OF MACROPOROUS POLYHEMA BEADS USING CULTURED CELLS

The tissue biocompatibility of polyHEMA has been well established (13,77-82). However, incompatibility of biopolymers is often caused by the presence of contaminants derived from the fabrication process,

which render the device incompatible. These contaminants can be leached from the device after implantation causing cell trauma and infection, leading to injury or death. A vast number of *in vitro* and *in vivo* tests have been devised to determine the tissue biocompatibility of polymers to be used in surgical implantation (163).

In order to establish the bicompatibility of macroporous polyHEMA beads manufactured by freeze-thaw polymerisation the beads were subjected to short-term cytotoxicity testing using cultured cells. The basic cytotoxicity test used was a modification of the Minimum Essential Medium (MEM) elution test, developed from the works of Wilsnack (164,165). This is an extremely sensitive test since cultured cells are directly exposed to a concentrated extract of substances which might be leached from the matrix. The cell line chosen for use in this study were L-929 mouse fibroblasts, chosen in accordance with the recommendations of the safety evaluation guidelines of North American Science Associates Incorporated (NAmSA Ohio - USA). L-929 cells are a sub line of NCTC, clone 929 (strain L), originating from C3H mouse areolar and adipose tissue (166). The cells are fibroblast and attachment dependant, forming epithelial-like monolayers in culture. The L-929 cell line is suggested for use by NAmSA in most cases

of cytotoxicity testing, since it is easy to culture and the supply of cells is unlimited and dependable.

2.8.1 Maintenance of stock cell cultures

Stock cultures of L-929 cells were routinely maintained in Eagle's minimum essential medium (modified) with Earle's salts and non-essential amino acids (EMEMA). The medium was supplemented with 10% foetal calf serum, 100µg/ml streptomycin and 100IU/ml penicillin. The stock cell cultures were maintained in 250ml Costar tissue culture flasks at 37°C in an humidified atmosphere of 95% air, 5% CO_2.

Media preparation

Eagle's minimum essential (modified) with Earle's salts and non-essential amino acids, was supplied in powdered form. Sufficient powder to make up 1l of medium was dissolved in 800ml of x 2 distilled water at room temperature and 0.85g of sodium bicarbonate added. The pH of the media was adjusted to 0.25 units below the desired final pH of 7.4 with 1M HCl, since the pH of the medium increased 0.2-0.3 units on filtering. The total volume of the medium, was then made up to 1L with x 2 distilled water. 20ml/l of a solution of penicillin (5,000IU/ml) and streptomycin (5,000µg/ml) was added to the medium and sterilization

effected by membrane filtration using a 0.22µm filter (Millipore UK Sterivex - GS, incorporating a filling bell) and aseptic collection into 250ml bottles. 10% foetal calf serum (FCS) was added to each 250ml bottle just prior to use.

Cell passaging

Adherent cells were brought into suspension for subculture, or passaging when the monolayer attained confluence and a few cells began to detach. Passaging was effected using a combined solution of trypsin and EDTA. Flasks to be passaged were first rocked gently to free any loose or dead cells and then spent medium was removed and replaced with 9ml trypsin (0.05% w/v)/EDTA (0.02% w/v). Each flask was then maintained at room temperature for one minute and the trypsin/EDTA poured off. A further 1ml of trypsin/EDTA was then added and the flasks were then incubated at 37°C (humidified air/5% CO_2) for a further 6-10 minutes to effect the complete detachment of cells. The action of trypsin was inhibited by the subsequent addition of 9ml of FCS supplemented EMEMA culture medium. The cell suspension was then centrifuged at 1,500 rpm (MSE Chillspin), for three minutes and the supernatant decanted off. The cell pellet was resuspended in 5ml of FCS supplemented culture medium and the number of live cells were

enumerated by trypan blue exclusion, using a haemocytometer. L-929 cells were re-seeded at an average density of 4×10^6 cells per 250ml tissue culture flask, containing 20ml of FCS supplemented EMEMA culture medium, routinely passaged once weekly and the passage number noted. Twice weekly, the spent culture medium was removed and replaced with fresh medium. The cell cultures were maintained at 37°C in humidified air/5% CO_2, using a temperature controlled incubator (Flow Laboratories, UK).

Plating efficiency

To determine the plating efficiency of L-929 cells, ie the percentage of individual cells which give rise to colonies when innoculated into new culture vessels after passaging, $2\text{-}3 \times 10^5$ cells from freshly trypsinised stocks were seeded into Nunc vented petri dishes (60 x 15mm) and incubated for 24 hours. The culture medium was then decanted off the monolayer and the number of cells in the supernatant was determined using a haemocytometer. The plating efficiency, P, of the L-929 cells was calculated using the following equation:

$$P\% = \frac{T - S}{T \times 100}$$

Where: T = cell count in initial innoculum
S = cell count in the supernatant

The plating efficiency of L-929 cells was found to be $87.2 \pm 3.7\%$ (n = 6).

Kinetics of cell growth

When cells are passaged from a confluent, stationary culture, there is an initial lag phase of some hours to days before growth commences. The length of the lag phase is dependant upon the cell strain and the growth conditions employed. The growth of the cells then proceeds steadily in an exponential fashion, ie the cells enter log phase growth (167). At the end of the log phase, the maximum population size is achieved and the cells enter the stationary phase (168). The stationary phase is the result of a combination of two factors, overcrowding, leading to a build up of toxic metabolites and nutrient depletion. During log phase growth, the cell population increases according to the equation below:-

$$N = No\ 2^{kt}$$

Where No = Number of cells in the initial innoculum

t = time

N = Number of cells at time t

k = a regression constant.

The term kt describes the generation number defined as the number of generations involved in the increase by doubling at each cell generation, from No to N. It follows that the mean generation, or doubling time, T, is represented by the inverse of k.

Rearranging the equation for k:-

$\text{Log } N = \log No + kt \log 2$

$\text{Log } N - \log No = kt \log 2$

since $\frac{1}{\log 2} = 3.32$

It follows that:

$3.32 (\log N - \log No) = kt$

Therefore $k = \frac{3.32 (\log N = \log No)}{t}$

and $T = \frac{1}{k}$

This calculation assumes that all the cells in the population divide and do so at the same rate. This can be assumed to be true for most cell cultures during log phase growth (168).

Growth curve for L-929 cells

The growth curve of L-929 cells was monitored over a five day period by counting the increase in cell number with time. 1.2×10^5 cells from freshly trypsinised stocks (stationary phase) were plated into 50ml Nunc tissue culture flasks containing supplemented medium and were maintained at 37°C in humidified air/5% CO_2. Four flasks per day were trypsinised and the number of live cells were enumerated by trypan blue exclusion, using a haemocytometer. Any remaining flasks were replenished with fresh medium on days 3 and 5. The growth curve of L-929 cells can be seen in Figure 2.12 and shows the three classical stages of growth. The lag phase was

FIGURE 2.12: Typical growth curve for L929 cells (Mean values ± SEM, n=6).

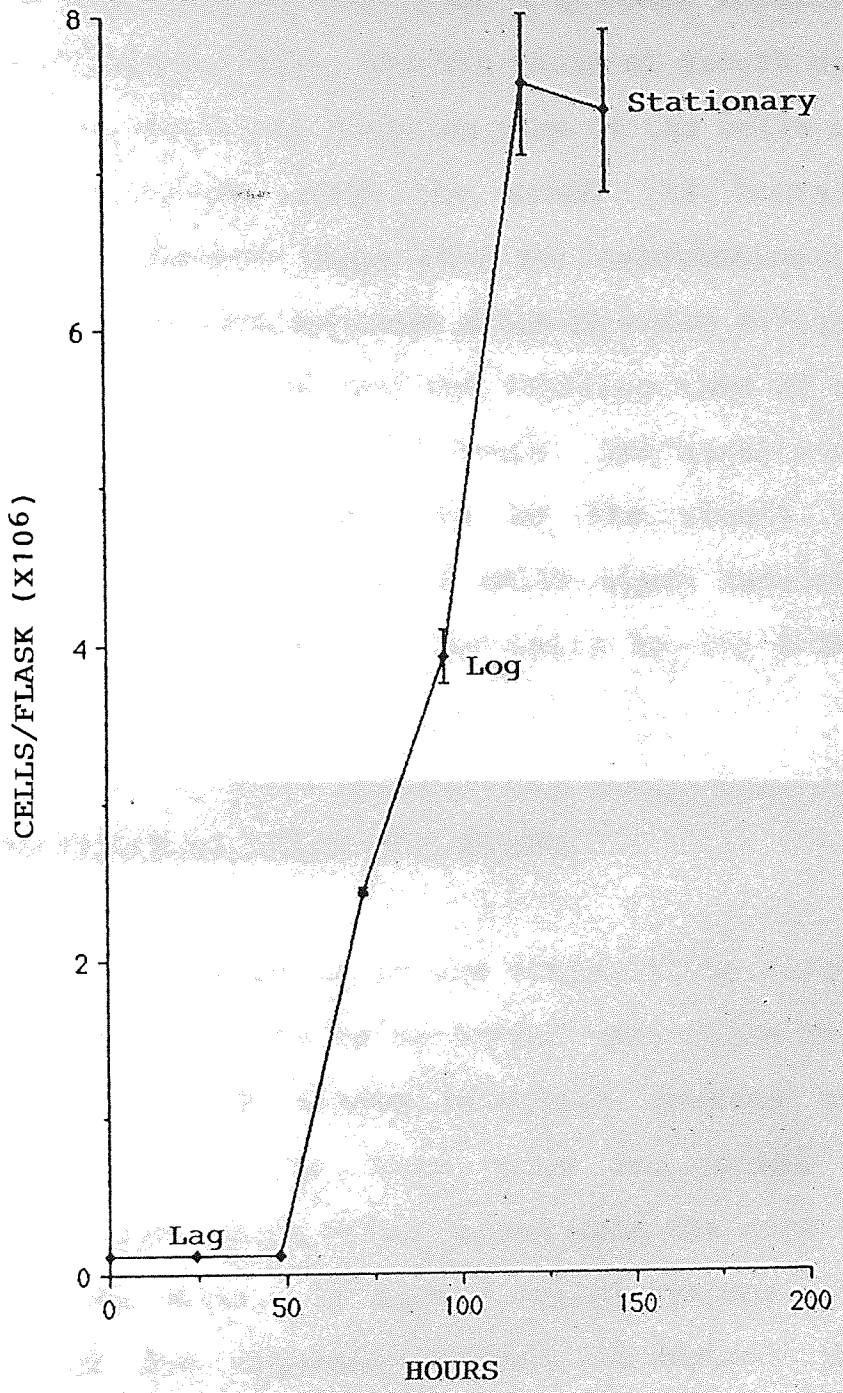

of the order of 50 hours. During the lag phase there is a build up of essential metabolites and growth factors by the initial innoculum, a process referred to as conditioning (168). The log phase of growth can be used to calculate the doubling time of the cells by direct extrapolation from the graph (14 hours), however, the equation (Page 145) for calculation of doubling time was more accurate since no curve fitting procedures were employed and the doubling time of L-929 cells was found to be 16.7 hours. The stationary phase observed was likely to be the result of overcrowding and detachment of cells since nutrient repletion failed to restore the cells to log phase growth.

Cryopreservation of L-929 cell stocks

The preservation of cells in the frozen state allows multiple experiments to be performed upon cells from the same stock and allows effective storage and transportation of cells. When cells are cooled to below 0°C changes occur which depend upon the rate of cooling of the cells. In slowly cooled systems, the build up of ice crystals spreads throughout the extracelluar solution. A build-up in extracelluar osmolarity occurs and the cells lose water by osmotic shrinkage. Slowly cooled cells become dehydrated but do not freeze intracellularly. Very rapid cooling

does not allow significant osmotic shrinkage of the cells and intracellular freezing occurs. If the rate of cooling is sufficiently slow that intracellular ice does not form to any great extent, but sufficiently rapid to ensure that cells are not damaged by high solute concentration or shrinkage the cells will survive the freezing and thawing process (169). Rapid thawing is required to prevent the conversion of the small ice crystals, formed at this intermediate cooling rate, into larger crystals, known as the recrystallisation of ice crystals (170). The rate of cooling suitable for survival depends on the cell type. The most commonly used cryoprotectant is dimethyl sulphoxide (DMSO) and this agent widens the 'preservation temperature window' particularly in the direction of overcoming injury caused by slow cooling. DMSO exerts its cryoprotective effect by preventing excessive increases in intracellular electrolyte concentrations (171-173).

(a) Freezing-down L-929 cells

4-6 x 10^6 L-929 cells from freshly trypsinised stocks, in the log phase of growth were suspended in 1ml of FCS supplemented EMEMA culture medium, containing 10% DMSO in 1.2ml Nunc cryo-ampoules. The cryo-ampoules were then prechilled in a refrigerator at 4°C for 20-30 minutes to allow equilibration of the DMSO. The

chilled cryo-ampoules were then loaded onto a Hand Freeze 35 HC freezing tray (Union Carbide, Indianapolis USA) set at position 3.5. When placed into a Union Carbide 35HC liquid nitrogen freezer, this position provided a freezing rate of approximately 3.5°C per minute (Data supplied by the manufacturer, shown in Appendix 4). After 20 minutes, the cryo-ampoules, maintained at approximately -65°C were loaded onto canes and plunged into liquid nitrogen at -196°C for storage.

(b) Thawing frozen cells

When frozen cells were required for culture, cryo-ampoules were rapidly thawed in a shaking water bath at 37°C. Thawing was complete in three minutes (thawing rate 80°C per minute). The contents of an ampoule was transferred into a 250ml tissue culture flask, containing 30ml of EMEMA culture medium, supplemented with 10% FCS. This, resulted in the dilution of the DMSO content to 0.3%. After 24 hours, the medium was replaced and cells subsequently cultured in the usual way.

2.8.2 MEM elution test

The basis of the MEM elution test is that the test material is extracted in cell culture medium, containing serum to simulate body fluids. Cell

cultures are then exposed to this extract and examined for cell death after 24, 28 and 72 hours (NAmSA, safety evaluation guidelines). The choice of extraction time and temperature is dependant upon the intended use of the device. USP permits the extraction of biomaterials at 121°C for 1 hour, 70°C for 24 hours or 50°C for 72 hours (NAmSa, safety evaluation guidelines), selected upon the basis of the resistance of the material to high temperatures. However, unless the product is to be autoclaved, these represent exaggerated conditions of extraction. The tests performed in the course of this work were not designed to conform to these exaggerated conditions, employed to allow a wide margin of error in biocompatibility assessment, but rather to investigate the possibility of toxic substances being leached from the beads under normal working conditions. Therefore, the extraction conditions chosen were 37°C for 24 hours and 4°C for 120 hours.

Preparation of test medium

Unloaded polyHEMA beads (500-1000μm) were washed for 5 minutes in x2 distilled water after fabrication and freeze-dried, then washed briefly in ethanol and rehydrated in sterile EMEMA tissue culture medium for 24 hours. 1g of beads was then transferred to 100ml of fresh culture medium and statically eluted for either 24 hours at 37°C or 120 hours at 4°C.

Preparation of cell cultures

A confluent layer of L-929 cells was trypsinised and seeded into 50ml tissue culture flasks containing EMEMA medium, at a cell density of approximately 1.2 x 10^5 cells per flask. The cultures were incubated for 72 hours to allow establishment of the freshly trypsinised cells, facilitating significant cell multiplication and the log phase of culture growth to commence. Prior to experimental work, the cells in six of the flasks were trypsinised and enumerated (time=0). This enumeration allowed the variation in the number of cells per flask, which arises from natural variation to be assessed before test or control medium was added to the cultures.

Experimental procedure

The test cell culture medium, containing eluates from the polyHEMA beads were fed to cultured cells during log phase growth (t=0). Live cell numbers were enumerated after 24, 48 and 72 hours using trypan blue exclusion. Control cell cultures were processed in the same way but were exposed to fresh culture medium alone. Positive control experiments were also set up to test the effect of HEMA monomer concentration on the growth of cultured cells. Cultured L-929 cells were exposed to EMEMA tissue culture medium containing either 1:1,000 or 1:100,000 distilled HEMA monomer and

live cell numbers were determined over 24, 48 and 72 hours. The effects of eluate extract test medium and HEMA monomer were illustrated by plotting the mean live cell number against time compared with control flask mean live cell numbers.

2.9 STATISTICAL ANALYSIS OF RESULTS

Results were generally expressed as mean values ± the standard error of the mean (± SEM). In order to establish whether there was any significant difference between the proportions of beads obtained in each size category for a particular bead fabrication procedure, two-way analysis of variance (174) (Two-way ANOVAR) was performed using a 'Statview^{R}' software package on an Apple Macintosh Plus^{R} microcomputer (175). This analysis could not however, confirm which of the size of categories were significantly different from each other. Therefore, when two-way ANOVAR provided a significant difference, Newan-Keuls multiple comparison test (176) was performed to establish which of the size categories were significantly different from each other.

To establish the effect of changing the fabrication parameters on the size distribution of the beads obtained, each size category was compared using either Student's unpaired t-test (177) (peristaltic pump

experiments), or one-way ANOVAR (178), followed by Newan-Keuls multiple comparison test (Brand dispenser experiments). One-way ANOVAR and Student's t-tests were also performed using the 'Statview^{R}' package. Any differences between mean total bead yields obtained from different manufacturing processes were confirmed using one-way ANOVAR. The effect of any alterations in monomer:solvent ratio or in percentage loading on the EWC of beads was established using one-way ANOVAR, followed by Newman-Keuls multiple comparison test.

The differences in the rates of release of BSA and GOD from polyHEMA beads under different experimental conditions were confirmed using Student's unpaired t-tests. The statistical comparison between the concentration of insulin, as determined by RIA, in fresh and freeze dried samples and in the concentrations of insulin assayed by the two different means of RIA were also established using Student's unpaired t-tests, as were the differences in the concentration of insulin in samples assayed by RIA and bioassay.

The statistical significance of the differences in the rates of release of different molecular weight FITC-linked dextrans and the rates of release of insulin exposed to different experimental conditions was established using two factorial ANOVAR (179), performed on a BBC microcomputer.

CHAPTER 3

DEVELOPMENT OF THE METHOD FOR THE PRODUCTION OF MACROPOROUS POLYHEMA BEADS

The main requirement for the production of bead form matrices by freeze-thaw polymerisation is the maintenance of frozen monomer beads in suspension until polymerisation is complete. The medium in which the monomer beads are suspended must be a non-solvent for the matrix monomers and must remain liquid when subjected to the very low temperatures required for freezing the monomer solution. The most suitable non-solvent liquids with these properties are the liquid hydrocarbons and n-hexane, cooled with powdered dry ice (solid CO_2), was the non-solvent used throughout the course of this work.

The basic pieces of equipment required for the production of polyHEMA beads by this method were a robust dewar flask for the safe containment of the hexane and frozen monomer beads at low temperatures, fitted with a low temperature thermometer. An automated delivery device was required to transfer the monomer solution rapidly from a monomer reservoir to the non-solvent as a discrete jet, which would allow the formation of frozen monomer droplets on contact with the cold hexane. It was necessary to stir the hexane in order to maintain the frozen monomer beads in suspension and a high power ultra-violet (UV)lamp was required to effect reliable photopolymerisation of the frozen beads.

The monomer used throughout the course of this work was 2-hydroxyethyl methacrylate (HEMA) crosslinked with ethylene dimethacrylate (EDM). x2 distilled water was the basic solvent used in the production of unloaded beads, containing ethylene glycol (EG) at a ratio of 80:20, H_2O:EG, the latter facilitated the incorporation of EDM without phase separation in the monomer solution and the depression of the freezing point of the solvent phase. For the successful production of macroporous beads it was important that all constituents of the monomer solution should remain in solution until separation of the phases occurred on freezing. Uranyl nitrate (UN) was selected as the photoinitiator since it was known to be water soluble and easily removed from the polymer matrix by washing.

Initial experiments designed to investigate the parameters governing bead size distribution and macromolecule release were carried out using a monomer: solvent molar ratio of 50:50 and a HEMA:EDM molar ratio of 10:1. These values were chosen in order to generate beads with an anticipated equilibrium water content of around 50% with good biocompatibility and an extensive macroporous network. During the course of this work a small change in EDM concentration was effected in order to accommodate a higher or lower solvent concentration whilst avoiding phase separation of the monomer solution these details

have been summarised in Table 1.3, (Page 57).

3.1 THE DEVELOPMENT OF THE METHOD FOR THE PRODUCTION OF MACROPOROUS POLYHEMA BEADS

For initial investigations into the method of production of macroporous polyHEMA beads and the parameters important in their fabrication, a basic experimental system was designed using the simple equipment illustrated in Figure 3.1. The production system was constructed and operated in a fume cupboard. Modifications were then made to this basic system to optimise bead production. The aim of the investigation was to develop a reproducible fabrication process, which would give a high yield of macroporous beads, of good spherical shape, within a predictable size range. Many modifications were made to the basic system as the fabrication technique evolved.

The non-solvent, hexane, was cooled to a temperature of -70°C by the addition of powdered dry ice. The temperature was checked routinely since it tended to increase during the polymerisation process, under the influence of heat generated by the UV lamp (250W. 250V, 3 pin glass type. Osram GEC ME/D). The quantity of each constituent of the monomer solution required to make one batch of beads with a HEMA:EDM molar ratio of 10:1 and monomer:solvent ratio of 50:50, have been

FIGURE 3.1: Basic experimental bench system for the production of macroporous polyHEMA beads.

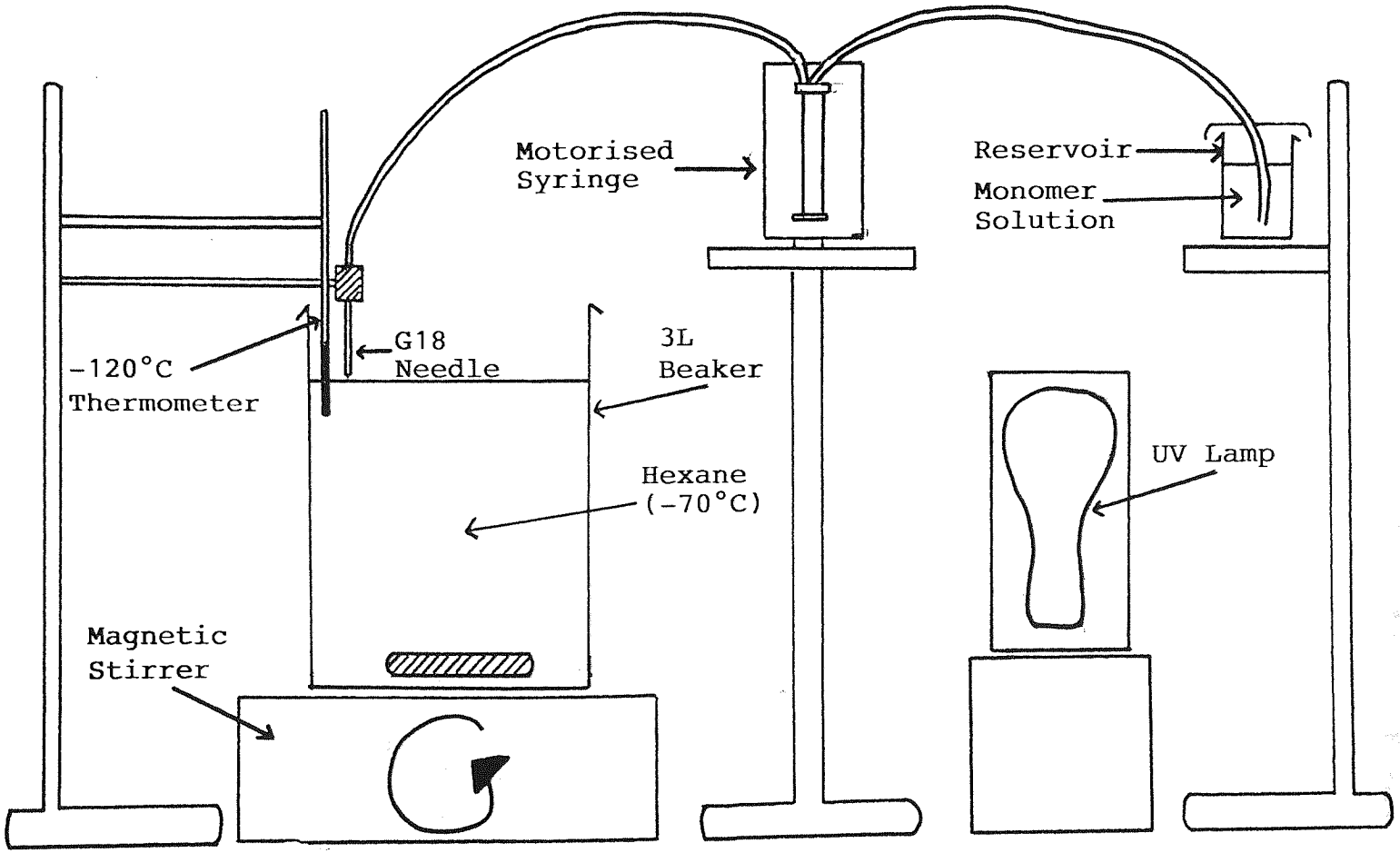

summarised in Table 2.1, (Page 79). 1.526g of EDM was added to 10.035g of HEMA and the two mixed. 2.312g of EG was combined with 9.249g of H_2O and this solvent phase mixed with the monomers. 0.251g (2%) of UN was dissolved in the monomer solution and the whole transferred to the monomer reservoir. A Fison's motorised syringe (type LFA/10) was initially used for the rapid delivery of the monomer solution. In order to deliver the monomer solution to the surface of the hexane as a discrete jet, a G18 needle was attached to the exit tubing from the motorised syringe and clamped close to the surface of the hexane. The hexane was stirred continuously by means of a magnetic stirrer and follower. The monomer solution was ejected into the hexane at the rate of 1.7ml/sec.

Polymerisation of the stirred, frozen droplets was effected with a compact UV light source, positioned 30cm away from the 3L beaker. Immediately after use the delivery system nozzle and tubing were thoroughly washed out with water to remove any residual monomer solution and prevent blockage. After 1½ hours polymerisation was judged to be complete and the product was harvested by decanting off the hexane through a 100µm mesh sieve. The hexane was then filtered and stored for subsequent reuse.

No satisfactorily shaped beads were produced by this means. This was because, during delivery, the jet of monomer solution hit the bottom of the beaker and formed a thick, frozen 'mat' which impeded the movement of the magnetic follower and encouraged further build up of fused polymer. It was clear that the 3L beaker was too small a vessel for use with the Fison's motorised syringe and the magnetic stirrer and follower proved to be an inadequate means of stirring. The contents of the 3L beaker was also subject to great fluctuations in temperature due to lack of thermal insulation.

The 3L beaker was replaced with a large vacuum sealed, double walled dewar flask with a capacity of 7L. The magnetic stirrer was replaced with a stirrer rod, powered by a Citenco motor (type KQPS/21 200-250V 60W), capable of stirrer speeds of between 100 and 600 rpm. The stirrer rod was fitted with an anchor shaped glass paddle, a style found to be optimal for bead formation by Atwal (180). The rest of the equipment used in the basic system was retained. Bead production, using this modified system, was carried out using stirrer speeds of 100, 150 and 300 rpm.

No problems of 'mat' formation were encountered but very few polymer beads were produced at any of the stirrer speeds. At 300 rpm large amounts of debris

were harvested, comprised of small threads of polymeric material suspended in hexane. This was presumably the result of the high stirrer speed causing a break-up of the frozen particles. When the stirring speed was reduced to 100 rpm most of the product proved to be polymeric debris, containing small clumps of fused beads. This suggested that the stirrer speed was too slow to keep the beads apart. Increasing the stirrer speed to 150 rpm did result in a small number of beads, with an average diameter of 350µm, although the bulk of the product consisted of thread-like debris.

The Fison's motorised syringe produced an intermittent, 'spurting' delivery due to air locks in the feed line and this was judged to be the cause of much of the polymer debris. The Fison's motorised syringe was subsequently replaced by more reliable delivery systems. During bead fabrication, the 7L dewar flask was found to be extremely cumbersome, harvesting polymer beads by decanting off the cold hexane proved very difficult and could not be accomplished with safety. In order to facilitate harvesting a smaller purpose built dewar flask (5L) was designed and constructed. The dewar was fitted with a spring loaded exit tap at its base, a lower 'skirt' to improve stability and improved vacuum between the inner and outer walls. This prevented the

hexane warming up too quickly under the influence of the high power UV lamp and thus minimised the effervescence of cold hexane on the addition of powdered dry ice during polymerisation. The 5L dewar was of sufficient depth to allow high speed delivery of the monomer solution without the problem of 'mat' formation. It also allowed the fabrication of large batches of beads, whilst retaining the ease of harvesting associated with a smaller, manageable vessel.

3.2 PARAMETERS AFFECTING THE SIZE DISTRIBUTION OF POLYHEMA BEADS

Preliminary experiments confirmed that a discrete, continuous jet of monomer solution was required for the production of bead form matrices. In addition, a sufficiently high stirrer speed was required to maintain the frozen monomer beads in suspension without fracture or clumping, until polymerisation was complete. Further work was conducted to establish more precisely, the contributions made by the rate of delivery of the monomer solution, the influence of stirrer speed and the ratio of monomer to solvent on the gross morphology, size distribution and total yield of the polymer beads. These experiments were also designed to assist in the establishment of an automated bench-scale manufacturing process which would ensure reproducible bead size ranges and yields and provide an optimal system for the production of

bead formed polyHEMA matrices. A summary of the various parameters investigated is shown in Table 3.1.

Table 3.1 A summary of the different delivery speeds, stirrer speeds and monomer:solvent ratios used in evaluating the size distribution of polyHEMA beads.

Dispenser	Delivery Speed (ml/sec)	Stirrer Speed (rpm)	Monomer: Solvent Ratio
Watson/Marlow Peristaltic Pump	0.3	150	50:50
Watson/Marlow Peristaltic Pump	0.3	200	50:50
Brand dispenser Speed I	7.1	300	50:50
Brand dispenser Speed I	7.1	250	50:50
Brand dispenser Speed IV	9.8	250	50:50
Brand dispenser Speed IV	9.8	400	50:50
Brand dispenser Speed IV	9.8	300	50:50
Brand dispenser Speed IV	9.8	300	40:60
Brand dispenser Speed IV	9.8	300	60:40

3.2.1 Use of a Watson/Marlow peristaltic pump for the delivery of monomer solution.

The use of a Watson/Marlow peristaltic pump was considered for the delivery of monomer solution. This pump provided a slow, continuous delivery of 0.3ml/sec without aeration, using autoanalyser tubing (2.05mm ID) and led to a greatly reduced debris formation. Bead fabrication was carried out at stirrer speeds of 150 and 200 rpm. In all experiments, polymerisation, harvesting and bead size range determination were carried out as described in Chapter 2 for the definitive method of bead production. (Pages 78-85).

The mean bead size (µm) distributions obtained using the peristaltic pump are shown in Figure 3.2. The size distributions obtained proved to be reproducible with a mean yield of >90%. Using a stirrer speed of 150 rpm there was an overall significant difference ($P<0.001$) between the proportions of beads in each size category and all proportions in each size category were found to be significantly different from each other ($P<0.001$). Most beads (55.8%) generated were greater than 1700µm in diameter whilst the smallest percentage of total yield was represented by 355-500µm beads (2.1%), Figure 3.2. When the stirrer speed was increased to 200 rpm there was an overall significant difference in the percentage of beads in each size category ($P<0.001$). There was, however no significant difference between the proportion of beads

FIGURE 3.2: The effect of stirrer speed on the mean size distribution of beads produced using the penstaltic pump at a delivery speed of 0.3ml/sec. (Mean values ± SEM, n=6).

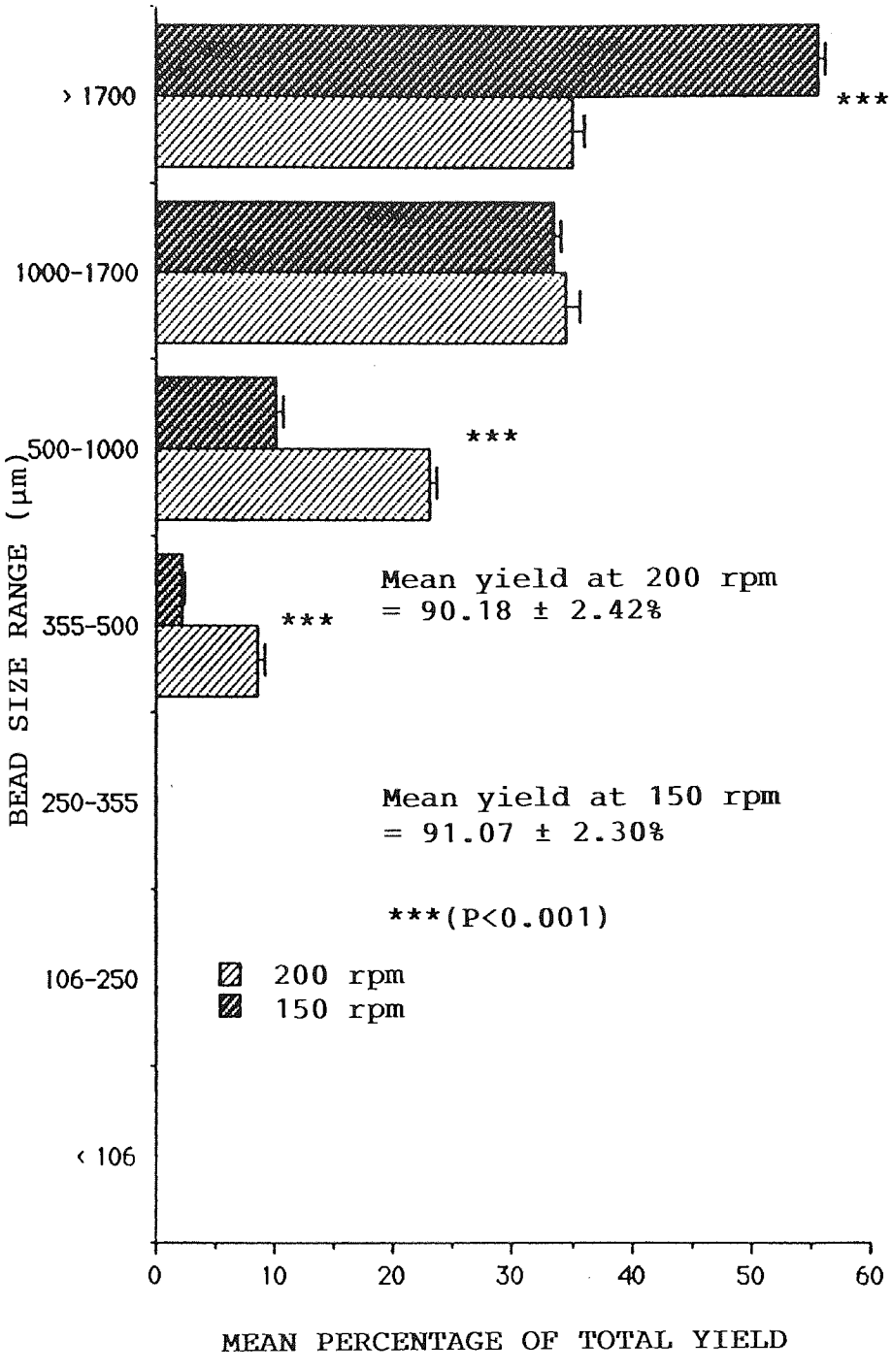

greater than 1700µm in diameter (35.4%) and the proportion of beads in the 1000-1700µm category (34.7%). The remaining two size categories (500-1000 and 355-500µm) contained significantly fewer beads than were found in the size range >1700µm and 1000-1700µm ($P<0.001$). The smallest proportion (8.6%) of the total yield appeared in the 355-500µm size category ($P<0.001$), Figure 3.2.

Increasing the stirrer speed from 150 - 200 rpm significantly increased the proportion of beads in the 355 - 500 and 500 - 1000µm categories ($P<0.001$), Figure 3.2, but reduced the proportion of large beads (>1700 µm). However, increasing the stirrer speed did not significantly influence the proportion of beads in the 1000 - 1700µm category. When using the peristaltic pump, there was a tendency to produce large beads, 1 - 3mm in diameter. Few of these beads were spherical, most were irregular in shape and many were 'pear shaped' possessing well defined projecting 'tails'. These 'tails' were formed when the large droplets of monomer, produced by the very slow delivery speed of the peristaltic pump, did not freeze instantaneously on contact with the cold hexane. This resulted in monomer droplets travelling down and around the flask before freezing, causing distortion of the bead shape. The tails tended to break from the beads increasing the proportion of debris. A stirrer

speed of 150 rpm was not adequate to keep the beads separated in the cold hexane during polymerisation. This led to the clumping of beads and their subsequent retention in the 1700µm mesh sieve. Increasing the stirrer speed to 200 rpm, increased the depth of the stirrer vortex and improved the separation of beads, reducing the proportion in the >1700µm size category.

These initial experiments suggested that stirrer speed was an important parameter which affected both the integrity and size distribution of the beads produced. More specifically, the stirrer speed appeared to have a pronounced effect on the proportion of beads generated at the two extremes of the size range distribution. Due to the production of large beads of irregular shape, the peristaltic pump was considered to be inappropriate for bead formation. Indeed, a means of delivery was required which would generate relatively smaller, spherical beads, over a variable, yet reproducible size range. The peristaltic pump was subsequently replaced with a 'Brand Multispenser' automatic dispenser.

3.2.2. Use of a 'Brand Multispenser' automatic dispenser for the delivery of monomer solution.

The 'Brand Multispenser' automatic dispenser provided a more rapid delivery of the monomer solution than any other delivery system used previously in this work.

The speed of delivery could be precisely controlled using four speed settings and calibration was carried out using a fixed (20ml) volume of water. The actual delivery speeds were calculated as shown in Table 3.2 below:-

Table 3.2: Calibration of the delivery speed using the 'Brand Multispenser' automatic dispenser.

Speed Setting	n=	Mean Time to Dispense 20ml water (sec)	Mean Delivery Speed ± SEM (ml/sec)
I	20	2.80	7.10 ± 0.03
II	20	2.50	8.0 ± 0.02
III	20	2.30	8.73 ± 0.02
IV	20	2.04	9.80 ± 0.03

PolyHEMA beads were generated using the fabrication process previously described (Pages 78-85) incorporating the Brand dispenser, set at a delivery speed setting of I (7.1ml/sec) or IV (9.8ml/sec). The monomer solution was dispensed in 10ml aliquots, perpendicular to the plane of the surface of the hexane, ensuring that the delivery nozzle was placed as close to the surface of the hexane as possible, without freezing the monomer solution in the tip of the tube. The stirrer motor speed was varied over the range 250 - 400 rpm, Table 3.1, (Page 163).

Figure 3.3 shows the effect of stirrer speed on the mean size distribution of beads produced using the Brand dispenser set at delivery Speed I (7.1 ml/sec). There were overall significant differences ($P<0.001$) between the proportions of beads produced in each size category at speeds of 250 and 300 rpm. At a stirrer speed of 250 rpm each size category was significantly different ($P<0.001$), from the next and the following bead distribution was produced according to the scheme below:

1000-1700μm > 500-1000μm > >1700μm > 355-500μm > 106-250μm

No beads smaller than 106μm were generated at this stirrer speed, Figure 3.3. Beads harvested in the >1700μm (13%) category were actually fused clumps of smaller beads that had not been separated by the 250 rpm stirrer speed. When the stirring speed was increased to 300 rpm a markedly different size distribution was obtained, Figure 3.3. The proportions of beads in each size range were significantly different from each other ($P<0.001$). A stirrer speed of 300 rpm generated the following bead size distribution;

500-1000μm > 355-500μm > 250-355μm > 106-250μm > 1000-1700μm > <106μm > >1700μm

FIGURE 3.3: The effect of stirrer speed on the mean size distribution of beads produced using the Brand dispenser at delivery speed I. (7.1ml/sec). (Mean Values ± SEM, n=6).

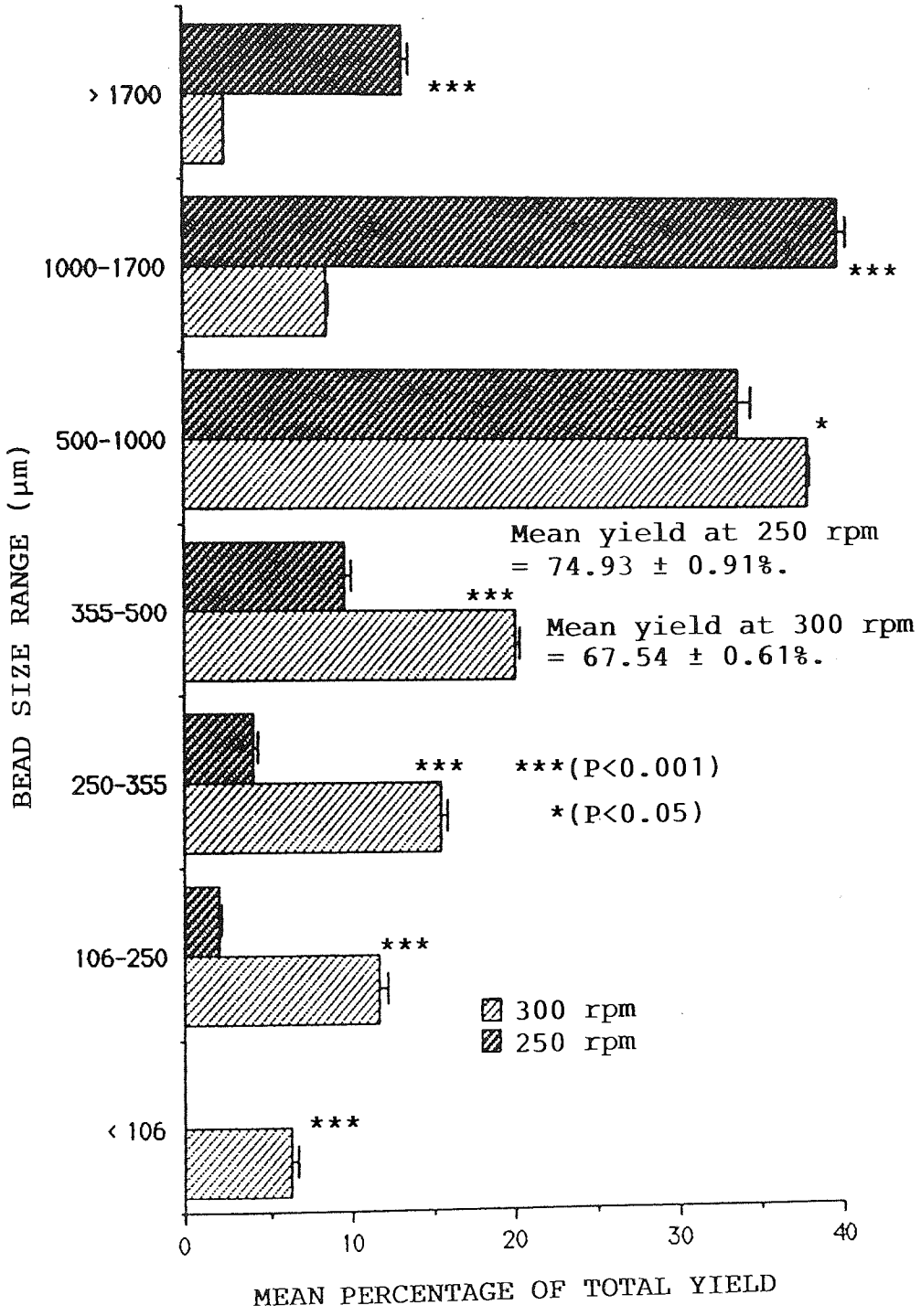

Bead clumping was eliminated and few (2.3%) very large beads were produced (>1700µm) because the stirring speed was sufficiently fast to stop the coagulation of smaller beads prior to polymerisation. In contrast to the profile obtained with a stirrer speed of 250 rpm, material was also harvested in the <106µm category (6.2%) Figure 3.3. This was not made up of beads but rather consisted of threads of debris, possibly caused by the collision of beads when subjected to the higher stirrer rate.

Significantly higher proportions of beads were obtained in the lower size ranges (<106- 500-1000µm) using the 300 rpm stirrer speed as shown in Figure 3.3 and hence increasing the stirrer speed from 250 to 300 rpm decreased the proportion of larger beads. No significant difference was found between the mean total bead yields obtained with each stirrer speed. In order to change the bead size distribution and to investigate further the effects of stirrer speed and delivery speed on the bead size distribution the delivery speed was increased to 9.8ml/sec (Speed IV). Figure 3.4.

There were significantly ($P<0.001$) different proportions of beads in the different size categories at stirrer speeds of both 250 and 300 rpm with the new delivery speed. At a stirring speed of 250 rpm all

FIGURE 3.4: The effect of stirrer speed on the mean size distribution of beads produced using the Brand dispenser at delivery speed IV. (9.8ml/sec). (Mean values ± SEM, n=9).

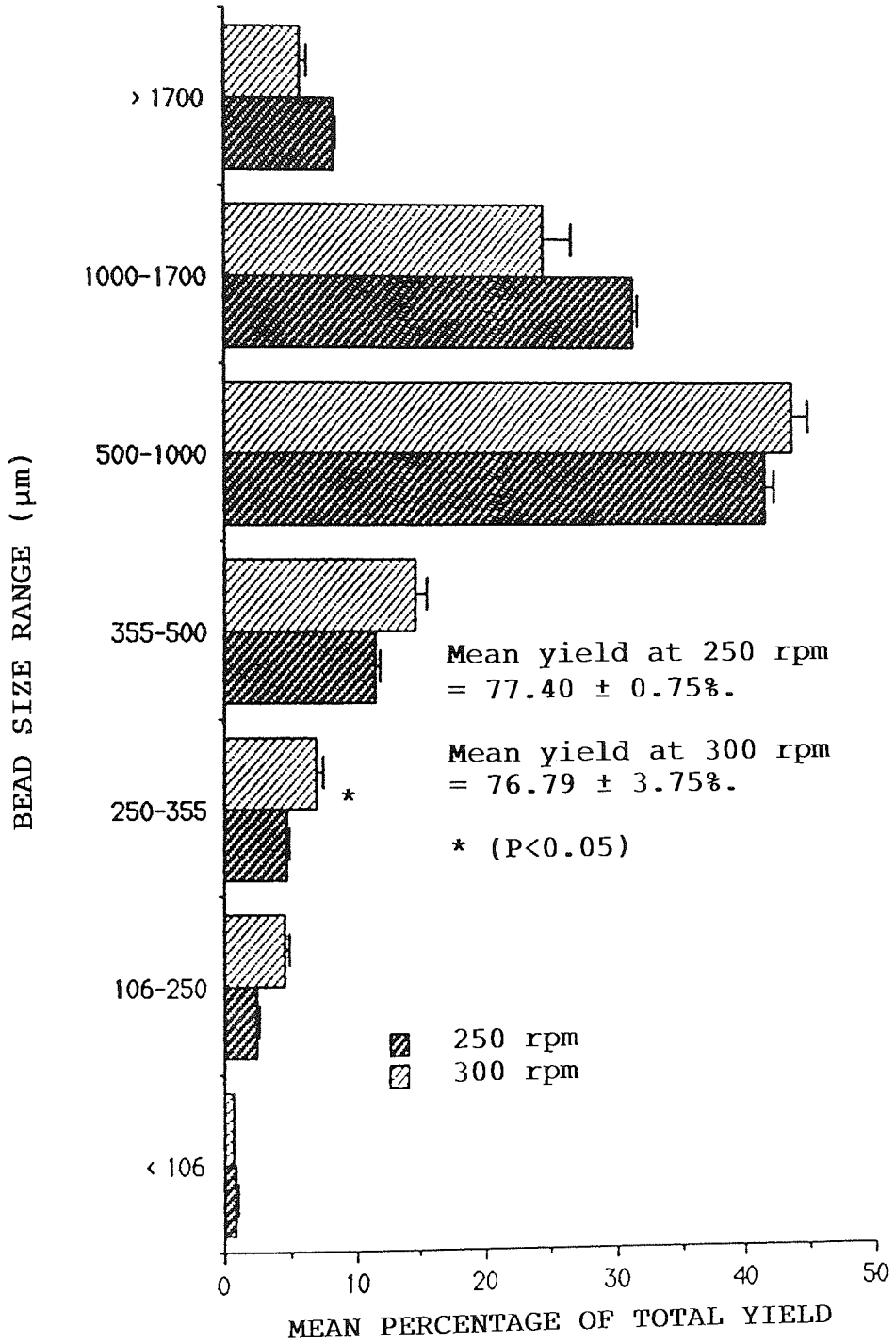

bead categories contained significantly different proportions of beads according to the following distribution:

500-1000µm >1000-1700µm >355-500µm >>1700µm >250-355µm >106-250µm ><106µm.

Using a stirrer speed of 300 rpm beads were produced in the categories according to the following scheme

500-1000µm >1000-1700µm >355-500µm >250-355µm = 106-250µm = >1700µm > <106µm.

No significant difference was observed between the mean total bead yields obtained at stirrer speeds of 250 and 300 rpm with speed setting IV on the Brand dispenser.

Increasing the stirring speed from 250-300 rpm significantly ($P<0.05$) increased the proportion of beads in the 250-355µm category alone, from 4.7 to 6.9% as shown in Figure 3.4. The difference in stirrer speed was probably too small to influence the bead size distribution in the larger bead size categories. At 300 rpm some clumping of beads was observed in the larger size categories, but very little debris (<106µm category) was produced (0.7%). The beads were generally discrete and spherical and 300 rpm was

subsequently taken as the optimum stirrer speed for a monomer solution delivery rate of 9.8 ml/sec.

The stirrer speed was increased to 400 rpm at delivery Speed IV (9.8ml/sec) in an attempt to eliminate the clumping of beads in the larger size categories and alter the size distribution to provide a greater proportion of small beads. The results of this manoeuvre are summarised in Figure 3.5. There were significant differences between the proportions of beads in each size category using a stirrer speed of 400 rpm ($P<0.001$). The proportions of beads in each size category showed the following distribution:

500-1000μm >355-500μm >250-355μm = 1000-1700μm >106-250μm = <106μm > >1700μm

There was a significant increase ($P<0.001$) in the proportion of beads in the smaller size categories (<106 - 355-500μm) when the stirrer speed was increased from 300 to 400 rpm and a decrease ($P<0.001$) in the proportion in the larger bead categories (1000-1700μm - <1700μm) as shown in Figure 3.5. Increasing the stirrer speed to 400 rpm did not significantly change the mean total bead yield. However, at this higher stirrer speed a larger proportion of debris (6.8%) was produced, in the <106μm category. The increased stirrer speed led to surface abrasion and

FIGURE 3.5: The effect of stirrer speed on the mean size distribution of beads produced using the Brand dispenser at delivery speed IV. (9.8 ml/sec). (Mean values ± SEM, n=9).

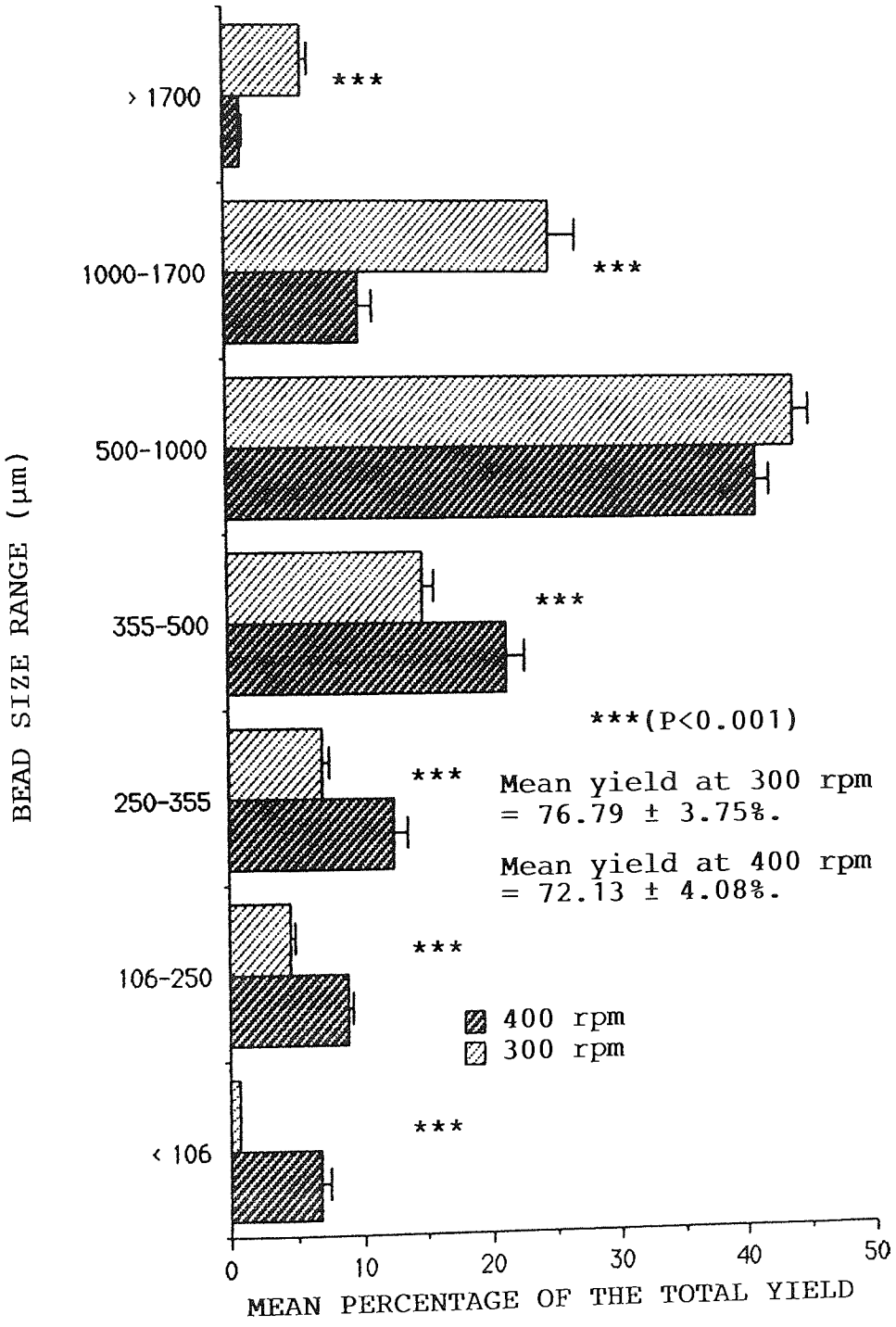

FIGURE 3.6: The effect of stirrer speed on the mean size distribution of beads produced using the Brand dispenser at delivery speed IV. (9.8ml/sec). (Mean values ± SEM, n= 9).

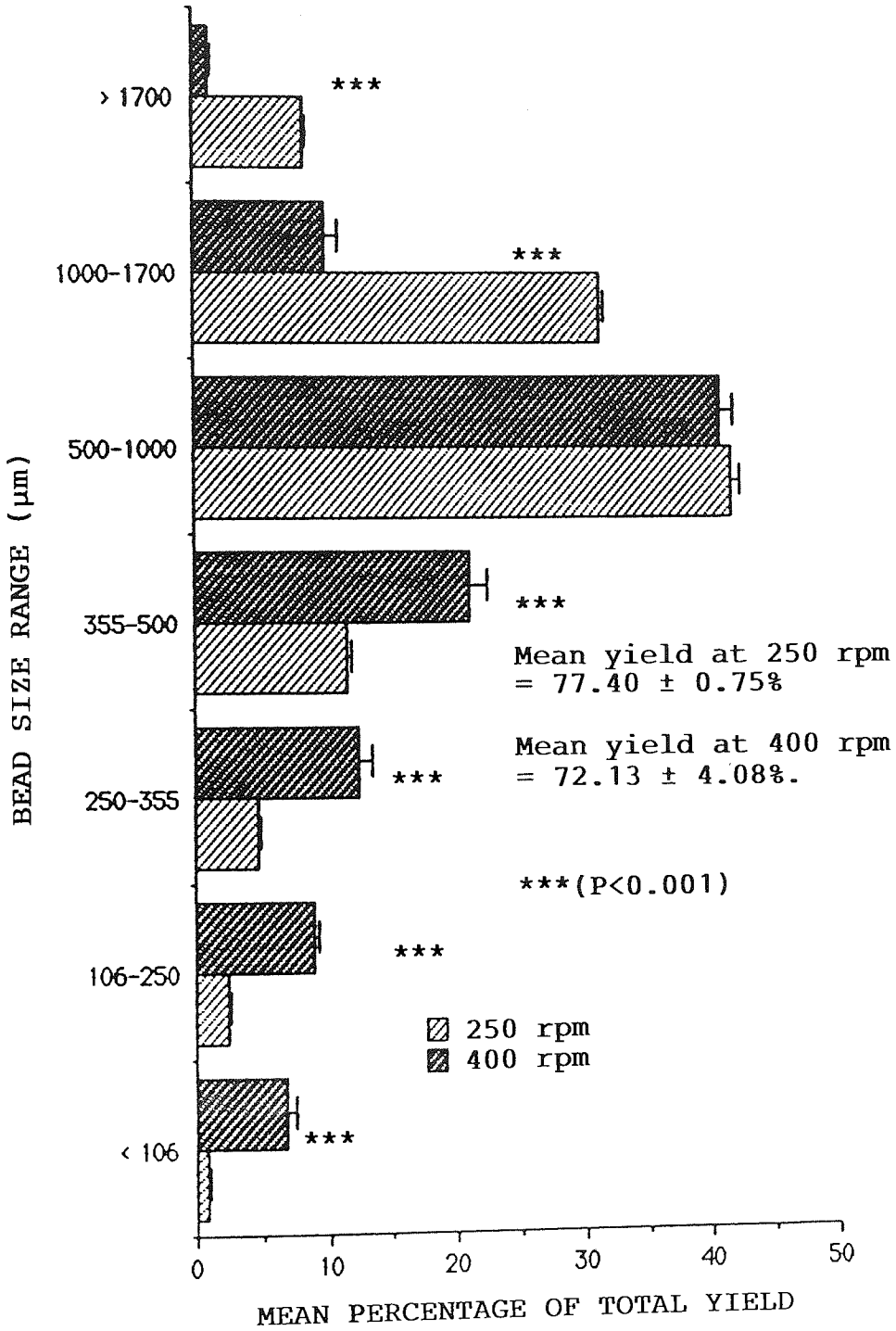

the breaking up of some of the frozen monomer droplets.

Increasing the stirrer speed did not significantly influence the proportion of beads in the 500-1000μm category Figure 3.5. This confirmed earlier observations suggesting that alteration in the stirrer speed only tended to influence the proportion of beads in the low and high size ranges. This effect is confirmed when the mean size distributions of beads obtained at 250 and 400rpm at a delivery speed of 9.8ml/sec are compared in Figure 3.6. It was therefore concluded that stirrer speed had a significant effect upon the size distribution and integrity of the beads produced but no significant effect on the mean total bead yield obtained.

In order to determine if the speed of delivery of the monomer solution was an important parameter influencing the size distribution of the beads generated, the speed of delivery was investigated at 7.1ml/sec (Speed I) and 9.8ml/sec (Speed IV) whilst the stirrer speed was maintained at 250 rpm as shown in Figure 3.7. Increasing the delivery speed from 7.1 to 9.8ml/sec significantly decreased the proportion of larger beads, in the 1000-1700μm - >1700μm categories but generally had no significant effect on the

FIGURE 3.7: The effect of delivery speed on the mean size distribution of beads produced using the Brand dispenser and a stirrer speed of 250 rpm. (Mean values ± SEM, n= 6).

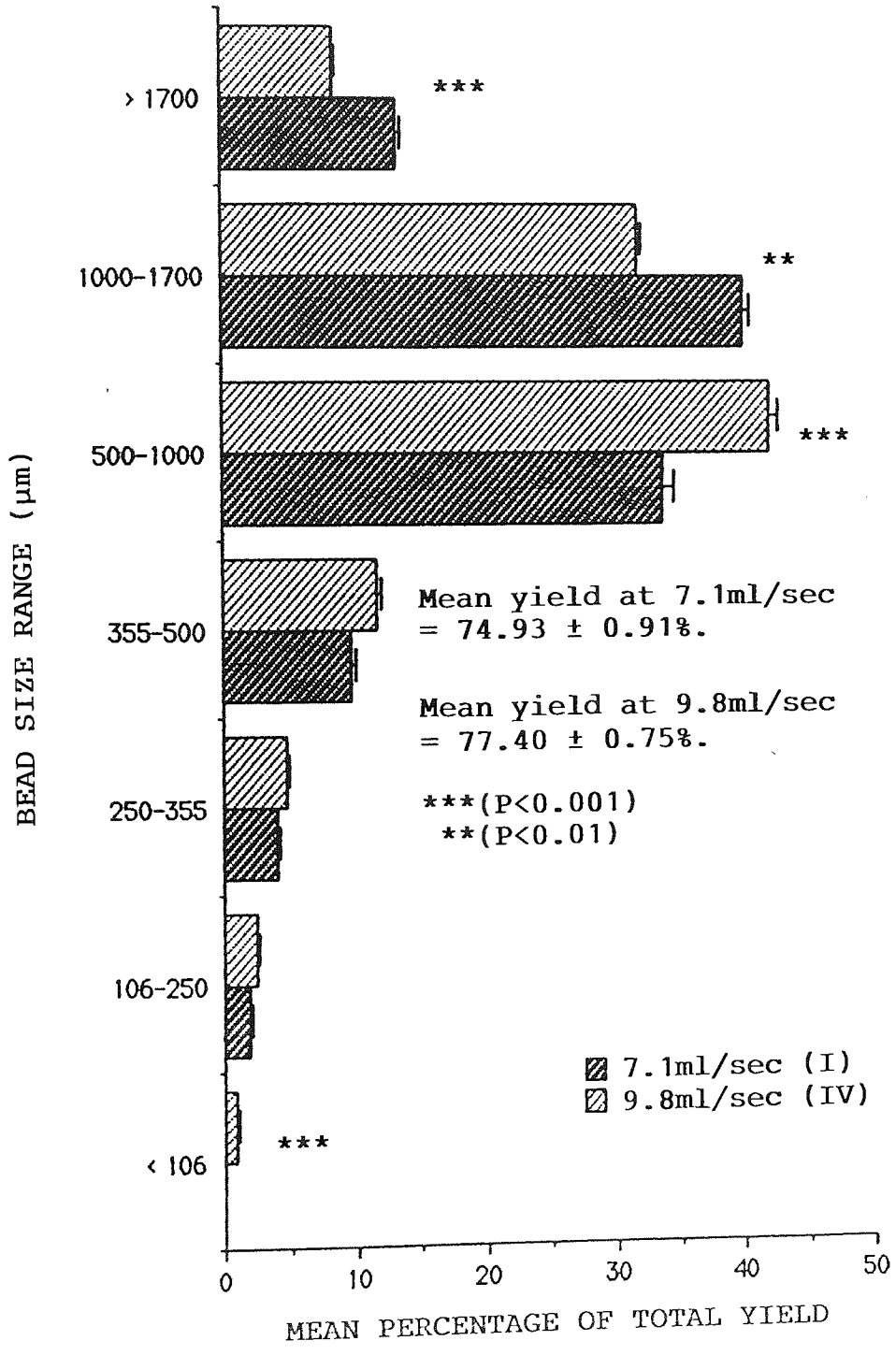

proportions of beads generated in the middle size ranges (<106-250-355-500μm). However, there was a significantly increased proportion of 500-1000μm and <106μm beads, Figure 3.7, when the delivery speed was increased to 9.8ml/sec.

Clumping of beads was not observed using the higher delivery speed. It appears that the fast delivery causes the jet of monomer solution to break up into small droplets, reducing the propensity to clumping at slow stirrer speeds and in turn significantly increasing the proportion of beads in the 500-1000μm size range. Increasing the delivery speed did not significantly influence the total mean bead yield, Figure 3.7.

When the stirrer speed was increased to 300 rpm the rate of delivery took on greater significance as regards the integrity of the beads produced. A delivery speed of 7.1ml/sec (Speed I) was too slow and a large amount of polymeric debris (<106μm, <5% total yield) was produced, Figure 3.8. A delivery speed of 9.8ml/sec (Speed setting IV), was more suited to a stirrer speed of 300 rpm with a much reduced production of debris and a bias towards the production of larger bead sizes, Figure 3.8.

Since altering stirrer speed and delivery speed did not significantly influence the total yield of beads

FIGURE 3.8: The effect of delivery speed on the mean size distribution of beads produced using the Brand dispenser and a stirrer speed of 300 rpm. (Mean values ± SEM, n=6).

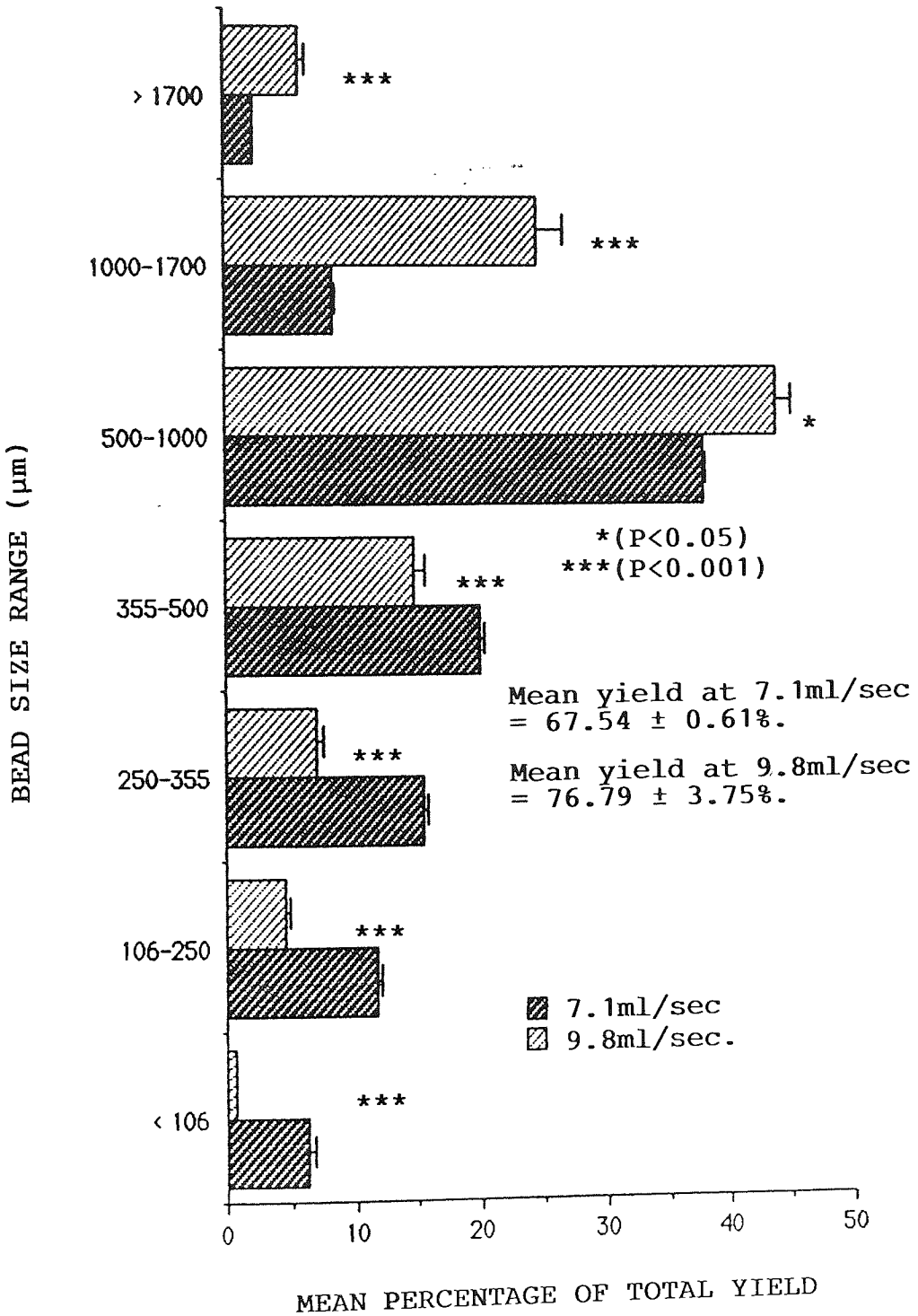

produced using the Brand dispenser, the mean total bead yield was not an important criterion for the determination of the optimum conditions of bead production. The reproducibility of the bead size profile, as judged by the size and variation in the standard error of the mean (±SEM) for each bead category proved to be good. A delivery speed of 9.8ml/sec (Speed IV) and a stirrer speed of 300 rpm was chosen for future bead production since the bulk of the yield was obtained in the middle size ranges and little debris was harvested. This enabled much of the bead harvest to be used in experimental work and little was discarded.

During the course of this development work the monomer:solvent ratios were altered to investigate the effects of monomer and solvent concentration on the macroporosity of the matrix and the release rates of incorporated macromolecules. In order to investigate the effect of monomer:solvent ratio on the bead size distribution, unloaded beads were fabricated, using standard conditions, ie. a delivery speed of 9.8ml/sec (Speed IV), a stirrer speed of 300 rpm and monomer:solvent ratios of 40:60, 50:50 and 60:40. Changing of the monomer:solvent ratio over the range 50:50, 40:60 and 60:40 had no significant effect on either the proportion of beads in each size category or the total mean bead yield, Figure 3.9.

FIGURE 3.9: The effect of monomer:solvent ratio on the mean size distribution of beads produced using the Brand dispenser at speed setting IV (9.8ml/sec) and a stirrer speed of 300 rpm. (Mean values ± SEM, n=9).

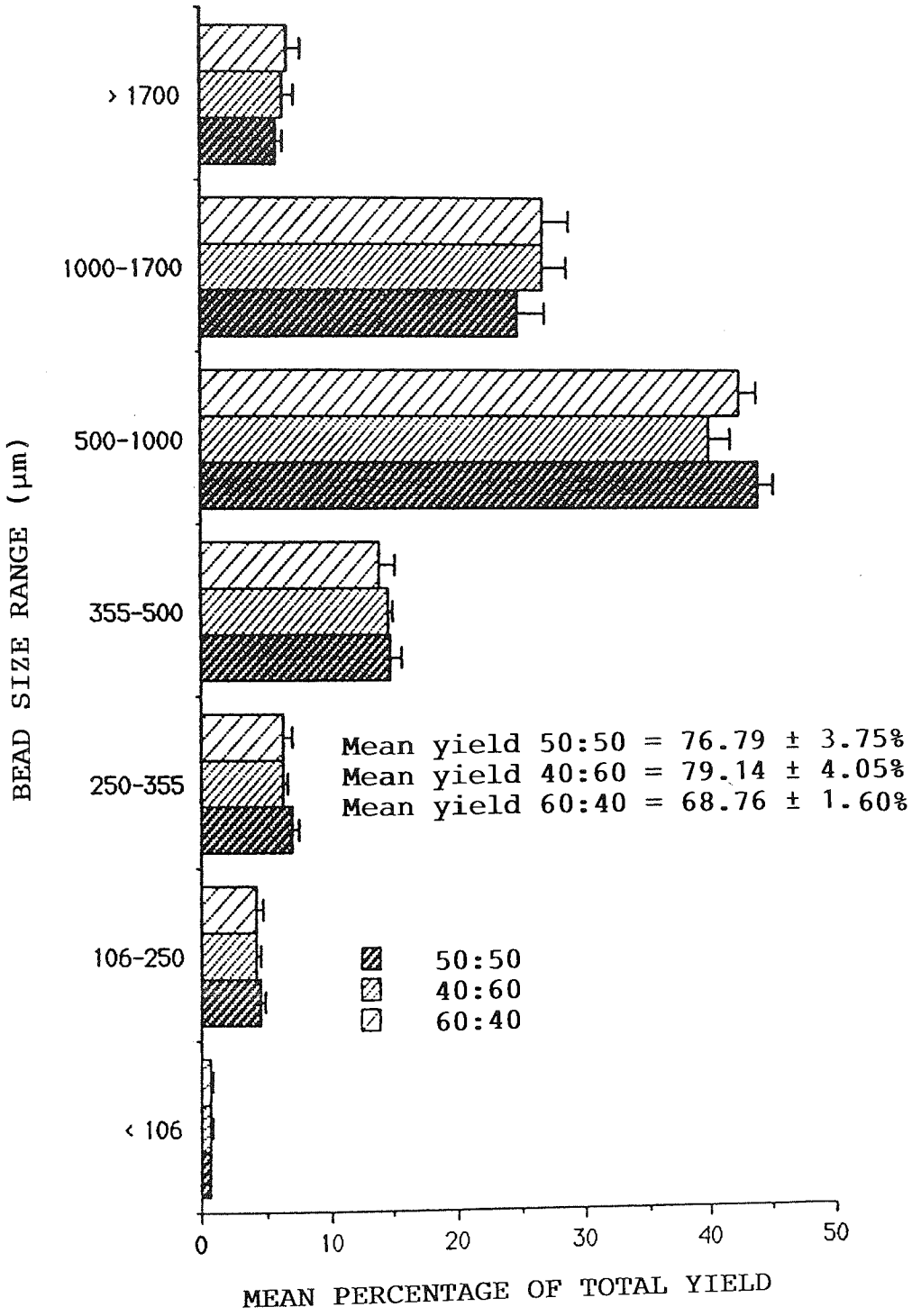

3.3 THE INCORPORATION OF PHYSIOLOGICAL BUFFERS INTO POLYHEMA BEADS.

In order to incorporate biologically active macromolecules into polyHEMA beads, in solution and in a stable state, they must be incorporated in appropriate physiological buffers which maintain optimal pH and provide the molecule with some protection against hydrolytic degradation. The supporting buffer is required to fulfil a number of criteria depending on the nature of the macromolecule itself and the chemical composition of the monomer solution. The buffer should not react chemically with any constituent of the monomer solution or interfere with either the photopolymerisation process or the formation of the macroporous matrix. A number of buffers were considered to be potentially useful carriers for biologically active macromolecules such as glucose oxidase, insulin and interleukin-2. The buffers selected for study were 0.04M phosphate buffer, 0.2M phosphate buffer and 0.01M sodium acetate/0.12M sodium chloride buffer. Their chemical compositions are given in Appendix A1. All buffers were freshly prepared and adjusted to physiological pH7.4 before use by the addition of either 1M HCl or NaOH as appropriate.

0.04M phosphate buffer pH7.4

This buffer is commonly used as the diluent buffer for the dilution of insulin standards and samples in the

radioimmunioassay of insulin and as such was thought to be suitable for buffering insulin solutions. Since the $H_2PO_4^-$ - HPO_4^{2-} system is a major intracellular buffer, it was considered likely that this buffer would be suitable for the incorporation of a large number of biologically active peptide macromolecules including glucose oxidase and interleukin-2.

0.2M phosphate buffer pH7.4

This buffer has a stronger buffering capacity than 0.04M phosphate buffer and had the capacity to buffer the 1M HCl initially used to take up insulin prior to the preparation of insulin solutions.

0.01M sodium acetate/0.12M sodium chloride buffer pH7.4

This buffer is used in commercially available injectable insulin preparations (Boots).

Bead fabrication was carried out as previously described and the appropriate buffer added as part of the aqueous phase in the monomer solution, ie 9.249g of buffer in a x 1 batch (as described in Table 2.1, Page 79) PolyHEMA beads were generated using the bench scale, standard apparatus as described in Chapter 2 (Pages 78-85). The general appearance of the combined monomer solution containing buffer was noted prior to polymerisation in order to check for signs of phase separation. After fabrication, the proportion

of beads produced in each size category was determined as described (Page 83). The equilibrium water content and morphology of the beads was also recorded. (See Section 3.4, Page 187).

0.2M phosphate buffer pH7.4

The use of 0.2M phosphate buffer in the aqueous phase of the monomer solution resulted in the formation of a white precipitate. Bead fabrication was attempted, but the HEMA failed to polymerise, even after extended (3 hours) exposure to UV light. The phosphate present in the buffer caused the photoinitiator, uranyl nitrate, to precipitate out of solution as uranyl phosphate and this buffer was therefore judged unsuitable for bead manufacture unless used with an alternative photoinitiator.

0.04M phosphate buffer pH7.4

The substitution of 0.04M phosphate buffer for the water content of the aqueous phase also resulted in a small amount of uranyl phosphate precipitation. However, the amount of precipitate was very much reduced and beads were successfully fabricated after an extended photopolymerisation time (3 hours). Despite this, it was concluded that this buffer would be unsuitable for the routine incorporation of peptide macromolecules because the precipitation of uranyl phosphate might lead to an uneven distribution of

inadequately buffered macromolecule in the bead. In addition, nitric acid is a bi-product of the reaction between uranyl nitrate and sodium phosphate and this could lead to the denaturation of the protein in solution.

Since phosphate buffers are widely used as physiological buffers, attempts were made to secure an alternative photoinitiator to uranyl nitrate. Three photoinitiators, known to bring about the successful polymerisation of HEMA, namely, benzoin, phenanthraquinone and benzil, were investigated. The initiators were used at the same concentration in the monomer solution as uranyl nitrate (2%). Benzil failed to bring about the polymerisation of HEMA in the presence of phosphate buffer. Benzoin and phenanthraquinone initiated the polymerisation of the monomer solution containing phosphate buffer. However, neither of these photoinitiators is water soluble and the final product required rigorous washing with dimethyl sulphoxide to remove the residual photoinitiator after polymerisation. Therefore, the distinct advantage of using an easily removable, water soluble photoinitiator, ie uranyl nitrate, would be lost if phosphate buffers were to be employed for peptide incorporation and it was therefore decided to avoid the use of phosphate buffers wherever possible in subsequent experimental work.

0.01M sodium acetate/0.12M sodium chloride buffer pH7.4

No change in the physical appearance of the monomer solution occurred when this buffer was included in the aqueous phase. Photopolymerisation time was not affected and beads were successfully fabricated with characteristic shape and size distribution. This buffer was subsequently used for the incorporation of insulin and other biologically active peptide macromolecules into macroporous polyHEMA beads.

These experiments highlight the importance of testing for chemical compatibility between any additions to the basic formulation and the monomer solution itself. It may be that the addition of buffers or the incorporation of macromolecule may influence the matrix structure of the beads and release kinetics. Each new constituent to the monomer solution may exert a different effect, which must be established. The equilibrium water content of all beads produced was routinely established and an ultrastructural examination of the macroporous matrix was carried out on all beads manufactured.

3.4 CHARACTERISATION OF POLYHEMA BEADS BY MEASUREMENT OF THE EQUILIBRIUM WATER CONTENT AND ULTRASTRUCTURAL EXAMINATION USING SCANNING ELECTRON MICROSCOPY

3.4.1 Equilibrium water content

The Equilibrium Water Content (EWC) of a hydrogel is a very important characteristic since it may influence

the permeability (hence possibly release kinetics), biocompatibility, mechanical and surface properties of the polymer (98). The EWC of all batches of beads was determined routinely by measuring the wet weight of a 7 days fully rehydrated sample of beads (in x2 distilled water), drying to constant weight and re-weighing. The EWC of the polymer was then calculated using the equation below (Chapter 2, Page 85).

$$EWC = \frac{\text{Weight of water in beads}}{\text{Total weight of hydrated beads}} \times 100\%$$

[At 20°C]

Any significant changes in the EWC of batches of beads, loaded or unloaded, generated using different bead formulations was confirmed statistically, using One-way ANOVAR and Newman-Keuls multiple comparison tests. Table 3.3 summarises the mean EWCs of batches of polyHEMA beads produced throughout the course of this work. In each case the EWC values obtained have been compared with those of unloaded beads, fabricated using a monomer:solvent ratio of 50:50, a solvent: ethylene glycol ratio of 4:1 and a HEMA EDM ratio of 10:1 (Standard EWC).

Increasing the proportion of HEMA monomer to solvent in the monomer solution led to a significant decrease in the EWC of the product polymer and vice versa. These observations are consistent with results obtained by other workers and it is well established that the EWC of heterogenous hydrogels is strongly

TABLE 3.3: Effect of monomer solution composition on the EWC of fabricated polyHEMA beads. (Mean values ± SEM). *** = P<0.001.

MONOMER:SOLVENT RATIO	n=	SOLVENT	MACROMOLECULE INCORPORATED	MEAN EWC % ± SEM	EFFECT ON EWC COMPARED COMPARED TO STANDARD
50:50	15	Water	-	60.02 ± 0.13	Standard
40:60	10	Water	-	69.51 ± 0.41	Increased (***)
60:40	10	Water	-	51.79 ± 0.35	Decreased (***)
50:50	15	Sodium acetate/ sodium chloride buffer.	-	71.70 ± 0.92	Increased (***)
50:50	10	Boric acid/ borate buffer.	-	62.34 ± 0.36	-
50:50	12	Water	BSA	57.08 ± 0.23	Decreased (***)
50:50	15	Sodium acetate/ sodium chloride buffer.	Glucose Oxidase	75.76 ± 0.74	Increased (***)
50:50	12	Sodium acetate/ sodium chloride buffer.	Insulin	73.08 ± 1.02	Increased (***)
40:60	12	Sodium acetate/ sodium chloride buffer.	Insulin	76.07 ± 0.69	Increased (***)
60:40	12	Sodium acetate/ sodium chloride buffer.	Insulin	72.44 ± 0.76	Increased (***)
50:50	10	Boric acid/ borate buffer.	FD-150	62.20 ± 0.31	-
50:50	10	Boric acid/ borate buffer.	FD-20S	62.60 ± 0.34	-

dependent on the monomer:solvent ratio (24,99,120).

Boric acid-borate buffer, pH7.4, had no significant effect on the EWC of polyHEMA beads, either alone, or when used to incorporate FITC-linked dextrans. However, the addition of sodium acetate/sodium chloride buffer to the HEMA monomer solution significantly increased the EWC of the product hydrogel. This effect has been shown to be a maximum at low (<0.2M) acetate concentrations (102). It has been suggested that acetate ions are adsorbed onto the polymer network and at low concentrations, the repulsive forces between acetate anions induce network swellings. At higher concentrations of acetate the charges may be shielded from one another, reducing the effect. On the other hand, chloride ions tend to reduce the EWC of polyHEMA, causing a strengthening of hydrophobic bonds in the polymer (102). However, at a concentration of 0.12M (0.7%) sodium chloride, the deswelling effect of the chloride anion is slight (103) and when the two anions are present together it appears that acetate exerts the greater effect, cancelling out the deswelling influence of the chloride ions and producing an overall increase in EWC.

The incorporation of macromolecules (insulin and glucose oxidase) into polyHEMA beads with sodium

acetate/sodium chloride buffer did not significantly affect the EWC of the beads, compared to the EWC of the beads fabricated using buffer alone. Alteration of the monomer solvent ratio had no significant effect on the EWC of beads fabricated with sodium acetate/sodium chloride buffer. The tendancy of the acetate anion to cause matrix swelling was presumably greater than the ability of the solvent concentration to alter the EWC of the polymer.

Loading beads with BSA at a level of 5% of the total matrix weight was found to significantly decrease the EWC of the polymer. The albumin may be acting in an occlusive fashion, blocking the ingress of water. This effect would be exaggerated with high concentrations of albumin which produce viscous solutions in water.

3.4.2 The ultrastructural morphology of macroporous polyHEMA beads determined using scanning electron microscopy.

Stereo scan electron microscopy (SEM) was employed to characterise the surface topography of the polyHEMA beads and to verify the extent and integrity of the macroporous structure. Routine monitoring of beads by SEM, allowed the impact of macromolecule incorporation on bead structure and macroporosity to be assessed. Methods for the processing and preparation of beads for SEM have been described in Chapter 2 (Page 86).

Plate 3.1: Interior of 50:50 monomer:solvent ratio unloaded polyHEMA bead. Mag x 5000.

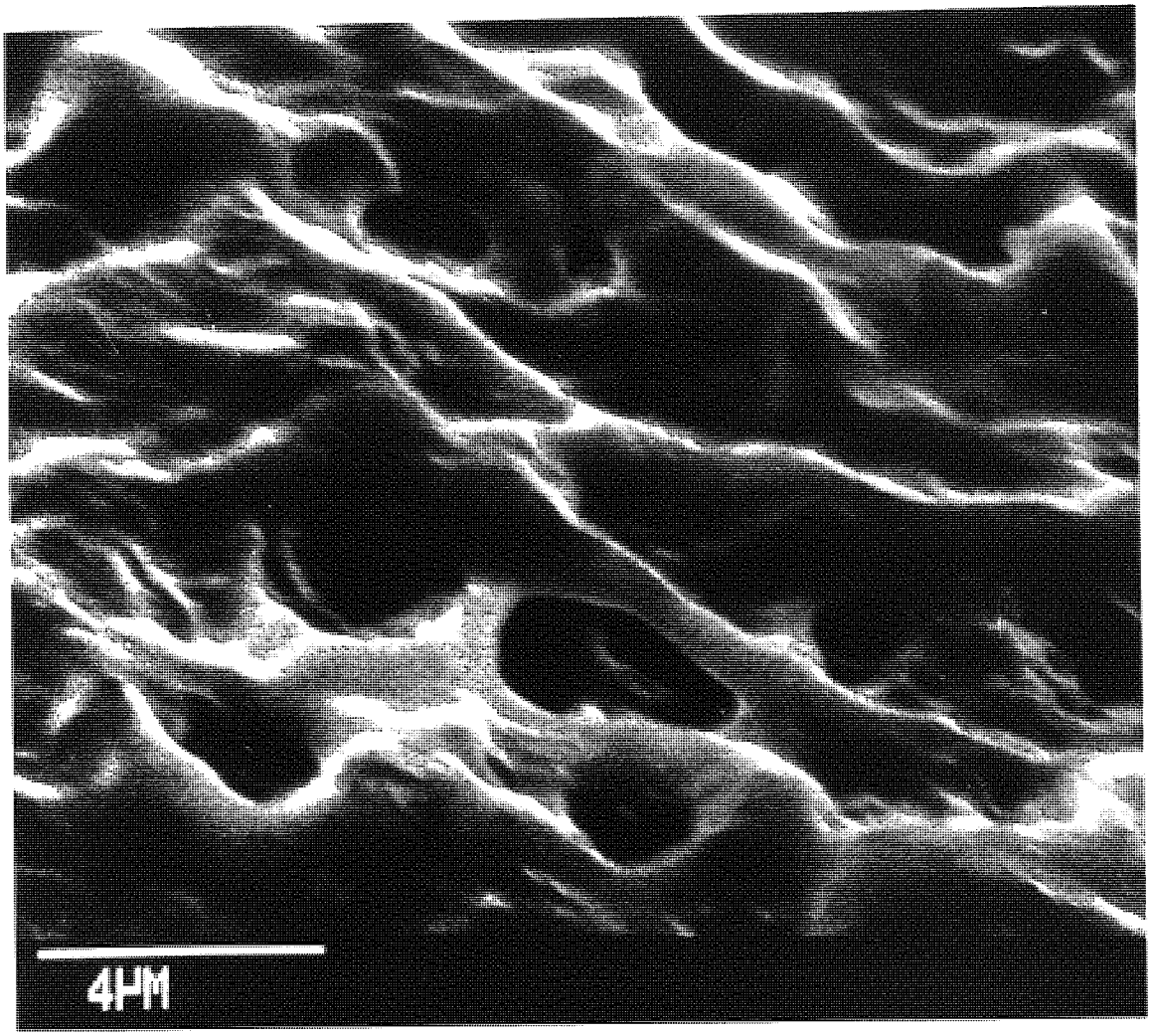

Plate 3.1 shows the macroporous structure of an unloaded bead fabricated using a monomer:solvent ratio of 50:50. The mean pore diameter in the interior of the bead was estimated to be of the order of 1.9μm, although pore sizes ranged from 1.5 to 2.9μm.

Plate 3.2 shows the sponge-like surface topography of a bead of the same composition.

Plate 3.2: Surface topography of 50:50 monomer:solvent ratio unloaded polyHEMA bead. Mag x 100

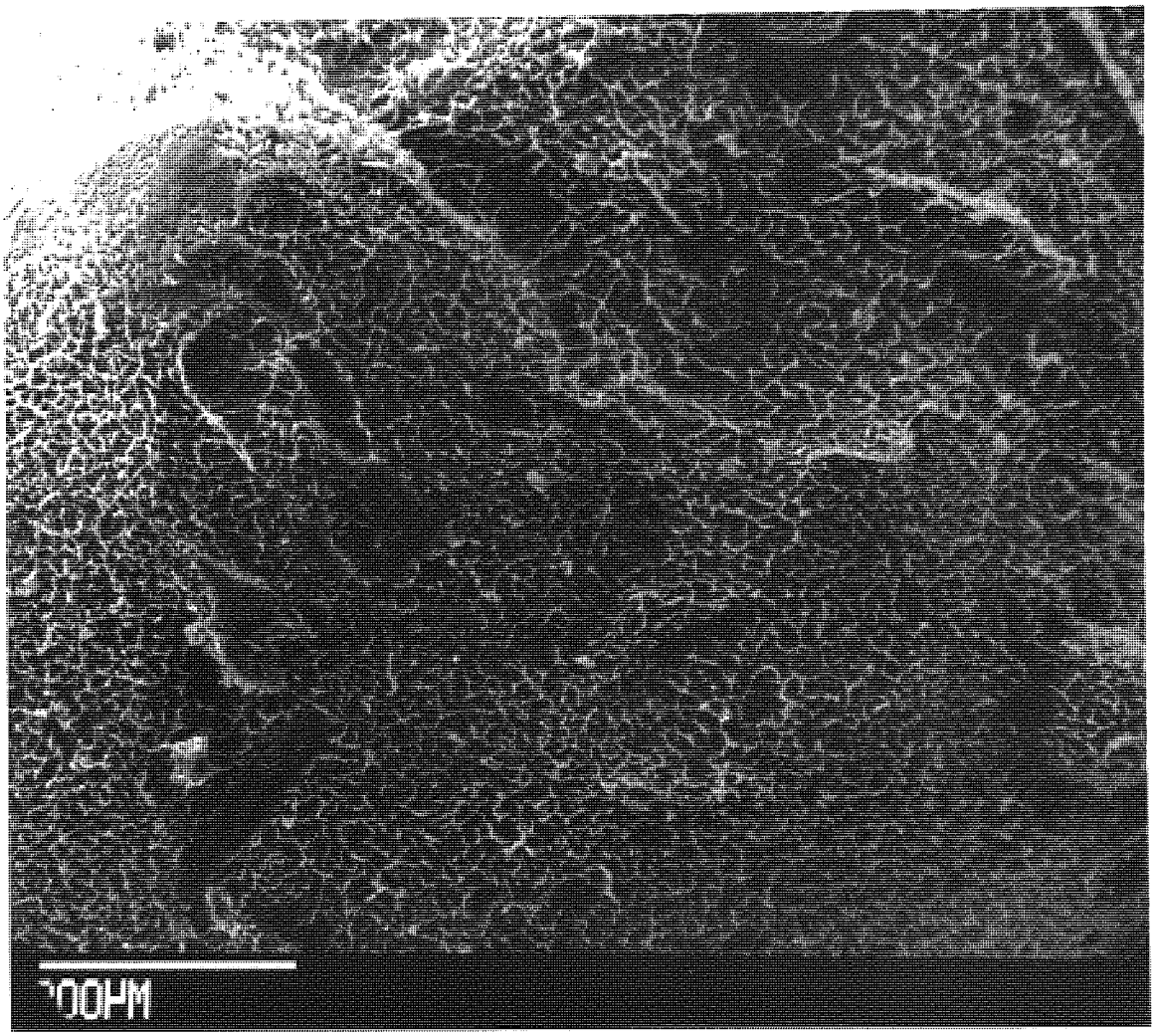

In this case, the magnification was rather too low to allow an accurate assessment of pore size to be made. However, the general appearance of the bead is illustrated, the surface of the bead is rough and undulating and the pores appear to be situated within distinct domains. This is seen more clearly on Plate 3.3 which shows the same bead at a higher magnification.

Plate 3.3: Surface of 50:50 monomer:solvent ratio unloaded polyHEMA bead showing surface pore domains. Mag x 2000.

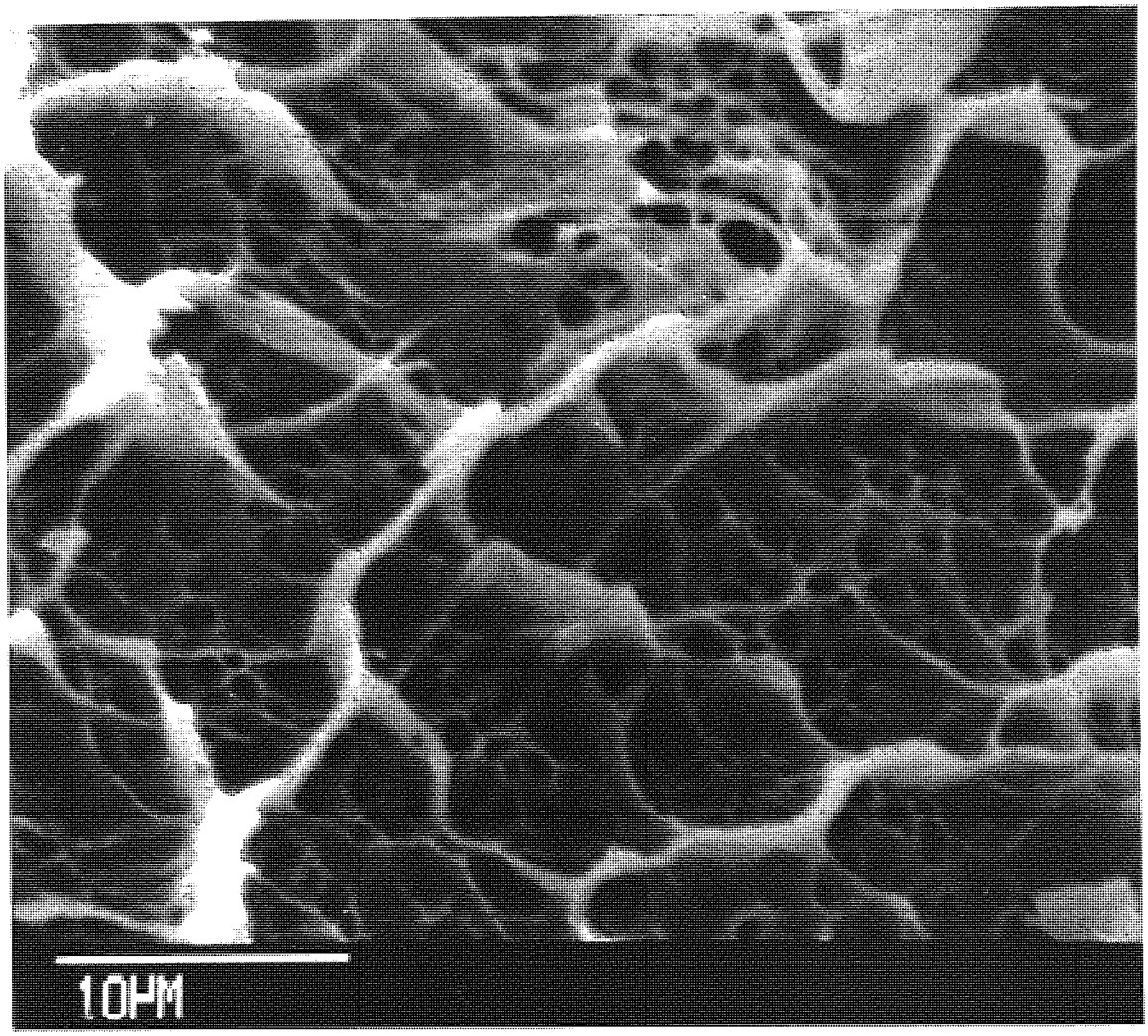

The average pore size was estimated to be 1.4µm with a range of 0.9 - 2.1µm. The pores within the ridged domains at the surface of the bead appear to be less widespread than the continuous pores in the interior. There is some indication that pores at the surface are somewhat smaller than those in the interior (1.4 compared to 1.9µm). It may be that the instantaneous

freezing of the bead on contact with the cold hexane during fabrication may not have allowed sufficient time for complete separation of the monomeric and aqueous phases to occur near the surface, reducing the size and frequency of the pores.

Plates 3.4 and 3.5 illustrate the effect of increasing the proportion of monomer to solvent from 50:50 to 60:40 on the size and extent of the pores at the surface and in the interior of the beads.

Plate 3.4. Interior pores of a polyHEMA bead manufactured using a monomer:solvent ratio of 60:40. Mag x 5000

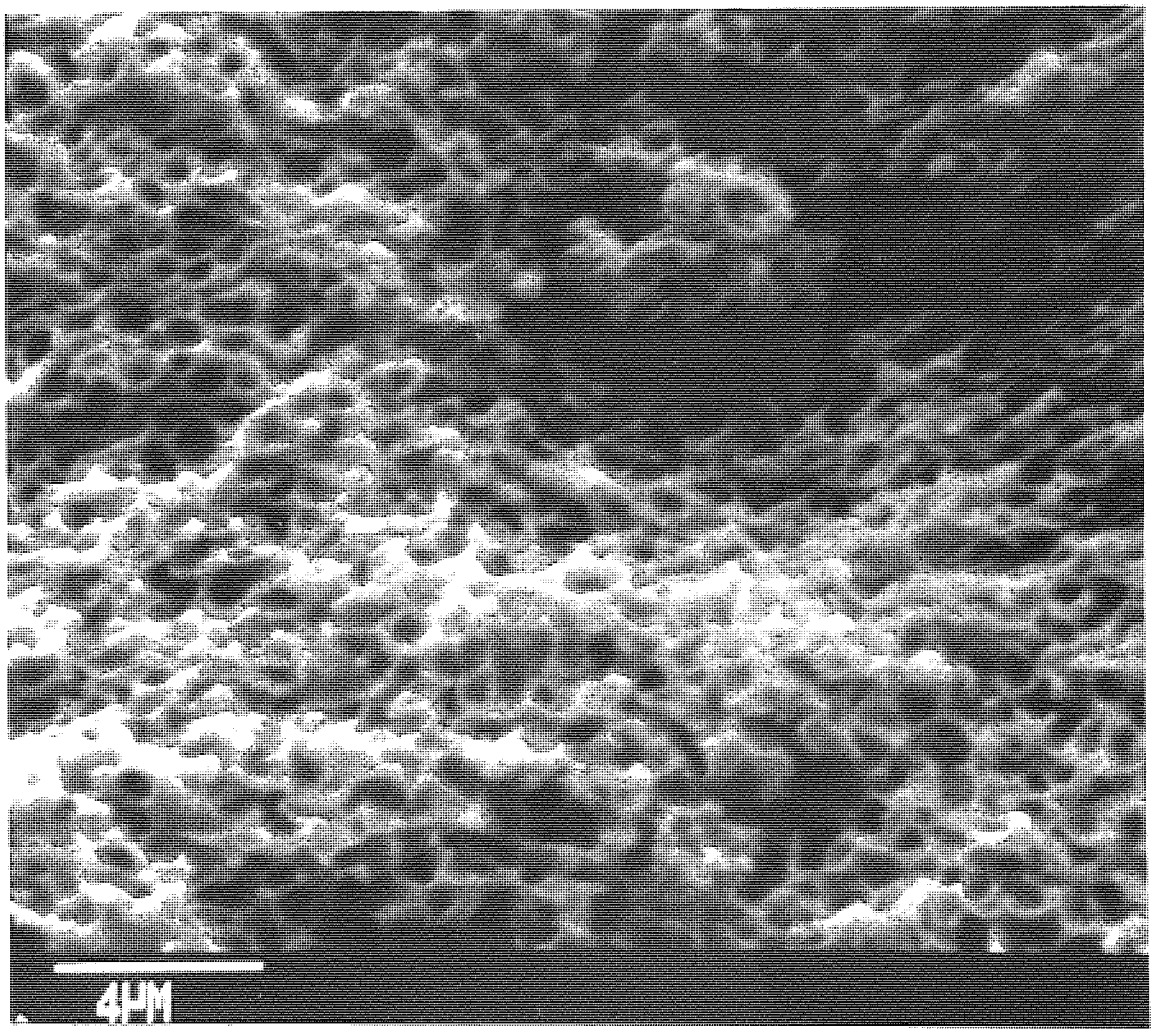

The mean interior pore size, Plate 3.4, was estimated to be 0.7µm and ranged from 0.5 to 0.9µm. The range of values was substantially lower than that recorded for beads manufactured with a 50:50 monomer:solvent ratio, Plate 3.1.

Plate 3.5. Surface pore domains of a polyHEMA bead manufactured using a monomer:solvent ratio of 60:40. Mag x 2000.

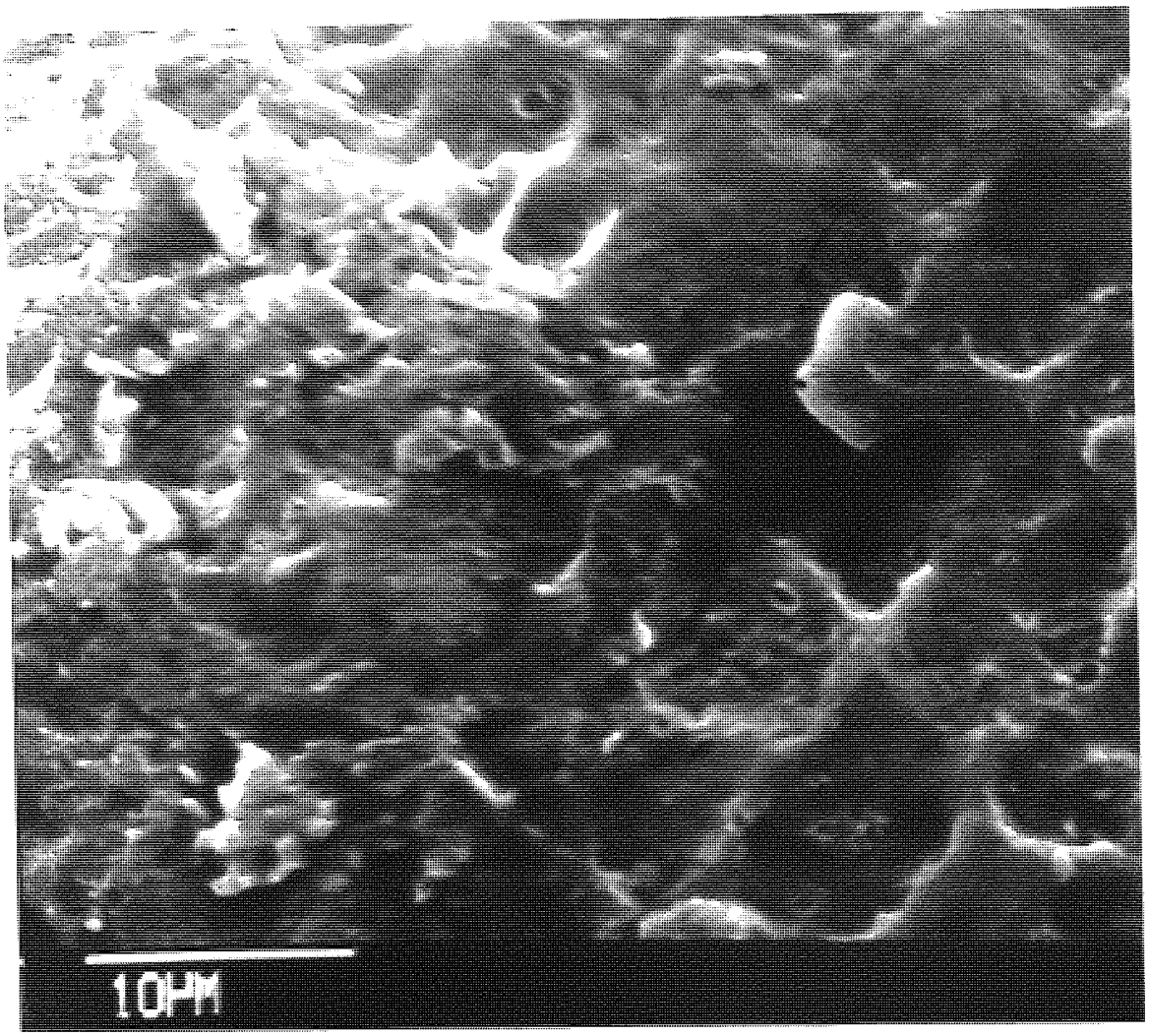

The surface topography of a 60:40 monomer:solvent ratio bead is shown in Plate 3.5. Pore sizes ranged from 0.5 to 0.8µm and averaged 0.7µm. This value was

much lower than the estimate of 1.4µm obtained for beads containing a 50:50 monomer:solvent ratio (Plate 3.2). There was no difference between the estimated pore size in the interior and at the surface of these beads. However, a comparison of Plates 3.4 and 3.5 shows that the macroporous network is much more extensive in the interior of the bead (Plate 3.4) than at the surface (Plate 3.5). The interior of an unloaded bead fabricated using a 40:60 monomer:solvent ratio is shown in Plate 3.6.

Plate 3.6. Interior of an unloaded polyHEMA bead fabricated using a 40:60 monomer:solvent ratio. Mag x 2000.

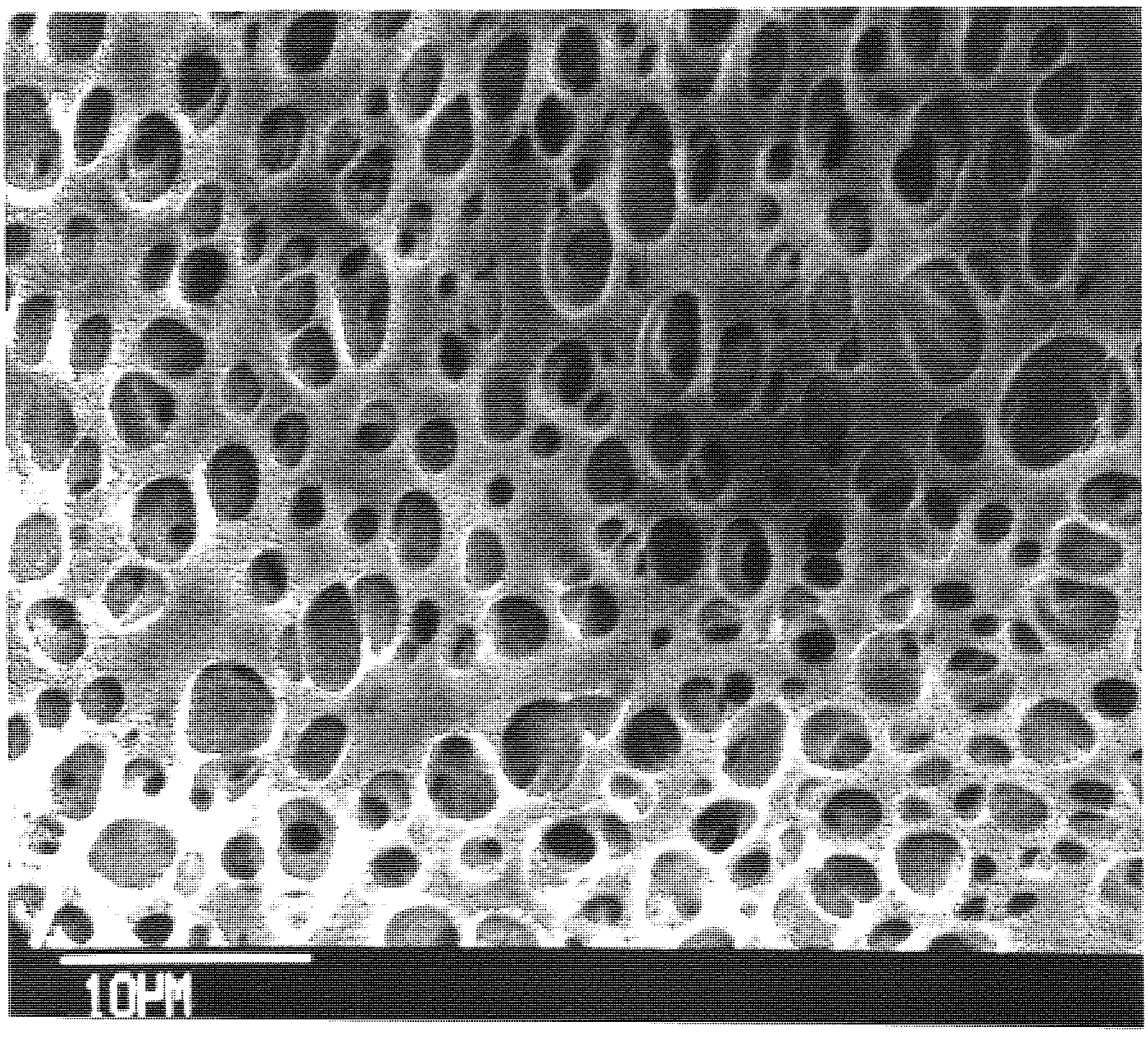

The mean pore size was estimated to be 2.6µm with a range of 1.9 to 3.9µm. The pore diameter in the interior of beads generated using a 40:60 ratio was considerably larger than that observed for beads fabricated using a 50:50 (Plate 3.1) and 60:40 (Plate 3.4) monomer:solvent ratio.

Plate 3.7. Surface topography of an unloaded polyHEMA bead fabricated using a 40:60 monomer:solvent ratio. Mag x 1000.

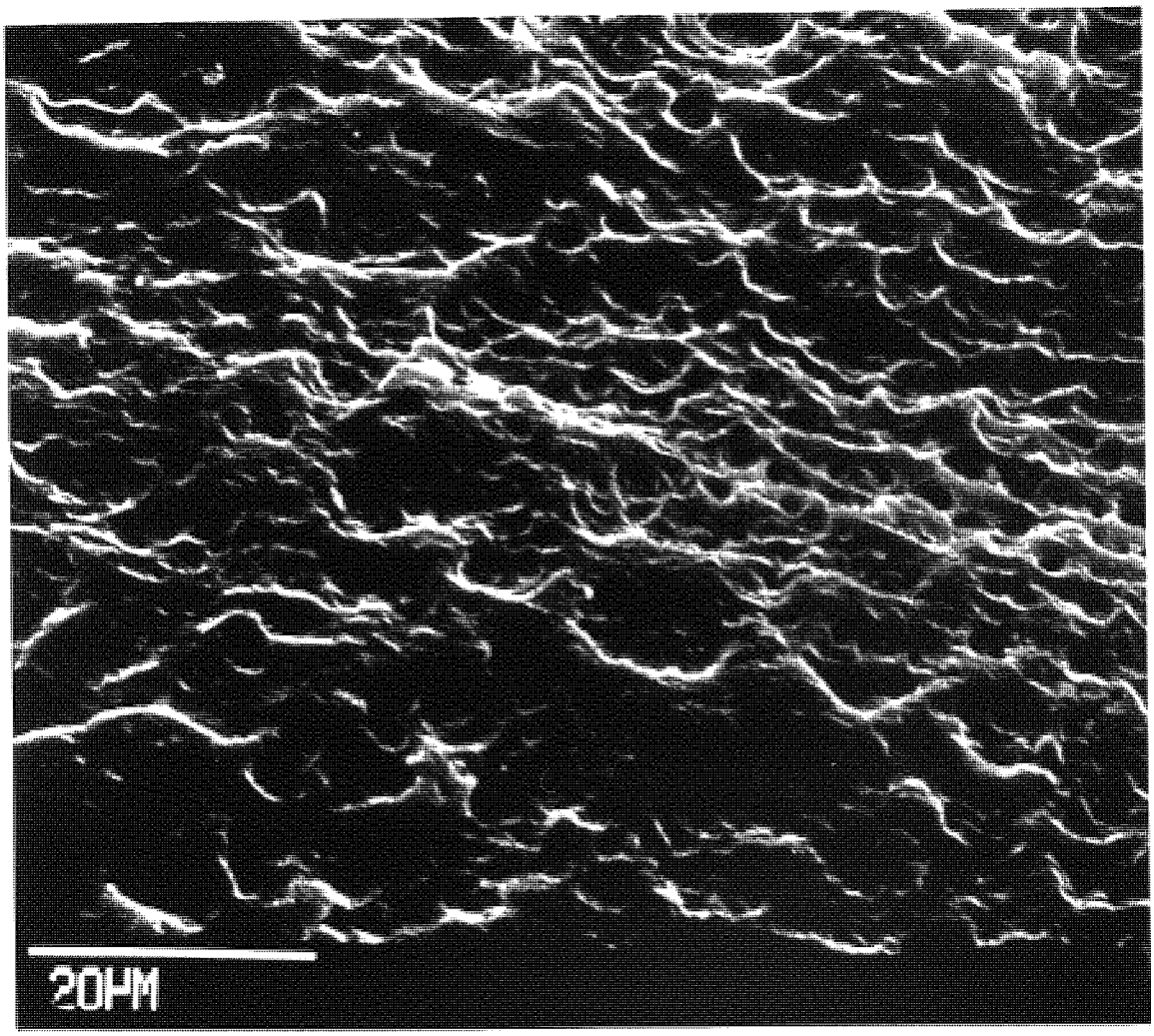

The mean pore diameter at the surface of beads formulated using monomer:solvent ratio of 40:60 (Plate 3.7) was 2.6μm and ranged from 1.9 to 3.8μm and were of the same order as those in the interior of beads of this formulation. However comparison of Plates 3.6 and 3.7 shows that there were far fewer pores at the surface of these beads than in the interior.

In general terms, these ultrastructural studies indicate that increasing the monomer concentration in relation to the solvent concentration, leads to a reduction in the number and diameter of macropores in the matrix. Comparison of Plates 3.1, 3.4 and 3.6 also indicate that at high (60%) solvent concentrations the path of the macropores through the bead become more ordered in appearance and have a less tortuous path.

Whilst the addition of sodium acetate/sodium chloride buffer to the monomer solution significantly increased the EWC of beads and caused a swelling of the matrix this buffer did not appear to affect the macroporosity, Plate 3.8.

Plate 3.8. Surface topography of polyHEMA beads fabricated using a 50:50 monomer solvent ratio with sodium acetate/sodium chloride buffer present in the solvent phase. Mag x 2000.

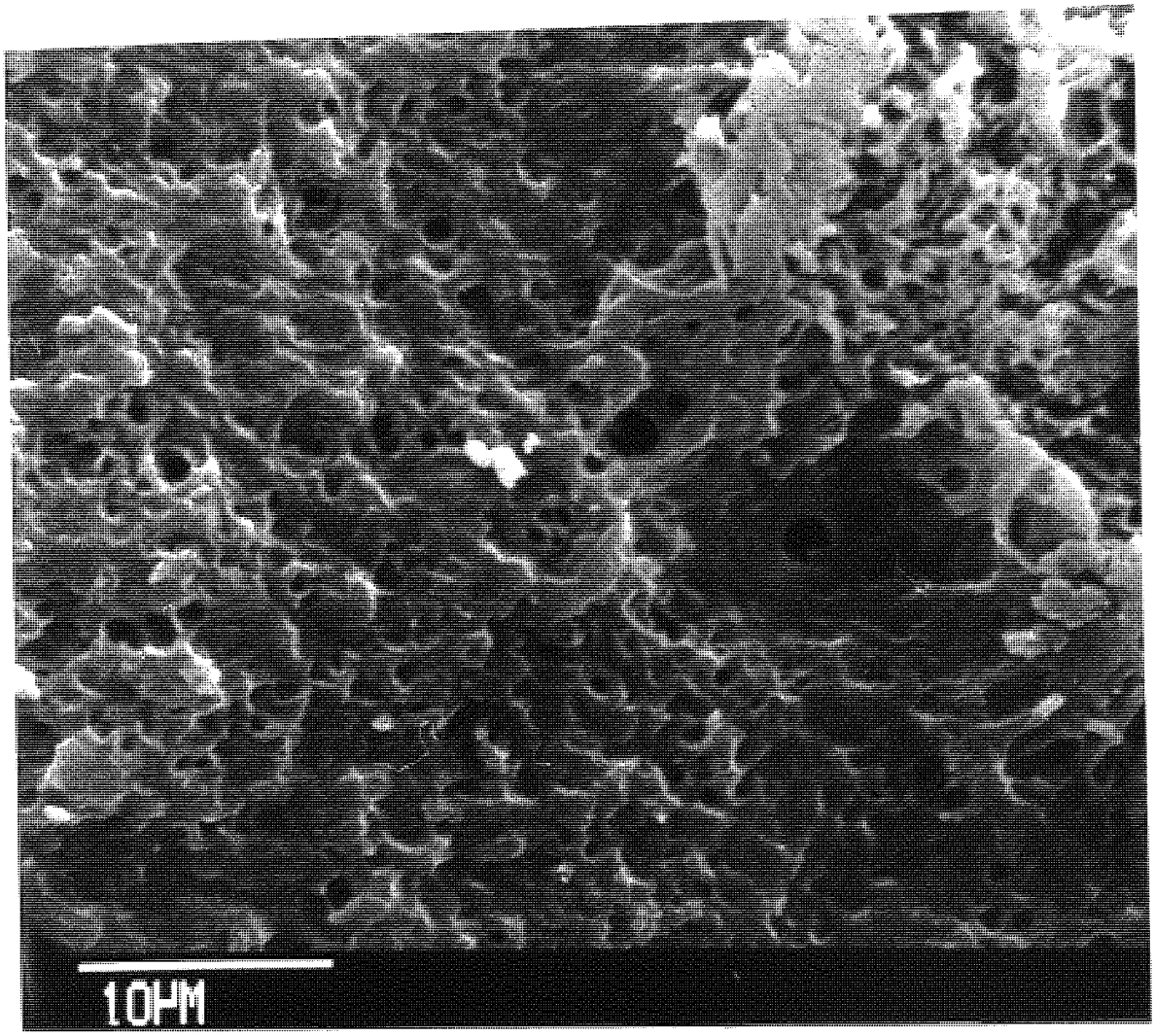

In this case (Plate 3.8) the mean pore size was found to be 1.2μm with a range of 0.6 - 1.8μm, not dissimilar from the pore diameters present at the surface of beads fabricated using distilled water in the solvent phase (0.9 - 2.1μm, Plate 3.3).

The ultrastructural morphology of all batches of beads produced during the course of this work was routinely monitored using SEM. The incorporation of macromolecules did not appear to affect the macroporosity of the matrix.

The parameters of stirrer speed and monomer delivery speed have been established as important factors controlling the size range of beads produced by freeze-thaw polymerisation and a reproducible and controllable bench system has been developed for the production of macroporous polyHEMA beads. The macroporosity of the beads has been confirmed by SEM. Although the EWC of the polymer may be affected by buffers such as sodium acetate/sodium chloride, the addition of buffers and macromolecules do not appear to affect the macroporous structure of the beads.

It is of paramount importance that vehicles formulated for the delivery of clinically useful macromolecules with potential for use as deep seated or subcutaneous implants, should be tissue biocompatible. PolyHEMA has been extensively tested and found to exhibit good biocompatibility (13,77-82). However, it is often the fabrication procedures which render a polymeric vehicle incompatible <u>in vivo,</u> rather than the nature of the polymer itself. With this in mind, the cytotoxicity

of macroporous polyHEMA beads was evaluated using MEM elution testing, Chapter 2 (Pages 149-152).

3.5 CYTOTOXICITY TESTING OF POLYHEMA BEADS FABRICATED BY FREEZE THAW POLYMERISATION

Cytotoxicity, or tissue culture testing is a rapid, economical, in vitro method of determining the biocompatibility of materials intended for use in medical devices. The cytotoxicity testing of fabrication materials used in the generation of delivery vehicles involves the production of a biomaterials extract. This is useful in establishing whether there are potential 'leachables' present in the vehicle that are capable of inducing a measurable degree of systemic toxicity, localised tissue irritation, sensitisation or other biological response. Mammalian tissue culture systems are extremely sensitive and results obtained which suggest a material to be cytotoxic must be viewed in conjunction with results of applicable in vivo studies and in the light of the intended use of the product. In the present study, the cytotoxicity testing of polyHEMA beads and HEMA monomer was carried out using minimum essential medium (MEM) elution tests in accordance with North America Science Associates Incorporated (NAmSA) Safety Evaluation Guidelines. Three cell lines are used at NAmSA; L-929, mouse fibroblast, WI-38, human embryonic lung and MRC-5, human embryonic lung. The L-929 cell line has been

suggested for use in most cases by NAmSA since it is the easiest to culture, the supply is unlimited and is very dependable. L-929 cells are a subclone of NCTC cells, clone 929, Strain L, originating from C3H mouse areolar and adipose tissue (166). The cells are fibroblasts and attachment dependent, forming epithelial-like monolayers in culture. Stock cell cultures were routinely maintained in Eagles minimum essential medium (modified) with Earle's salts, as described previously in Chapter 2, (Pages 141-143) and MEM elution tests were carried out as described, Chapter 2, (Pages 149-152).

The effect of exposure of L-929 cells to one days static bead eluant, obtained at 37°C is shown in Figure 3.10. The eluant significantly reduced the growth rate of L-929 cells after 48 and 72 hours by 25% and 24% respectively when compared to the growth curve of control cells, but substantial cell growth was still maintained. When L-929 cells were exposed to 5 day low temperature eluate (4°C), no significant change in log phase growth could be detected after 48 and 72 hours in culture, Figure 3.11, although there was a marginal reduction in the number of cells detected in culture after 24 hours. The results of the cytotoxicity testing of polyHEMA beads suggest the presence of a minimal amount of toxic leachable substance in the polymeric matrix, probably introduced

FIGURE 3.10: The effect of a one day test eluate from 1g polyHEMA beads per 100ml medium at 37°C on the growth of L929 cells. (Mean values ± SEM, n=6).

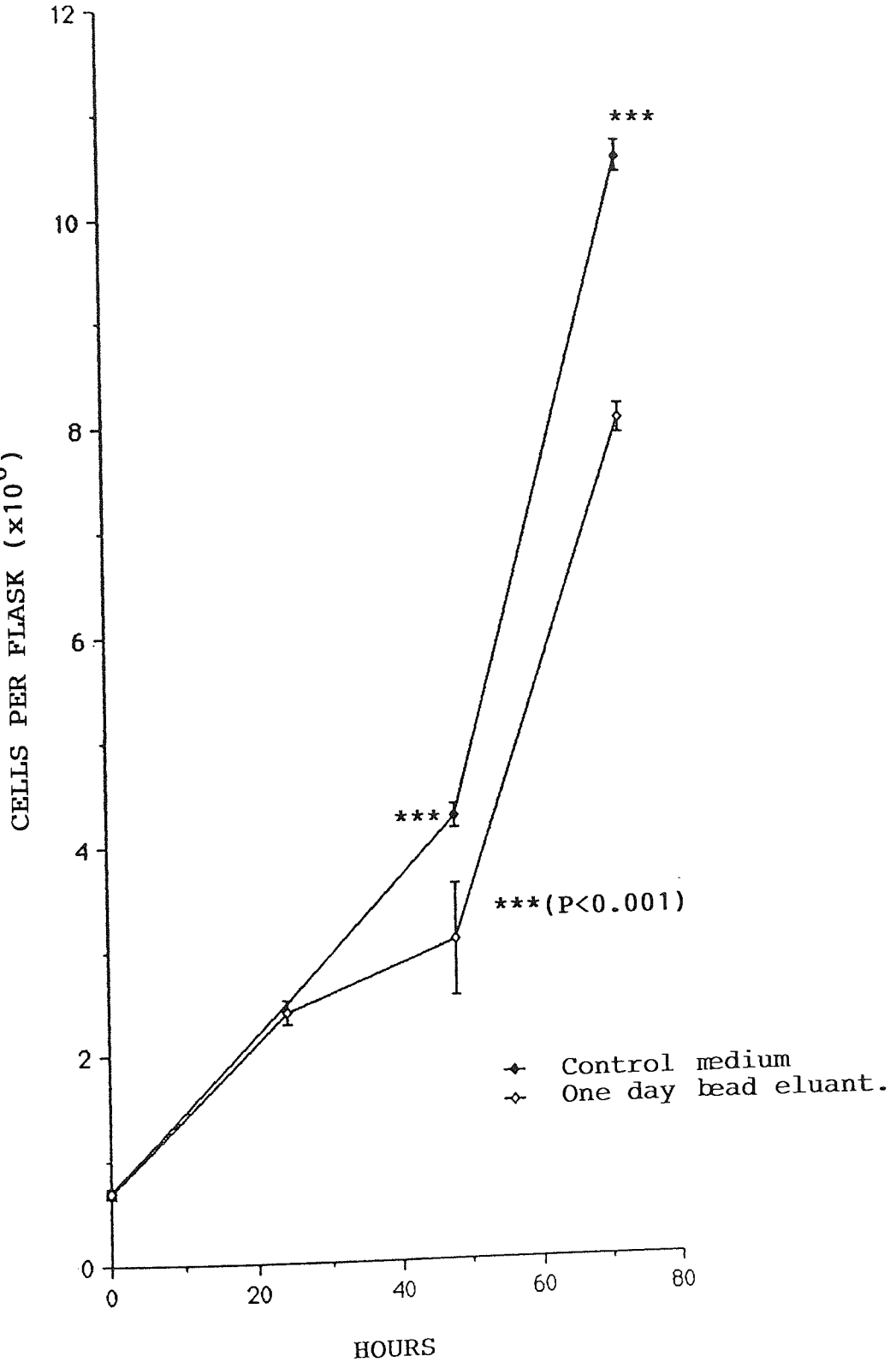

FIGURE 3.11: The effect of a 5 day test eluate from 1g polyHEMA beads per 100ml medium at4°C on the growth of L929 cells. (Mean values ± SEM, n=6).

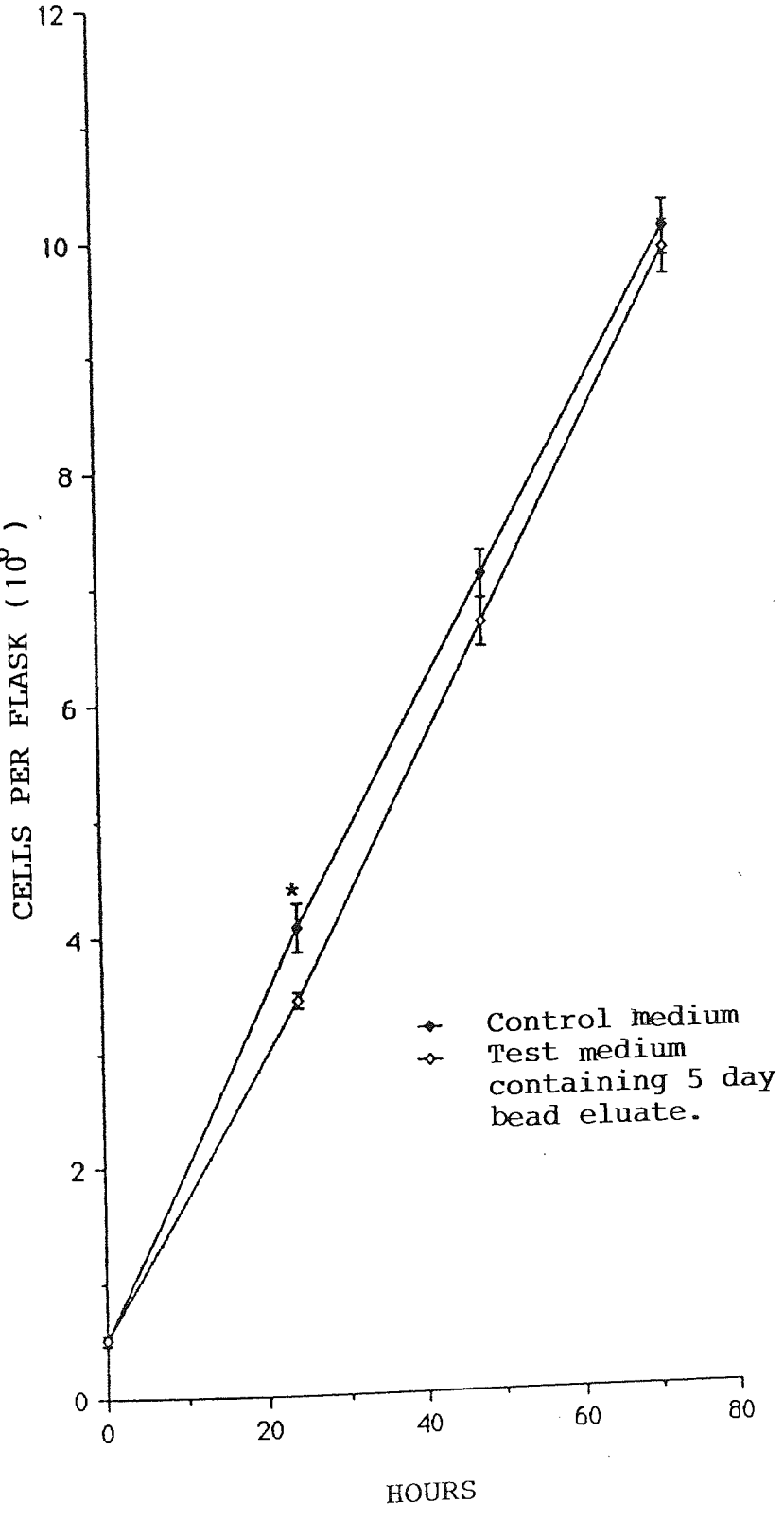

at the fabrication stage of bead production. However, the substance is not present at a concentration sufficient to cause cell death and a significant growth of L-929 cells was maintained. The addition of HEMA monomer to the tissue culture medium at low concentrations (1:1000 and 1:100,000) significantly inhibited the growth of L-929 cells, Figures 3.12 and 3.13. Total cell death occurred within 48 hours of the administration of HEMA monomer at a concentration of one part per thousand, Figure 3.12. However the cell line did show some recovery from exposure to one part per hundred thousand HEMA monomer after 70 hours, Figure 3.13.

These data do not indicate the precise nature of the contaminant(s) leached from the beads which affected cell growth in culture. It is possible that a range of contaminants such as hexane, unreacted monomer, and uranyl nitrate or ethylene glycol might be present at very low concentrations, giving rise to a reduction in the rate of growth of the cells. The toxicity of HEMA monomer (69) is confirmed by these cell culture experiments and the requirement for the complete polymerisation of polyHEMA beads emphasised.

This study indicates that polyHEMA beads fabricated using the method of free-thaw polymerisation require more extensive washing than utilised here,

FIGURE 3.12: The effect of one part per thousand HEMA monomer on L929 cells in log phase growth. (Mean values ± SEM, n=6).

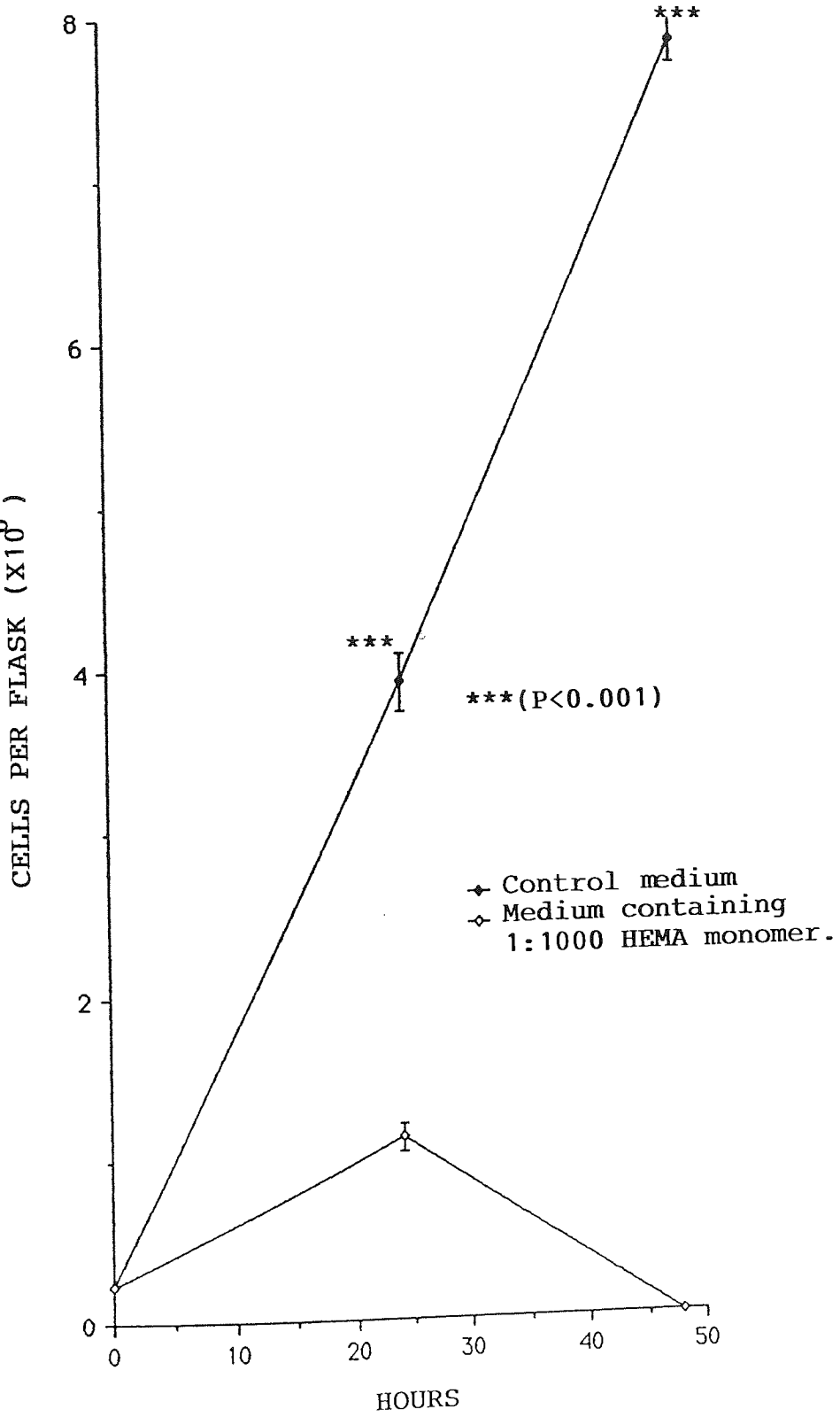

FIGURE 3.13: The effect of one part per hundred thousand HEMA monomer on L929 cells in log phase growth.
(Mean value ± SEM, n=6).

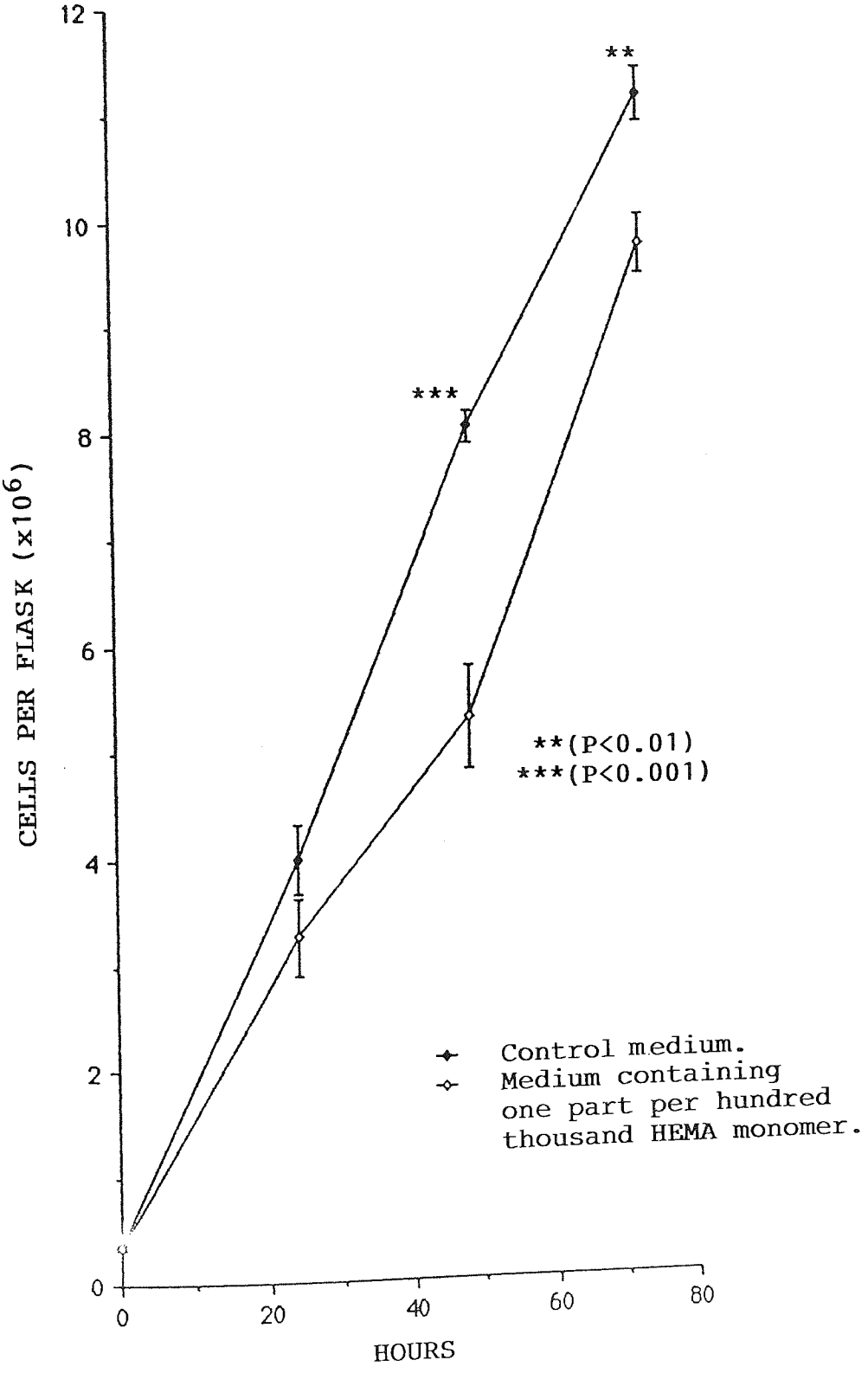

(5 minutes in x2 distilled water) to preserve cell biocompatibility. Since the leaching of contaminant(s) was greater at 37°C it may be that a warm washing procedure (37°C) might be a more efficient means for removing contaminants than the room temperature x2 distilled water wash currently employed.

CHAPTER 4

THE RELEASE OF SURROGATE PROTEIN MACROMOLECULES FROM MACROPOROUS POLYHEMA BEADS

4.1 THE RELEASE OF BOVINE SERUM ALBUMIN FROM MACROPOROUS POLYHEMA BEADS.

Bovine serum albumin (BSA) fraction V (MW 68,000) was considered a convenient surrogate macromolecule for incorporation into polyHEMA beads because it is relatively stable in solution and when frozen at -20°C has a reasonable shelf life. BSA can be assayed conveniently and sensitively using the bicinchoninic acid assay procedure (Pages 89-97), as described in Chapter 2.

BSA was loaded into polyHEMA beads by dissolving in the water component of the aqueous phase of the monomer solution at a concentration of 60mg BSA per ml water (5% of the total polymer matrix weight), and beads were fabricated using the standard procedure described previously (Pages 78-85).

After harvesting, beads were washed in x2 distilled water at room temperature for five minutes. Half the yield was air dried at room temperature (21°C) and half was freeze-dried overnight at a temperature of -65°C under a vacuum of 0.2 atmospheres (Edwards 4K Modulyo freeze-drier). BSA containing beads from a number of batch preparations were similarly processed and pooled for use in release BSA experiments. Cumulative release profiles were constructed and differences in the rates of release of BSA obtained in

response to the various treatment conditions were computed using Student's unpaired t-tests.

4.1.1 The effect of drying procedure on the release of BSA from macroporous polyHEMA beads.

The release experiments were set up as described in Chapter 2 (Pages 87-88) using air and freeze-dried beads in the 500-1000μm size range. Water was used as the incubation medium and BSA release was monitored for 20 days. Control studies, using unloaded beads, indicated the presence of some contaminant, apparently leached from the polyHEMA beads into the incubation medium, which affected the BCA assay used for protein measurement. Control samples showed an apparent protein concentration of the order of 0.1mg/ml per day. The cause of this effect could not be identified as any constituent of the monomer solution, nor the non-solvent, hexane. Therefore this control value was subtracted from the measured amount of protein per day.

Freeze drying significantly ($P<0.001$) increased the rate of release of BSA from polyHEMA beads, Figure 4.1. Freeze dried beads released about five times more BSA than air dried beads over a 20 day period. After 18 days air dried beads ceased to release detectable amounts of BSA. It may be that BSA contained in air dried beads was either degraded during the drying process or dried to a water resistant film. Lyophilised protein is more

FIGURE 4.1: THE EFFECT OF FREEZE-DRYING ON THE MEAN CUMULATIVE RELEASE OF BSA FROM 5% LOADED BEADS (500-1000μm) (MEAN VALUES ± SEM, n=9).

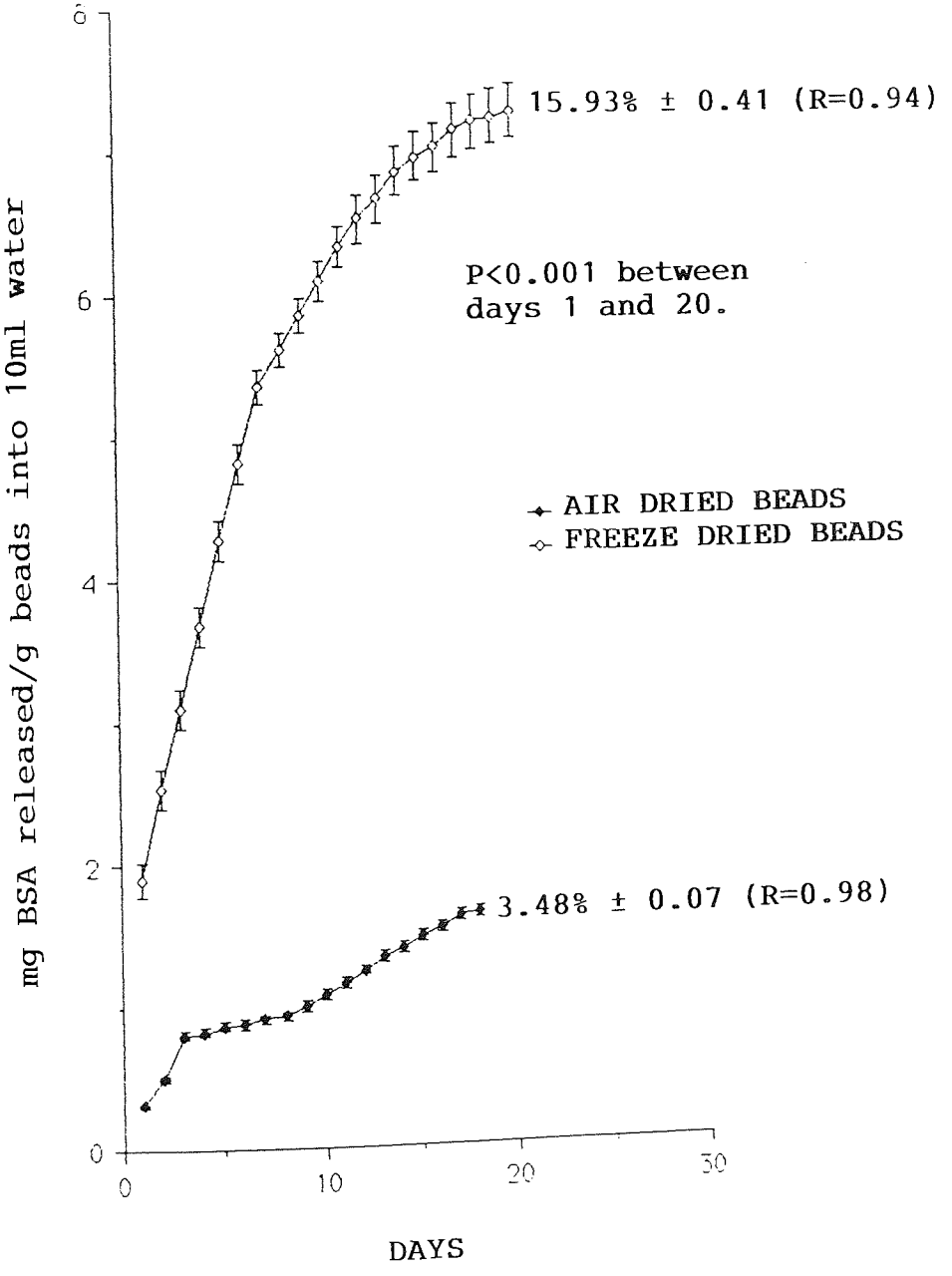

hydrolytically stable than air dried protein, less prone to degradation by microorganisms, and more easily water soluble than air dried material.

Both freeze-dried and air dried beads showed a characteristic burst release of BSA over the first few days. This may be the result of the release of BSA from the bead surface and superficial layers of the matrix. It is also possible that some BSA may have been sublimed through the matrix pores, to the surface of the beads during the freeze drying process, potentiating the prolonged burst release seen with freeze dried beads.

The regression coefficients for the release profiles of air dried and freeze dried beads were high and approximated to zero order. These studies demonstrate that the freeze drying of beads is a reliable means of bead processing, prior to prolonged storage and facilitates the dissolution and release of the surrogate macromolecule on rehydration. In subsequent experimental work, polyHEMA beads were freeze-dried immediately after fabrication and stored at -20°C until required.

4.1.2 The effect of agitation on the release of BSA from freeze-dried macroporous polyHEMA beads.

Freeze-dried beads loaded with 5% BSA were generated and the release of BSA monitored as described in

FIGURE 4.2: THE EFFECT OF AGITATION ON THE MEAN CUMULATIVE RELEASE OF BSA FROM 5% LOADED BEADS (500-1000μm) (MEAN VALUES ± SEM, n=9).

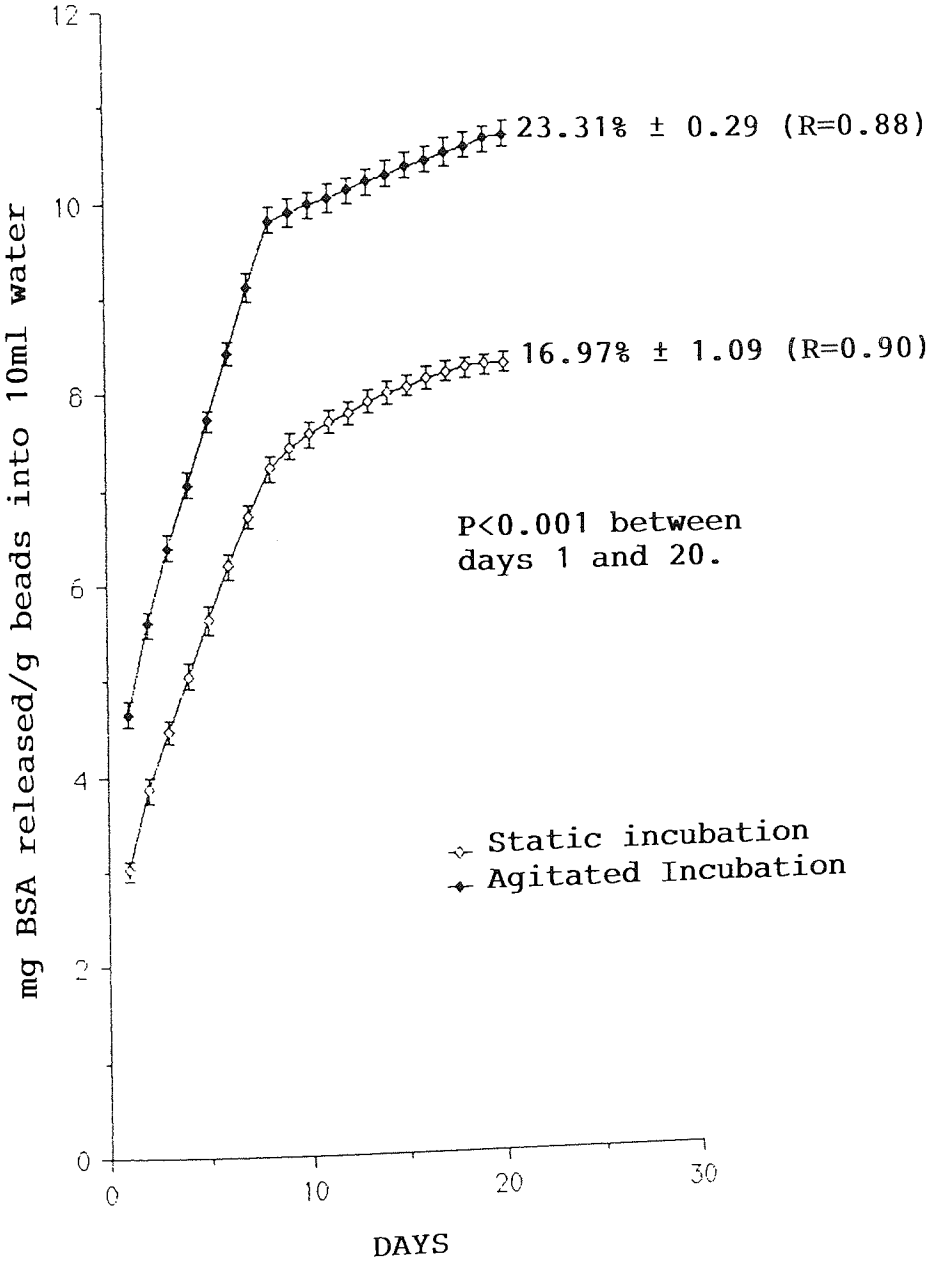

Chapter 2 (Pages 87-88). Half the flasks, each containing 1g freeze-dried beads, were continuously agitated at room temperature on a Luckhams RS200 Recipro-Shake Major (220/240V, 50/60 Hz) at 70 cpm. The remaining flasks were maintained at room temperature and not shaken.

Figure 4.2 shows the cumulative release of BSA from agitated and statically incubated polyHEMA beads at room temperature. Agitation significantly increased ($P<0.001$) the rate of BSA release from polyHEMA beads compared with static incubation. Both profiles showed a marked burst release of BSA over the first 8 days and agitation tended to exaggerate the burst effect. Agitation probably increases the rate of diffusion of the incubation medium in and out of the polymer matrix, encouraging increased BSA efflux from the beads.

4.2 THE RELEASE OF FLUORESCEIN ISOTHIOCYANATE DEXTRANS (FITC-LINKED DEXTRANS) FROM MACROPOROUS POLYHEMA BEADS

The rate of release of macromolecules by diffusion through and from a hydrophilic matrix may be a function of molecular weight. With this in mind, polyHEMA beads were loaded with FITC-linked dextrans of differing molecular weights. The linking of FITC to dextran allows direct monitoring of dextran concentration by spectrophotometry. Two FITC-linked

dextrans were selected for study, a relatively low molecular weight species (FD-20S, MW = 17,500) and a high molecular weight species (FD-150, MW = 148,900). 100mg of each FITC linked dextran was loaded into polyHEMA beads (0.86% loading) in 0.2M boric acid - borate buffer pH7.4 (Appendix A1) via the aqueous phase of the monomer solution. This buffer was also used as the incubation medium for release studies. Boric acid-borate buffer (buffering capacity pH7.4 - pH9) was used to specifically stabilise the absorption maxima of the FITC-linked dextrans (132) and incubation of the beads was carried out in the dark since FITC-linked dextran is light sensitive (132). The absorption maxima of FD-20S and FD-150 in borate buffer, pH7.4 were confirmed as 491nm and 495nm respectively. FITC-linked dextran loaded beads were fabricated in the usual way, and the release experiments were set up as described previously (Pages 87-88), using 355 - 500μm and 500 - 1000μm beads. The effects of incubation temperature (4°C and 37°C) and bead size were investigated on the rate of release of both FD-20S and FD-150 over a 20 day period. Cumulative release profiles were constructed and differences in the rates of release obtained in response to the various treatment conditions were computed using two factorial ANOVAR.

4.2.1 The effect of bead size and incubation temperature of the release of FITC-linked dextrans from macroporous polyHEMA beads.

The effect of bead diameter and incubation temperature on the rates of release of FD-150 and FD-20S are summarised in Figures 4.3 and 4.4 respectively.
The mean cumulative release of FD-150 dextran was significantly greater at 37°C than at 4°C irrespective of bead size, over a period of 14 days, Figure 4.3. The release profile for FD-150, was characterised by a significant initial burst release lasting about 5 days. The rate of release then declined to very low levels. After 14 days at 37°C, release of FD-150 ceased, whilst at 4°C a low level of release was maintained up to the conclusion of the experiment at 21 days. A significantly greater proportion of the total loading of FD-150 was released at 37°C than at 4°C irrespective of bead size, Figure 4.3.

Increasing the incubation temperature to 37°C significantly elevated the rate of release of FD-20S dextran from polyHEMA beads, Figure 4.4. Like FD-150, the release profile for FD-20S was characterised by an initial burst release lasting approximately 5 days, followed by a low level release for the remainder of the time period up to 21 days. However, unlike FD-150 dextran, beads loaded with FD-20S and

FIGURE 4.3: THE EFFECT OF BEAD SIZE AND INCUBATION TEMPERATURE ON THE MEAN CUMULATIVE RELEASE OF FD-150 FROM 0.86% LOADED BEADS (MEAN VALUES ± SEM, n=6).

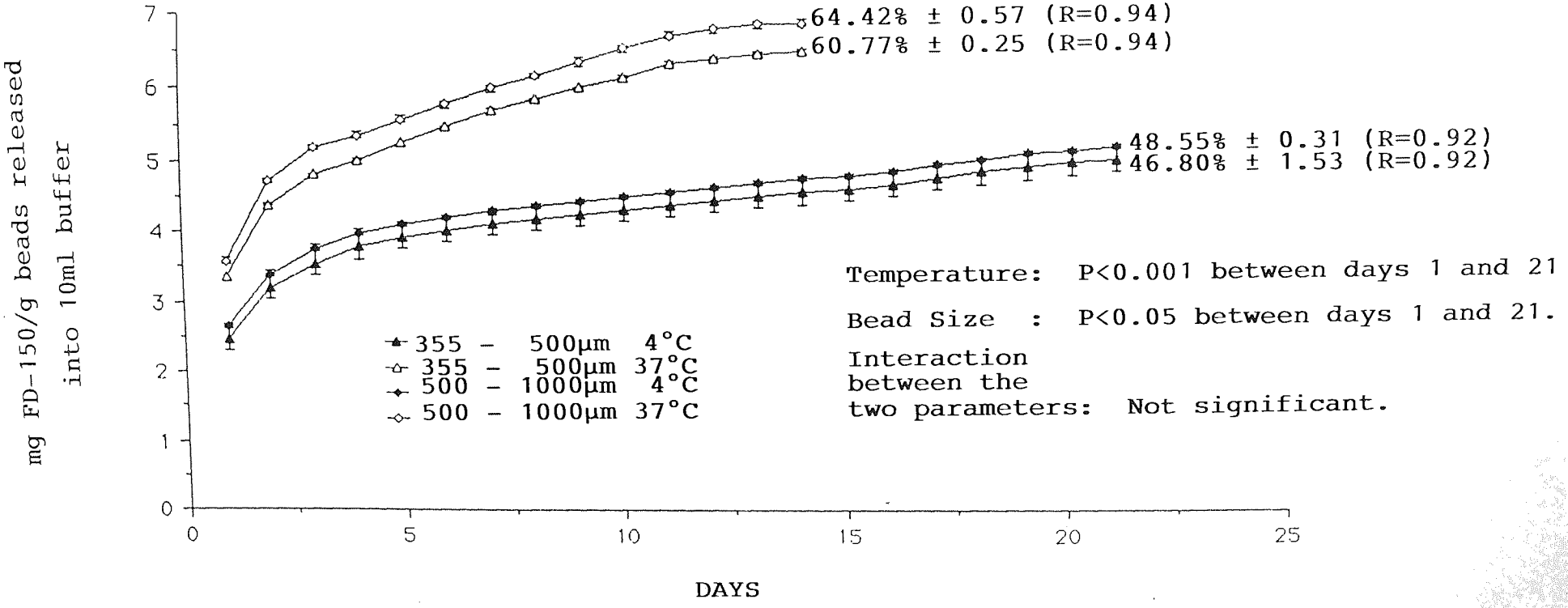

FIGURE 4.4 THE EFFECT OF BEAD SIZE AND INCUBATION TEMPERATURE ON THE MEAN CUMULATIVE RELEASE OF FD-20S FROM 0.86% LOADED BEADS (MEAN VALUES ± SEM, n= 6).

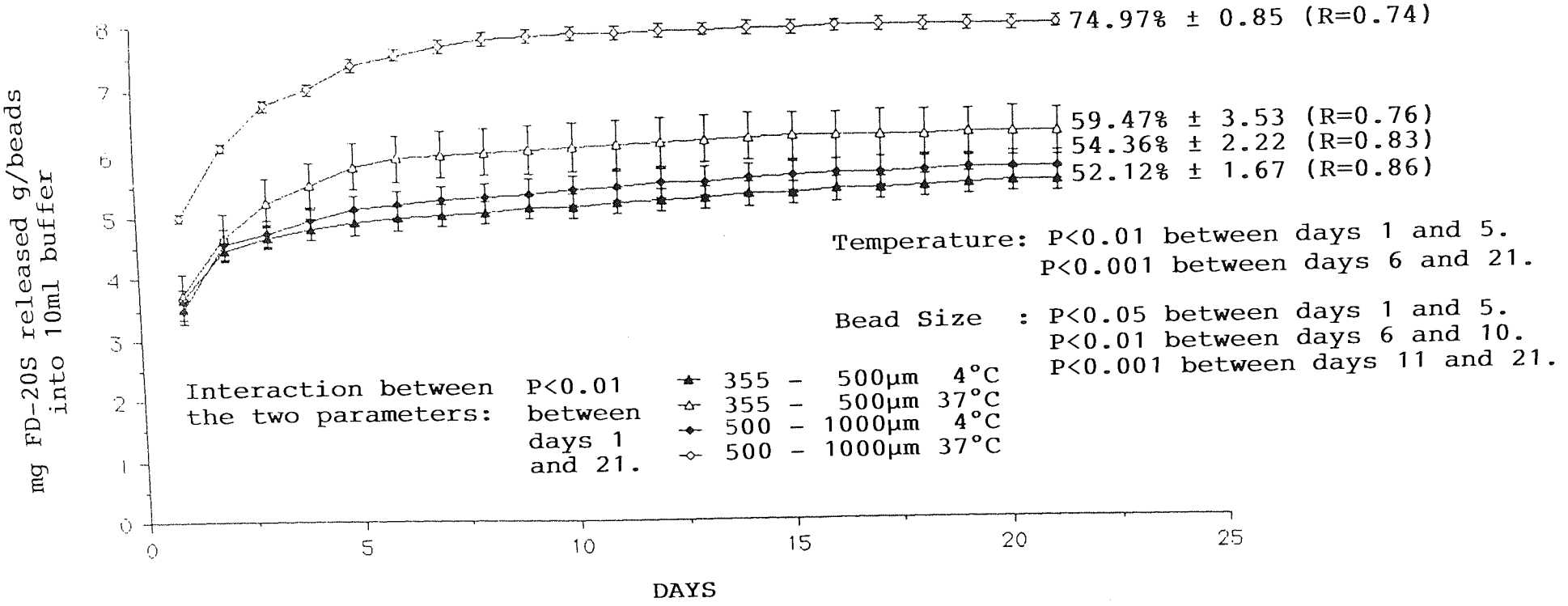

incubated at 37°C continued to release dextran at a low level for up to 21 days.

PolyHEMA beads of 500 - 1000µm diameter consistently released a greater proportion of the total incorporated FITC-linked dextran than smaller beads (355 - 500µm), irrespective of incubation temperature and the molecular weight of the dextran, Figures 4.3 and 4.4. Analysis of the release data for FD-150 dextran showed that incubation temperature and bead size had independent effect on the release rate, ie there was no significant interaction between incubation temperature and bead size, but this was not the case for the release of FD-20S dextran. The temperature induced elevation of FD-20S dextran release was significantly greater from 500 - 1000µm beads than from 355 - 500µm beads.

Although the dextrans used in these experiments were of moderately high molecular weight, dextran molecules tend to be filamentous in solution, resulting in long chains of molecules, rather than a 'globular' shape as is generally found with high molecular weight proteins. This is probably the reason for the relatively rapid release of FITC-linked dextrans from the macroporous matrix. The increased rate of dextran release at 37°C indicated that the rate of diffusion

of the macromolecule was the main factor controlling the release of FITC-linked dextran.

The fact that FITC-linked dextran release was greater from 500 - 1000μm beads than from 355 -500μm beads was rather surprising. The amount of dextran incorporated into 1g of beads was theoretically the same, irrespective of the final size of the beads produced and small beads would be expected to show faster release rates than large beads due to their increased total surface area. However, small beads were likely to have lost a high proportion of their incorporated dextran from their surface at the washing stage after bead production. Larger beads have a reduced surface area and greater reservoir capacity, hence, most of the dextran in the larger beads will be in the interior and potentially less at the surface, protecting the bulk of the incorporated dextran from elution at the washing stage. This would leave proportionately more dextran within the larger beads for release during incubation.

4.2.2 The effect of molecular weight on the release of FITC-linked dextrans from macroporous polyHEMA beads.

Molecular weight significantly influenced the rate of FITC-linked dextran release from the polyHEMA beads, Figure 4.5. At 4°C and 37°C a significantly greater proportion of FD-20S dextran was released than

FIGURE 4.5 THE EFFECT OF MOLECULAR WEIGHT OF THE MEAN CUMULATIVE RELEASE OF FD-150 AND FD-20S FROM 0.86% LOADED BEADS (500-1000μm) (MEAN VALUES ± SEM, n=6).

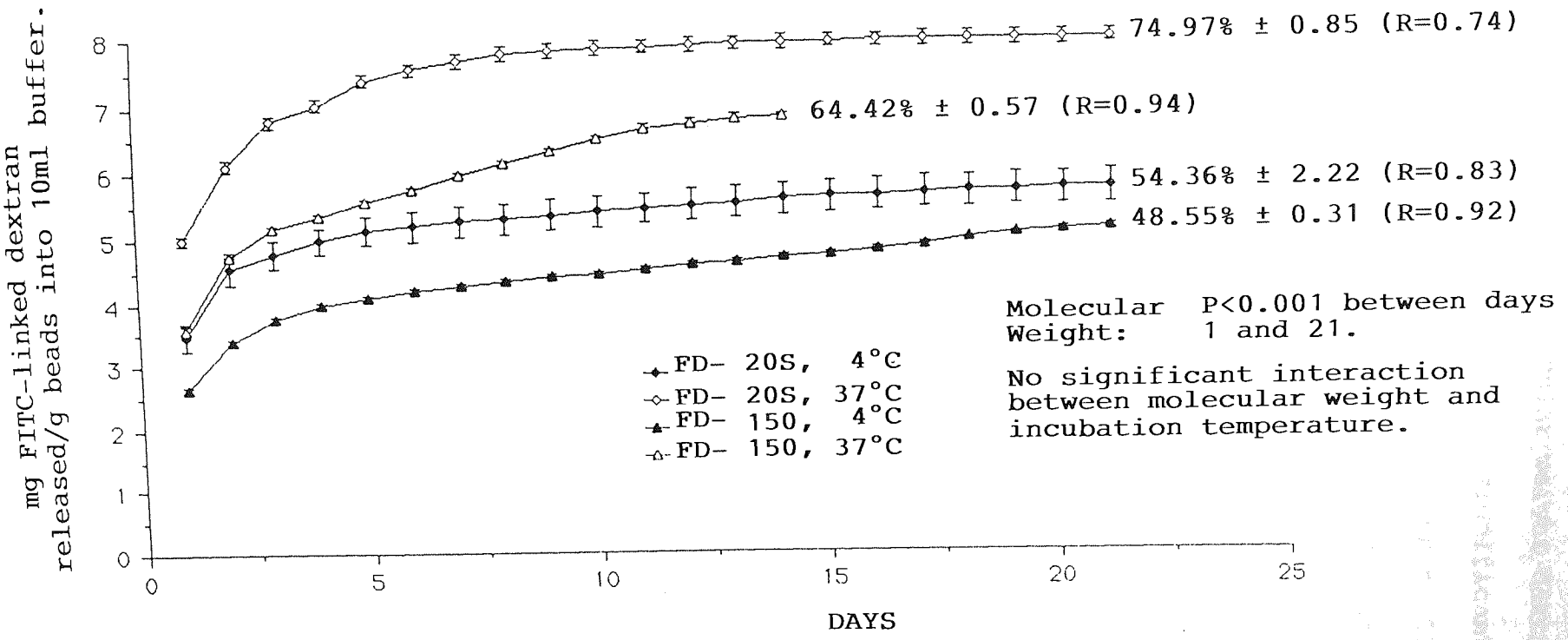

FD-150 dextran. Clearly, low molecular weight dextran diffuses out of the macroporous matrix significantly faster than the high molecular weight dextran. This observation is consistent with the rate of diffusion the macromolecule being the main controlling factor affecting the release of dextrans from macroporous polyHEMA beads. There was no significant interaction between the effects of temperature and molecular weight on the rate of FITC-linked dextran release, ie each parameter acted independently of the other in affecting release rates.

Studies so far have investigated the incorporation and release of surrogate macromolecules with no relevant biological activity. In order to investigate whether the process of incorporation into polyHEMA beads influences the biological activity of the subsequently released macromolecule, beads were manufactured containing the representative enzyme glucose oxidase, EC 1.1.3.4. The assay of glucose oxidase provides direct information on the biological activity of the macromolecule. Preliminary attempts were also made to incorporate and monitor the release of an important immunomodulating peptide, interleukin-2. The tissue culture bioassay of this cytokine provides direct information concerning the biological potency of the macromolecule after incorporation into and subsequent release from a bead formed hydrophilic matrix.

4.3 THE RELEASE OF THE ENZYME GLUCOSE OXIDASE (EC 1.1.3.4) FROM MACROPOROUS POLYHEMA BEADS

Enzyme determinations provide a direct measure of the biological activity of an enzyme protein and the effect of bead incorporation on biological activity after release from the polymeric matrix can be assayed directly. The enzyme chosen for study was glucose oxidase (EC 1.1.3.4, GOD). This enzyme is a specific and commonly used enzyme for the determination of glucose in biological fluids (MW 154,000). It is employed extensively, either as a reagent solution or immobilised on supporting surfaces in autoanalyser systems.

GOD was incorporated into polyHEMA beads using 0.01M sodium acetate/0.12M sodium chloride buffer, (Appendix A1) at a loading level of 0.32% (19,200U/x 4 batch). Beads were fabricated (Pages 78-85) and release experiments set up as described previously (Pages 87-88). Beads in the size range of 355 - 500µm and 500 - 1000µm were used for the study and incubation was carried out at room temperature. Units of GOD released per day were determined using the GOD enzyme assay method previously described (Pages 102-104). Cumulative release profiles were constructed and differences in the rates of GOD obtained in response to treatment conditions were computed using Student's unpaired t-test.

FIGURE 4.6 THE EFFECT OF BEAD SIZE ON THE MEAN CUMULATIVE RELEASE OF GLUCOSE OXIDASE FROM 0.32% LOADED BEADS (MEAN VALUES ± SEM, n=5).

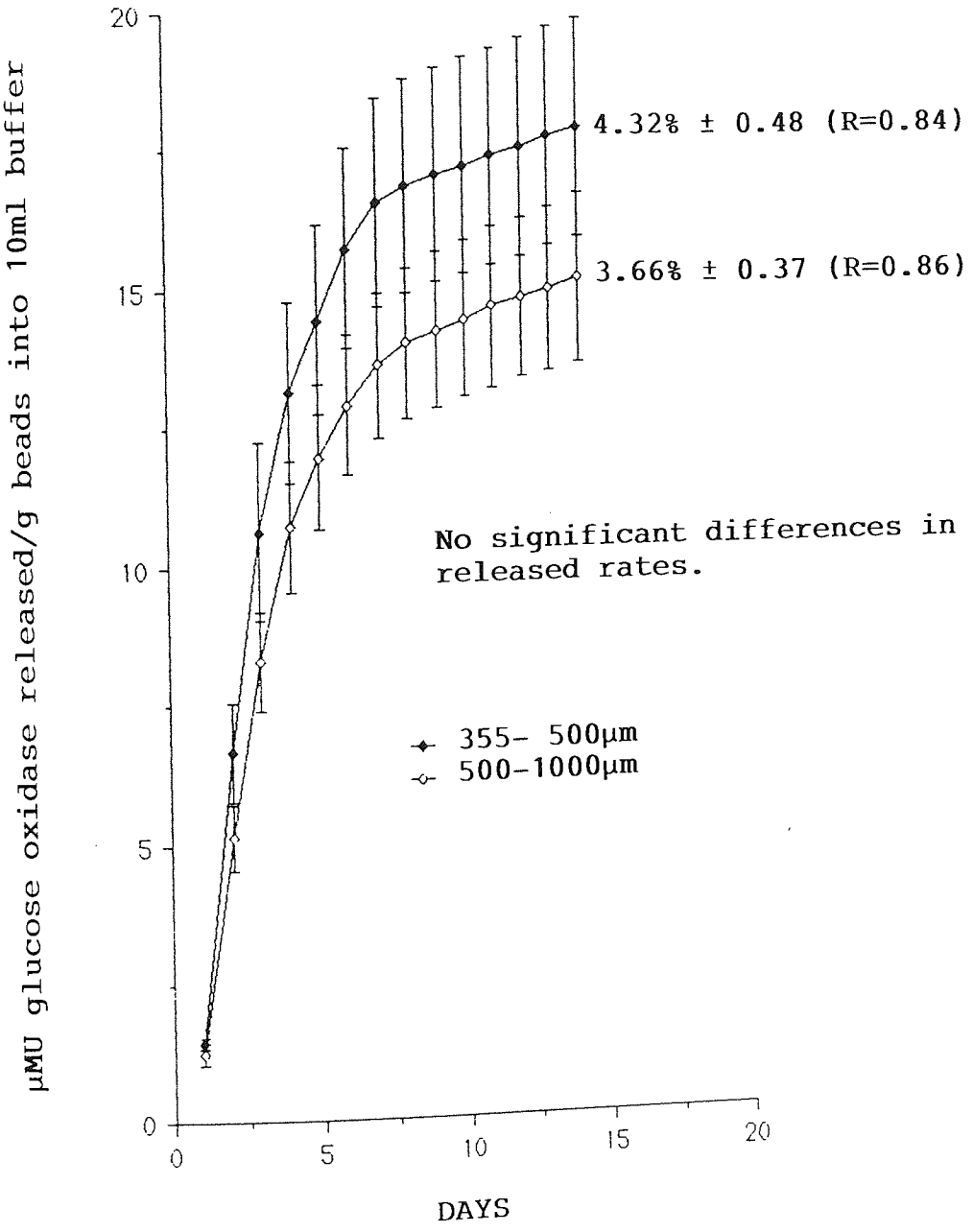

Bead size had no significant effect on the mean cumulative release of GOD at room temperature as shown in Figure 4.6. A marked burst release was observed over the first 4 days but the rate quickly declined thereafter, until by day 14, no further enzyme release could be detected. Approximately 4% of the GOD load was released over a 14 day period, irrespective of the bead size used. This rather small proportion may have been the result of enzyme activity being destroyed by the fabrication process, hydrolytic and/or microbial degradation of the enzyme in solution, or enzyme immobilisation in or on the polymeric matrix itself. Clearly, significant GOD release from polyHEMA beads could be monitored for at least 14 days and the enzyme was released in a biologically active form.

4.4 THE RELEASE OF INTERLEUKIN-2 (IL-2) FROM MACROPOROUS POLYHEMA BEADS

The term cytokine is an umbrella term used to describe soluble proteins which influence cells of the immune system . Cytokines are produced and act in extremely low concentrations. Recombinant DNA technology has enabled the production of large quantities of pure cytokines which are now available for physiological, biochemical, immunochemical and clinical investigation. Cytokines have great potential in controlling the extent and type of immune response against tumours, infectious agents, tissue grafts and

disorders affecting the immune system per se such as leukaemias and immune deficiencies. Interleukin-2 (IL-2) acts on T cells, B cells and macrophages and is a polypeptide produced by activated T cells, with a molecular weight of 14-16,000. The IL-2 molecule contains a single disulphide bond between cystine residues 58 and 105 and reduction of this bond leads to a loss in biological activity (181). The present study was carried out using highly purified human IL-2, with a molecular weight of 15,500, a monomer ortho-glycosylated and generated via chromosome 4 (a gift from Biotest-Folex Ltd, UK). The material was supplied as a solution of specific activity 100K Units per ml in 0.01M phosphate buffer, pH7.4, containing 1% human serum albumin and 0.15M sodium chloride. The manufacturer indicated that IL-2 activity may be significantly reduced on freeze-drying, something of the order of an 8-10% reduction in activity, but the small amount of IL-2 available for study and the replacement expense of the cytokine did not allow control tests to be performed.

Bead production was carried out in the usual way but using half the normal batch quantities (Pages 78-85). IL-2 was loaded, via 0.01M phosphate buffer (Appendix A1) into the aqueous phase of the monomer solution at a level of 200K Units in 2ml 0.01M phosphate buffer

(loading,0.003%). Early studies indicated that phosphate buffer was incompatible with the bead production system, causing precipitation of uranyl phosphate. However, the low molarity phosphate buffer used here did not produce significant precipitation prior to polymerisation and the morphology of the product beads appeared normal. The IL-2 loaded beads were briefly sterilised in 75% ethanol and release studies were carried out using 0.5g rather than 1g beads, incubated in 5ml of RPMI 1640 culture medium supplemented with 10% foetal calf serum. The aspirated culture medium was frozen for subsequent analysis and replaced with fresh culture medium daily. The release samples obtained were frozen with dry ice and transported to Dr A J H Gearing at the National Institute for Biological Standards and Controls, South Mimms, for the assay of IL-2.

IL-2 was assayed using the IL-2 dependent cell line CTL-L2. 2 x 10^5 cells per ml were cultured in RPMI 1640 containing 10% foetal calf serum with and without 1ml of 1 in 10 diluted IL-2 sample, for 18 hours. Controls were used to account for the IL-2 content of the foetal calf serum. The cells were then pulsed with 0.5µCi of [methyl-^{3}H] thymidine (specific activity 5Ci/mmol, 5µCi/µg) from 18 hours to 24 hours in multiwells. The cells were then harvested on glass fibre discs and counted in a scintillation counter

(counting efficiency ≈40%). Cells cultured in the presence of IL-2 showed a graded thymidine incorporation, measured in cpm x 10^3 and expressed as U/ml of IL-2 by reference to a standard curve. The assay maximum was 80 x 10^3cpm.

At the time of assay, no standardised unit had been confirmed for IL-2 so one unit was taken to be equivalent to the reciprocal of the dilution factor required to give 50% maximum incorporation of [methyl -^{3}H] thymidine into the CTL - L2 cell line. The rates of release of IL-2 from small (250 - 355μm) medium (355 - 500μm) and large beads (500 - 1000μm) are shown in Figure 4.7. Due to the expense of IL-2 and thus the restricted availability of IL-2 loaded beads, meaningful SEMS or statistical analysis could not be computed. However, the cumulative release profiles showed the familiar pattern of burst release for up to 6 days, followed by a significant and sustained low level release which was maintained for at least 16 days. These studies confirmed the biological activity of incorporated and subsequently released IL-2. The small beads (250 - 355μm) produced the highest burst release of IL-2 which was presumably a function of the increased surface area of polymer available for diffusional release. The percentage yield of biologically active IL-2 released after 16 days was 2.23% (250 - 355μm), 1.85% (355 - 500μm) and 1.98% (500 - 1000μm). These results suggest capacity to

FIGURE 4.7 THE CUMULATIVE RELEASE OF IL-2 FROM 0.5g POLYHEMA BEADS INCUBATED AT 37°C.

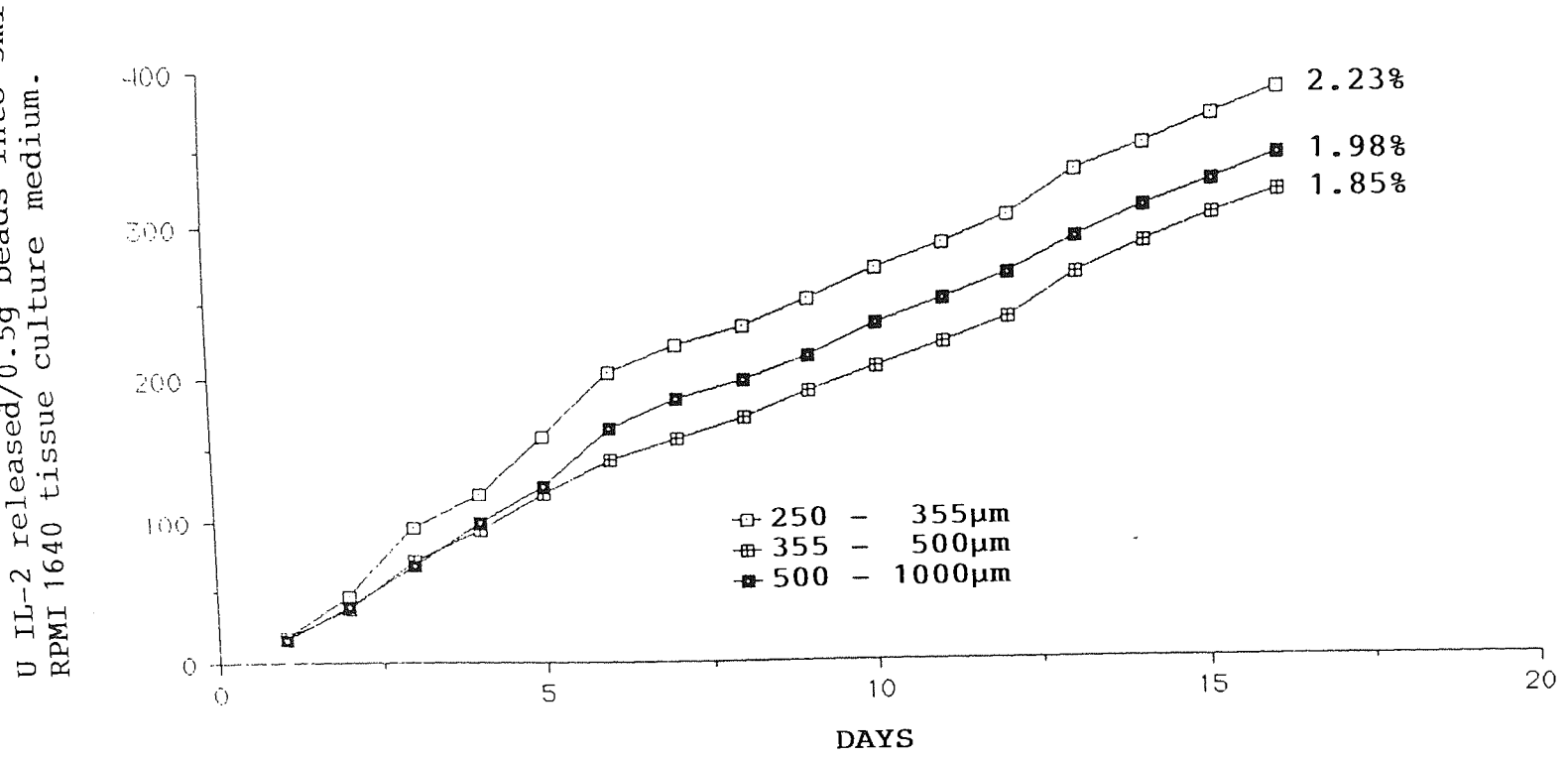

sustain a release rate of approximately 17.5U of IL-2 per day for some considerable time. Although statistical analysis of these results was not possible due to the small sample size, this study did demonstrate that significant sustained release of a biologically active macromolecule was possible from macroporous polyHEMA beads produced by the method developed in this work.

The release profiles for all surrogate and biologically active macromolecules studied so far have demonstrated an initial burst release in the first few days of incubation. This may have been due to the presence of macromolecule at the surface of the bead and in the superficial layers of the matrix. In order to try and reduce this burst release,the washing procedure was extended to 10 minutes in the hope that the majority of the surface protein could be removed before release experiments were initiated. A burst release would be unacceptable if a device were to be used as an implant for the delivery of clinically useful macromolecules, since the dosage must be constant and reliable, without a potentially dangerous pulse of release.

To further evaluate the feasibility of using polyHEMA beads as a controlled delivery device for clinically useful macromolecules, bovine insulin was selected for

study in detail. Insulin concentration is relatively easy to measure in a large amount of samples, using radioimmunoassay and a biological assay can also be performed to confirm the bioactivity of the released insulin molecule.

CHAPTER 5

THE CONTROLLED RELEASE OF BOVINE INSULIN FROM MACROPOROUS POLYHEMA BEADS

Crystalline bovine insulin (MW5660) consists of two polypeptide chains, crosslinked by three disulphide bridges. Native insulin from a number mammalian species is structurally very similar to human insulin. Porcine insulin differs from human insulin only in the substitution of an alanine for a threonine at B30 and bovine insulin, in addition to this substitution has two further substitutions. Both these animal insulins approach the biological potency of human insulin in man and have been widely used for the treatment of diabetes mellitus.

Prior to the fabrication of insulin loaded beads, the effect of freeze drying and subsequent storage at -20°C on the integrity of insulin solutions, of known concentration was determined. This was carried out in order to investigate the suitability of freeze drying and low temperature storage for insulin loaded beads whilst retaining the immunoreactivity of the incorporated insulin. A range (6.25-200µU/ml) of neutral insulin concentrations was made up in 0.01M sodium acetate/0.12M sodium chloride buffer, pH7.4. (Appendix A1). The solutions were freeze dried and stored at -20°C for one week, then thawed and reconstituted with x2 distilled water. A range of freshly prepared insulin solutions was then prepared in sodium acetate/sodium chloride buffer, pH7.4

in the same range of concentrations and the insulin content of both sets of solutions was determined by RIA for comparison.

Table 5.1: Comparison of the insulin content of fresh insulin solutions and freeze-dried insulin solutions, stored at -20°C and reconstituted.

STANDARD INSULIN CONCENTRATION (μU/ml)	n=	INSULIN CONCENTRATION DETERMINED BY RIA (±SEM) (μU/ml)		P
		FRESH	FREEZE DRIED	
6.25	6	5.59 ± 0.8	9.67 ± 2.6	ns
12.5	6	17.82 ± 3.7	12.87 ± 1.4	ns
25	6	28.74 ± 1.6	37.53 ± 2.7	ns
50	6	53.96 ± 2.4	62.02 ± 3.5	ns
100	6	106.41 ± 2.8	118.81 ± 5.7	ns
200	6	201.68 ± 3.9	212.80 ± 4.2	ns

ns = No significant difference in values (Student's unpaired t-test).

Compared with fresh insulin solutions, freeze drying and storage at -20°C for one week had no significant deleterious effect upon the insulin content of reconstituted solutions as determined by RIA, Table 5.1.

Crystalline bovine insulin was incorporated into bead form matrices at loading levels of 0.004, 0.02 and 0.4% of the total weight of the polymer, ie. 2, 10 and 200mg of crystalline insulin per x 4 batch of beads (Page 79). The crystalline insulin was incorporated in solution via 0.01M sodium acetate/0.12M sodium chloride buffer, pH7.4 (Appendix A1).

For the incorporation of insulin as a neutral solution the hormone was dissolved in a minimum of 0.01M hydrochloric acid, 0.1M sodium hydroxide was then added in a dropwise fashion and the insulin precipitated out of solution at around pH7, but redissolved as the pH was increased to approximately pH8. The amount of buffer to replace the water part of the solvent phase of the monomer solution (9.249g per x 1 batch) was then added to the insulin solution and the pH adjusted to 7.4 with 0.01M hydrochloric acid, resulting in a solution of insulin at physiological pH, 7.4. Once the insulin was in buffered solution bead production was carried out in the usual way (Pages 78-85). Fabricated beads were washed for an extended period of 10 minutes, freeze dried and stored in a desiccator over silica gel at -20°C until required. Beads from a number of fabrication batches were pooled for use in release experiments. Release experiments were set up as described previously (Page 87-88). Insulin release

from polyHEMA beads was routinely monitored by radioimmunoassay (RIA). Control studies, using unloaded beads, confirmed that no substances were leached from the polymeric matrix during incubation which would affect the insulin RIA standard curve. Cumulative release profiles were constructed and differences in the rates of insulin release obtained in response to various treatment conditions were computed using two factorial ANOVAR.

5.1 THE EFFECTS OF AGITATION AND BEAD SIZE ON THE RELEASE OF INSULIN FROM 0.4% INSULIN LOADED POLYHEMA BEADS, INCUBATED AT ROOM TEMPERATURE.

Figure 5.1 shows the cumulative release of insulin over 30 days from 0.4% insulin loaded beads under static and agitated (70cpm) conditions at room temperature. In contrast to other macromolecules investigated, insulin did not show an initial burst release but rather, a short initial 'lag' phase of 3-5 days, during which the release of insulin was very low. This 'lag' phase may represent the time taken to fully rehydrate the matrix and for the dissolution of the insulin within the matrix pores and its subsequent diffusion to the exterior. It may be that the extended washing procedure removed any insulin from the surface and superficial layers of the matrix prior to freeze drying. The relatively low loading level of insulin in the beads may have contributed to the absence of an initial burst release.

FIGURE 5.1: THE EFFECTS OF AGITATION AND BEAD SIZE ON THE MEAN CUMULATIVE RELEASE OF INSULIN FROM 0.4% INSULIN LOADED BEADS AT ROOM TEMPERATURE (MEAN VALUES ± SEM, n=6).

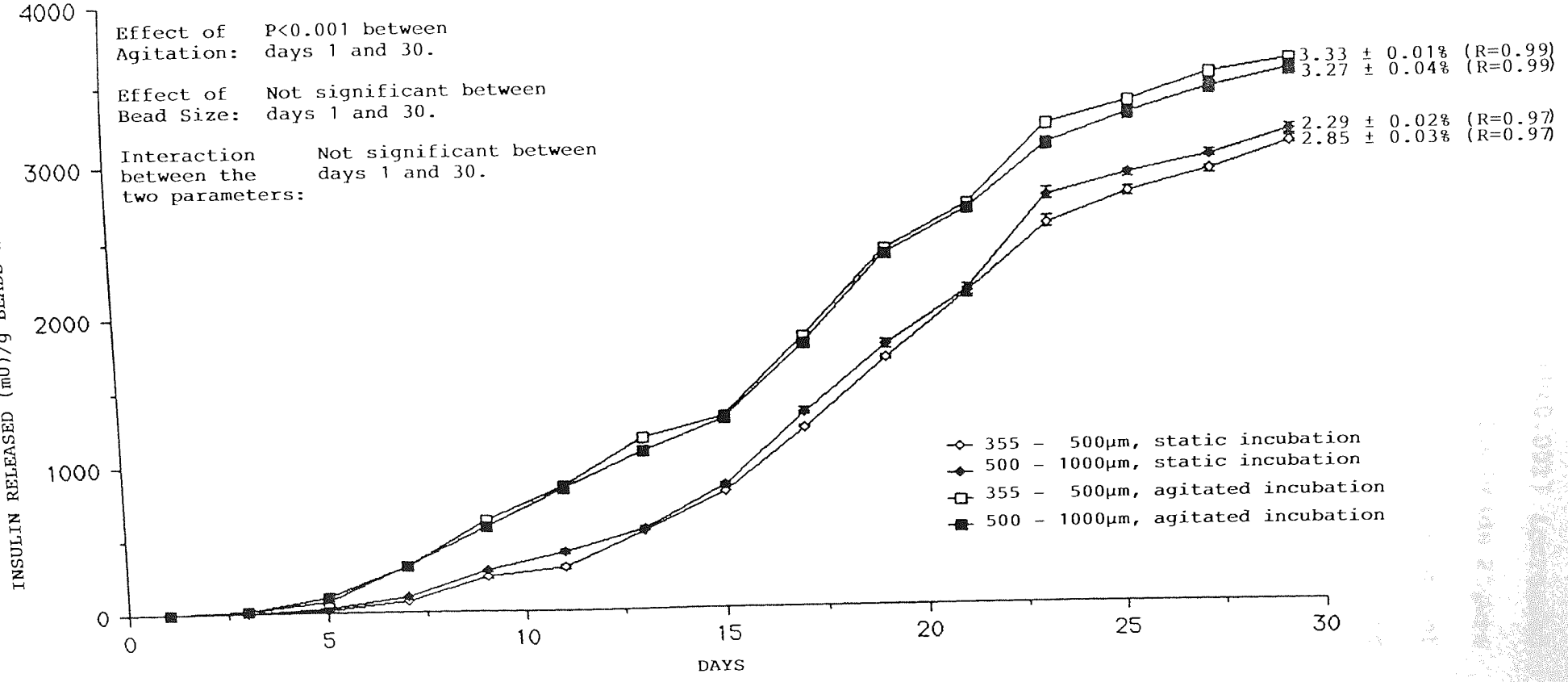

Moderate agitation significantly ($P<0.001$) increased the rate of insulin release from polyHEMA beads Figure 5.1, presumably by encouraging the diffusion of insulin out of the peripheral layers of the matrix and setting up a favourable diffusion gradient at the matrix/buffer interface. Bead diameter did not significantly influence the rate of release of insulin, Figure 5.1. The amount of insulin released after 30 days as a proportion of the total insulin incorporated was very low (approximately 3%) under both static and agitated conditions, irrespective of bead diameter. However, insulin release was reproducible and sustainable over a period of at least one month, at room temperature in the absence of any preservative. The rate of insulin release closely approximated to zero order, especially under agitated conditions.

It may be that the rather small proportion of the total insulin load released over 30 days was due to hydrolytic or microbial degradation of the insulin, since these release experiments were not carried out under aseptic conditions. It was therefore decided to add a preservative to the buffer system to combat possible microbiological deterioration. In addition, the concentration of insulin released from beads and appearing in release samples was very high, relative to the sensitivity of the RIA for insulin. Samples

had to be diluted considerably (up to 1:3,000) to fit the standard curve of the insulin assay. This dilution invariably caused errors in the precision of the insulin assay and hence the loading levels of insulin used in subsequent experimental work were greatly reduced.

5.2 THE EFFECTS OF INCUBATION TEMPERATURE AND PRESERVATIVE ON THE RELEASE OF INSULIN FROM POLYHEMA BEADS.

PolyHEMA beads were fabricated containing bovine insulin at a loading of 0.02% and 0.004% of the total polymer weight, as described previously (Pages 78-85). Release experiments were set up using beads in the 500-1000μm size range (Pages 87-88) in the absence and presence of 2.5% thiomersalate added to the sodium acetate/sodium chloride buffer as a preservative. In addition, flasks were incubated at either 37°C (physiological temperature) or 4°C, on the premise that incubation at the reduced temperature, although unphysiolgical, might aid the preservation of insulin in solution.

5.2.1 The effects of incubation temperature and preservative on the release of insulin from 0.02% insulin loaded beads

The cumulative release of insulin from 0.02% insulin loaded beads in the absence and presence of thiomersalate preservative is shown in Figure 5.2. An initial lag phase, lasting approximately 5 days was observed, followed by a substantial level of insulin release, the amount and duration of which was dependant upon incubation conditions. Insulin release, irrespective of incubation temperature and the presence of preservative approximated to zero order release which was sustained at 4°C in the presence of thiomersalate, Figure 5.2.

After 13 days incubation the release of insulin at 4°C was significantly greater ($P<0.001$) than release at 37°C, both in the absence and presence of preservative. A reduction in the rate of insulin release per day can be seen as a flattening of the release profile, indicating a low level of daily release of insulin. This occurred around day 10 at 37°C and day 17 when incubated at 4°C in the absence of preservative. When thiomersalate was added to the incubation buffer, a reduction in the amount of insulin in solution was not observed until day 15 at 37°C and no fall off in the rate of insulin release was observed over the 45 day incubation period when

FIGURE 5.2: THE EFFECTS OF INCUBATION TEMPERATURE AND PRESERVATIVE ON THE MEAN CUMULATIVE RELEASE OF INSULIN FROM 0.02% INSULIN LOADED BEADS (500-1000μm) (MEAN VALUES ± SEM, n = 9).

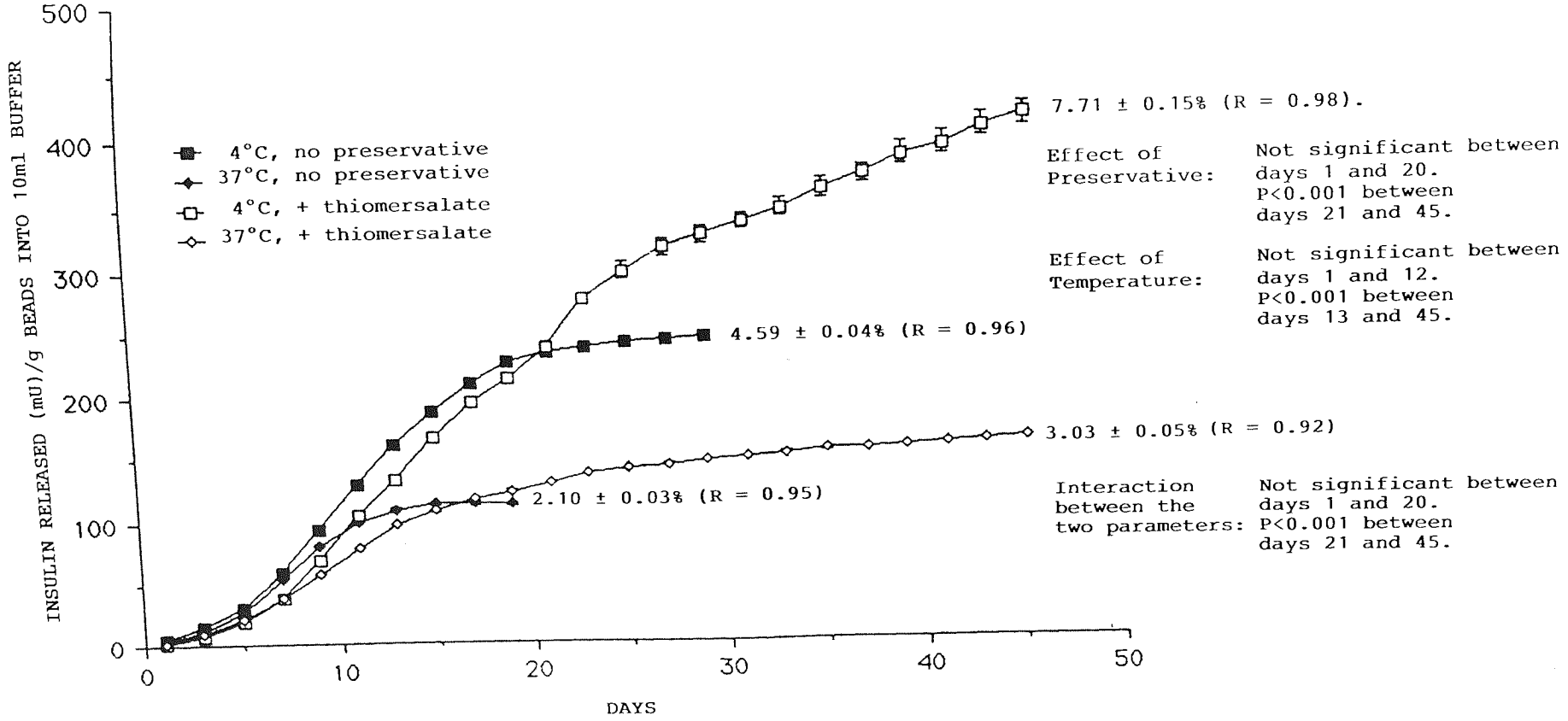

the beads were incubated at 4°C in the presence of thiomersalate.

The addition of 2.5% thiomersalate to the incubation buffer significantly increased ($P<0.001$) the total amount of insulin released after 45 days incubation at both 4°C and 37°C, Figure 5.2. However, the addition of preservative had no significant effect on the rate of release of insulin at 37°C up to day 21 at which time, beads incubated in the absence of preservative had ceased to release immunoreactive insulin. The same was true for beads incubated at 4°C up to day 21 after which time, beads incubated in the presence of thiomersalate released significantly more insulin and continued to release significant amounts of insulin at a rate of approximately 5mU insulin/g beads/day after 45 days. The release of insulin from these beads was monitored for 70 days, at which time approximately 2mU of insulin/g beads/day, continued to be released.

There was significant interaction ($P< 0.001$) between the effects of incubation temperature and preservative on the release of insulin from polyHEMA beads, Figure 5.2. The presence of preservative in the incubation medium influenced the rate of insulin release at the two incubation temperatures in different ways. At 37°C the addition of thiomersalate to the incubation buffer served to extend the time period over which

insulin release could be detected from 19 to 45 days, but did not significantly increase the absolute amount of insulin released per day up to day 21 when beads incubated at 37°C without preservative released no further insulin. Even in the presence of preservative, the amount of insulin released per day at 37°C was small (approximately 0.9mU insulin/g beads/day). However, the combination of low incubation temperature (4°C) and the addition of preservative significantly increased insulin release after day 21 and extended the period over which significant insulin release could be measured. Increasing the incubation temperature from 4°C to 37°C appears to reduce the rate of release of insulin, presumably by acceleration of hydrolytic and/or microbial degradation of insulin in solution. Hydrolytic degradation, accelerated at 37°C appears to significantly affect insulin levels after about 13 days, while microbial breakdown, enhanced in the absence of thiomersalate does not begin to significantly influence insulin levels until after about 3 weeks incubation.

5.2.2 The effects of incubation temperature and preservative on the release of insulin from 0.004% insulin loaded beads

The cumulative release of insulin from 0.004% insulin loaded beads at 4°C and 37°C in the absence and

presence of preservative is shown in Figure 5.3. The inferences drawn from these release profiles are largely the same at those drawn from release profiles obtained with 0.02% insulin loaded beads Figure 5.2. The release rates of insulin approximate to zero order most closely when thiomersalate is added to the incubation medium. The lower incubation temperature (4°C) served to significantly preserve insulin in solution after about 13 days of incubation whilst the thiomersalate showed a significant effect after approximately 25 days incubation. As was seen in the case of 0.02% insulin loaded beads, there was significant interaction between the effects of temperature and preservative after 25 days, when the addition of thiomersalate to the release medium at 4°C caused an increase in the rate of release of insulin as well as an extension of the time period over which insulin was released. A decrease in the percentage of insulin incorporated into polyHEMA beads from 0.02% to 0.004% produced a proportional reduction in the rate of insulin release, and the percentage of the total insulin load released after 35 days from 0.02% and 0.004% insulin loaded beads was of the same order. In the presence of preservative, beads loaded with 0.004% insulin released 5.9% of their total insulin load at 4°C and 2.6% at 37°C after 35 days, while beads loaded with 0.02% insulin released 6.4% at 4°C and 2.9% at

FIGURE 5.3: THE EFFECTS OF INCUBATION TEMPERATURE AND PRESERVATIVE ON THE MEAN CUMULATIVE RELEASE OF INSULIN FROM 0.004% INSULIN LOADED BEADS (500-1000μm) (MEAN VALUES ± SEM, n= 9). 50:50 MONOMER SOLVENT RATIO

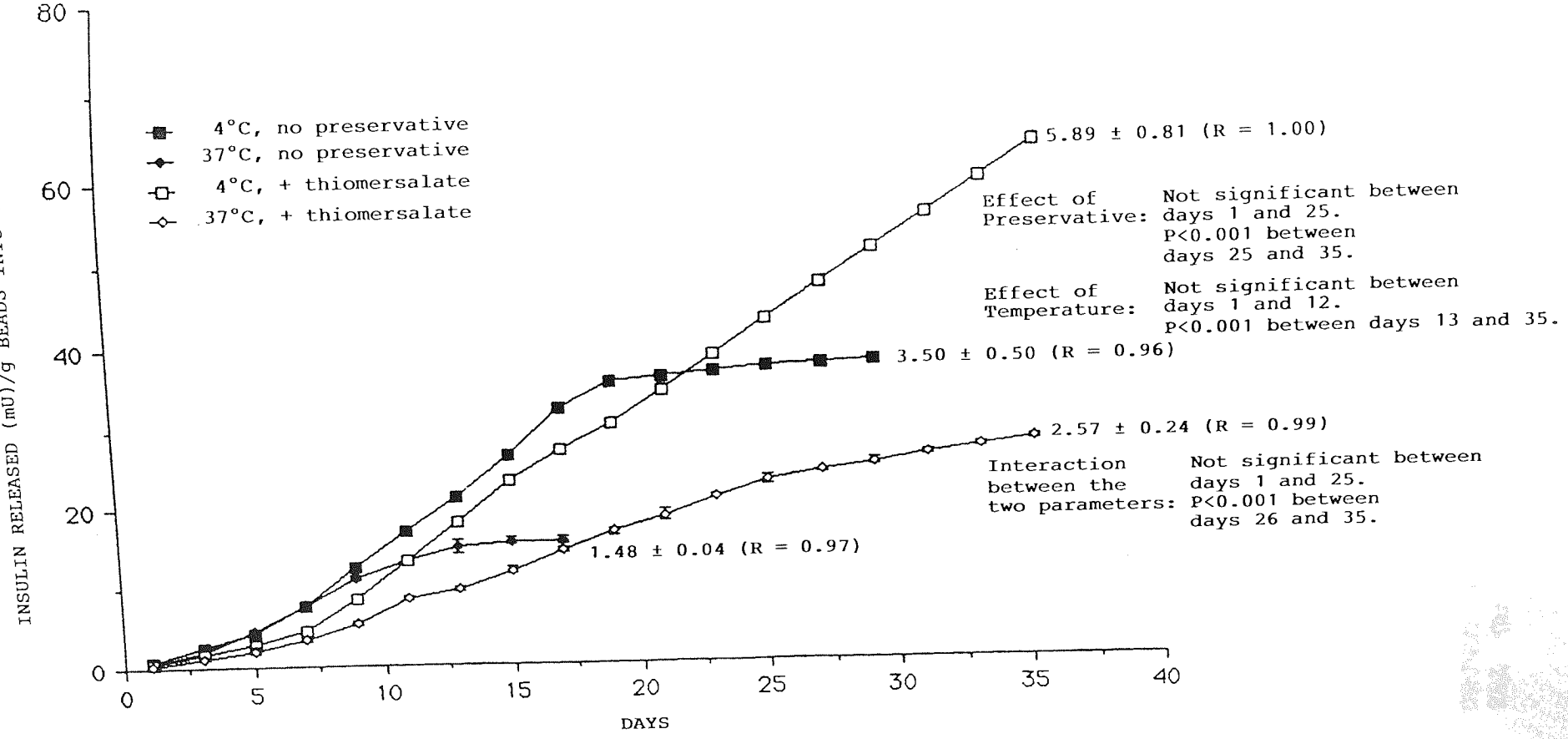

37°C after 35 days incubation in medium containing thiomersalate.

5.3 THE EFFECT OF MONOMER:SOLVENT RATIO ON THE RELEASE OF INSULIN FROM 0.004% INSULIN LOADED BEADS.

0.004% insulin loaded polyHEMA beads were fabricated, with 40, 50 and 60% HEMA monomer in the monomer solution, using the method previously described (Pages 78-85) and 2.5% thiomersalate was used routinely in the incubation medium as a preservative. The effects of incubation temperature and bead size on the rate of release of insulin from polyHEMA beads fabricated with a 40:60 monomer:solvent ratio and a 60:40 monomer:solvent ratio are shown in Figures 5.4 and 5.5 respectively. Bead diameter had no significant effect on the rate of insulin release from beads fabricated with different monomer:solvent ratios and the release at 4°C was always significantly greater than at 37°C after the first 11 days of incubation. Figures 5.6 and 5.7 summarise the release of insulin at 4°C and 37°C respectively from 500-1000μm beads, fabricated using 40, 50 and 60% HEMA monomer concentrations. Decreasing the monomer concentration from 50% to 40% HEMA, resulted in a significant ($P< 0.001$) increase in the rate of insulin release, from 5.89% of the total insulin incorporated, released at 4°C from beads fabricated with 50% monomer to 10.21% of incorporated insulin released from beads fabricated with 40% monomer, over the 35 day release period, Figure 5.6.

FIGURE 5.4: THE EFFECTS OF INCUBATION TEMPERATURE AND BEAD SIZE ON THE MEAN CUMULATIVE RELEASE OF INSULIN FROM 0.004% INSULIN LOADED BEADS FABRICATED WITH A MONOMER:SOLVENT RATIO OF 40:60 (MEAN VALUE ± SEM, n = 9).

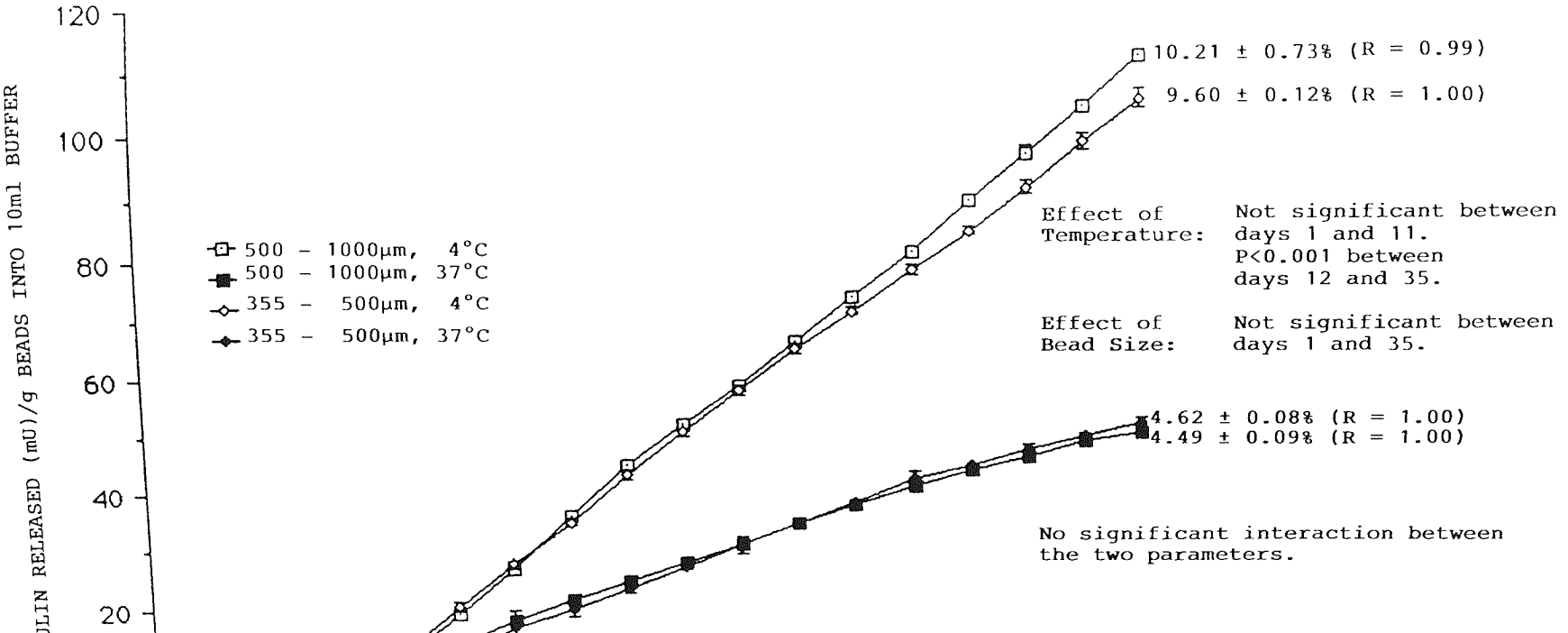

FIGURE 5.5: THE EFFECTS OF INCUBATION TEMPERATURE AND BEAD SIZE ON THE MEAN CUMULATIVE RELEASE OF INSULIN FROM 0.004% INSULIN LOADED BEADS FABRICATED WITH A MONOMER:SOLVENT RATIO OF 60:40. (MEAN VALUE ± SEM, n = 9).

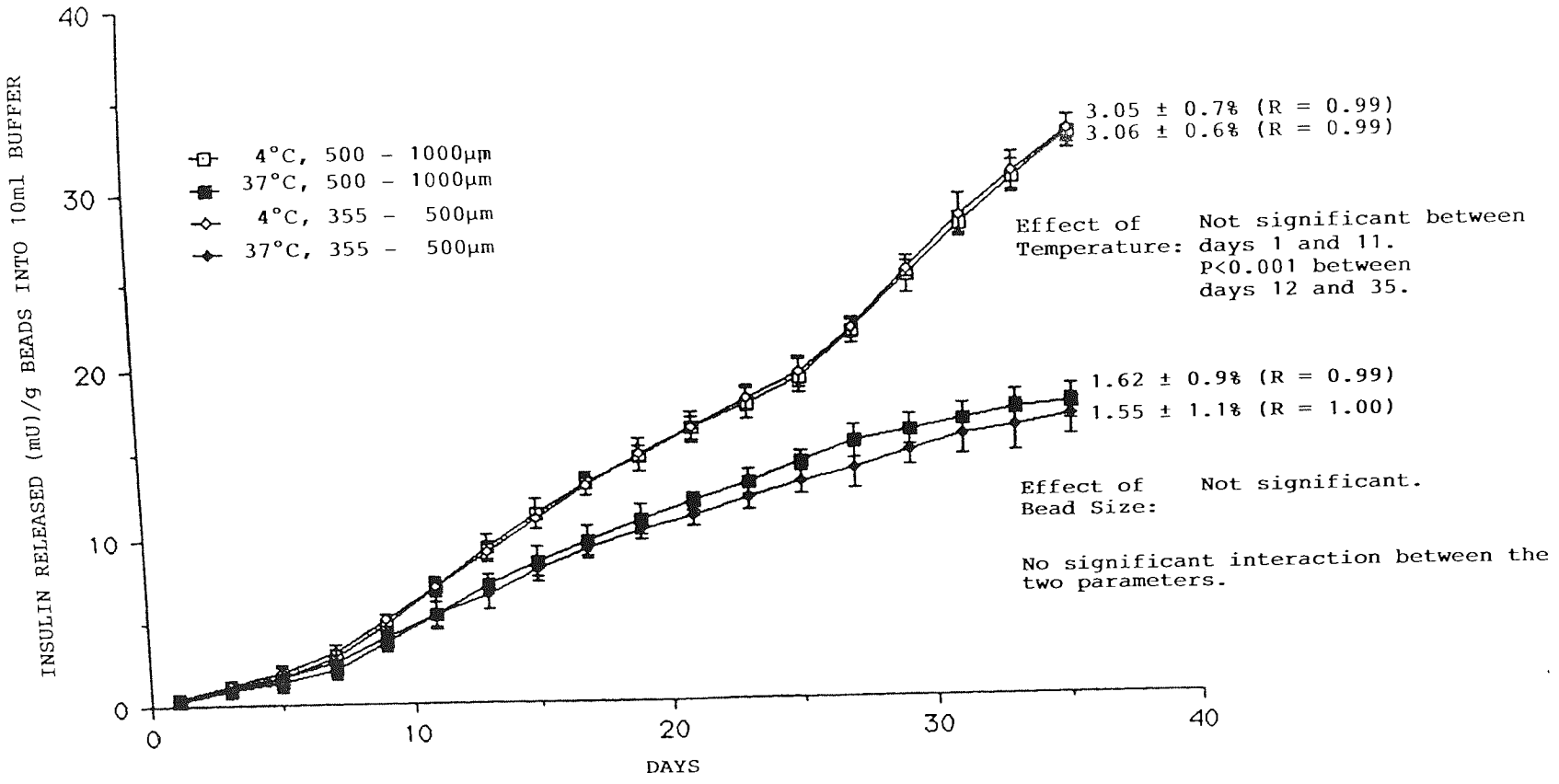

FIGURE 5.6: THE EFFECT OF ALTERATION OF THE MONOMER:SOLVENT RATIO ON THE MEAN CUMULATIVE RELEASE OF INSULIN FROM 0.004% INSULIN LOADED BEADS (500-1000μm) AT AN INCUBATION TEMPERATURE OF 4°C (MEAN VALUES ± SEM, n = 9)

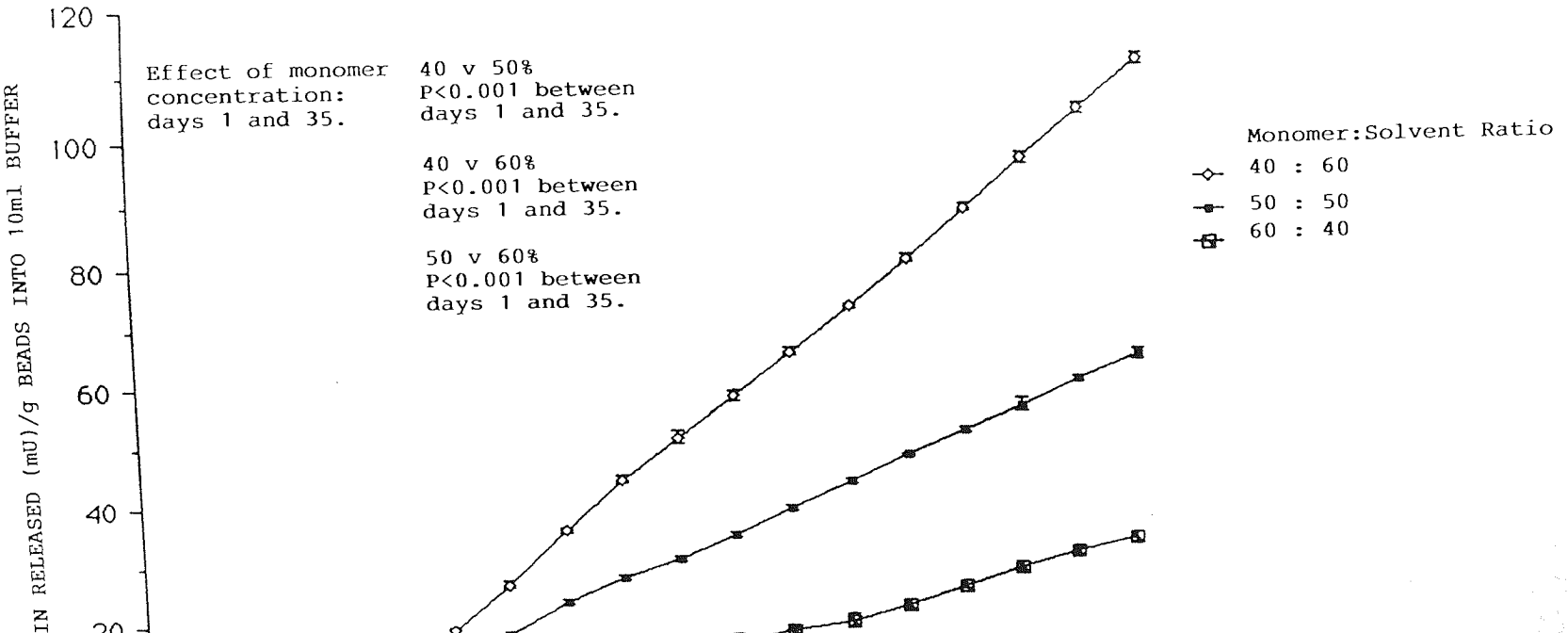

FIGURE 5.7: THE EFFECT OF ALTERATION OF THE MONOMER SOLVENT RATIO ON THE MEAN CUMULATIVE RELEASE OF INSULIN FROM 0.004% INSULIN LOADED BEADS (500-1000μm) AT AN INCUBATION TEMPERATURE OF 37°C (MEAN VALUES ± SEM, n = 9).

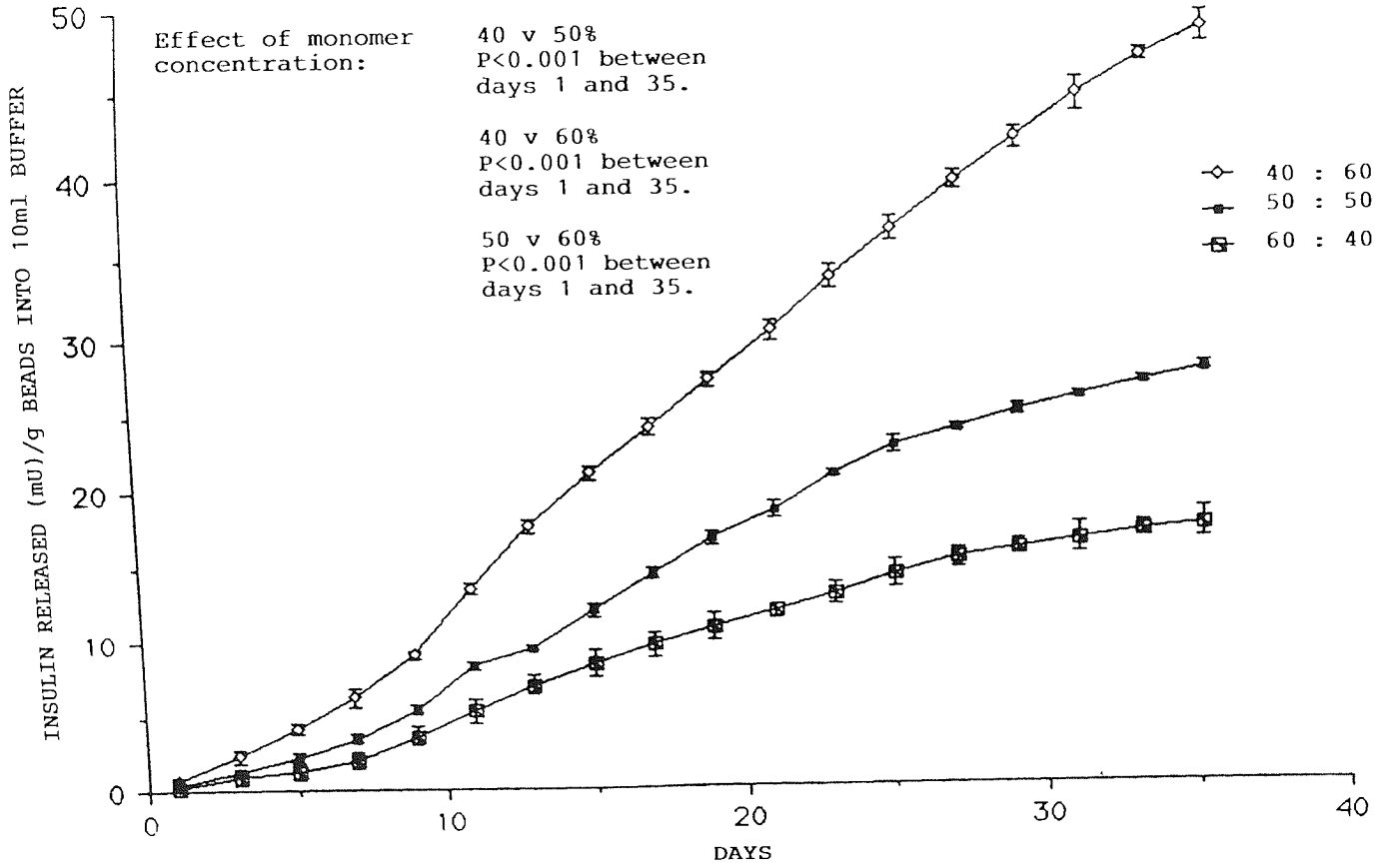

Increasing the HEMA monomer content of the beads, resulted in a significant ($P<0.001$) reduction in the percentage of incorporated insulin released over 35 days at 4°C from 5.89% released from beads fabricated with 50% HEMA monomer to 3.06% from beads fabricated with 60% monomer, Figure 5.6. This effect of monomer concentration was also seen at an incubation of 37°C, Figure 5.7.

PolyHEMA beads containing 40% monomer were found to have the largest pore diameter (2.6µm interior and surface, Plates 3.6 and 3.7, Pages 197 and 198) compared to beads of other formulations produced. Increasing the monomer concentration to 50% resulted in a reduction of the mean pore diameter to 1.9µm in the interior of the bead and 1.4µm at the surface (Plates 3.1 and 3.3, Pages 192 and 194). Further increasing the monomer concentration to 60% led to a reduction in mean pore size to 0.7µm both in the interior and at the surface of the beads, (Plates 3.4 and 3.5, Pages 195 and 196). It may be that the decreasing rate of insulin release seen with increasing monomer concentration is due to the reduction in the size of the macropores within and at the surface of the polyHEMA beads. Ultrastructural studies of polyHEMA beads of varying formulations also revealed that the macroporous network within the bead becomes more tortuous with increasing monomer concentration. The reduction of the rate of insulin

release due to increasing monomer concentrations may also be due to the more tortuous diffusion pathway the insulin must travel for release. At high (60%) monomer concentrations, the macropores are not only smaller in diameter but also fewer in number. This reduction in pore number may also be a factor which leads to reduced release rates from polyHEMA beads fabricated with high monomer concentrations.

The assay of insulin by RIA, although specific and very sensitive only provides information on the immunoreactivity of the insulin molecule and does not necessarily confirm that the insulin released from the beads is still biologically active. With this in mind, the biological activity of insulin samples released from polyHEMA beads was assayed using a well characterised biological technique, involving the rate of insulin stimulated glucose oxidation by isolated rat epididymal fat pads (156-162).

5.4 THE ASSESSMENT OF THE BIOLOGICAL ACTIVITY OF INSULIN RELEASED FROM MACROPOROUS POLYHEMA BEADS.

It was important to establish whether the immunoreactivity of bovine insulin, incorporated and released from polyHEMA beads determined by RIA, also reflected the biological activity of the insulin. The bioactivity of insulin was determined using the rate of insulin stimulated D-[U-^{14}C] - glucose (200µCi/ml)

oxidation to $^{14}Co_2$ by portions of rat epididymal fat pad as described in Chapter 2 (Pages 129-139). Insulin samples were collected from release experiments involving the use of 0.02% insulin loaded beads. No preservative was added to the incubation buffer in case it interfered with the metabolic activity of the adipose tissue or the assay method itself. Concomitant control studies utilised incubation buffer from unloaded polyHEMA beads and confirmed whether the buffer itself or any material leached from the polymeric matrix during incubation had any effect on the rate of glucose oxidation by the adipose tissue. Insulin samples and their controls, collected after 5, 6, 15, 25 and 28 days of release at 4°C and 37°C were assayed for bioactivity. The concentration of insulin in each sample was estimated by reference to a standard curve, constructed for each assay batch, using a range of bovine insulin standard concentrations (0.5, 5 and 50ng/ml). A typical standard curve is shown in Figure 2.11, Page 138. The concentration of biologically active insulin in release samples was expressed in ng/ml.

In this study it was found that the distal portion of the epididymal fat pad was significantly ($P< 0.001$) more sensitive to insulin than the proximal portion, whilst the rates of glucose oxidation shown by the two regions of the pad in the absence of exogenous insulin

(basal rate) was not significantly different, as shown in Table 5.2. In all subsequent studies involving the assay of the bioactivity of the insulin released from polyHEMA beads only the distal portion of the fat pad was used and was cut in a longitudinal fashion.

Table 5.2: Rate of glucose oxidation by distal and proximal portions of the epididymal fat pad under basal conditions and standard insulin concentrations.

INSULIN CONCENTRATION (ng/ml)	n=	MEAN RATE OF INSULIN STIMULATED GLUCOSE OXIDATION ABOVE BASAL (±SEM) (μ mol/mg fat/hr)		P (*** = P< 0.001)
		PROXIMAL	DISTAL	
0.5	6	15.57 ± 2.04	23.99 ± 6.72	***
5	6	24.69 ± 5.84	45.81 ± 8.00	***
50	6	26.22 ± 6.93	52.36 ± 10.45	***
BASAL RATE OF GLUCOSE OXIDATION	6	8.71 ± 1.94	9.01 ± 1.72	***

ns = no significant difference in values (Student's unpaired t-test).

Results obtained from the bioassay of insulin samples show that the insulin released from polyHEMA beads, irrespective of incubation temperature was indeed bioactive. A comparison of the concentrations of insulin in samples released from 0.02% insulin loaded beads, measured by both bioassay and RIA has been summarised in Table 5.3. Results obtained by RIA have been converted to ng/ml (25μU = 1ng). Up to day 6 of incubation at both 4°C and 37°C and on day 15 at 4°C, significantly ($P < 0.01$) higher concentrations of insulin were detected by RIA than by bioassay. By day 15, bioactive and immunoreactive insulin could only be detected in samples from beads incubated at 4°C. Control samples, containing no insulin did not significantly alter the basal rate of glucose oxidation by adipose tissue.

The maximum sensitivity of the bioassay for insulin using the rat epididymal fat pad has been stated to be of the order of 250μU or 10ng/ml of insulin (159). The present work confirms these values and whilst the highest standard insulin concentration used was 50ng/ml, the standard curves obtained (Figure 2.11, Page 138) only demonstrated linearity up to a value of about 12ng/ml of insulin. Therefore the bioactivity of samples containing greater than 12ng/ml of insulin could not be measured without dilution. The need to dilute insulin samples and the high SEMs obtained for

TABLE 5.3: A comparison of the concentration of insulin released from 0.02% insulin loaded beads, determined by bioassay and radioimmunoassay (mean values ± SEM).

DAY	SAMPLE	n=	INSULIN MEASURED BY RIA (ng/ml)			INSULIN MEASURED BY BIOASSAY (ng/ml)			P
DAY 5	4°C	6	48.12	±	0.65	39.9	±	2.51	**
	37°C	6	47.53	±	0.44	36.6	±	1.70	**
	Control 4°C	6	0				ns		
	Control 37°C	6	0				ns		
DAY 6	4°C	6	42.48	±	0.60	38.3	±	1.77	**
	37°C	6	51.23	±	0.84	41.9	±	2.23	**
	Control 4°C	6	0				ns		
	Control 37°C	6	0				ns		
DAY 15	4°C	6	51.60	±	0.84	42.3	±	2.50	**
	37°C	6	0.02	±	0.003		ns		
	Control 4°C	6	0				ns		
	Control 37°C	6	0				ns		
DAY 25	4°C	6	4.09	±	0.23	5.6	±	0.88	
	37°C	6	0				ns		
	Control 4°C	6	0				ns		
	Control 37°C	6	0				ns		
DAY 28	4°C	6	4.07	±	0.23	5.3	±	0.55	
	37°C	6	0				ns		
	Control 4°C	6					ns		
	Control 37°C	6	0				ns		

ns = No significant change in basal rate of glucose oxidation.

** = $P<0.01$ compared with sample measured by RIA.

mean values using the bioassay method may have led to the significant differences between insulin concentrations measured by bioassay and RIA on days 5 and 6 at both incubation temperatures and day 15 at 4°C. When using samples containing low insulin concentrations, which did not require dilution, the amounts of insulin measured by the two methods were the same. These studies confirm that insulin released from polyHEMA beads remains biologically active and that RIA is a reliable estimate of the bioactivity of the insulin present. However, the bioassay was known to be less sensitive and reproducible than RIA with values of minimum sensitivity of 10μU of insulin/ml (161,162) and 5μU of insulin/ml respectively (Table 2.6, Page 121).

CHAPTER 6

GENERAL DISCUSSION

The present work has extended the principle of freeze-thaw polymerisation, previously described by Haldon and Lee (24) for the production of macroporous polyHEMA films, to the fabrication of macroporous polyHEMA bead formed matrices. In our laboratory, macroporous polyHEMA beads were initially fabricated by Skelly (182) and Atwal (180) with a view to their use as bead formed adsorbants for artificial liver support systems. However, these workers did not characterise the physio-chemical parameters which influence the mean bead yield, size distribution or pore size of the beads obtained.

Initial investigations, using a simple bench production system demonstrated the requirement for discrete, non-turbulent delivery of the monomer solution to the surface of the hexane, a sufficiently large vessel for the containment of the hexane and its adequate stirring for the production of discrete polyHEMA spheres. A 5L dewar flask was designed and constructed to allow the safer and more convenient production and harvesting of the polyHEMA beads. A Watson/Marlow peristaltic pump was initially used to obtain a slow (0.3ml/sec) delivery of the monomer solution and the effect of the rate of stirring of the hexane on the mean total bead yield and bead size distribution at this slow delivery speed indicated that increasing the stirrer speed from 150 to 200 rpm

resulted in an increase in the proportion of relatively small beads (355-500, 500-1000μm) and a decrease in the proportion of large beads (>1700μm) whilst the proportion in the middle size range (1000-1700μm) were unaffected (Figure 3.2, Page 165). Stirrer speed did not influence the mean total bead yield. The replacement of the Watson/Marlow peristaltic pump with the Brand Multispenser automatic dispenser and increase in delivery speed resulted in improved spherical shape of the beads without the formation of the 'tails', found when using the Watson/Marlow peristaltic pump and enabled precise, variable control of the rate of delivery of the monomer solution. The rate of delivery of the monomer solution by the Brand dispenser was very much faster than that obtained with the peristaltic pump and could be varied between 7.1 and 9.8 ml/sec. This increase resulted in the generation of much smaller beads than were fabricated using the peristaltic pump. The delivery speed of 0.3ml/sec, obtained using the peristaltic pump and did not result in the production of beads smaller than 355μm, irrespective of stirrer speed, whilst spherical beads were routinely obtained in the size range 106-250μm when using the Brand dispenser. Increasing the delivery speed of the monomer solution from 7.1 to 9.8 ml/sec generally led to a decrease in the proportion of large beads (>1000μm), whilst increasing the percentage of the

bead yield which was less than 106µm in diameter. The proportion of beads 106-500µm in diameter were not significantly influenced by the change in delivery speed. However, this influence of delivery speed depended on the stirring speed of the hexane. If the stirring speed was too fast in relation to the delivery speed, for example, a stirrer speed of 300 rpm with a delivery speed of 7.1ml/sec (Figure 3.8, Page 180), increasing the delivery speed to 9.8 ml/sec increased the proportion of large beads (500->1700µm) whilst resulting in a significant decrease in the proportion of small (<500µm) beads produced. This was because a stirrer speed of 300 rpm caused break-up of the monomer droplets in the hexane, at a delivery speed of 7.1ml/sec, resulting in the production of a large amount of debris. The effect that increasing the rate of stirring of the hexane had on increasing the proportion of smaller beads in the total yield, noted in earlier experiments using a slow delivery rate (0.3ml/sec), was confirmed using fast monomer delivery rates. For example, at a monomer delivery rate of 9.8ml/sec increasing the stirrer speed from 250-400 rpm (Figure 3.6, Page 176) resulted in a significant decrease in the proportion of beads in the two largest size categories, 1000-1700µm and >1700µm and a significant increase in the amount of smaller beads produced (<106µm - 500µm) while the proportion of beads in the middle size range (500 - 1000µm) was

unaffected by the change in stirrer speed. Delivery speed and stirrer speed had no significant effect on the mean total bead yield. Also, the loading of the beads with buffers as part of the monomer solution, with or without an incorporated macromolecule and alteration of the monomer:solvent ratio, had no significant effect on either the mean total bead yield or the bead size distribution. When the delivery speed of the monomer solution was increased, to alter the bead size distribution and give a greater proportion of small beads, the stirrer speed had to be increased to avoid 'clumping' of the beads due to an insufficient rate of stirring or conversely, debris formation which occurred when the non-solvent was stirred too quickly.

These developmental studies allowed the fabrication of predictable bead sizes and an optimal bench system for the production of macroporous polyHEMA beads was produced. This comprised the Brand dispenser set at speed setting IV (9.8ml/sec) and the stirrer set at a speed of 300 rpm (Figure 2.1, Page 84). These fabrication conditions resulted in high mean total bead yields (76.8%) with the majority of beads in a medium size range (500 - 1000µm) which were a convenient bead size for release studies. Large batches of beads could be conveniently fabricated by multiplying up the quantity of fabrication materials and a x4 batch was easily accommodated by the optimal

bench system. The small standard error of the means for each bead size category indicated good reproducibility of the bead fabrication method.

Ultrastructural examination of the polyHEMA bead formed matrices using scanning electron microscopy, revealed the presence of a well defined macroporous matrix, containing a comprehensive pore system which appeared to be interconnecting with a tortuous path through the beads. Pores on the surface of the beads were less widely distributed than in the interior and appeared to be organised into discrete domains. This different distribution is thought to be the result of insufficient phase separation at the surface of the beads, due to instantaneous freezing as it comes into contact with the cold hexane.

The mean pore diameter, both at the surface and in the interior of the beads varied over the range 0.7µm (60% monomer) to 2.6µm (40% monomer), depending on monomer concentration. Previous studies undertaken by Skelly (182) and Atwal (180) did not involve routine pore size measurements, although Skelly stated that the mean pore diameter at the surface of a polyHEMA bead, fabricated with a monomer:solvent ratio of 50:50 appeared to be of the order of 2µm. The present work has confirmed this observation and established that the mean pore diameter at the surface of a polyHEMA

bead of 50:50 monomer:solvent ratio was 1.4μm (range of 0.9 - 2.1μm, Plate 3.3, Page 194). The mean pore diameter in the interior of beads with the same monomer concentration was 1.9μm (1.5 - 2.9μm range, Plate 3.1, Page 192). Haldon and Lee measured approximate pore sizes from photomicrographs of polyHEMA films and obtained values of 1-2μm for pores in fast frozen films and 0.5-1.0μm for pores in slowly cooled films (24). Increasing the monomer concentration from 50 to 60% resulted in the reduction of mean pore diameter on the surface of polyHEMA beads from 1.4μm to 0.7μm (Plate 3.5,Page 196) and in the interior of the beads from 1.9μm to 0.7μm (Plate 3.4, Page 195). This may have been the result of a reduction in the amount of water available to form the ice crystal network and hence subsequent macropore formation. Conversely, decreasing the monomer concentration from 50 to 40% increased the mean pore diameter to 2.6μm (Plates 3.6 and 3.7,Pages 197 & 198) both in the interior and on the surface of the beads. Reducing the monomer:solvent ratio to 40% solvent also resulted in a reduced number of pores at the bead surface than were seen with solvent concentrations of 50 and 60% and the structure of the pore matrix appeared more tortuous, whilst increasing the solvent concentration to 60% resulted in a more extensive porous network which seemed to cause straighter channels through the beads. Skelly noted an increased

tortuosity of the pores at the interior of the beads due to a slower rate of freezing (182). It may be that the monomer solution froze more quickly at high (60%) water content, leading to a reduced tortuosity of the pore matrix whilst at lower solvent (40%) concentrations, the freezing point of the monomer solution was lower and hence the slower freezing rate increased tortuosity. Manipulation of the monomer:solvent ratio provided a simple and predictable means of significantly altering the mean pore diameter and pore frequency of the macroporous bead formed matrices.

The change in the pore diameter of unloaded polyHEMA beads by altering the monomer:solvent ratio was reflected in the changes in EWC of the beads. Beads obtained using a 50% monomer concentration were found to have a mean EWC of 60.02%. Increasing the monomer:solvent ratio to 60:40 resulted in a decrease in the mean EWC to 51.79% and decreasing the monomer concentration to 40% caused an increase in the mean EWC to 69.51% (Table 3.3, Page 189). These results confirmed the observations of Haldon and Lee on polyHEMA films. These workers suggested that the EWC of a polymer made by freeze-thaw polymerisation was not directly proportional to its initial water content since the ice separated from different solution concentrations at different temperatures (24).

Results obtained by Skelly for macroporous polyHEMA beads showed that using a monomer:solvent concentration of 50:50 produced an EWC of 52% while at 60% monomer an EWC of 43% was obtained (182). In general, EWC values obtained during the course of this work were somewhat higher than those obtained by Skelly. This probably reflects the difficulty in obtaining an accurate measurement of the hydrated weight of polyHEMA beads, due to the persistence of a thin film of water around the polymer bead. Although the hydrated beads were carefully blotted with dry filter paper prior to weighing, no control was made for evaporation, different room temperatures or humidity.

The use of sodium acetate/sodium chloride and boric acid - borate buffers, used as carrier buffers for macromolecules in the monomer solution, had no effect on the mean pore size of the macroporous polyHEMA beads, however, an increase in EWC of the beads was observed with the use of sodium acetate/sodium chloride buffer, (Table 3.3, Page 189). It has been reported that the swelling of the matrix is due to repulsive forces between adsorbed acetate ions in the matrix (102). Clearly, this effect would not influence the size of macropores observed in dehydrated bead samples. The swelling caused by the acetate anion was sufficient to keep the EWC of the

polyHEMA beads at approximately 75% irrespective of any change in pore size brought about by changing the monomer:solvent ratio of the monomer solution. This confirms the importance of monitoring pore size within the matrix by scanning electron microscopy. In addition, the incompatibility of phosphate buffer with the photoinitiator used in the monomer solution supports the need for careful selection of the constituents of the monomer solution before incorporation of a macromolecule. The absence of any effect caused by the use of buffer, or the process of macromolecule incorporation, on the pore size of polyHEMA beads, may be the result of the low molarity of buffers (<0.2M) and the low loading levels of macromolecules (<5%) employed. HEMA monomer solution with a 50:50 monomer:solvent ratio, containing 10% EDM and a 1:4 EG:H_2O ratio freezes at around -10°C (24). Since a temperature of -70°C was employed for bead fabrication, the addition of macromolecules and/or buffer salts at low concentrations would be unlikely to exert any further lowering of the freezing point sufficient to influence pore structure. For example, at the molarity used in this work, sodium acetate/sodium chloride buffer only lowers the freezing point between 3 and 7°C (183).

Cytotoxicity testing, involving the exposure of cultured L929 mouse fibroblasts to bead extracts

indicated the presence of a small quantity of cytotoxic leachable material, sufficient to cause a reduction in the rate of growth of L929 cells, but not sufficiently toxic to eliminate cell growth. The MEM elution test is extremely sensitive and the modest cytotoxic effect demonstrated for bead extracts must be weighed against the large body of evidence supporting the tissue biocompatability of polyHEMA (13,77-82). However, these results demonstrated the need for a thorough washing of the polymer beads after fabrication. The acute toxicity of HEMA monomer to cells in culture, confirmed in the present work, underlines the importance of ensuring complete polymerisation of the polymeric matrix. The bead formed polymeric matrices generated in this work were designed with their future use as an implant and in vivo biocompatibility very much in mind. The small size of the beads produced by freeze-thaw polymerisation (mean 500-1000μm) tended to minimise the possibility of incomplete polymerisation of the matrix and hence reduced the likelihood of any significant amounts of residual monomer being leached from the matrix. The UV exposure time required to polymerise small beads was kept to a functional minimum to reduce the possibility of the UV denaturation of incorporated macromolecules. The water content of the polyHEMA beads produced is relatively high, since high water content has been

shown to reduce the tendency of proteins to adsorb to the surface of a hydrogel (116,118). The denaturation of proteins adsorbed on the surface of a polymer may serve as a trigger for phagocytic attack *in vivo* (117). However, the water content of the polyHEMA matrices in the present work was kept below 70% to reduce the likelihood of calcification on implantation (86-88).

Evaluation of the release kinetics of the surrogate macromolecule bovine serum albumin (BSA) demonstrated that freeze drying greatly improved the rate of release of the BSA, compared with air drying of the polyHEMA matrix, from about 3.5 to 16% over 20 days (Figure 4.1, Page 213). Lyophilisation and cold temperature storage are often used for the storage of biologically active macromolecules, allowing the preservation of bioactivity on reconstitution. Lyophilisation freezes the molecules in solution prior to the removal of water by sublimation under vacuum. This may allow the macromolecule to be more easily dissolved on rehydration and hence lead to greater *in vitro* release rates. Investigation of the influence of drying and storage procedures on the subsequent biological activity and rate of release of incorporated macromolecules has received little attention in the literature.

In the present work, approximately 16% of the total BSA incorporated was released into x2 distilled water at room temperature, from freeze-dried polyHEMA beads over 20 days. Agitation of the release medium significantly increased this total release to around 23% of BSA incorporated (Figure 4.2, Page 215). The influence of agitation on the rate of release of incorporated macromolecules was also confirmed in subsequent experiments, involving the release of insulin. Agitation appears to increase the rate of release of the macromolecule by encouraging diffusion away from the matrix, setting up a more favourable concentration gradient. The increased rate of release caused by agitation emphasised the dependence of the rate of release of the macromolecule on its rate of diffusion from the matrix. The effect of agitation may be important when considering the likely rate of release of macromolecule *in vivo*. Brown and coworkers showed that *in vivo* and *in vitro* rates of release of BSA, ß-lactoglobulin and inulin were identical from ethylene vinyl acetate copolymer devices, if the matrices were subjected to agitation *in vitro* (19). Agitation of the polymeric device is likely to give incubation conditions closer to physiological conditions than static incubation, since *in vivo*, the macromolecule would have almost infinite sink

conditions for release, whereas a local build up of macromolecule around the polymeric beads in vitro under static incubation conditions would tend to reduce the concentration gradient and hence the diffusion rate of the macromolecule.

In order to investigate the influence of molecular weight of the macromolecule on its rate of release from macroporous bead formed matrices, the incorporation and rate of release of two molecular weight species of FITC-linked dextran were studied, FD-20S (MW 17,500) and FD-150 (MW 148,900). The low molecular weight species was released significantly faster than the high molecular weight species and increasing the incubation temperature from 4°C to 37°C led to a significant increase in the rates of release of both macromolecules. These observations confirm that diffusion from the matrix is the mechanism controlling the rate of release of these molecules. However, the rates of release of both FITC-linked dextrans were very fast, compared with the release rates of other macromolecules studied. 54.4% of the total FD-20S and 48.6% of FD-150 incorporated was released over 21 days at 4°C increasing to 75% and 64.4% respectively at 37°C (Figure 4.5, Page 223). BSA (MW 68,000) has a lower molecular weight than FD-20S and yet only 16% of the total incorporated load was released after 20 days incubation at room

temperature. This difference in release rate was probably due to the relatively lower solubility of BSA in water compared with the solubility of FITC-linked dextrans in buffer. Glucose oxidase (GOD, MW 154,000) has a molecular weight similar to FD-150 and yet less than 4% of the enzyme incorporated was released into buffer solution over a 14 day incubation at room temperature (Figure 4.6, Page 226). The low rate of release of GOD may have been due to either the hydrolytic or microbial degradation of the enzyme in solution, or its immobilisation within the matrix.
It is clear that the molecular weight of the macromolecule per se is not an important factor governing the rate of release and that the solubility and stability of the macromolecule in solution and its molecular radius may be more important factors controlling release rates. Langer and coworkers confirmed that there is no clear influence of molecular weight of a macromolecule on its rate of release from a polymeric matrix comprised of ethylene vinyl acetate copolymers (12-14).

The incorporation and subsequent biological assay of GOD and interleukin-2 (IL-2) released from macroporous polyHEMA bead formed matrices, confirmed the property of this polymeric device to release macromolecules in a biologically active form. Both these macromolecules required the assay of their biological activity for

detection. The incorporation of buffered solutions of these hydrolytically unstable peptides, at low temperatures into polyHEMA beads and their subsequent freeze drying and storage at -20°C preserved the biological activity of the macromolecules. Freeze drying the macromolecules in buffered solution within the matrix and their subsequent release into the same buffer maximised their solubility. The release of GOD was characterised by a large burst release which extended over 4 days. The release rate then quickly fell away and no further release was detectable after 14 days (Figure 4.6, Page 226). It is unclear whether the low (≈4%) release of GOD was due to degradation of the released enzyme in solution at room temperature, or possibly due to immobilisation of the enzyme within or on the matrix. The release of IL-2 showed a similar burst release profile and at the termination of the IL-2 release studies, about 2% of the total incorporated IL-2 had been released from the matrix after 16 days at 37°C (Figure 4.7, Page 231). IL-2 release at this time was sustained, low level and could probably have continued for a considerable period of time.

The parameters which control the release of biologically active macromolecules from macroporous polyHEMA matrices were further investigated by monitoring the rate of release of the clinically

significant macromolecule bovine insulin. Insulin released from beads was routinely monitored by RIA. Agitation of the incubation buffer significantly increased the proportion of total incorporated insulin released from 0.4% insulin loaded beads (500-1000μm), from 2.29% to 3.27% over 30 days at room temperature, in the absence of preservative (Figure 5.1, Page 239). This effect, as with the increased release of BSA seen with agitation, was thought to be due to the rapid removal of the macromolecule in solution from the microenvironment around the beads, setting up a more favourable concentration gradient for release. Increasing the incubation temperature from 4°C to 37°C resulted in a decrease in the rate of release of insulin, an observation at variance with the effect of temperature on the rate of release of FITC-linked dextrans. The rate and duration of insulin release was increased at 4°C compared with 37°C. This was attributed to the increased hydrolytic and microbial degradation of insulin in solution at 37°C. The addition of the preservative thiomersalate (2.5%) to the incubation medium extended the time period over which insulin release could be detected, presumably by decreasing the microbial degradation of the macromolecule in solution. 0.02% insulin loaded beads released 2.1% of the total insulin incorporated over 19 days at 37°C in the absence of preservative in the buffer (Figure 5.2, Page 243). The addition of

preservative did not significantly increase the amount of insulin released over the first 19 days, but did preserve immunoassayable insulin release for 45 days. A similar effect for preservative was seen at 4°C, increasing the percentage of the total loading of insulin released from 4.6% over 30 days to 7.7% over the 45 day release period at a rate of about 5mU of insulin a day (Figure 5.2, Page 243). These studies highlighted the difficulty of monitoring the rate of release of easily degradable macromolecules in vitro. It was possible to minimise the microbial degradation of insulin in solution, but hydrolytic degradation, especially at 37°C could not be avoided. Despite the problems of degradation, immunoassayable insulin was released from macroporous polyHEMA beads (0.02% insulin loaded) for over 70 days, at the rate of 2mU of insulin per day. Insulin release from polyHEMA beads was directly proportional to the initial loading level. 5.9% and 2.6% of the total insulin loading was released from 0.004% insulin loaded beads in the presence of thiomersalate at 4°C and 37°C respectively after 35 days incubation (Figure 5.3, Page 247). Beads loaded with 0.02% insulin released 6.4% and 2.9% of the total insulin loaded at 4°C and 37°C respectively, under the same incubation conditions. Bead diameter did not appear to be a significant factor in controlling the rate of release of macromolecules from polyHEMA beads. It appears that

macromolecule stability and also perhaps solubility were more significant factors influencing the rate of release of biologically active macromolecules than was the bead diameter.

The monomer:solvent ratio of the monomer solution into which insulin was loaded, in buffer via the water phase, was a significant parameter affecting the rate of release of insulin. An increase in the proportion of total HEMA monomer from 50% to 60% resulted in a significant decrease in the percentage of the total incorporated insulin subsequently released from 0.004% insulin loaded beads (500-1000μm), from 5.9% to 3.1% at an incubation temperature of 4°C in the presence of thiomersalate, over a 35 day incubation period. Decreasing the HEMA monomer concentration to 40% of the total monomer solution, resulted in an increase of the proportion of the total insulin load released at 4°C to 10.2% over the same time period (Figure 5.6, Page 251). There was however, no significant difference in the EWC of 0.004% insulin loaded beads fabricated with 40, 50 or 60% HEMA monomer due to the swelling of the matrix caused by the sodium acetate/sodium chloride buffer used for insulin incorporation. The monomer:solvent concentration did, however, affect the macroporosity of the polyHEMA beads loaded with insulin. It was assumed that the release of incorporated macromolecules occurred via

the macropores and not through the low water content polymer matrix per se, due to the large size of the macromolecules and hence, any change in the water content of the matrix polymer would be unlikely to affect the rate of release of macromolecules. The macropore sizes in the interior of 0.004% insulin loaded beads increased with decreasing monomer content, ie 0.7μm at 60% monomer, 1.9μm at 50% monomer and 2.6μm at 40% monomer. Insulin usually exists as a dimer in solution with dimensions of 0.02 x 0.04μm (184). It is therefore unlikely that frictional or steric hinderance to the insulin molecule passing through a reduced pore diameter would account for the reduction in insulin release seen at lower solvent concentrations. However, at low solvent concentrations, the pores are not only smaller than at high solvent concentrations, but also fewer in number and it may be that it is the reduced number of pores which leads to a reduction in the rate of insulin release at low solvent concentrations. Increasing the solvent concentration to 60% not only produced larger, more numerous pores, but also appeared to reduce the tortuosity of the matrix, giving the pore network a much more ordered appearance. The lack of tortuosity may also be responsible for the increased rate of insulin release from polyHEMA beads fabricated with 60% solvent. The results of these experiments show that the structure of the polymeric matrix itself is

also an important factor in affecting the release rates of macromolecules. Since the EWC of insulin loaded beads is not influenced by monomer:solvent ratio due to the swelling effect of the sodium acetate/sodium chloride buffer, the hydration of the polymeric matrix per se does not appear to be an important factor in controlling insulin release rates. However, the swelling of the matrix brought about by the buffer increases the amount of hydration, increasing the EWC. The larger the pore size the greater will be the amount of water within the polymeric matrix and this could lead to the easier dissolution of the insulin molecule.

The biological assay of insulin samples released from polyHEMA beads was carried out using the insulin stimulated rate of glucose oxidation by rat epididymal fat pads. Insulin radioimmunoassay was known to be an accurate and convenient method of measuring the amount of immunoereactive insulin in a sample but it was not known if immunoreactivity was a reliable estimate of biological activity. The studies undertaken in this work established that the biological activity and the immunoreactivity of released insulin were closely related and that the insulin released from polyHEMA beads retained its biological activity.

In the present study, the typical cumulative release profile observed for surrogate macromolecules generally consisted of a short burst release, followed by a period of sustained release, approaching zero order, followed by a gradual decline in the rates of release. This type of release profile is a common feature of diffusion from a monolith or matrix type system (14). However, this type of profile was not observed for insulin release from bead form polyHEMA matrices. Insulin release was characterised by an initial 'lag' phase, lasting approximately 5 days, followed by a period of increased insulin release and a subsequent period of lower, but sustained release. The absence of a period of burst release may have been due to the very low percentage loading levels of insulin employed (0.4 - 0.004%). The insulin would have been widely dispersed throughout the macroporous matrix. Also, a longer period of washing probably removed much of the insulin from the surface layers of the beads, suppressing a burst release of insulin. The washing procedure was standardised as far as possible so that the amount of macromolecule lost through washing was kept relatively constant. A period of zero order insulin release was observed in all studies involving insulin release. However, zero order release was best achieved over approximately 40 days after the initial lag phase, from 0.004% insulin loaded beads, incubated at 4°C in the presence of

thiomersalate. This may have been the result of a comprehensive dispersal of insulin within the polymer and the subsequent control of insulin released by fewer, smaller pores at the matrix surface than in the interior of the bead. The adsorption of proteins onto the internal surface of the macropores might also have contributed to the overall release profile, although this would be expected to be minimal because of the high water content of the hydrogel (116,118).

The process by which macromolecules have been incorporated into polyHEMA matrices and their release subsequently monitored is unique to this study. There are few reports of the release of protein macromolecules from polymeric delivery devices in the literature and no report of protein macromolecules being contained within macropores prior to release. The first documented instance of the release of insulin in a biologically active form from polyacrylamide pellets was reported in 1971 by Davis (185). In this study, the recorded release of insulin was low and only sustained for a few days. Also the polymer used, polyacrylamide, is known to cause significant inflammation on implantation (13,82). In 1976, Langer and Folkman described a method of incorporation of protein macromolecules for sustained release, by the incorporation of the protein into an ethylene vinyl acetate copolymer (EVAc) solution, in

a powdered crystalline form (12). The powdered macromolecule formed a network of channels within the polymer and on rehydration the protein dissolved and was released from the polymer. As the incubation medium penetrates, more macromolecule is dissolved and diffuses through gaps in the polymer vacated by macromolecule nearer the surface (13). EVAc is relatively hydrophobic and so the rate of protein release from this polymer depended on the rate of influx of the environmental medium as the macromolecule dissolved. Macromolecules which have been incorporated into this EVAc system include BSA, ß-lactoglobulin, catalase, lysozyme and alkaline phosphatase (12-14). Macromolecule particle size has been found to be a significant factor controlling release rates in the EVAc system (14). However, this feature is not important in the macroporous polyHEMA matrices used in the present work because the macromolecule is incorporated in solution. EVAc pellets have been utilised in vivo for the controlled release of insulin in diabetic rats. Release rates of 2U of insulin per day have been achieved for up to 1 month (15), which increased to 5U of insulin per day when a more soluble insulin preparation was used (16). This demonstrates the high dependence of this type of system on the solubility of the incorporated macromolecule. Release rates of insulin achieved by these workers were high, but these rates also required

a high level of insulin loading, (30% wt/wt to achieve 5U/day) and a highly soluble sodium insulin preparation. It may be possible to incorporate such an insulin into polyHEMA matrices used in the present work, to test the influence of the solubility of the macromolecule on its subsequent rate of release. It is however, difficult to compare the in vitro insulin release rates obtained in the present work, with in vivo values of insulin release reported by other workers.

Polymer-based delivery vehicles, of various types, have been used for the controlled delivery of many substances including steroids (8,9,35,186,187) narcotic antagonists (33,34) and anticancer agents (56,57). Controlled delivery vehicles are already available for the delivery of low molecular weight species such as these and the technology is well understood. However, the controlled release of biologically active macromolecules such as hormones, enzymes and growth factors is an area which is currently underexploited. The prevention of the long term complications of diabetes, such as neuropathy, nephropathy and retionopathy is a major goal in diabetes research. Insulin dependant diabetics (IDD) normally inject insulin at least once and generally twice a day, in an attempt to maintain normoglycaemia. This is not only extremely inconvenient for the

individual, but more importantly, fluctuations in blood glucose can occur, especially just prior to and after injections. These periodic fluctuations in blood glucose are thought to be responsible for the distressing side effects of the disease (188). In 1976, the American Diabetes Association issued a statement, supporting the view that the control of hyperglycaemia may reduce the risk of long term complications, that the therapeutic regimens available, such as insulin injections and dietary control, were only partly effective and that more physiologically sound insulin delivery systems needed to be developed (189).

Animal studies have yielded persuasive data regarding the benefits of good control of blood sugar levels on the development of diabetic complications (190-194). However, results from human studies have not proved conclusive since ethical constraints and the long time period between onset of diabetes and the appearance of complications make human studies difficult. The availability of continuous insulin infusion pumps (188) has enabled the affects of tight control of blood sugar to be investigated more easily. Christensen and coworkers compared the effects of continuous subcutaneous insulin infusion (CSII) and conventional insulin treatment (CIT) on the kidney function of long term IDD patients (195). These

authors concluded that the improved control over blood sugar levels obtained by CSII was associated with normalization of renal hyperfunction found in long term IDD patients, whilst no improvement was found in patients receiving CIT. However, there was no reduction in the associated nephromegaly over the two year period of the study. Bibergeil and colleagues found that the metabolic control of patients undergoing CSII was significantly better than those receiving CIT and intensified conventional insulin treatment (ICT) and stated that CSII had a positive effect on the early stages of microangiopathy and neuropathy (196).

Insulin is not necessarily the most suitable or the most convenient macromolecule for use in controlled delivery devices. There are problems of hydrolytic stability, solubility, biological activity of the insulin molecule and sterilization prior to pharmaceutical formulation to be overcome. However, the production of a convenient, implantable delivery device to sustain a basal level of insulin release would be a significant step forward in the treatment of insulin dependant diabetes. However, an additional bolus of insulin would still be required to combat post-prandial hyperglycaemia. There have been some attempts to overcome this problem via the development of the magnetically modulated systems, in which a

basal level of insulin release is supplemented by an increased rate of release on the application of an external oscillating magnetic field (61-66). A recent development involving insulin releasing polymer based implants has provided a means for the feedback control of insulin release from the implant. An ethylene vinyl acetate copolymer device has been developed, containing insulin and the enzyme glucose oxidase (197). The enzymic conversion of glucose to gluconic acid by glucose oxidase reduces the pH in the polymer microenvironment. Since the solubility of insulin increases at acid pH, the release of insulin tends to increase with increases in glucose concentration.

The advent of recombinant DNA technology has allowed the production of immunoregulatory cytokines, in significant quantities with high specific activities. Those cytokines which have been cloned include interleukins 1-6 (IL-1-IL-6), γ-interferon (INF-γ) and tumour necrosis factor (TNF) (198). The availability of these molecules has provided the potential for their use in the treatment of tumours and disorders of the immune system. Interleukin-2 (IL-2) promotes the clonal expansion of activated T cells, T-helper and T-cytotoxic cells are critically dependant on IL-2 for proliferation (199). IL-2 also plays a part in B-cell proliferation (200), induces secretion of

INF-γ by T-cells (201) and causes an increase in natural killer (NK) and lymphocyte activated killer cell (LAK) activity beyond that attributable to induction of INF-γ (202) IL-2 also activates macrophages to kill tumour targets (203). From these actions of IL-2, it can be seen that this molecule has enormous potential for controlling the immune response. Rosenberg and colleagues have demonstrated that the administration of IL-2, in combination with a population of a patient's own lymphocytes which have been activated in culture with IL-2 (LAK), can result in regression of a variety of tumours (204). Renal carcinoma, melanoma and colorectal carcinoma have all been treated in this way. There was, however, significant toxicity associated with the treatment. The IL-2 gave rise to leaky capillaries and this resulted in fluid retention which caused dose limiting toxicity. The half life of a cytokine is only minutes in the circulation (205) and therapeutic benefit is only likely to be achieved on the maintenance of high levels, leading to toxic side effects, or the persistence of the molecule at the required site, at lower doses to avoid toxicity. Hence, IL-2 is an ideal candidate for the application of controlled release technology.

Other cytokines, such as the interferons have clinical potential as antiviral and anticancer agents (206) and

would also benefit from the application of controlled release technology. The incorporation of cytokines within a polymeric matrix allows the possibility of a 'cocktail' of cytokines to be delivered. This would be of great potential use in cytokine therapy, since it has been shown that some cytokines act synergistically, for example, maximal reduction of pulmonary metastases in mice was found when a combination of IL-2 and INF-α were used (207). Other macromolecules which could be used in controlled release vehicles include human growth hormone, for the treatment of dwarfism in children and leutinising hormone releasing hormone (LHRH) which has been extensively investigated as an antitumourigenic agent for the treatment of hormone sensitive breast and prostate cancer (208-211) and also as hormone for use in contraception (212-213). Controlled release vehicles also have a role to play in the delivery of agriculturally important molecules such as pesticides. Highly toxic, yet non-persistent pesticides, such as the insecticide methyl parathion (214) could be rendered persistent locally, without the need for frequent administration.

Numerous advantages are to be gained from the use of controlled delivery systems and many macromolecules are likely to become candidates for controlled release. There are, however, some potential

disadvantages to the controlled release of macromolecules from implanted polymer based delivery vehicles. Invasive or superficial surgical procedures will be required to implant and also remove the spent vehicle, unless it is bioerodible/biodegradable. This is unlikely to be a major problem since implants are likely to be small and probably positioned superficially or subcutaneously. Some initial inflammation on implantation is likely, however, any trauma on implantation must be weighed against the benefit derived.

The work carried out in this thesis has led to a reproducible and controllable method for the fabrication of macroporous polyHEMA bead formed matrices. The incorporation and release of surrogate macromolecules and biologically active macromolecules has been demonstrated in vitro. It has been shown that the rate of release of a macromolecule, from the macroporous polyHEMA matrices fabricated in this work, is dependant upon the interaction of a number of factors, namely, macromolecule solubility and loading level, incubation conditions, the method of drying of the loaded matrix and the monomer:solvent ratio of the monomer solution used to fabricate the macroporous matrix.

An important problem associated with the determination of the release of biologically active macromolecules

in vitro, is the extent of their hydrolytic degradation in solution. Estimation of the amount of degraded macromolecule present in solution by a method such as separation down a Sephadex column would allow the extent of degradation of the molecule in solution to be assessed. A means of estimating the amount of macromolecule within the matrix after a given period of incubation would be useful in assessing the amount of macromolecule lost in the fabrication and washing procedures. The control of macromolecule release rates by manipulation of the monomer:solvent ratio has been confirmed in the present work. Further control over the rate of release may be achieved by coating the bead formed matrix with a layer of bioerodible polymer. Its gradual degradation would permit the passage of macromolecules to the exterior from the polyHEMA matrix whilst initially controlling the burst release of macromolecules observed at high loadings. It may also be possible to modify the polyHEMA matrix itself to make the polymer bioerodible. This would be useful since implants would not require further surgery for removal. Implantation of polyHEMA beads containing insulin, would provide details of *in vivo* release rates and allow the amelioration of diabetes induced in experimental animals to be studied.

The present work has resulted in the development of a novel method of production of a macroporous polyHEMA

bead formed matrix for the controlled delivery of macromolecules. Biologically active macromolecules, including clinically significant proteins have been incorporated into the matrix and their bioactivity on release from the delivery vehicle has been demonstrated *in vitro*. The polymeric delivery vehicle designed in this work has potential application as implantable delivery devices for the controlled release of biologically active macromolecules of clinical significance. As such, this work represents a significant contribution to the currently underexploited field of controlled delivery of macromolecules.

REFERENCES

1. Smolen V.F. (1984) Optimally controlled drug bioavailability in theory and products. In Controlled Drug Bioavailability. Volume I. Drug Product and Design. Eds. Smolen. V.F., Ball L.A. John Willey and Sons, London. pp 3 - 33.

2. Ziegler A., Kiel D. (1987) Pharmacodynamic effects of a changed rate of drug deposition. In Controlled Drug Delivery. International Symposium of the Association for Pharmaceutical Technology (APV). Bad Homburg. Ed. Müller B.W. Wissenschaftliche Verlagsgesellschaft mbH Stuttgart. pp 13 - 28.

3. Langer R.S. (1980). Polymeric delivery systems for controlled drug release. Chem. Eng. Commun **6** 1 - 48.

4. Langer R.S., Peppas N.A. (1981). Present and future applications of biomaterials in controlled drug delivery systems Biomaterials **2** 201 - 214.

5. Kim S.W., Petersen R.V.,Feijen J. (1980) Polymeric drug delivery systems. In Drug Design Volume 10. Ed. Ariëns E.J. Academic Press Inc. New York pp 193 - 250.

6. Craig L.C., Konisberg W.(1961) Dialysis studies. III Modification of pore size and shape in cellophane membranes. J. Phys. Chem. **65** 166 - 172.

7. Zenter G.M., Cardinal J.R., Feijen J, Song S.K. (1979) Progestin permeation through polymer membranes. IV Mechanism of steroid permeation and functional group contributions to diffusion through hydrogel films. J. Pharm. Sci. **68** 970 - 975.

8. Place V.A., Pharriss B.B. (1974). Progress in the development of the Progestasert 65 progesterone therapeutic system for contraception. J. Reprod. Med. **13** 66 - 68.

9. Zador G, Nilsson B.A., Nilsson B, Sjoberg N.D., Westrom L.,Wiese J. (1976). Clinical experience with the uterine progesterone system. (Progestasert) Contraception **13** 559 - 568.

10 Worthen D.M., Zimmerman T.J., Wind C.A. (1974). An evaluation of the pilocarpine Ocusert. Invest. Opthalmol. **13** 296 - 299.

11 Stewart R.H., Novak S (1978). Introduction of the Ocusert ocular system to an opthalmic practice. Ann. Opthalmol. **10** 325 - 330.

12 Langer R., Folkman J. (1976) Polymers for the sustained release of proteins and other macromolecules. Nature **263** 797 - 800.

13 Langer R.S., Folkman J. (1978) Sustained release of macromolecules from polymers. In Polymeric Delivery Systems. Midland Macromolecular Monographs Volume 5. Ed. Kostelnik R.J. Gordon and Breach Science Publishers Ltd., London. pp 175 - 196.

14 Rhine W.D., Hsieh D.S.T., Langer R. (1980) Polymers for sustained macromolecule release. Procedures to fabricate reproducible delivery systems and control release kinetics. J. Pharm. Sci **69** 265-270.

15 Creque H.M., Langer R.,Folkman J. (1980) One month of sustained release of insulin from a polymer implant. Diabetes **29** 37 - 40.

16 Brown L., Siemer L., Munoz C., Langer R (1986) Controlled release of insulin from polymer matrices in vitro kinetics. Diabetes **35** 684 - 691

17 Brown L., Munoz C., Siemer L., Edelman E., Langer R. (1986) Controlled release of insulin from polymer matrices. Control of diabetes in rats. Diabetes **35** 692 - 697.

18 Miyazaki S., Yokouchi C., Takada M. (1988) Sustained release of insulin from a hydrophilic polymer matrix implanted in diabetic rats. Chem. Pharm. Bull. **36** 3689 - 3691.

19 Brown L.R., Wei C.L., Langer R (1983) In vivo and in vitro release of macromolecules from polymeric drug delivery systems. J Pharm. Sci. **72** 1181 - 1185

20 Siegel R.A., Langer R (1984) Controlled release of polypeptides and other macromolecules. Pharm. Res. **1** 2 - 10.

21 Gurny R., Doelker E., Peppas N.A. (1982) Modelling of sustained release of water-soluble drugs from porous, hydrophobic polymers. Biomaterials **3** 27 - 32.

22 Peppas N.A. (1983) A model of dissolution - controlled solute release from porous drug delivery polymeric systems. J. Biomed. Mat. Res. **17** 1079 - 1087.

23 Tsong-Pin Hsu T., Langer R (1985) Polymers for the controlled release of macromolecules. Effect of molecular weight of ethylene-vinyl acetate copolymer. J. Biomed. Mat. Res. **19** 445 -460.

24 Haldon R.A., Lee B.E. (1972) Structure and permeability of porous films of poly (hydroxyethyl methacrylate) Br. Polym. J. **4** 491 - 501.

25 Williams D.F. (1982) Biodegradation of surgical polymers. J. Mat. Sci **17** 1233 - 1246.

26 Gilbert R.D., Stannet V., Pitt C.G., Schindler A (1982) The design of biodegradable polymers, two approaches. In Developments in Polymer Degradation-4. Ed. Grassie N. Applied Science Publishers Ltd., London. pp 259 - 293.

27 Gilding D.K. (1981) Biodegradable polymers. Biocompat. Clin. Implant. Mater **2** 209 - 232.

28 Graham N.B., Wood D.A. (1982) Hydrogels and biodegradable polymers for the controlled delivery of drugs. Polymer News **8** 230 - 236.

29 Heller J (1983) Synthesis of biodegradable polymers for biomedical utilisation. ACS Symposium Series **212** 373 - 392.

30 Langer R., Peppas N. (1983) Chemical and physical structure of polymers as carriers for controlled release of bioactive agents. A review J.M.S. Rev. Macromol. Chem. Phys. **C23** (1) 61 - 126.

31 Holland S.J., Tighe B.J., Gould P.L. (1985) The scope of bioerosion for controlled release of macromolecules. Department of Chemistry. University of Aston, Birmingham. Unpublished report.

32 Heller J. (1980) Controlled release of biologically active compounds from bioerodible polymers. Biomaterials **1** 51 - 57.

33 Schwope A.D., Wise D.L., Howes J.F. (1975) Lactic/glycolic acid polymers as narcotic antagonist delivery systems. Life Sciences **17** 1877 - 1886.

34 Wise D.L., Schwope A.D., Harrigan S.E., McCarty D.A., Howes J.F. (1978) Sustained delivery of a narcotic antagonist from lactic/glycolic acid copolymer implants. In Polymeric Delivery Systems. Ed Kostelnik R.J. Midland Macromolecular Monographs. Volume 5. Gordon and Breach Science Publishers Ltd., London. pp 75 - 89.

35 Beck L.R., Tice T.R. (1983) Poly (lactic acid) and poly (lactic acid-co-glycolic acid) contraceptive delivery systems. In Advances in Human Fertility and Reproductive Endocrinology. Volume 2. Long acting steroid contraception. Ed. Mishell D.R. Raven Press, New York. pp 175 - 199.

36 Torchilin V.P., Tischenko E.G., Smirnov V.N., Chazov E.I. (1977). Immobilisation of enzymes on slowly soluble carriers. J. Biomed. Mat. Res.**11**. 223 - 235.

37 Heller J., Baker R.W. (1980). Theory and practice of controlled drug delivery from bioerodible polymers. In Controlled Release of Bioactive Materials. Ed. Baker R.W. Academic Press, New York. pp 1 - 17.

38 Heller J., Helwing R.F., Baker R.W., Tuttle M.E. (1983) Controlled release of water-soluble macromolecules from bioerodible hydrogels. Biomaterials **4** 262 - 266.

39 Chu C.C. (1981) Hydrolytic degradation of poly glycolic acid: Tensile strength and crystallinity study. J. Appl. Poly. Sci. Part A-1 **26** 1727 - 1734.

40 Chu C.C. (1981) An <u>in vitro</u> study of the effect of buffer on the degradation of poly (glycolic acid) sutures. J. Biomed. Mat. Res. **15**. 19 - 27.

41 Chu C.C. (1981) The <u>in vitro</u> degradation of poly (glycolic acid) sutures. Effect of pH. J. Biomed. Mat. Res. **15** 795 - 804.

42 Chu C.C. (1982) A comparison of the effect of pH on the biodegradation of two synthetic adsorbable sutures. Ann. Surg. **195** 55 - 59.

43 Chu C.C., Campbell N.D. (1982) Scanning electron microscopic study of the hydrolytic degradation of poly (glycolic acid) suture. J. Biomed. Mat. Res. **16** 417 - 430.

44 Chu C.C., Moncreif G.(1983) An in vitro evaluation of the stability of mechanical properties of surgical suture materials in various pH conditions. Ann. Surg. **198** 223-228.

45 Pitt C.G., Schindler A (1980) The design of controlled drug delivery systems based on biodegradable polymers. In Progress in Contraceptive Delivery Systems. Ed. Hafez E.S.E. M.T.P. Publishers, Lancaster. pp 17 - 46.

46 Pitt C.G., Gratzl M. M. Kimmel G.L., Surles J., Schindler A (1981) Aliphatic polyesters 2. The degradation of poly (D, L-lactide), poly (- caprolactone) and their copolymers in vivo Biomaterials **2** 215 - 220.

47 Hopfenberg H.B. (1976) Controlled release from erodible slabs, cylinders and spheres. In Controlled Release Polymeric Formulations Eds. Paul D.R., Harris F.W. ACS Symposium Series No 33. pp 26 - 32.

48 Vezin W.R., Florence A.T. (1980) In vitro heterogenous degradation of poly (n-alkyl - cyanoacrylates). J. Biomed. Mat. Res. **14** 93 - 106.

49 Courvreur P. (1988) Polyalkylcyanoacrylates as colloidal drug carriers. Crit. Rev. Ther. Drug Carrier Syst. **5** 1 - 20.

50 Brasseur F., Courvreur P., Kante B., Deckers-Passau L., Roland M., Deckers C., Speiser P. (1980) Actinomycin D adsorbed on polymethyl-cyanoacrylate nanoparticles. Increased efficiency against an experimental tumour. Europ. J. Cancer **16** 1441 - 1445.

51 Laurencin C.T., Koh H.J., Neenan T.X., Allcock H.R., Langer R (1987). Controlled release using a new bioerodible polyphosphazine matrix system J. Biomed. Mat. Res. **21** 1231 - 1246.

52 Allcock H.R., Fuller T.J., Mack D.P., Matsumura K., Smeltz K.M. (1977) Synthesis of poly [(amino acid-alkylester)phosphazenes]. Macromolecules **10** 824 - 830.

53 Allcock H.R., Fuller T.J., Matsumura K (1982) Hydrolysis pathways for aminophosphazenes. Inorg. Chem. **21** 515 - 521.

54 Wade C.W.R., Gourlay S., Rice R., Hegyeli A., Singler R., White J. (1978) Biocompatability of eight poly (organophosphazenes). In Organometallic Polymers. Eds. Carracher C.E., Sheats J.E., Pittman C.U. Academic Press, New York. pp 283 - 288.

55 Trouet A. (1978) Carriers for bioactive materials. In Polymeric Delivery Systems. Midland Macromolecular Monographs. Volume 5. Ed Kostelnik R.J. Gordon and Breach Science Publishers Ltd., London. pp 157 - 174.

56 Goldberg E.P. (1978) Polymeric affinity drugs. In Polymeric Delivery Systems. Midland Macromolecular Monographs Volume 5. Ed. Kostelnik R.J. Gordon and Breach Science Publishers Ltd., London. pp 227 - 235.

57 Rowland G.F., O'Neill G.J., Davies D.A.L. (1975) Suppression of tumour growth in mice by a drug-antibody conjugate using a novel approach to linkage. Nature **255** 487 - 488.

58 Peppas N.A. (1987) Swelling controlled release systems. Recent developments and applications. In Controlled Drug Delivery. International Symposium of the Association for Pharmaceutical Technology (APV). Bad Homburg. Ed Müller B.W. Wissenschaftliche Verlagsgesellschaft mbH. Stuttgart. pp 161 - 173.

59 Peppas N.A., Korsmeyer R.W. (1987). Dynamically swelling hydrogels in controlled release applications. In Hydrogels in Medicine and Pharmacy. Volume III. Properties and Applications Ed. Peppas N.A. CRC Press Inc., Florida. pp 109 - 135.

60 Good W.R. (1978) Diffusion of water soluble drugs from initially dry hydrogels. In Polymeric Delivery Systems. Midland Macromolecular Monographs Volume 5. Ed Kostelnik R.J. Gordon and Breach Science Publishers Ltd., London. pp 139 - 156.

61 Hsieh D.S.T., Langer R., Folkman J. (1981) Magnetic modulation of release of macromolecules from polymers. Proc. Nat. Acad. Sci. **78** 1863-1867.

62 Hsieh D.S.T., Langer R (1981) Experimental approaches for achieving both zero-order and modulated controlled release from polymer matrix systems. Controlled Release of Pesticides and Pharmaceuticals Proc. 7th Int. Symp. **7** 5 - 15.

63 Edelman E.R., Linhardt R.J., Bobeck H. Kost J., Rosen H.B., Langer R.(1984). Polymer based drug delivery. Magnetically modulated and bioerodible systems. In Polymers as Biomaterials. Eds Shalaby S.W., Hoffman A.S., Ratner B.D., Horbett T.A. Plenum Publishing Corp. New York. pp 279 -292.

64 Edelman E., Kost J. Bobeck H. Langer R.(1985) Regulation of drug release from polymer matrices by oscillating magnetic fields. J Biomed. Mat. Res. **19** 67 - 83.

65 Kost J., Noecker R., Kunica E., Langer R (1985) Magnetically controlled release systems. Effect of polymer composition. J Biomed. Mat. Res. **19** 935 - 940.

66 Kost J., Wolfrum J., Langer R. (1987) Magnetically enhanced insulin release in diabetic rats. J Biomed. Mat. Res. **21** 1367 - 1373.

67 Williams D.F. (1981) Biomaterials and biocompatability. An introduction, In Fundamental Aspects of Biocompatability Volume I. Ed. Williams D.F. CRC Press Florida. pp 2 - 7.

68 Stol M., Cífková I., Brynda E (1988) Irritation effects of residual products derived from poly (2-hydroxyethyl methacrylate) gels I. Testing of some model compounds. Biomaterials **9** 273 - 276.

69 Cathers S.J., Kaminski E.J., Osetek E.M. (1984) The cellular response to Hydron within the rat peritoneal cavity. J Endodon. **10** 173 - 181.

70 Autain J. (1981) Toxicological aspects of implantable plastics and plastics used in medical and paramedical applications. In Fundamental Aspects of Biocompatability Volume II. Ed Williams D.F., CRC Press, Florida. pp 63 - 86.

71 Lawrence W.H. (1983) Acute and chronic evaluations of implanted polymeric materials. In Controlled Drug Delivery. Volume II Clinical Applications. Ed Bruck S.D. CRC Press, Florida. pp 1 - 43.

72 Williams D.F. (1981) Biodegradation in the human body. In Fundamental Aspects of Biocompatability Volume II. Ed Williams D.F. CRC Press, Florida. pp 129 - 138.

73 Williams D.F. (1987) Biodegradability and toxicity of polymers as adjuvants for parenteral drug delivery systems. In Controlled Drug Delivery. Inernational Symposium of the Association for Pharmaceutical Technology (APV) Bad Homburg. Ed Müller B.W. Wissenschaftliche Verlagsgesellschaft mbH Stuttgart. pp 49 - 55.

74 Autain J, Singh A.R., Turner J.E., Hung G.W.C., Nunez L.J., Lawrence W.H. (1976) Carcinogenic activity of a chlorinated polyether polyurethan. Cancer Res. **36** 3973 - 3977.

75 Bischoff F. Bryson G. (1964) Carcinogenesis through solid state surfaces. Prog. Exp. Tumor. Res. **5** 85 - 133.

76 Wichterle O., Lím D (1960) Hydrophilic gels for biological use. Nature **185** 117 - 118.

77 Barvic M., Kliment K., Zavadil M. (1967) Biologic properties and possible uses of polymer-like sponges. J Biomed. Mat. Res **1** 313 - 323.

78 Kocvara S., Kliment C.H., Kubát J. Stol M, Ott Z, Dvorák J. (1967) Gel-fabric prostheses of the ureter. J. Biomed. Mat. Res. **1** 325 - 336.

79 Warren A., Gould F.E., Capulong R., Glotfelty E., Boley S.J., Calem W.S., Levowitz B.S. (1967) Prosthetic applications of a new hydrophilic plastic. Surg. Forum **18**. 183 - 185.

80 Levowitz B.S., LaGuerre J.N., Calem W.S., Gould F.E., Scherrer J., Schoenfeld H. (1968) Biologic compatability and applications of Hydron. Trans. Am. Soc. Artif. Int. Org. **14** 82 - 87.

81 Cerny E., Chromecek R., Opletal A., Papousek F., Otoupalová J. (1970) Tissue reaction in laboratory animals to some varieties of glycometacrylate polymers Scripta Medica **43** 63 - 75.

82 Langer R., Brem H., Tapper D. (1981) Biocompatability of polymeric delivery systems for macromolecules. J. Biomed. Mat. Res. **15.** 267 - 277.

83 Aaronson S.B., Horton R.C. (1971) Mechanisms of the host response in the eye. Arch. Opthalmol. **85** 306 - 308.

84 Henkind P. (1978) Ocular neovascularization. Am. J. Opthalmol. **85** 287 - 301.

85 Winter C.D., Simpson B.J. (1969) Heterotopic bone formed in a synthetic sponge in the skin of young pigs. Nature **223** 88 - 90.

86 Sprincl L., Kopecek J., Lím D. (1971) Effect of porosity of heterogenous poly (glycol monomethacrylate) gels on the healing-in of test implants. J. Biomed. Mat. Res. **4** 447 - 458.

87 Sprincl L., Vacík J., Kopecek J. (1973) Biological tolerance of ionogenic hydrophilic gels. J. Biomed. Mat. Res. 7 123 - 136.

88 Sprincl L., Kopecek J., Lím D. (1973) Effect of the structure of poly (glycol monomethacrylate) gel on the calcification of implants. Calc. Tiss. Res **13** 63 - 72.

89 Brynda E., Stol M., Chytry V., Cífková I.(1985). The removal of residuals and oligomers from poly (2-hydroxyethyl methacrylate). J. Biomed. Mat. Res. **19** 1169 - 1179.

90 Ratner B.D., Hoffman A.S. (1976) Synthetic hydrogels for biomedical applications. ACS Symposium Series **31** 1 - 36.

91 Larke J.R., Ng C.O., Tighe B.J. (1971) Hydrogel polymers in contact lens applications. A survey of existing literature. Part 1. The Optician **162** 12 - 16.

92 Skelly P.J. (1979) The design of hydrogel polymers for artificial liver support systems. Aston University. PhD Thesis Chapter I Hydrogels pp 2 -53.

93 Hasa J., Janacek J. (1967) Effect of diluent content during polymerisation on equilibrium deformational behaviour and structural parameters of polymer networks. J. Polym. Sci. **16** Part C 317 - 328.

94 Peppas N.A., Mikos A.G. (1986) Preparation methods and structure of hydrogels. In Hydrogels in Medicine and Pharmacy. Volume I Fundamentals. Ed Peppas N.A. CRC Press, Florida. pp 1 - 25.

95 Peppas N.A., Moynihan H.J. (1987) Structure and physical properties of poly (2-hydroxyethyl methacrylate) hydrogels. In Hydrogels in Medicine and Pharmacy. Volume II Polymers. Ed Peppas N.A. CRC Press, Florida. pp 49 - 64.

96 Sevcík S., Stamberg J., Schmidt P. (1967) Chemical transformations of polymers: IV Chemical reactions of glycol methacrylate gels. J. Polym. Sci. **16** Part C 821 - 831.

97 Stamberg J., Sevíck S. (1966) Transformations of polymers. III Selective hydrolysis of a copolymer of diethylene glycol methacrylate and diethylene glycol methacrylate. Collect. Czech. Chem. Commun. **31** 1009 - 1016.

98 Pedley D.G., Skelly P.J., Tighe B.J. (1980) Hydrogels in biomedical applications. Br. Polym. J. **12** 99 - 109.

99 Refojo M.F., Yasuda H. (1965) Hydrogels from 2-hydroxyethyl methacrylate and proplylene glycol monomethacrylate J. Appl. Polym. Sci. **9** Part A-1 2425 - 2435.

100 Wichterle O. (1971) Hydrogels. In Encyclopedia of Polymer Science and Technology. Volume 15. Interscience, New York. pp 273 - 291.

101 Dusek K., Janácek J. (1975) Hydrophilic gels based on copolymers of 2-hydroxyethyl methacrylate with methacrylamide and acrylamide. J. Appl. Polym. Sci. **19** Part A-1 3061 - 3075.

102 Refojo M.F. (1967) Hydrophobic interactions in poly (2-hydroxyethyl methacrylate) hydrogels. J. Polym. Sci. **5** Part A-1 3103 - 3113.

103 Dusek K., Bohdanecky M., Vosicky Y. (1977) Solubilisation of poly (2-hydroxyethyl methacrylate) with aqueous salt solutions; Swelling of Gels. Collect. Czech. Chem. Commun. **42** 1599 - 1613.

104 Ratner B.D., Miller I.F. (1972) Interaction of urea with poly (2-hydroxyethyl methacrylate) hydrogels. J. Polym. Sci. **10** Part A-1 2425 - 2445.

105 Mack E.J., Okano T., Kim S.W. (1987) Biomedical applications of poly (2-hydroxyethyl methacrylate) and its copolymers. In Hydrogels in Medicine and Pharmacy. Volume II Polymers. Ed Peppas N.A. CRC Press, Florida. pp 65 - 93.

106 Jhon M.S., Andrade J.D. (1973) Water and hydrogels. J. Biomed. Mat. Res. **7** 509 - 522.

118 Hoffman A.S., Cohn D., Hanson S.D., Harker L.A., Horbett T.A., Ratner B.D., Reynolds L.O. (1983) Application of radiation-grafted hydrogels as blood contacting biomaterials. Rad. Phys. Chem. **22** 267 - 283.

119 Yasuda H., Gochin M., Stone W. (1966) Hydrogels of poly (hydroxyethyl methacrylate) and hydroxyethyl methacrylate-glycerol monomethacrylate copolymers. J. Polym. Sci. **4** Part A-1 2913 - 2927.

120 Skelly P.J. (1979) The design of hydrogel polymers for artificial liver support systems. Chapter 6. Macroporous membranes. Aston University, PhD Thesis pp 250 - 292.

121 Wood J.M., Attwood D., Collett J.H. (1983) Characterisation of poly (2-hydroxyethyl methacrylate) gels. Drug Dev. Ind. Pharm. **9** 93 - 101.

122 Wood J.M., Attwood D., Collett J.H. (1982) The influence of gel formulation on the diffusion of salicylic acid in polyHEMA hydrogels. J. Pharm. Pharmacol. **34** 1 - 4.

123 Hsieh D.S.T., Rhine W.D., Langer R. (1983) Zero-order controlled release polymer matrices for micro and macromolecules. J. Pharm. Sci. **72** 17 - 22.

124 Cobby J., Mayersohn M., Walker G.C. (1974) Influence of shape factors on kinetics of drug release from matrix tablets. I Theoretical. J. Pharm. Sci **63** 725 - 731.

125 Cobby J., Mayersohn M., Walker G.C. (1974) Influence of shape factors on kinetics of drug release from matrix tablets. II Experimental J. Pharm. Sci. **63** 732 - 737.

126 Lee E.S., Kim S.W., Kim S.H., Cardinal J.R., Jacobs H. (1980) Drug release from hydrogel devices with rate-controlling barriers. J. Memb. Sci. **7** 293 - 303.

127 Refojo M.F., Leong F.L. (1979) Microscopic determination of the penetration of proteins and polysaccharides into poly (hydroxyethyl methacrylate) and similar hydrogels. J. Polym. Sci. Polym. Symp. **66** 227 - 237.

128 Chien Y.W., Lambert H.J. (1974) Controlled drug release from polymeric delivery devices. II Differentiation between partition-controlled and matrix controlled drug release mechanisms. J. Pharm. Sci **63** 515 - 519.

129 Langer R.S., Rhine W.D., Hsieh D.S.T, Bawa R.S. (1980) Polymers for the sustained release of macromolecules. Applications and control of release kinetics. In Controlled Release of Bioactive Materials. Ed. Baker R. Academic Press Inc. New York. pp 83 - 98.

130 Smith P.K., Krohn R.I., Hermanson G.T., Mallia A.K., Gartner F.H., Provenzano M.D., Fujimoto E.K., Goeke N.M., Olson B.J., Klenk D.C. (1985) Measurement of protein using bicinchoninic acid. Anal. Biochem. **150** 76 - 85.

131 Lowry O.H., Rosebrough N.J., Farr A.L., Randal R.J. (1951) Protein measurement with Folin-Phenol reagent. J. Biol. Chem. **193** 265 - 275.

132 Holland S.J. (1986) Novel polymeric controlled release systems. Aston University PhD Thesis. pp 87 - 88.

133 Spiro R.G. (1966) Section 1: Analytical methods: Part 1 Analysis of sugars found in glycoproteins. In Methods in Enzymology. Vol VIII. Acadamic Press London. pp 3 - 26.

134 Hales C.N., Randle P.J. (1963) Immunoassay of insulin with insulin-antibody precipitate. Biochem. J. **88** 137 - 146.

135 Heding L.G. (1966) A simplified insulin radioimmunoassay method. In Labelled Proteins in Tracer Studies Ed. Donato L. Euration. Brussels. pp 345 - 350.

136 Yalow R.S., Berson S.A. (1960) Immunoassay of endogenous plasma insulin in man. J. Clin. Invest. **39** 1157 - 1175.

137 Berson S.A., Yalow R.S., Bauman A., Rothschild M.A., Newerly K. (1956) ^{131}I-insulin metabolism in human subjects. Demonstration of insulin binding globulin in the circulation of insulin treated subjects. J. Clin. Invest. **35** 170 - 190

138 Grodsky G.M., Forsham P.H. (1960) An immunological assay of total extractable insulin in man. J. Clin. Invest. **39** 1070 - 1079.

139 Genuth S., Frohman L.A., Lebowitz H.E. (1965) A radioimmunological assay method for insulin using ^{125}I and gel filtration. J. Clin. Endocrin. Metab. **25** 1043 - 1049.

140 Goetz F.C., Beryl Z., Greenberg B.Z., Ellis J. Meinert C. (1963) A simple immunoassay for insulin: Application to human and dog plasma. J. Clin. Endocrin. **23** 1237 - 1246.

141 Morgan C.R., Lazarow A. (1963) Immunoassay of insulin: Two antibody system. Diabetes **12** 115 - 126.

142 Heding L.G. (1972) Determination of total serum insulin in insulin treated diabetic patients Diabetologia **8** 260 - 266.

143 Hunter W.M., Greenwood F.C. (1962) Preparation of ^{131}I labelled human growth hormone of high specific activity. Nature **194** 495 - 496.

144 Freedlender A., Cathou R.E. (1971) Iodination. In Radioimmunoassay Methods. Eds Kirkham K.E., Hunter M.W. Churchill Livingstone, Edinburgh. pp 94 - 96

145 Gliemann J. Sonne O., Linde S., Hansen B (1979) Biological potency and binding affinity of monoiodoinsulin with iodine in tyrosine A14 or tyrosine A19. Biochem. Biophys. Res. Commun. **87** 1183 - 1190.

146 De Meyts P. (1976) Insulin and growth hormone receptors in human cultured lymphocytes and peripheral blood monocytes. In Methods in Receptor Research Part 1. Ed. Belcher M. Marcel Dekker, New York. pp 301 - 383.

147 Freychet P., Roth J., Neville D.M. (1971). Monoiodoinsulin: Demonstration of its biological activity and binding to fat cells and liver membranes. Biochem. Biophys. Res. Commun. **43** 400 - 408.

148 Wilson M.A., Miles L.E.M. (1977) Radioimmunoassay of insulin. In Handbook of Radioimmunoassay. Ed. Abraham G.E. Clinical and Biochemical Analysis Volume 5. Marcel Dekker New York. pp 275 - 297.

149 Jϕrgensen K., Binder C. (1966) ^{125}I-insulin as a tracer of insulin in different chemical processes. In Labelled Proteins in Tracer Studies Ed. Donato L. Euration, Brussels. pp 329 - 333.

150 Olefsky J.M. (1976) The insulin receptor: its role in insulin resistance of obesity and diabetes Diabetes **25** 1154 - 1162.

151 Chech J.M., Freeman R.B., Caro J.F., Amatruda J.M. (1980) Insulin action and binding in isolated hepatocytes from fasted streptozotocin-diabetic and other, older spontaneously obese rats. Biochem J. **188** 839 - 845.

152 LeMarchand -Brustel Y., Freychet P. (1979) Effect of fasting and streptozotocin diabetes and insulin binding and action in the isolated mouse soleus muscle. J. Clin. Invest. **64** 1505 - 1515.

153 Czech M.P. (1980) Insulin action and the regulation of hexose transport. Diabetes **29** 399 - 409.

154 Levin R. (1982) Insulin: The effects and mode of action of the hormone. Vitamins. Horm. **39** 145 - 175.

155 Ashcroft S.J.H., Weerasinghe L.C.C., Basset J.M., Randle P.J. (1972) The pentose cycle and insulin release in mouse pancreatic islets. Biochem. J. **126** 525 - 532.

156 Winegrad A.F., Renold A.E. (1958) Studies on rat adipose tissue in vitro. I Effects of insulin on the metabolism of glucose, pyruvate and acetate. J. Biol. Chem. **233** 267 - 272.

157 Ball E.G., Martin D.B., Cooper O. (1959) Studies on the metabolism of adipose tissue. I Effect of insulin on glucose utilisation as measured by the manometric determination of CO_2 output. J.Biol. Chem. **234** 774 - 780.

158 Renold A.E., Martin D.B., Dagenais Y.M., Steinke J. , Nickerson R.J. , Sheps M.C. (1960) Measurement of small quantities of insulin-like activity using rat adipose tissue I A proposed procedure. J. Clin. Invest. **39** 1487 - 1498.

159 Gjedde F. (1968) Studies of the insulin-like activity of serum. I Normal values determined by the rat epididymal fat pad and by the rat diaphragm method. Acta Endocrinologica **57** 330 - 352.

160 Beigelman P.M. (1962) Additional studies with insulin bioassay employing glucose uptake by rat adipose tissue. Metabolism **11** 1315 - 1324.

161 Martin D.B., Renold A.E., Dagenais Y.M. (1958) An assay for insulin-like activity using rat adipose tissue. The Lancet **2** 76 - 77.

162 Rodbell M. (1964) Metabolism of isolated fat cells. I Effects of hormones on glucose metabolism and lipolysis. J. Biol. Chem. **239** 375 - 380.

163 Autain J. (1973) The new field of plastics toxiocology. Methods and results. CRC Critical Reviews in Toxicology **2** 1 - 40.

164 Wilsnack R.E., Meyer F.J., Smith J.G. (1973) Human cell culture toxicity testing of medical devices and correlation to animal tests. Biomat. Med.Dev. Artif. Org. **1** 543 - 562.

165 Wilsnack R.E. (1976) Quantitative cell culture biocompatibility testing of medical devices and correlation to animal tests. Biomat. Med. Dev. Artif. Org. **4** 235 - 261.

166 Earle W.R. (1943) Production of malignancy in vitro: IV The mouse fibroblast cultures and changes seen in the living cells. J. Natl. Cancer Inst. **4** 165 - 212.

167 Davis B.D. (1980) Bacterial nutrition and growth. In Microbiology. 3rd Edition. Ed Davis B.D., Dulbecco R., Eisen H.N., Ginsberg H.S. Harper and Row Publishers Inc. USA Chapter 5. pp 60 - 70.

168 Holley R.W. (1975) Control of growth in mammalian cells. Nature **258** 487 - 490.

169 Farrant J. (1980) General observations on cell preservation. In Low Temperature Preservation in Medicine and Biology. Ed. Ashwood-Smith M.J. Farrant J. Pitman Medical Ltd., Kent. Chapter 1. pp 1 - 17.

170 Rey L.R. (1957) Studies on the action of liquid nitrogen on cultures in vitro of fibroblasts. Proc. Roy. Soc. (B) **147** 460 - 466.

171 Lovelock J.E. (1953) The haemolysis of human red blood cells by freezing and thawing. Biochem. Biophys. Acta. **10** 414 - 426.

172 Lovelock J.E. (1953) Net mechanism of the protective action of glycerol against harmolysis by freezing and thawing. Biochem. Biophys. Acta **11** 28 - 36.

173 Lovelock J.E. (1954) The protective action of neutral solutes against haemolysis by freezing and thawing. Biochem J. **56** 265 - 270.

174 Chatfield C. (1983) The design and analysis of experiments 1. Comparative experiments. In Statistics for Technology. A course in applied statistics. 3rd Edition. Chapman and Hall, London. pp 224 - 256.

175 Statview ™(1985) Feldman D., Gagnon J. The graphic statistics utility for the Macintosh ™ Brain Power Inc. 24009, Ventura Boulevard, Suite 250, Calabasas, CA 91302, USA.

176 Zar J.H. (1984) Multiple comparisons. In Biostatistical Analysis. 2nd Edition. Prentice-Hall Inc. USA. pp 185 - 205.

177 Zar J.H. (1984) Two sample hypothesis In Biostatistical Analysis 2nd Edition. Prentice-Hall Inc. USA. pp 122 - 149.

178 Snedecor G.W., Cochran W.G. (1980) One way classifications; analysis of variance. In Statistical Methods. 7th Edition. The Iowa State University Press USA. pp 215 - 237.

179 Chatfield C. (1983) The design and analysis of experiments 2. Factorial experiments. In Statistics for Technology. A course in applied Statistics. 3rd Edition. Chapman and Hall, London. pp 257 - 287.

180 Atwal U.S. (1985) Novel polymers for artifical liver support systems. Chapter 3. Synthesis of hydrogel particulates; Freeze-thaw polymerisation. pp 108 - 171.

181 Robb R.J. (1984) Interleukin-2: the molecule and its function. Immunol Today **5** 203 - 209.

182 Skelly P.J. (1979) The design of hydrogel polymers for artifical liver support systems. Chapter 7. Macroporous beads. Aston University PhD Thesis. pp 293 - 320.

183 Murphy S.M., Skelly P.J., Tighe B.J. (1989) The controlled release of macromolecules from hydrophilic polymer matrices. Synthetic hydrogels: 10. Preparation and characterisation of macroporous hydrophilic matrices. Speciality Materials Research Group, Aston University, Unpublished Report.

184 Adams M.J., Blundell T.L., Dodson E.J., Dodson G.G., Vijayan M., Baker E.N., Harding M.M., Hodgkin D.C., Rimmer B., Sheat S. (1969) Structure of rhombohedral 2 zinc insulin crystals. Nature **224** 491 - 495.

185 Davis B.K. (1971) Control of diabetes with polyacrylamide implants containing insulin. Experentia **28** 348.

186 Heller J., Baker R.W., Gale R.M., Rodin J.O. (1978) Controlled drug release by polymer dissolution. I Partial esters of maleic anhydride copolymers - Properties and theory. J. App. Poly. Sci. **22** 1991 - 2009.

187 Heller J., Trescony P.V. (1979) Controlled drug release by polymer dissolution II Enzyme-mediated device. J. Pharm. Sci. **68** 919 - 921.

188 Blackshear P.J. Rohde T.D. (1983) Artificial devices for insulin infusion in the treatment of patients with diabetes mellitus: In Controlled Drug Delivery. Volume II. Clinical Applications Ed. Bruck S.D. CRC Press Florida. pp 112 - 147.

189 Cahill G.F., Etzwiler D.D., Freinkel N. (1976) Blood glucose control in diabetes. Diabetes **25** 237 - 238.

190 Bloodworth J.M.B. Jr. Engerman R.L. (1971) Spontaneous and induced diabetic microangiopathy. Acta. Diabetol. Lat. **8** (Suppl) 263 - 301.

191 Mauer S.M., Sutherland D.E.R., Steffes M.W., Leonard R.J., Najarian J.S., Michael A.F., Brown D.M. (1974) Pancreatic islet transplantation. Effects on the glomerular lesions of experimental diabetes in the rat. Diabetes **23** 748 - 753.

192 Mauer S.M., Steffes M.W., Sutherland D.E.R., Najarian J.S., Michael A.F., Brown D.M. (1975) Studies of the rate of regression of the glomerular lesions in diabetic rats treated with pancreatic islet transplantation. Diabetes **24** 280 - 285.

193 Gray B.N., Watkins E. (1976) Prevention of vascular complications of diabetes by pancreatic transplantation. Arch. Surg. **111** 254 - 257.

194 Engerman R.L., Bloodworth J.M.B. Jr., Nelson S. (1977) Relationship of microvascular disease in diabetes to metabolic control. Diabetes **26** 760 - 769.

195 Christensen C.K., Christiansen J.S., Schmitz A., Christensen T., Hermansen K., Mogensen C.E. (1987) Effect of continuous subcutaneous insulin infusion on kidney function and size in IDDM patients; a two year controlled study. J. Diabetic Complic. **1** 91 - 95.

196 Bibergeil H. Huttl I., Felsing W., Felsing U., Seidlein I., Herfurth S., Dabels J., Reichel G., Luder C., Albrecht G. (1987) 36 months continuous subcutaneous insulin infusion (CSII) in insulin dependant diabetics (IDDM)-influence on early stages of retinopathy, nephropathy and neuropathy-psycologic analysis. Exp. Clin. Endocrin **90** 51 - 61.

197 Fischel-Ghodsian F., Brown L., Mathiowitz E., Brandenburg D., Langer R. (1988) Enzymatically controlled drug delivery. Proc. Natl. Acad. Sci. USA **85** 2403 - 2406.

198 Hamblin A.S. (1988) Lymphokines. In Lymphokines Ed. Male D. IRL Press Ltd., Oxford. pp 1 - 12.

199 Watson J. (1979) Continuous proliferation of murine antigen-specific helper T-lymphocytes in culture. J. Exp. Med. **150** 1510 -1519.

200 Gordon J., Guy G.R. (1987) The molecules controlling B lymphocytes. Immunol. Today **8** 339 - 344.

201 Farrar J.J., Benjamin W.R., Hilfiker M.L., Howard M., Farrar W.L., Fuller-Farrar J. (1982) The biochemistry, biology and role of interleukin-2 in the induction of cytotoxic T cell and antibody-forming B cell responses. J. Immunol. Rev. **63** 129 - 166.

202 Henney C.S., Kuribayashi K., Kern D.E., Gillis S. (1981) Interleukin-2 augments natural killer cell activity Nature **291** 335 - 338.

203 Hamblin A.S. (1988) Lymphokines in haematopoiesis, cytotoxicity and inflammation. In Lymphokines. Ed. Male D. IRL Press Ltd., Oxford. pp 45 - 53.

204 Rosenberg S.A., Lotze M.T., Muul L.M., Leitman S., Chang A.E., Ettinghausen S.E., Matory Y.L., Skibber J.M., Shiloni E., Vetto J.T., Seipp C.A., Simpson C., Reichert C (1985). Observations on the systemic administration of autologous lymphokine-activated killer cells and recombinant interleukin-2 to patients with metastatic cancer. New England J. Med.**313** 1485-1492

205 Hamblin A.S. (1988) Lymphokines in pathology and therapy. In Lymphokines. Ed. Male D. IRL Press Ltd., Oxford. pp 53 - 61.

206 White D.O. (1984) Interferons. In Antiviral Chemotheraphy, Interferons and Vaccines. Ed. Melnick J.L. Monographs in Virology. Volume 16. Karger, Switzerland. pp 7 - 35.

207 Kim B., Stein S., Warnaka P., Franceschi D. (1988) Enhanced in vivo therapy of pulmonary metastases with interferon and interleukin-2 J. Surg. Res. **45** 66 - 73.

208 Nicholson R.I., Walker K.J., Davies P., Turkes A., Turkes A.O., Dyas J., Blamey R.W., Williams M., Robinson M.R.G., Griffiths K. (1984) Use and mechanism of action of the LH-RH agonist ICI 118630 in the therapy of hormone sensitive breast and prostate cancer. In Progress in Cancer Research and Therapy. Volume 31. Hormones and Cancer 2. Proc. 2nd Int. Conf. Eds. Bresciani F., King R.J.B., Lipman M.E., Namer M., Raynaud J.P. Raven Press, New York, pp 519 - 532.

209 Labrie F., Dupont A., Bélanger A., Labrie C., Lacourcière Y., Raynaud J.P., Husson J.M., Emond J., Houle J.G., Girard J.G., Monfette G., Paquet J.P., Vallières A., Bossé C. Delisle R. (1984) Combined antihormonal treatment in prostate cancer. A new approach using an LH-RH agonist or castration and an antiandrogen. In Progress in Cancer Research and Therapy Volume 31. Hormones and Cancer 2. Proc. 2nd Int. Conf. Eds. Bresciani F., King R.J.B., Lipman M.E., Namer M. Raynand J.P., Raven Press, New York. pp 533 - 547.

210 Debruyne F.M. (1988) Results of a Dutch trial with the LH-RH agonist, buserelin in patients with metastatic prostate cancer and results of EORTC studies in prostate cancer. Am. J. Clin. Oncol. **11** (Suppl.1) S 33 - 35.

211 Swanson L.J., Seely J.M., Garnick M.B. (1988) Gonadotropin - releasing hormone analogs and prostatic cancer. CRC Crit. Rev. Oncol. Hematol. **8** 1 - 26.

212 Labrie F., Bélanger A., Pelletier G., Séguin C., Cusan L., Kelly P.A., Lemay A., Auclair C., Raynaud J.P. (1980) LH-RH agonists. Inhibition of testicular functions and possible clinical applications. In Regulation of Male Fertility. Eds. Cunningham G.R., Schill W.B., Hafez E.S.E., Martinus Nijhoff, London pp 65 - 76.

213 Corbin A, Bex F.J. (1980) Inhibition of male reproductive processes with an LH-RH agonist. In Regulation of Male Fertility Eds. Cunningham G.R., Schill W.B., Hafez E.S.E. Martinus Nijhoff, London pp 55 - 63.

214 Ware G.W. (1978) The Pesticide Book. W.H. Freeman and Company, San Francisco. pp 25 - 58.

APPENDICES

APPENDIX A1 - THE PREPARATION OF BUFFERS

0.5M phosphate buffer, pH7.4, for insulin iodination

73g Na_2HPO_4 was combined with 14.04g $NaH_2PO_4.2H_2O$ and dissolved in 800ml x2 distilled water. The pH was adjusted to 7.4 and the buffer made up to 1 litre with x2 distilled water.

0.5M phosphate buffer, pH7.4, for insulin iodination

7.3g Na_2HPO_4 was combined with 1.404g $NaH_2PO_4.2H_2O$ and dissolved in 800ml x2 distilled water. The pH was adjusted to 7.4 and the buffer made up to 1 litre with x2 distilled water.

RIA diluent buffer, pH7.4, for the radiommunoassay of insulin by the double antibody method.

6.2g $NaH_2PO_4.2H_2O$, 0.25g thiomersalate (as a preservative) and 5.1g BSA (fraction V, RIA grade) were combined and dissolved in 800ml x2 distilled water. The pH was adjusted to 7.4 and the buffer made up to 1 litre with x2 distilled water.

Diluent phosphate buffer, pH7.4 for the radioimmunoassay of insulin by the ethanol precipitation method.

6.2g $NaH_2PO_4.2H_2O$, 0.25g thiomersalate, 1.00g BSA (fraction V, RIA grade) and 6.00g NaCl were combined and dissolved in 800ml x2 distilled water. The pH was adjusted to 7.4 and the buffer made up to 1 litre with x2 distilled water.

Modified Kreb's bicarbonate buffer, pH7.4, for insulin bioassay.

6.92g NaCl, 0.35g KCl, 0.14g $CaCl_2$, 0.16g KH_2PO_4, 0.29g $MgSO_4.7H_2O$, 2.10g $NaHCO_3$, 5.00g BSA (fraction V, RIA grade) and 1.00g glucose were combined and dissolved in 1 litre x2 distilled water. After 30 minutes oxygenation with 95% O_2:5%CO_2 the pH was routinely found to be 7.4.

0.04M phosphate buffer

5.84g $Na_2HPO_4$and 1.12g $NaH_2PO_4.2H_2O$ were combined and dissolved in 800ml x2 distilled water. The pH was adjusted to 7.4 and the buffer made up to 1 litre with x2 distilled water.

0.2M phosphate buffer, pH7.4

7.164g $Na_2HPO_4.2H_2O$ was dissolved in 100ml of x2 distilled water and 3.12g NaH_2PO_4 was dissolved in 100ml of x2 distilled water. 30.5ml of $Na_2HPO_4.2H_2O$ solution and 19.5ml of NaH_2PO_4 solution were combined, the pH was adjusted to 7.4 and the buffer made up to 100ml with x2 distilled water.

0.01M sodium acetate/0.12M sodium chloride buffer, pH7.4

1.36g $C_2H_3NaO_2.3H_2O$ and 7g NaCl were dissolved in 800ml x2 distilled water. The pH was adjusted to 7.4 and the buffer made up to 1 litre with x2 distilled water.

Boric acid-borate buffer, pH7.4 0.2M in terms of boric acid.

12.37g H_3BO_3 was dissolved in 800ml x2 distilled water, the pH adjusted to 7.4 and made up to 1 litre with x2 distilled water. 19.07g $Na_2B_4O_7.10H_2O$ was dissolved in 800ml x2 distilled water, the pH adjusted to 7.4 and made up to 1 litre with x2 distilled water (0.05M). 100ml of sodium tetraborate solution was then combined with 900ml boric acid solution.

0.01M phosphate buffer, pH7.4

1.46g Na_2HPO_4 was combined with 0.28g $NaH_2PO_4.2H_2O$ and dissolved in 800ml distilled water. The pH was adjusted to 7.4 and the buffer was made up to 1 litre with x2 distilled water.

APPENDIX A2 - DECAY CORRECTION CURVE FOR ^{125}I.

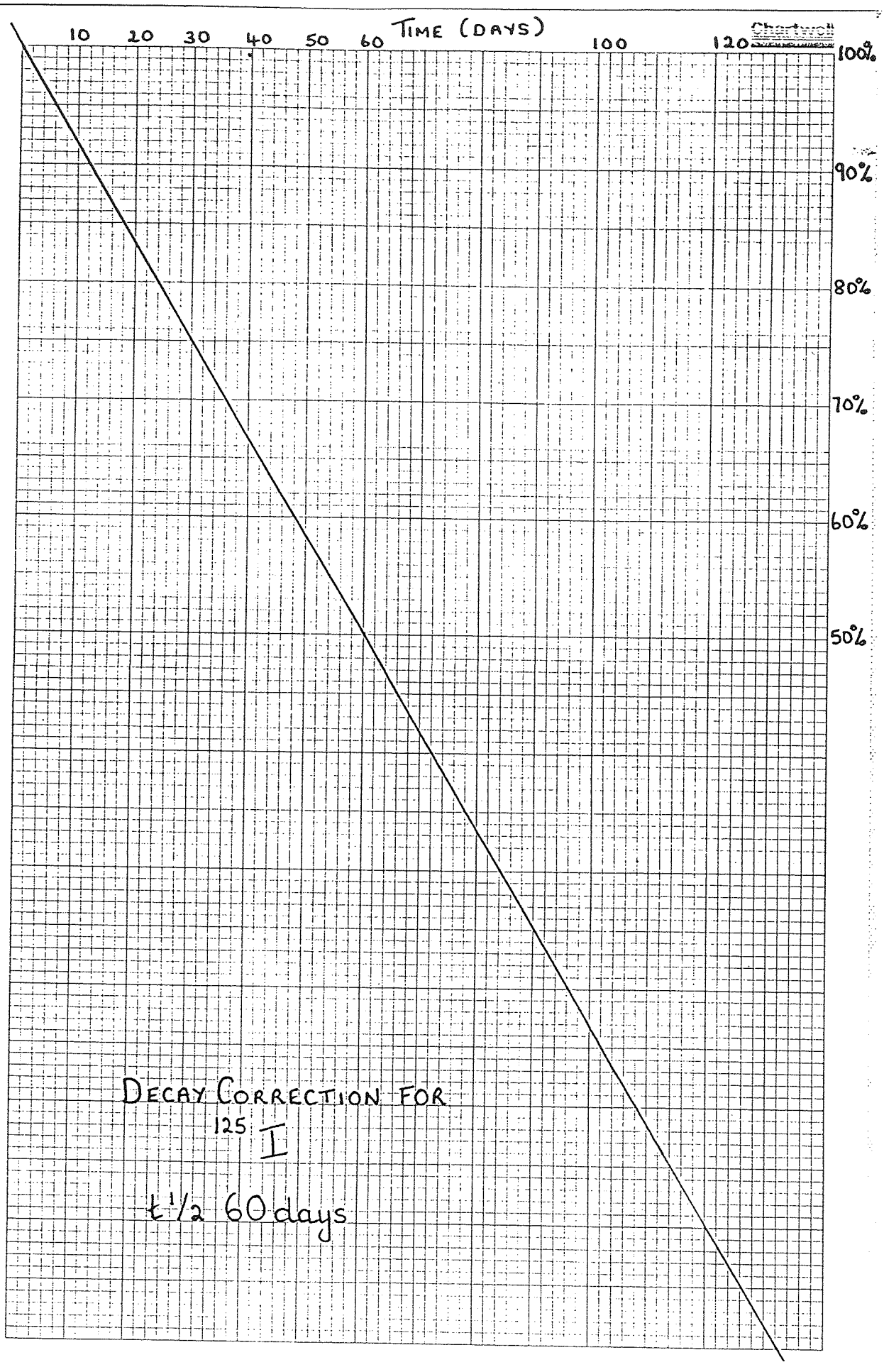

APPENDIX A3 - TYPICAL PRINTOUTS FOR INSULIN RADIOIMMUNOASSAY

1. Double antibody method of insulin radioimmunoassay.

```
 1 LISTING          Y
 2 DUAL LABEL       N
 3 STD TIME         30
 4 UNK TIME         30
 5 COUNTS           900000
 6 WINDOW           035-110
 7 METHOD           6
 8 UNK BLAN         0
 9 UNK REPL         1
10 CONC.FACTORS     N
11 CURVE EDIT       Y
12 FREE FRACTION    N
13 PRINT            -1-2-4-6-7-8-9-10-11-12

14 CODING           POS-CODE
                    001-TOA
                    004-BLA
                    007-6.25
                    010-12.5
                    013-25
                    016-50
                    019-100
                    022-200
                    025-UNKS
```

POS	CODE1	CTIME	COUNTS1	COR.CPM1	ERR1%	RATIO1	S.E1%	CONC.1	TOT.1%
001	TOA	30	5247	10572.0	1.4				
002	TOA	30	5078	10230.7	1.4				
003	TOA	30	5592	11269.2	1.3				
	MEAN			10690.6	0.8		2.9		
004	BLA	30	427	858.1	4.8				
005	BLA	30	438	880.2	4.8				
006	BLA	30	476	956.6	4.6				
	MEAN			898.3	2.7		3.3		
007	6.25	30	1100	2211.4	3.0				
008	6.25	30	425	854.1	4.9				
009	6.25	30	1024	2058.5	3.1				
	MEAN			1708.0	2.0	1.0000	25.1		
010	12.5	30	917	1843.3	3.3	1.0792			
011	12.5	30	844	1696.5	3.4	0.9933			
012	12.5	30	903	1815.1	3.3	1.0627			
	MEAN			1785.0	1.9	1.0451	2.5		
013	25	30	886	1780.9	3.4	1.0427			
014	25	30	768	1543.7	3.6	0.9038			
015	25	30	811	1630.1	3.5	0.9544			
	MEAN			1651.6	2.0	0.9670	4.2		
016	50	30	617	1240.0	4.0	0.7260			
017	50	30	793	1593.9	3.6	0.9332			
018	50	30	608	1221.9	4.1	0.7154			
	MEAN			1352.0	2.2	0.7916	9.0		
019	100	30	683	1372.8	3.8	0.8037			
020	100	30	568	1141.5	4.2	0.6684			
021	100	30	477	958.6	4.6	0.5612			
	MEAN			1157.6	2.4	0.6778	10.4		
022	200	30	388	779.7	5.1	0.4565			
023	200	30	520	1045.0	4.4	0.6119			
024	200	30	511	1026.9	4.4	0.6013			
	MEAN			950.6	2.7	0.5565	9.0		

N = 2
S = 1.500
F = .096

STAN.	CONC.	CPM DIFF.(%)	CONC.	WEIGHT(%)
1	6.250	-15.2784	147.0302	25.1304
2	12.500	.9075	-5.5274	10.9406
3	25.000	5.0212	-24.9493	11.8106
4	50.000	-1.2207	5.8507	14.3896
5	100.000	-.9233	3.8634	16.7763
6	200.000	-1.8518	6.2855	20.3932

SUM D = 75932.0
SUM W = 373560.1
RATIO = .2033

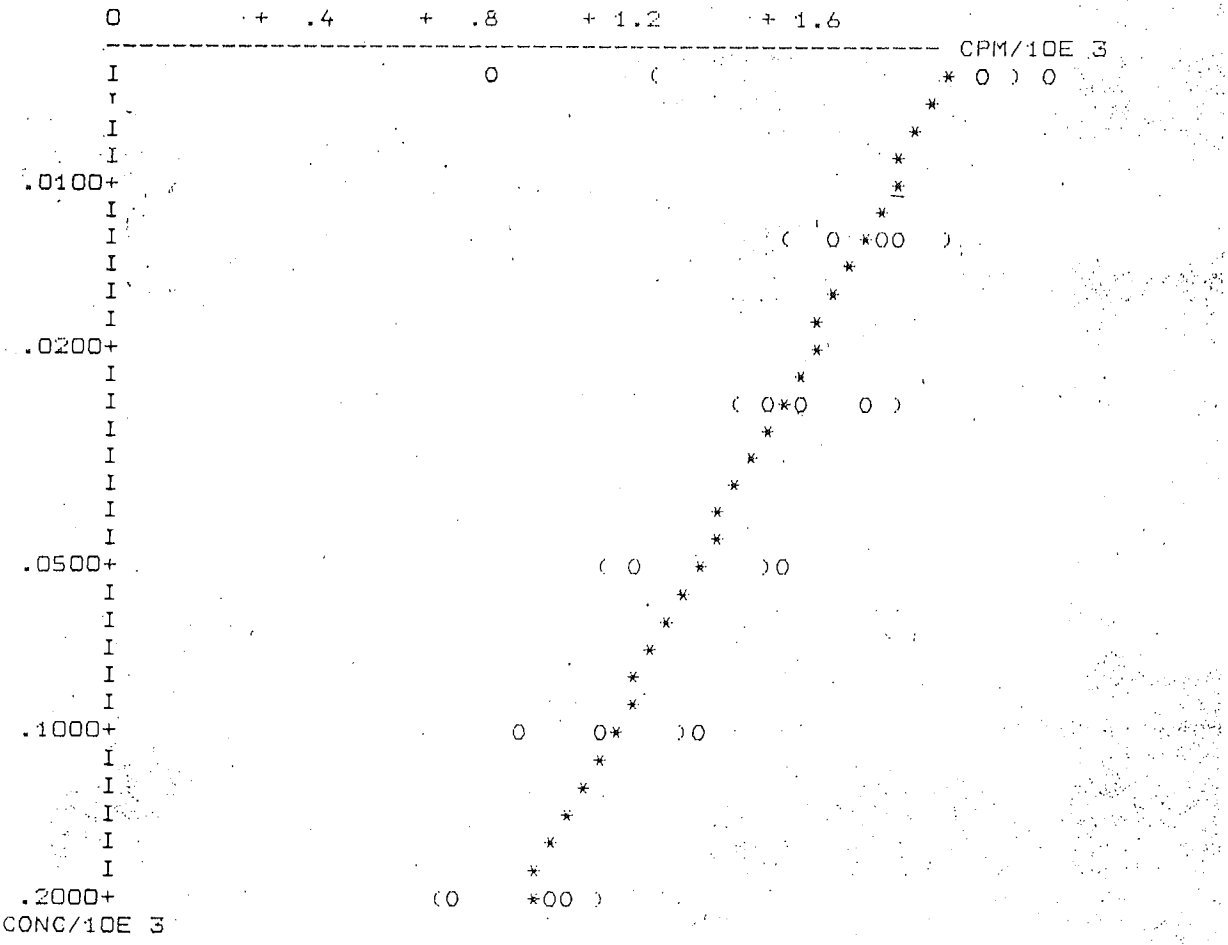

2. Ethanol precipitation method of insulin radioimmunoassay.

1	LISTING	Y
2	DUAL LABEL	N
3	STD TIME	60
4	UNK TIME	60
5	COUNTS	900000
6	WINDOW	035-110
7	METHOD	6
8	UNK BLAN	0
9	UNK REPL	1
10	CONC.FACTORS	N
11	CURVE EDIT	Y
12	FREE FRACTION	N
13	PRINT	-1-2-4-6-7-8-9-10-11-12
14	CODING	POS-CODE 001-TOA 004-BLA 007-6.25 010-12.5 013-25 016-50 019-100 022-UNKS

POS	CODE1	CTIME	COUNTS1	COR.CPM1	ERR1%	RATIO1	S.E1%	CONC.1	TOT
001	TOA	60	17734	17901.2	0.8				
002	TOA	60	17867	18036.1	0.7				
003	TOA	60	18091	18263.5	0.7				
	MEAN			18066.9	0.4		0.6		
004	BLA	60	852	856.1	3.4				
005	BLA	60	766	769.7	3.6				
006	BLA	60	769	772.7	3.6				
	MEAN			799.5	2.0		3.5		
007	6.25	60	3475	3494.2	1.7				
008	6.25	60	3280	3298.0	1.7				
009	6.25	60	3272	3289.9	1.7				
	MEAN			3360.7	1.0	1.0000	2.0		
010	12.5	60	3649	3669.3	1.7	1.0916			
011	12.5	60	2606	2619.8	2.0	0.7795			
012	12.5	60	3048	3064.5	1.8	0.9119			
	MEAN			3117.9	1.0	0.9277	9.8		
013	25	60	2778	2792.8	1.9	0.8310			
014	25	60	2491	2504.1	2.0	0.7451			
015	25	60	2288	2299.9	2.1	0.6844			
	MEAN			2532.3	1.2	0.7535	5.6		
016	50	60	1951	1961.0	2.3	0.5835			
017	50	60	1795	1804.1	2.4	0.5368			
018	50	60	2282	2293.9	2.1	0.6826			
	MEAN			2019.6	1.3	0.6010	7.1		
019	100	60	1534	1541.7	2.6	0.4587			
020	100	60	1322	1328.5	2.8	0.3953			
021	100	60	1482	1489.4	2.6	0.4432			
	MEAN			1453.2	1.5	0.4324	4.4		

N = 2
S = 1.250
F = .150

STAN.	CONC.	CPM	DIFF.(%) CONC.	WEIGHT(%)
1	6.250	-2.2028	11.2879	5.0468
2	12.500	5.2423	-20.9873	9.7554
3	25.000	2.2963	-8.0510	6.6653
4	50.000	1.2778	-3.7197	8.3319
5	100.000	-4.1532	9.1007	11.5408

SUM D = 39885.4
SUM W = 206210.6
RATIO = .1934

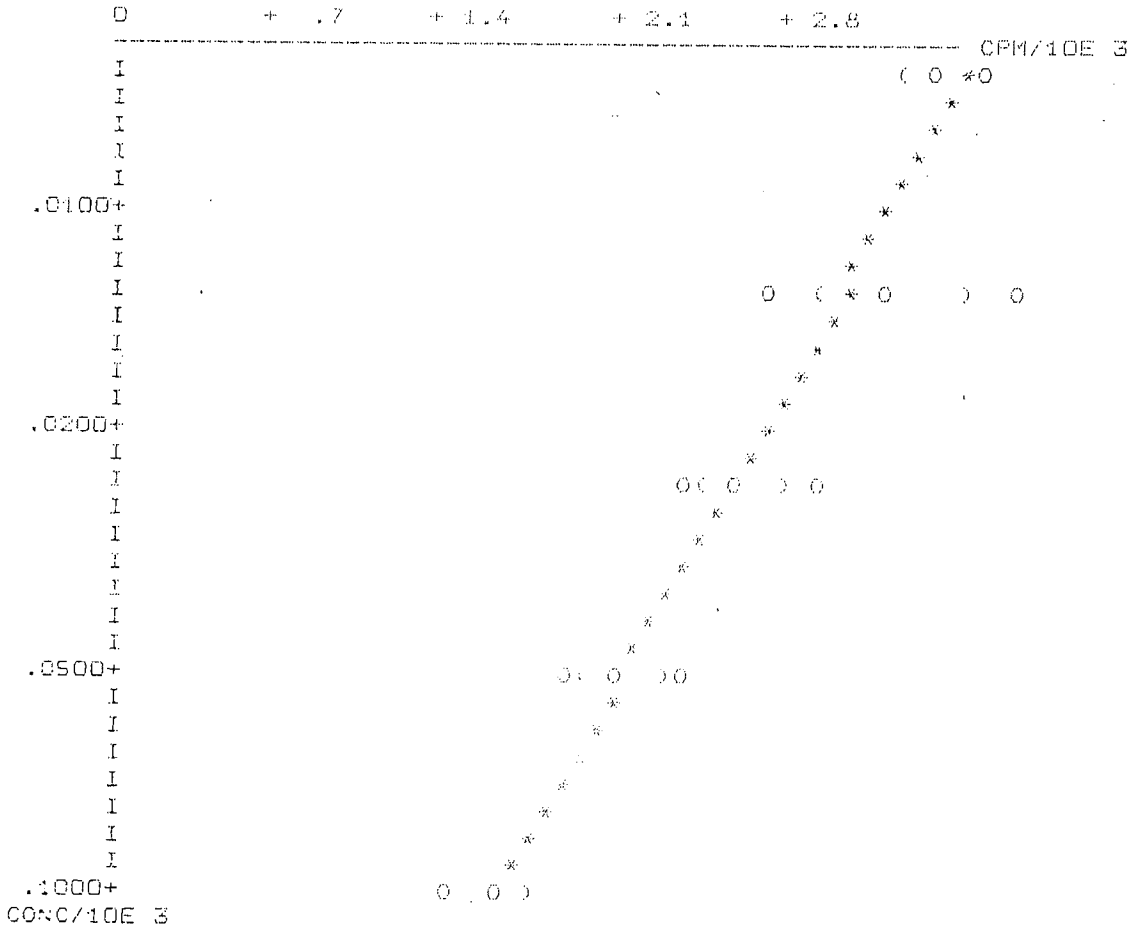

APPENDIX A4 - PERFORMANCE CHARACTERISTICS OF THE UNION CARBIDE HANDI FREEZE TRAY WHEN INSERTED INTO A 35HC FREEZER NECK TUBE.

TRAY POSITION NUMBER	TEMPERATURE AFTER 20 MINUTES (°C)	CALCULATED FREEZING RATE (°C/MINUTE)
1	-160	8.2
2	-100	5.4
3	-80	4.2
4	-50	2.7
5	-40	2.2
6	-70	0.7